



**Cyclic di-GMP-mediated regulation of the Pga
exopolysaccharide secretion machinery in
*Escherichia coli***

Inauguraldissertation

zur

Erlangung der Würde eines Doktors der Philosophie

vorgelegt der

Philosophisch-Naturwissenschaftlichen Fakultät

der Universität Basel

von

Samuel Steiner

aus Walterswil (BE), Schweiz

Basel, 2012

Originaldokument gespeichert auf dem Dokumentenserver der Universität Basel edoc.unibas.ch



Dieses Werk ist unter dem Vertrag „Creative Commons Namensnennung-Keine kommerzielle Nutzung-Keine Bearbeitung 2.5 Schweiz“ lizenziert. Die vollständige Lizenz kann unter creativecommons.org/licenses/by-nc-nd/2.5/ch eingesehen werden.



Namensnennung-Keine kommerzielle Nutzung-Keine Bearbeitung 2.5 Schweiz

Sie dürfen:



das Werk vervielfältigen, verbreiten und öffentlich zugänglich machen

Zu den folgenden Bedingungen:



Namensnennung. Sie müssen den Namen des Autors/Rechteinhabers in der von ihm festgelegten Weise nennen (wodurch aber nicht der Eindruck entstehen darf, Sie oder die Nutzung des Werkes durch Sie würden entlohnt).



Keine kommerzielle Nutzung. Dieses Werk darf nicht für kommerzielle Zwecke verwendet werden.



Keine Bearbeitung. Dieses Werk darf nicht bearbeitet oder in anderer Weise verändert werden.

- Im Falle einer Verbreitung müssen Sie anderen die Lizenzbedingungen, unter welche dieses Werk fällt, mitteilen. Am Einfachsten ist es, einen Link auf diese Seite einzubinden.
- Jede der vorgenannten Bedingungen kann aufgehoben werden, sofern Sie die Einwilligung des Rechteinhabers dazu erhalten.
- Diese Lizenz lässt die Urheberpersönlichkeitsrechte unberührt.

Die gesetzlichen Schranken des Urheberrechts bleiben hiervon unberührt.

Die Commons Deed ist eine Zusammenfassung des Lizenzvertrags in allgemeinverständlicher Sprache: <http://creativecommons.org/licenses/by-nc-nd/2.5/ch/legalcode.de>

Haftungsausschluss:

Die Commons Deed ist kein Lizenzvertrag. Sie ist lediglich ein Referenztext, der den zugrundeliegenden Lizenzvertrag übersichtlich und in allgemeinverständlicher Sprache wiedergibt. Die Deed selbst entfaltet keine juristische Wirkung und erscheint im eigentlichen Lizenzvertrag nicht. Creative Commons ist keine Rechtsanwalts-gesellschaft und leistet keine Rechtsberatung. Die Weitergabe und Verlinkung des Commons Deeds führt zu keinem Mandatsverhältnis.

Genehmigt von der Philosophisch-Naturwissenschaftlichen Fakultät auf Antrag von

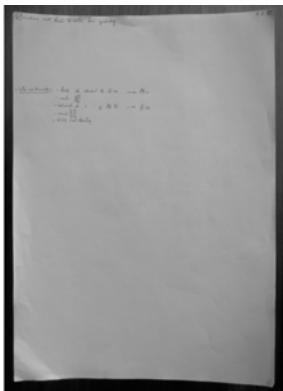
Prof. Dr. Urs Jenal

Prof. Dr. Dirk Bumann

Basel, den 24. April 2012

Prof. Dr. Martin Spiess

Dekan



Abstract

The ubiquitous bacterial second messenger c-di-GMP plays a central role as a controller of the bacterial 'lifestyle' transition. High cellular c-di-GMP levels promote surface attachment and biofilm formation, while low levels favor single cell behavior, motility and virulence. In response to largely unknown internal and environmental cues, c-di-GMP is synthesized by diguanylate cyclases (DGCs) and turned over by specific phosphodiesterases (PDEs). Within a multicellular biofilm structure, bacteria are enclosed in a self-produced extracellular polymeric matrix that is mainly composed of different exopolysaccharides (EPS). Biofilms formed by the model organism *Escherichia coli* that are based on one specific EPS, poly- β -1,6-*N*-acetylglucosamine (poly-GlcNAc), are in the main focus of this work. The cellular processes that underlie the induction of poly-GlcNAc-dependent biofilm formation in response to external stress are addressed at first, while the main part of this work focuses on the investigation of the molecular mechanisms behind c-di-GMP-stimulated poly-GlcNAc production.

In Boehm & Steiner et al. (2009), the molecular principles triggering poly-GlcNAc-dependent biofilm induction in response to subinhibitory concentrations of translation inhibitors were investigated. We present evidence that translational stress at the ribosome causes a SpoT-mediated reduction of ppGpp levels that results in the specific derepression of PgaA, an essential component of the poly-GlcNAc secretion machinery. In addition, we show that c-di-GMP that is mainly produced by the dedicated DGC YdeH strongly stimulates poly-GlcNAc-dependent biofilm formation and upregulates PgaD, another essential component of the secretion machinery. Evidence is provided that ppGpp and c-di-GMP play synergistic roles in controlling the poly-GlcNAc secretion machinery on a post-transcriptional level.

In the second and main part of this work, we show that the Pga machinery, which is involved in the production and secretion of poly-GlcNAc, is allosterically activated by c-di-GMP and we identify the inner membrane-bound PgaCD complex composed of the glycosyltransferase PgaC and the small protein PgaD as a novel type c-di-GMP receptor that relies on the tight interplay between two proteins for specific ligand binding. We present biochemical and genetic data to suggest that c-di-GMP binds to both proteins within the complex. Based on the analysis of gain-of-function, loss-of-function and truncated mutants, we propose a model in which PgaD integrates its two transmembrane helices into the core of transmembrane helices formed by PgaC to trigger the opening of a pore for poly-GlcNAc translocation across the cytoplasmic membrane upon c-di-GMP binding. Additionally, as PgaD, one subunit of the c-di-GMP receptor, gets rapidly degraded at low cellular c-di-GMP concentrations, we suggest a role for PgaD in shutting-off the Pga

machinery in response to c-di-GMP fluctuations and in temporarily uncoupling it from c-di-GMP signalling. In summary, this study not only unravels how c-di-GMP controls poly-GlcNAc synthesis, but furthermore presents a novel model for the molecular basis of specificity of c-di-GMP signalling systems.

Index

Abstract	i
Index	iii
1 Introduction	2
1.1 Cyclic di-GMP receptor proteins.....	2
1.1.1 PilZ domain-containing proteins	3
1.1.2 Degenerate GGDEF and EAL domain proteins	4
1.1.3 Transcription factors	6
1.1.4 Others	8
1.2 The Pga exopolysaccharide secretion system of <i>E. coli</i>	8
1.2.1 The Pga machinery	9
1.2.2 Regulation of the <i>pgaABCD</i> operon	10
1.2.3 The homologous Hms system of <i>Y. pestis</i>	12
2 Aim of the thesis	15
3 Results	17
3.1 Second messenger signalling governs <i>Escherichia coli</i> biofilm induction upon ribosomal stress	17
3.2 Allosteric activation of exopolysaccharide synthesis through cyclic di-GMP- mediated protein-protein interplay in <i>Escherichia coli</i>	58
3.3 Additional results	125
3.3.1 Results and interpretations.....	125
3.3.2 Additional figures, tables and figure legends.....	131
3.3.3 Materials and methods	141
4 Conclusions & perspectives	144
5 Bibliography	147
6 Appendix.....	156
7 Acknowledgements	158
8 Curriculum vitae	160

I N T R O D U C T I O N

1 Introduction

1.1 Cyclic di-GMP receptor proteins

The bacterial second messenger bis-(3'-5')-cyclic dimeric GMP (c-di-GMP) plays a central role in integrating environmental and cellular cues to control the 'lifestyle' transition by disfavoring motility and single cell behavior and by promoting biofilm formation (Figure 1).

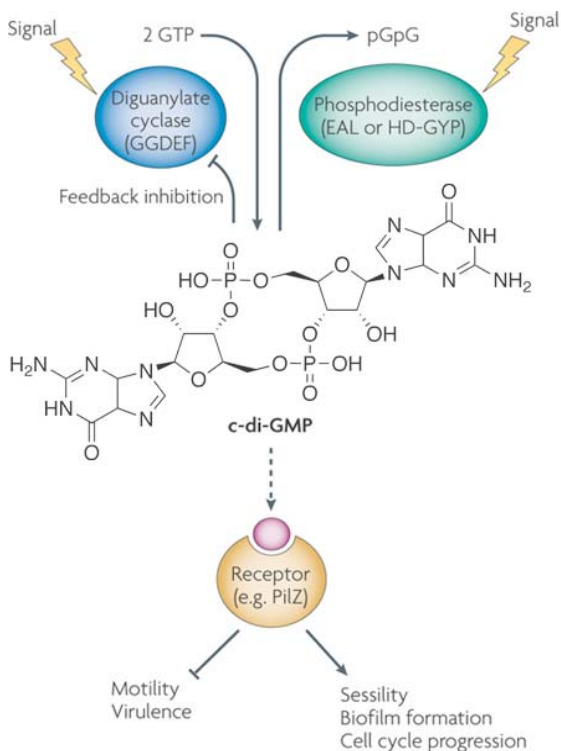


Figure 1: Minimal functional unit of a c-di-GMP signalling pathway. Cellular c-di-GMP concentrations are modulated by the action of DGCs with a GGDEF domain and PDEs with an EAL or HD-GYP domain. The activity of these enzymes is usually controlled by accessory signal input domains. C-di-GMP is sensed by receptor proteins that elicit stimulatory or inhibitory effects on particular cellular functions upon ligand binding. Figure adapted from (Schirmer & Jenal, 2009).

The small molecule was first described by Benziman and co-workers in 1987 as an allosteric activator of the cellulose synthase of *Gluconacetobacter xylinus* (Ross *et al*, 1987). C-di-GMP is synthesized from GTP by diguanylate cyclases (DGCs) that harbor a conserved GGDEF domain (Paul *et al*, 2004) and is degraded to pGpG by c-di-GMP-specific phosphodiesterases (PDEs) that typically harbor a conserved EAL domain (Christen *et al*, 2005; Hengge, 2009; Schirmer & Jenal, 2009). Certain bacterial species including e.g. *Pseudomonas aeruginosa*, but not *Escherichia coli* contain a second, unrelated type of c-di-GMP hydrolyzing domain, the so called HD-GYP domain

(Ryan *et al*, 2006). While DGCs and PDEs have been analyzed in detail, both structurally and functionally, relatively little is known about how c-di-GMP acts on downstream targets. The small molecule is known to interfere with cellular signalling on several levels, including transcription, translation, protein activity and protein stability (Schirmer & Jenal, 2009). The few c-di-GMP-specific receptor protein families that have been described up to now will be introduced and discussed in this chapter.

1.1.1 PilZ domain-containing proteins

The PilZ domain (named after the protein PilZ of *P. aeruginosa*) is the first c-di-GMP binding domain that was identified. Like the GGDEF and EAL domains, it is widely distributed among bacterial species and was found using a bioinformatical approach. PilZ domains exist either as stand-alone domain proteins or are associated with regulatory (e.g. DNA-binding domains), enzymatic (e.g. glycosyltransferase domains) or transport domains (Amikam & Galperin, 2006). Within the domain, the two conserved N-terminally located motifs RXXXR and D/NXSXXG were shown to be critical for binding of c-di-GMP with a sub-micromolar affinity (Ryjenkov *et al*, 2006; Christen *et al*, 2007; Merighi *et al*, 2007; Pratt *et al*, 2007). Structures of single PilZ domain proteins and of PilZ proteins with an N-terminal YcgR-like domain (YcgR-N) that have recently been solved in their apo and holo forms by NMR and crystallography (Benach *et al*, 2007; Ramelot *et al*, 2007; Christen *et al*, 2007; Ko *et al*, 2010; Habazettl *et al*, 2011) revealed a six-stranded antiparallel β -barrel fold and shed light on the mechanisms of c-di-GMP-dependent PilZ activation and signalling to downstream targets.

In PlzD of *Vibrio cholerae*, a single c-di-GMP molecule binds right at the junction between the N-terminal YcgR-N domain and the C-terminal PilZ domain, which leads to a conformational change (the c-di-GMP switch), causing the two domains to come into close proximity and to wrap around c-di-GMP. Thus, in the holo form, c-di-GMP sits in the interface of the YcgR-N and PilZ domains. These dramatic structural changes may affect the interaction with downstream targets and processes (Benach *et al*, 2007). In contrast to PlzD, binding of an intercalated c-di-GMP dimer was reported to trigger a dimer to monomer transition in the YcgR-N-PilZ family protein PP4397 from *Pseudomonas putida* (Ko *et al*, 2010).

On the other hand, a single PilZ domain that lacks the N-terminal YcgR-N domain is sufficient for c-di-GMP binding. Apo and holo NMR structures of PA4608 from *P. aeruginosa* were reported (Ramelot *et al*, 2007; Christen *et al*, 2007; Habazettl *et al*, 2011; Shin *et al*, 2011). Upon binding of a c-di-GMP dimer to the monomeric PilZ domain, the unstructured N-terminus containing the RXXXR PilZ domain motif gets ordered and wraps around the intercalated ligand dimer. This

structural rearrangement goes along with the reorientation of the C-terminal part of the protein, bringing the C-terminus in close proximity to the ligand binding site (c-di-GMP switch) (Habazettl *et al*, 2011; Shin *et al*, 2011). As these conformational changes lead to a severe rearrangement of surface charges, it was hypothesized that the newly generated molecular surface might serve as a readout of PilZ receptors by providing a highly charged interaction surface for downstream target proteins (Habazettl *et al*, 2011).

The fact that PilZ domain proteins seem to exhibit different c-di-GMP binding stoichiometries and quaternary structures, may suggest that these differences play a role in generating diverse forms of c-di-GMP-mediated output regulation. The existence of a tetrameric PilZ domain structure as discovered in *Xanthomonas campestris* may point into the same direction (Li *et al*, 2011).

The detailed mechanisms by which PilZ domains relay c-di-GMP signalling information upon ligand binding remain to be investigated. Protein-protein interactions seem to generally play a central role in mediating downstream biological outputs. One of the best-studied examples is YcgR that regulates c-di-GMP-dependent motility in *E. coli* and other enterobacteria. Upon c-di-GMP binding, the cytosolic protein YcgR gets recruited to the flagellar motor protein MotA to negatively affect motor activity in a brake-like fashion (Boehm *et al*, 2010). Other studies reported that c-di-GMP-loaded YcgR interacts with the FliG/FliM subunits of the flagellum switch complex to induce a bias in the change of flagellum rotation direction (Fang & Gomelsky, 2010; Paul *et al*, 2010).

In addition, PilZ domains have been implicated in the c-di-GMP-dependent regulation of exopolysaccharide (EPS) secretion systems in several bacterial species. For example the cellulose synthase BcsA of *G. xylinus*, which was the first enzyme found to be allosterically activated by c-di-GMP (Ross *et al*, 1987, 1990), harbors a C-terminal PilZ domain. The PilZ domain that is known to activate alginate biogenesis in *P. aeruginosa* is located in the cytoplasmic N-terminus of Alg44, an essential subunit of the alginate biosynthesis machinery (Merighi *et al*, 2007; Oglesby *et al*, 2008).

A third PilZ-dependent functional output that has been described is the stimulation of DNA binding of a transcriptional activator. The PilZ-containing protein MrkH of *Klebsiella pneumoniae* was shown to activate biofilm formation through c-di-GMP-mediated expression of type 3 fimbriae (Wilksch *et al*, 2011).

1.1.2 Degenerate GGDEF and EAL domain proteins

Degenerate GGDEF and EAL domains that lack enzymatic activity constitute a second group of c-di-GMP receptors. Several examples have been identified in the past. The first example is PelD, an

inner membrane-bound component of the PEL EPS biosynthesis machinery that is required for pellicle formation of *P. aeruginosa* (Lee *et al*, 2007). Secondary structure prediction indicated some structural similarity between the C-terminus of this protein and GGDEF domains, especially within the region of the RXXD motif that is reminiscent of the I-site known to be involved in feedback inhibition of DGCs (Chan *et al*, 2004; Christen *et al*, 2006). PelD was shown to specifically bind c-di-GMP with a high affinity and alanine substitutions within the RXXD motif were found to totally abrogate c-di-GMP binding as well as c-di-GMP-dependent PEL EPS synthesis (Lee *et al*, 2007). However, the mechanistic details behind this allosteric activation remain to be clarified. It can only be speculated that c-di-GMP binding would generate a large conformational change in the receptor protein similar to what was observed for binding of a c-di-GMP dimer to the I-site of enzymatically active DGCs (Chan *et al*, 2004; Wassmann *et al*, 2007).

PopA states a second example of a protein that harbors a degenerate GGDEF domain, which specifically binds c-di-GMP via its RXXD I-site motif (Duerig *et al*, 2009). This cytoplasmic protein is known to participate in the regulation of cell cycle progression in the asymmetrically dividing bacterium *Caulobacter crescentus*. During the G1-to-S phase transition, PopA dynamically localizes to the stalked pole of a differentiating cell in response to c-di-GMP binding. There it helps to recruit and sequester proteins involved in the degradation of the replication initiation inhibitor CtrA (Duerig *et al*, 2009).

Very recently, a third example of this group of c-di-GMP receptors was described. SgmT from *Myxococcus xanthus* is a cytoplasmic sensor histidine kinase that harbors a C-terminal degenerate GGDEF domain and that phosphorylates the DNA binding response regulator DigR. While c-di-GMP binding to SgmT does not seem to affect the kinase activity, it is needed for the proper spatial sequestration of SgmT. The distinct localization of SgmT and/or DigR may insulate this two-component system from cross-talk with other signalling pathways (Petters *et al*, 2012).

Besides degenerate GGDEF domains, also degenerate EAL domains are known to function as receptors for c-di-GMP. The structural and functional basis of allosteric regulation of FimX, a protein involved in the regulation of type IV pili-based twitching motility and biofilm formation in *P. aeruginosa* (Mattick, 2002; Huang *et al*, 2003), has been carefully investigated (Navarro *et al*, 2009; Qi *et al*, 2011). The cytoplasmic protein consists of an N-terminal receiver domain that is followed by a PAS domain, an enzymatically inactive GGDEF domain that also lacks the I-site motif and a degenerate non-catalytic EAL domain. In contrast to the stacked c-di-GMP dimers that bind to I-sites of DGCs, c-di-GMP binds to the degenerate EAL domain of FimX as a monomer. The conserved amino acid residues that are involved in ligand coordination are very much the same than in other known catalytically active or inactive EAL domains (Navarro *et al*, 2009). Mutations

in the EVL motif of the EAL domain abrogate high affinity c-di-GMP binding *in vitro* and cause a mislocalization of FimX *in vivo* (Kazmierczak *et al*, 2006; Qi *et al*, 2011). The fact that ligand binding to the C-terminal EAL domain triggers a long-range conformational change in the N-terminal receiver domain and adjacent linker region suggests that FimX participates in c-di-GMP-dependent protein-protein interactions that are important for the assembly of type IV pili (Qi *et al*, 2011).

Another member of this group of c-di-GMP receptors is the inner membrane-bound protein LapD from *Pseudomonas fluorescens* that is involved in biofilm formation (Newell *et al*, 2009). It is composed of an N-terminal periplasmic domain and a cytosolic HAMP domain that is followed by degenerate GGDEF and EAL domains. Binding of c-di-GMP to the degenerate EAL domains of a LapD heterodimer results in a strong conformational change that is propagated through the HAMP domains to the periplasmic part of the proteins, causing the sequestration and inhibition of the periplasmic protease LapG that under low c-di-GMP conditions (e.g. due to the activity of the PDE RapA in response to phosphate starvation) causes the release of the biofilm-promoting large outer membrane adhesin LapA through cleavage of its N-terminus (Newell *et al*, 2011; Navarro *et al*, 2011). Based on structural and biochemical analysis, c-di-GMP binding triggers the dimerization of the two EAL domains, which are physically separated in the ligand-free state. Furthermore, only a c-di-GMP-bound receptor is thought to be capable of binding LapG in the periplasm. This inside-out signal transduction mechanism, which allows cells to react to phosphate starvation by promoting biofilm detachment, is the first example of an inner membrane-bound c-di-GMP binding protein that controls the activity of a periplasmic enzyme (Navarro *et al*, 2011).

1.1.3 Transcription factors

Several structurally heterogeneous c-di-GMP receptor proteins act as DNA binding transcription factors. FleQ, which activates the expression of flagella genes and represses *pel* EPS biosynthesis genes in *P. aeruginosa*, was the first member of this group that was identified. Upon c-di-GMP binding (presumably to the AAA+ ATPase domain), FleQ dissociates from the DNA, thereby causing derepression of transcription from the *pel* promoter (Hickman & Harwood, 2008).

A crystal structure of the transcriptional regulator VpsT from *V. cholerae* in complex with an intercalated c-di-GMP dimer has recently been solved (Krasteva *et al*, 2010). VpsT consists of an N-terminal non-canonical receiver domain, which has an additional helix (α_6) at its C-terminus, and a C-terminal helix-turn-helix domain and is known to inversely regulate the expression of motility and *vps* EPS production genes in a c-di-GMP-dependent manner (Lim *et al*, 2006; Beyhan

et al, 2007). VpsT is a member of the FixJ, LuxR and CsgD family of prokaryotic response regulators. Binding of a c-di-GMP dimer to the conserved motif W[F/L/M][T/S]R at the base of helix α_6 of the receiver domain induces VpsT dimerization and DNA binding. Within the binding motif, the tryptophan and arginine side chains were found to form π -stacking interactions with the purine rings of the nucleotide (Krasteva *et al*, 2010). Whether analogous mechanisms play a role in the large family of homologous transcription factors that harbor an extended receiver domain remains to be seen. Only very recently, CpsQ, a VpsT homologue of *Vibrio parahaemolyticus*, was shown to activate the expression of *cps* capsular polysaccharide genes upon c-di-GMP binding (Ferreira *et al*, 2012). Interestingly, the expression of *vpsT* in *V. cholerae* is c-di-GMP-dependent itself. It is induced by the c-di-GMP binding transcription factor VpsR, which like FleQ harbors an AAA+ ATPase domain (Srivastava *et al*, 2011).

The Clp protein of plant pathogenic *Xanthomonas* spp. (XcCLP) is a paralog of the classical cAMP binding CRP protein of enterobacteria (CRP/FNR superfamily) that has evolved to specifically bind c-di-GMP (Leduc & Roberts, 2009; Tao *et al*, 2010; Chin *et al*, 2010). XcCLP negatively regulates the expression of several virulence genes in response to high cellular c-di-GMP concentrations (He & Zhang, 2008). In contrast to classical CRP-like proteins, XcCLP is intrinsically competent to bind to target DNA sites in the absence of any ligand and the DNA binding activity is allosterically inhibited upon the interaction with its effector c-di-GMP. The apo crystal structure of XcCLP was recently solved and revealed that the protein consists of an N-terminal β -barrel domain and a C-terminal helix-turn-helix DNA-binding domain that are coupled via a long α -helix dimerization domain (Chin *et al*, 2010). The potential c-di-GMP binding site that lies in the interface of the N- and C-terminal domains of XcCLP was identified with a molecular modeling approach. An aspartate, a histidine and several arginine residues that reside in a locally positively charged region were suggested to make contact with the ligand through salt bridges and π -stacking interactions. Alanine substitutions of the corresponding residues abrogated the c-di-GMP-dependent release of XcCLP from target promoter DNA. The slight tilting of two α -helices upon c-di-GMP binding is thought to open up the protein conformation, rendering it unable to bind to DNA (Chin *et al*, 2010). In marked contrast to XcCLP, c-di-GMP binding to an unknown site in the CRP/FNR family protein Bcam1349 from *Burkholderia cenocepacia* was reported to strengthen the protein-DNA interaction and to activate the expression of cellulose EPS biosynthesis genes (Fazli *et al*, 2011). Further structural studies have to investigate the differences between the molecular mechanisms of XcCLP and Bcam1349.

1.1.4 Others

A few other proteins that do not belong to one of the three classes discussed above were also shown to bind c-di-GMP. In *E. coli*, a macromolecular RNase E- and polynucleotide phosphorylase (PNPase)-containing ribonucleoprotein complex that is involved in RNA processing and degradation was found to copurify with the oxygen-sensing DGC and PDE couple DosC/DosP (Tuckerman *et al*, 2009, 2011). The c-di-GMP, which is locally produced by DosC under anaerobic conditions, directly binds to an unknown site within PNPase and activates its 3' polyribonucleotide polymerase activity. Under aerobic conditions however, DosP activity is dominant causing PNPase inactivation. It remains to be investigated what determines the specificity for certain RNAs to be preserved and/or degraded in response to changing oxygen conditions (Tuckerman *et al*, 2011).

BdcA from *E. coli* was described as a c-di-GMP binding protein that inversely regulates biofilm formation and dispersal. Since it is thought to fulfill its general role in controlling c-di-GMP-mediated phenotypes by scavenging unbound c-di-GMP molecules in the cell, it was proposed to be an interesting candidate to be developed as a tool for synthetic biology (Ma *et al*, 2011; Hong *et al*, 2012).

Very recently, the discovery of the first eukaryotic c-di-GMP binding protein was reported (Burdette *et al*, 2011). Membrane-bound STING that is essential for the IFN response to bacteria-specific cyclic dinucleotides in HEK293T cells acts as an immunosensor by directly binding to c-di-GMP. Interestingly, STING does not seem to share homology with any of the known c-di-GMP receptor proteins of bacteria (Burdette *et al*, 2011).

Besides the proteinaceous c-di-GMP receptors described in this chapter, a few c-di-GMP binding RNA riboswitches were recently discovered and characterized (Sudarsan *et al*, 2008; Kulshina *et al*, 2009; Smith *et al*, 2009; Lee *et al*, 2010; Smith *et al*, 2011; Smith & Strobel, 2011). They will however not be discussed here in more detail.

1.2 The Pga exopolysaccharide secretion system of *E. coli*

Once cells have adhered to surfaces via fimbriae, pili or other adhesins, exopolysaccharides (EPS) are synthesized and secreted to allow the formation of a mature biofilm matrix (Branda *et al*, 2005; Beloin *et al*, 2008). Besides colanic acid and cellulose, *E. coli* produces the EPS poly- β -1,6-*N*-acetylglucosamine (poly-GlcNAc; also called PGA, PNAG, ICA) to permanently colonize surfaces (Wang *et al*, 2004). This linear homopolymer was recently implicated to play a role in biofilm formation in a wide variety of pathogenic bacteria including *Staphylococcus epidermidis* and *S.*

aureus (Mack *et al*, 1996; O’Gara, 2007), *Yersinia pestis* (Hinnebusch *et al*, 1996; Bobrov *et al*, 2008), *Actinobacillus pleuropneumoniae* (Izano *et al*, 2007), *Aggregatibacter actinomycetemcomitans* (Izano *et al*, 2008), *Acinetobacter baumannii* (Choi *et al*, 2009), *Bordetella* spp. (Parise *et al*, 2007; Conover *et al*, 2010), *Pectobacterium atrosepticum* (Pérez-Mendoza *et al*, 2011), *Chromobacterium violaceum* (Becker *et al*, 2009) and *Burkholderia* spp. (Yakandawala *et al*, 2011). In many of these species, poly-GlcNAc promotes virulence and antibodies against this EPS were shown to protect mice against infections with e.g. *S. aureus*, uropathogenic *E. coli*, *A. baumannii* and *Burkholderia* spp. (Maira-Litrán *et al*, 2005; Cerca *et al*, 2007; Bentancor *et al*, 2012; Skurnik *et al*, 2012).

1.2.1 The Pga machinery

In *E. coli*, poly-GlcNAc is synthesized and secreted by the cell envelope-spanning Pga machinery, which is encoded by the *pgaABCD* operon (Wang *et al*, 2004, 2005). Interestingly, this genetic locus differs in its G+C content from the *E. coli* average (44% versus 51% for the genome), suggesting that the Pga system was acquired by horizontal gene transfer (Wang *et al*, 2004). While PgaA and PgaB are needed for poly-GlcNAc export, PgaC and PgaD are necessary for poly-GlcNAc synthesis (Figure 2) (Itoh *et al*, 2008).

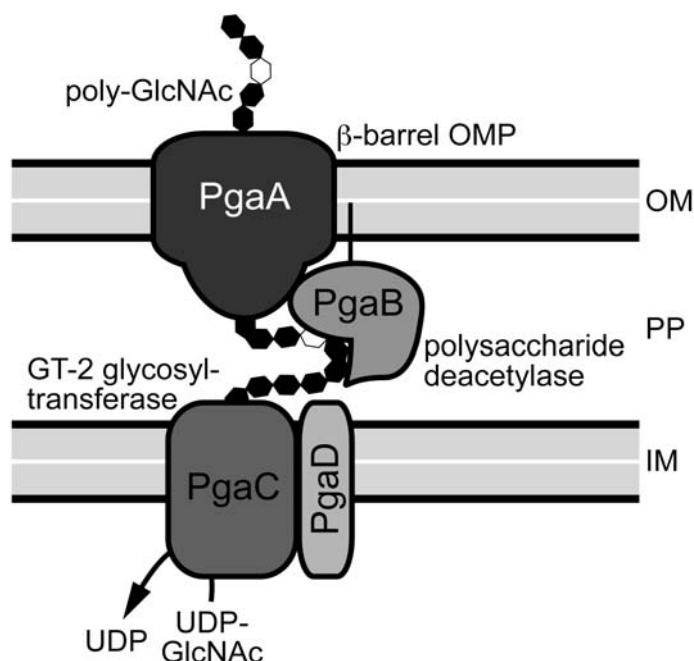


Figure 2: The Pga machinery is involved in polymerization and secretion of poly-GlcNAc. A model for Pga protein localization and poly-GlcNAc biogenesis. See text for explanations. IM = inner membrane, OM = outer membrane, PP = periplasm, OMP = outer membrane protein. Black irregular hexagons indicate GlcNAc residues, while white irregular hexagons depict glucosamine residues (deacetylated GlcNAc).

PgaA (807 aa) is an outer membrane protein with an N-terminal periplasmic domain and a predicted β -barrel structure at the C-terminus that likely serves as a porin to translocate growing poly-GlcNAc chains to the cell surface (Itoh *et al*, 2008). PgaB (672 aa) is a putative outer membrane lipoprotein that contains a predicted poly-GlcNAc binding and a polysaccharide *N*-deacetylase domain. Its catalytic activity was shown to be essential for poly-GlcNAc export through PgaA (Wang *et al*, 2004; Itoh *et al*, 2008). NMR analysis of purified poly-GlcNAc from *E. coli* revealed that about 3% of the GlcNAc residues are unacetylated (Wang *et al*, 2004). PgaC (441 aa) is a putative inner membrane-bound processive (invertig) β -glycosyltransferase (GT) of the GT-2 family with a conserved 'D, D, D35QXXRW' motif that polymerizes poly-GlcNAc from uridine 5'-diphosphate-*N*-acetylglucosamine (UDP-GlcNAc) (Saxena & Brown, 1997; Wang *et al*, 2004; Itoh *et al*, 2008). The catalytic domain of GT-2 family members is thought to be exposed to the cytoplasm (Heldermon *et al*, 2001; Ciocchini *et al*, 2006; Bobrov *et al*, 2008) and the sugar transfer through the cytoplasmic membrane likely functions independently of an undecaprenyl phosphate lipid carrier, as shown for the PgaC homologue IcaA from *S. epidermidis* (Gerke *et al*, 1998). Finally, PgaD (137 aa) is a small protein with two predicted N-terminal transmembrane helices. Its function is unknown and it does not show any obvious similarity to other protein families or domains. However, because PgaD is essential for poly-GlcNAc synthesis (Wang *et al*, 2004), it was suggested to assist the GT in polymerizing poly-GlcNAc (Itoh *et al*, 2008). The small protein IcaD of *S. epidermidis* is required to fully activate the IcaA GT *in vitro* (Gerke *et al*, 1998). Even though PgaD and IcaD are not related in sequence, these proteins may function similarly.

1.2.2 Regulation of the *pgaABCD* operon

Transcriptional regulation. Transcription of *pgaABCD* operon from a single promoter requires the LysR-type transcription factor NhaR, which responds to elevated Na^+ concentrations and alkaline pH (Goller *et al*, 2006). NhaR was first described as an activator of the two-gene operon *nhaAR*, in which *nhaA* encodes for a Na^+/H^+ antiporter that fulfills an important role in pH homeostasis (Rahav-Manor *et al*, 1992). Since NhaR is essential for cell survival under high NaCl concentrations, high pH and certain oxidative stresses, its role in promoting poly-GlcNAc-dependent biofilm formation was suggested to be part of a network that provides protection against a variety of biological and chemical stresses (Goller *et al*, 2006).

Translational regulation. The expression of the *pga* operon is negatively controlled on the translational level by the action of the RNA binding global regulator CsrA (carbon storage regulator A). CsrA binding to six sites on the *pgaABCD* 5' untranslated mRNA leader sequence

competes with binding of the 30S ribosomal subunit, thus blocks translation initiation and destabilizes the *pgaABCD* mRNA (Wang *et al*, 2005).

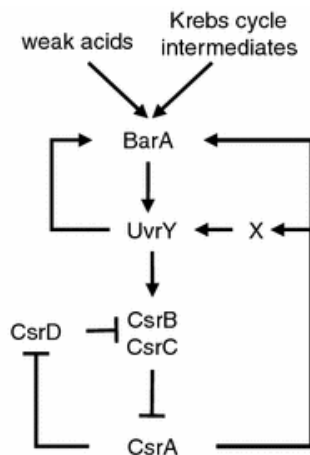


Figure 3: The Csr circuitry. See text for explanations. Figure adapted from (Timmermans & Van Melder, 2010).

CsrA (and its orthologues RsmA and RsmE from *Pseudomonas* spp.) is a small dimeric global regulatory protein that generally activates exponential phase processes while repressing stationary phase functions. It is known to control numerous biological pathways including carbon metabolism, EPS production, motility, quorum sensing and virulence in many eubacteria (Romeo *et al*, 1993; Timmermans & Van Melder, 2010). Binding of CsrA homodimers to the 5' untranslated leader sequence of mRNAs mostly represses translation, but also a few examples of positive regulation are known (Timmermans & Van Melder, 2010). The two non-coding small RNAs (sRNAs) CsrB and CsrC (RsmY and RsmZ in *Pseudomonas* spp.), which are predicted to form multiple stem-loops containing conserved CsrA target sites, antagonize CsrA activity through CsrA binding and sequestration (Babitzke & Romeo, 2007; Lapouge *et al*, 2008). The expression of both sRNAs is under positive control of the BarA-UvrY (GacS-GacA in *Pseudomonas* spp.) two-component system (TCS) (Suzuki *et al*, 2002) that was shown to react to the metabolic end-products formate and acetate in *E. coli* (Chavez *et al*, 2010) and to yet uncharacterized density-related signals and Krebs cycle intermediates in *Pseudomonas* spp. (Lapouge *et al*, 2008; Takeuchi *et al*, 2009). The Csr circuitry (Figure 3) is completed by the fact that CsrA activates the BarA-UvrY TCS via a yet unknown mechanism (Gudapaty *et al*, 2001; Suzuki *et al*, 2002; Weilbacher *et al*, 2003). Finally, CsrD, the newest identified component of the Csr cascade that harbors degenerate GGDEF and EAL domains specifically targets CsrB and CsrC for degradation by RNase E in a c-di-GMP-independent manner (Suzuki *et al*, 2006). Its expression seems to be repressed by CsrA in *Salmonella Typhimurium* as well as in *E. coli* (Suzuki *et al*, 2006; Jonas *et al*, 2008, 2010).

Very recently, it was found that CsrA not only directly affects *pga* expression, but also indirectly by repressing the translation of NhaR, the essential transcriptional activator of the *pga* operon (Pannuri *et al*, 2012).

Interestingly, *pga* translation was suggested to be activated by the CRP-regulated sRNA McaS that also seems to control *csgD*, the transcription regulator of curli biogenesis, and *flhDC*, the master transcription regulator of flagella synthesis. However, the detailed molecular mechanism and the physiological role behind this finding remain to be unraveled (Thomason *et al*, 2012).

c-di-GMP-dependent regulation. It was shown that the second messenger c-di-GMP that is derived from the DGC YdeH, the main DGC under the tested conditions, post-transcriptionally (in respect to *pga* operon transcription) activates poly-GlcNAc-dependent biofilm formation via a yet unknown mechanism (Boehm *et al*, 2009). Interestingly, the expression of *ydeH* and *ycdT*, another DGC-encoding gene that is divergently located to the *pga* operon, stands under translational repression by CsrA (Jonas *et al*, 2008). This thus strongly suggests that the expression of the Pga machinery and c-di-GMP signalling proteins is coupled via CsrA and implies that this coupling is part of a coordinated biofilm-promoting signalling response.

In addition to the post-transcriptional control mechanism, a recent report suggested the existence of a c-di-GMP-responsive regulatory protein that activates *pga* operon transcription in a DGC YddV-specific manner. This study extends the impact of c-di-GMP on *pga* regulation and proposes a model of multiple levels of control for c-di-GMP-dependent poly-GlcNAc production (Tagliabue *et al*, 2010).

1.2.3 The homologous Hms system of *Y. pestis*

The four proteins that make up the poly-GlcNAc-synthesizing and -secreting Hms machinery of *Y. pestis* are close homologues of the Pga proteins of *E. coli* and fulfill the same functions (Forman *et al*, 2006; Bobrov *et al*, 2008; Abu Khweek *et al*, 2010). The Hms system has been extensively studied due to its critical role in bubonic plague. *Y. pestis* is transmitted by bites of infected fleas that carry Hms-dependent biofilms occluding their proventriculus. This blockage begins to form due to a temperature-dependent control mechanism as soon as a flea ingests a blood meal from an infected mammalian host (Hinnebusch *et al*, 1996; Perry *et al*, 2004; Hinnebusch & Erickson, 2008).

Biochemical and genetic studies that have been performed on the Hms system revealed that the two outer membrane proteins HmsH and HmsF (the homologues of PgaA and PgaB of *E. coli*) as well as the two inner membrane proteins HmsR and HmsS (the homologues of PgaC and PgaD

of *E. coli*) interact (Bobrov *et al*, 2008; Abu Khweek *et al*, 2010). Most interestingly, the *hms*-dependent surface attachment is controlled by c-di-GMP via a yet unknown molecular mechanism. *Y. pestis* encodes only three enzymatically active c-di-GMP signalling proteins (Sun *et al*, 2011; Bobrov *et al*, 2011). Among them, the DGC HmsT, whose gene is divergently located to the *hms* operon, and the PDE HmsP are the main controllers that inversely regulate biofilm formation (Kirillina *et al*, 2004; Bobrov *et al*, 2005). Because HmsP was found to interact with HmsT and maybe also with HmsR, an allosteric activation mechanism of c-di-GMP was proposed, which relies on the existence of an inner membrane complex composed of HmsR, HmsS, HmsT and HmsP that was suggested to generate a physically isolated c-di-GMP signalling entity (Kirillina *et al*, 2004; Bobrov *et al*, 2008).

A I M O F T H E T H E S I S

2 Aim of the thesis

The second messenger c-di-GMP has emerged as a central controller of the transition from a motile, single cell 'lifestyle' to a biofilm 'lifestyle' in many bacterial species. However, relatively little is known about the mechanistic details on how c-di-GMP acts on downstream targets to mediate cellular responses. It was previously found that c-di-GMP stimulates poly-GlcNAc-dependent biofilm formation in *E. coli*. The main aim of this PhD thesis was to find out on which level and how c-di-GMP controls the poly-GlcNAc-synthesizing and -secreting Pga machinery. The goal was to unravel the details of the underlying molecular mechanisms and to gain insight into the functional consequences of this regulation using a variety of different genetic and biochemical approaches.

R E S U L T S

3 Results

3.1 *Second messenger signalling governs Escherichia coli biofilm induction upon ribosomal stress*

Alex Boehm*, **Samuel Steiner***, Franziska Zaehringer, Alain Casanova, Fabienne Hamburger, Daniel Ritz, Wolfgang Keck, Martin Ackermann, Tilman Schirmer and Urs Jenal

* Both authors contributed equally to this work.

Molecular Microbiology (2009) 72(6), 1500–1516.

Statement of my work: The main experimental contribution to this work has been done during my Master thesis (2006-2007) under the supervision of Dr. Alex Boehm. However, within the first eight months of my PhD studies, several experiments were redone for publication reasons as well as new data was generated.

Second messenger signalling governs *Escherichia coli* biofilm induction upon ribosomal stress

Alex Boehm,^{1*†} Samuel Steiner,^{1†}
Franziska Zaehring,¹ Alain Casanova,¹
Fabienne Hamburger,¹ Daniel Ritz,² Wolfgang Keck,²
Martin Ackermann,³ Tilman Schirmer¹ and Urs Jenal¹

¹Biozentrum, University of Basel, Klingelbergstrasse 50/70, 4056 Basel, Switzerland.

²Actelion Pharmaceuticals Ltd, Gewerbestrasse 16, 4123 Allschwil, Switzerland.

³ETH Zurich, Institute of Biogeochemistry and Pollutant Dynamics, and EAWAG, Department of Environmental Microbiology, 8092 Zurich, Switzerland.

Summary

Biofilms are communities of surface-attached, matrix-embedded microbial cells that can resist antimicrobial chemotherapy and contribute to persistent infections. Using an *Escherichia coli* biofilm model we found that exposure of bacteria to subinhibitory concentrations of ribosome-targeting antibiotics leads to strong biofilm induction. We present evidence that this effect is elicited by the ribosome in response to translational stress. Biofilm induction involves upregulation of the polysaccharide adhesin poly- β -1,6-N-acetyl-glucosamine (poly-GlcNAc) and two components of the poly-GlcNAc biosynthesis machinery, PgaA and PgaD. Poly-GlcNAc control depends on the bacterial signalling molecules guanosine-bis 3', 5'(diphosphate) (ppGpp) and bis-(3'-5')-cyclic di-GMP (c-di-GMP). Treatment with translation inhibitors causes a ppGpp hydrolase (SpoT)-mediated reduction of ppGpp levels, resulting in specific derepression of PgaA. Maximal induction of PgaD and poly-GlcNAc synthesis requires the production of c-di-GMP by the dedicated diguanylate cyclase YdeH. Our results identify a novel regulatory mechanism that relies on ppGpp signalling to relay information about ribosomal performance to the Pga machinery, thereby inducing adhesin production and biofilm formation. Based on the important synergistic roles of ppGpp and c-di-GMP in this process, we

suggest that interference with bacterial second messenger signalling might represent an effective means for biofilm control during chronic infections.

Introduction

In response to various stress conditions, bacteria like *Escherichia coli* can form communities of aggregated, surface-attached cells called biofilms. Cells in a biofilm typically express proteinaceous adhesive organelles, e.g. pili or fimbriae and secrete exopolysaccharides, including alginate, cholanolic acid, cellulose or poly- β -1,6-N-acetylglucosamine (poly-GlcNAc) (Branda *et al.*, 2005). These factors constitute a species-specific extracellular matrix, which serves as protective encasement against physical or chemical stress and against predation by the host immune system. Importantly, cells in a biofilm display a strongly decreased susceptibility to antibiotics and the host immune system (Mah and O'Toole, 2001; Furukawa *et al.*, 2006). Resistance is mediated by the protective properties of the extracellular matrix and by subpopulations of metabolically dormant cells. These biofilm-associated persister cells are believed to be the base for latent and recurrent infections (Costerton *et al.*, 1999; Lewis, 2007). While acute infections can be treated effectively in most cases, chronic infections like endocarditis, infections linked to prosthetic implants or recurring urinary tract infections, are notoriously difficult to eradicate and represent a public health problem of increasing importance (Fux *et al.*, 2005).

In recent years it was shown that bacteria display species-specific, antibiotic-specific and dose-dependent transcriptional responses upon challenges with subminimal inhibitory concentrations (sub-MIC) of antibiotics (Goh *et al.*, 2002; Tsui *et al.*, 2004; Yim *et al.*, 2006). These findings have led to the hypothesis that antibiotics can be intercellular or even interspecies signalling molecules and that the presence of low levels of antibiotics can evoke beneficial adaptational responses (Yim *et al.*, 2007; Fajardo and Martinez, 2008). A number of bacterial species, including major human pathogens, respond to the presence of sub-MIC levels of antibiotics with increased biofilm formation (Bisognano *et al.*, 1997; Rachid *et al.*, 2000; Blickwede *et al.*, 2004; Hoffman *et al.*, 2005; Linares *et al.*, 2006). In one report it was suggested

Accepted 9 May, 2009. *For correspondence. E-mail alexander.boehm@unibas.ch; Tel. (+41) 61 2672091; Fax (+41) 61 2672118. †Both authors contributed equally to this work.

that biofilm induction in response to antibiotic challenge is mediated by the intracellular signalling molecule cyclic di-GMP, a bacterial second messenger that is known to stimulate biofilm formation in a wide range of bacteria (Hoffman *et al.*, 2005; Cotter and Stibitz, 2007). However, knowledge about the molecular details underlying bacterial adaptation to sub-MIC of antibiotics in general, and biofilm induction in particular is scarce (Fajardo and Martinez, 2008). In patients undergoing antimicrobial chemotherapy, pathogens can be exposed to subinhibitory concentrations of drugs for several hours (Craig, 1998). Also, widespread usage of antibiotics in farm animals and agriculture might lead to increasing exposure of individuals to low levels of antibiotics (Smith *et al.*, 2002). Together, this suggests that biofilm formation and bacterial persistence can be a specific adaptation to antibiotic stress in the host. We sought to systematically analyse the effects of subinhibitory concentrations of antimicrobials on biofilm formation in order to define the cellular and molecular mechanisms involved in this phenomenon. As a model we chose an *E. coli* K-12 *csrA::Tn5* mutant strain (Romeo *et al.*, 1993; Timmermans and Van Melder, 2008) that forms biofilms under laboratory conditions. These biofilms rely entirely on the polysaccharide adhesin poly-GlcNAc (Wang *et al.*, 2004). Four proteins that reside in the cell envelope catalyse poly-GlcNAc biosynthesis and export. These include PgaA, which forms a pore across the periplasm and the outer membrane, and together with the N-acetyl-glucosamine deacetylase PgaB is required for export of the polymer (Itoh *et al.*, 2008). The glycosyltransferase PgaC resides in the inner membrane and catalyses poly-GlcNAc polymerization from the precursor UDP-GlcNAc. The role of PgaD is less clear, but it is known to be an inner membrane protein (Daley *et al.*, 2005) and is essential for poly-GlcNAc biosynthesis (Wang *et al.*, 2004; Itoh *et al.*, 2008). The *pga* genes are arranged in an operon, *pgaABCD*, which is negatively controlled on the mRNA level by the RNA binding protein CsrA (Wang *et al.*, 2005). CsrA activity is governed by a complex signal transduction cascade that controls the levels of two small regulatory RNAs (CsrB and CsrC), which sequester CsrA and thereby prevent CsrA activity (Suzuki *et al.*, 2006; Babitzke and Romeo, 2007). Poly-GlcNAc is utilized as an adhesin by a number of important bacterial human pathogens, including *Yersinia* (Bobrov *et al.*, 2008), *Staphylococcus* (Gotz, 2002) and *Bordetella* (Parise *et al.*, 2007). Importantly, a majority of clinical isolates of uropathogenic *E. coli* (UPEC) express poly-GlcNAc in the host environment, where it contributes to *in vivo* virulence (Cerca *et al.*, 2007). Likewise, the response regulator UvrY that controls the levels of CsrB and CsrC has been shown to be a virulence factor in a uropathogenic *E. coli*-based bladder infection model (Tomenius *et al.*, 2006). However, the host signals that

feed into the regulatory cascade controlling *pga* expression are unknown. Therefore, we chose the *csrA::Tn5* mutant as a biofilm model. This model system allows basal level expression of poly-GlcNAc and biofilm formation and thus represents a valid *in vitro* approximation of the situation in the host. Exploiting the simple biofilm readout provided by this strain in combination with the powerful genetic tools available for *E. coli* K-12, we set out to dissect the molecular mechanisms underlying biofilm induction by sub-MIC levels of antibiotics. We show that poly-GlcNAc-dependent biofilm formation is strongly induced by sublethal doses of all tested translation inhibitors. This effect is triggered by the ribosome itself and information about the ribosomal status is transmitted to the poly-GlcNAc machinery via the bacterial signalling molecule ppGpp. In addition, we show that poly-GlcNAc production and maximal biofilm formation require another bacterial signalling molecule, c-di-GMP. Together, these second messengers control biofilm formation by specifically regulating the cellular levels of two proteins of the poly-GlcNAc biosynthesis complex. Thus, our study identifies the sensory, signal transduction and output mechanisms underlying bacterial adaptation to antibiotic challenges.

Results

Translation inhibitors induce biofilm formation

To define the spectrum of compounds inducing a biofilm response, a comprehensive chemical library including more than 200 antimicrobials and related substances was screened. *csrA::Tn5* mutant cells were grown in microtiter plates containing tryptone broth (TB) medium supplemented with four different concentrations of each of the various antimicrobials. After 24 h, the optical density (cell density) was recorded, the planktonic phase was discarded, the wells were washed vigorously and the surface-attached biomass was quantified. The ratio of attached biomass divided by the cell density is a measure for biofilm formation (see *Experimental procedures*). As expected, the vast majority of antimicrobial substances displayed a progressive growth-inhibitory effect with increasing concentrations (Table S1). The presence of many different individual antibiotics, targeting a wide range of cellular processes, led to induction of biofilm. However, whereas most classes of antibiotics, e.g. the β -lactams or the quinolones, had no coherent effect on biofilm formation (some members of a group induced biofilm while others inhibited biofilm), all antibiotics that target the ribosome strongly induced biofilm formation in a concentration-dependent fashion (Table S1). Because of this striking pattern and the prominent role of translation inhibitors as anti-infectives, we decided to focus on this

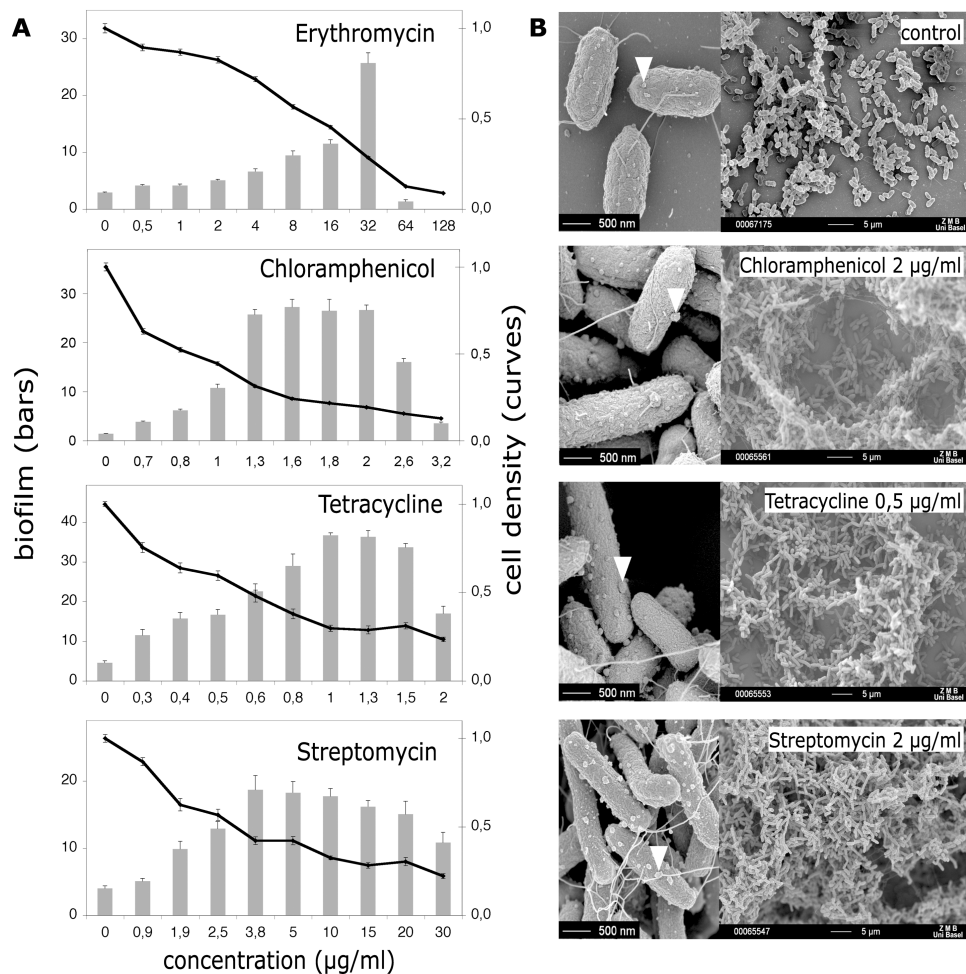


Fig. 1. Induction of biofilm formation by representative translation inhibitors.

A. *csrA::Tn5* cells were exposed to the indicated antibiotics for 24 h and their cell density and surface attachment was measured. Bars represent biofilm formation (surface-attached biomass divided by optical density of total cells) with standard errors of the mean. Biofilm values are indicated on the left *y*-axis. Curves represent relative optical density of total cells (optical density divided by the value of optical density in the absence of antibiotics) with standard errors. Values for normalized cell density are indicated on the right *y*-axis.

B. Scanning electron micrographs of biofilms. *csrA::Tn5* cells exposed to the indicated antibiotics are compared with a control without antibiotic. Scale bars are indicated. Arrows indicate cell surface-associated poly-GlcNAc spheres (see text).

group of antibiotics and to analyse the underlying molecular principles of biofilm induction. Towards this goal, four antibiotics representing the major chemical classes of translation inhibitors were tested. At increasing concentrations, all four drugs led to a strong increase of biofilm formation, with the strongest induction observed at concentrations that reduced cell density by 50–70% (Fig. 1A). As the antibiotics approached the MIC, biofilm formation rapidly declined, most likely as a consequence of a cumulative effect on cell growth.

To corroborate these findings we analysed the fine structure of the biofilms using scanning electron microscopy. In the absence of antibiotics, *E. coli* cells formed flat and fragile surface structures. Upon exposure to sub-MIC levels of translation inhibitors these developed into a thick, three-dimensional mesh of cells (Fig. 1B).

Filamentous appendages and spherical, knob-like structures were prominently visible on the cell surface (Fig. 1B). The filamentous structures, which were identified as flagella, did not contribute to antibiotic-induced biofilm formation (Fig. S1). In contrast, the knob-like surface structures, which are reminiscent of poly-GlcNAc-associated surface structures in *Staphylococcus epidermidis* or *Yersinia pestis* (Vuong *et al.*, 2004; Erickson *et al.*, 2008), correlated with biofilm formation and increased in size upon exposure to antibiotics (Fig. 1B). Likewise, cells grown in the presence of translation inhibitors displayed a stronger signal when probed with an antibody raised against poly-GlcNAc (Fig. S2). Strains with deletions in the poly-GlcNAc biosynthesis genes ($\Delta pgaABCD$) (Wang *et al.*, 2004) showed no biofilm formation or induction (Fig. 3A and B), failed to display the

knob-like surface structures (Fig. S3), and showed a background signal when probed with the poly-GlcNAc antibody (not shown). From this we concluded that the knob-like structures represent surface-exposed poly-GlcNAc and that antibiotic treatment induces biofilms through the upregulation of this amino-sugar polymer.

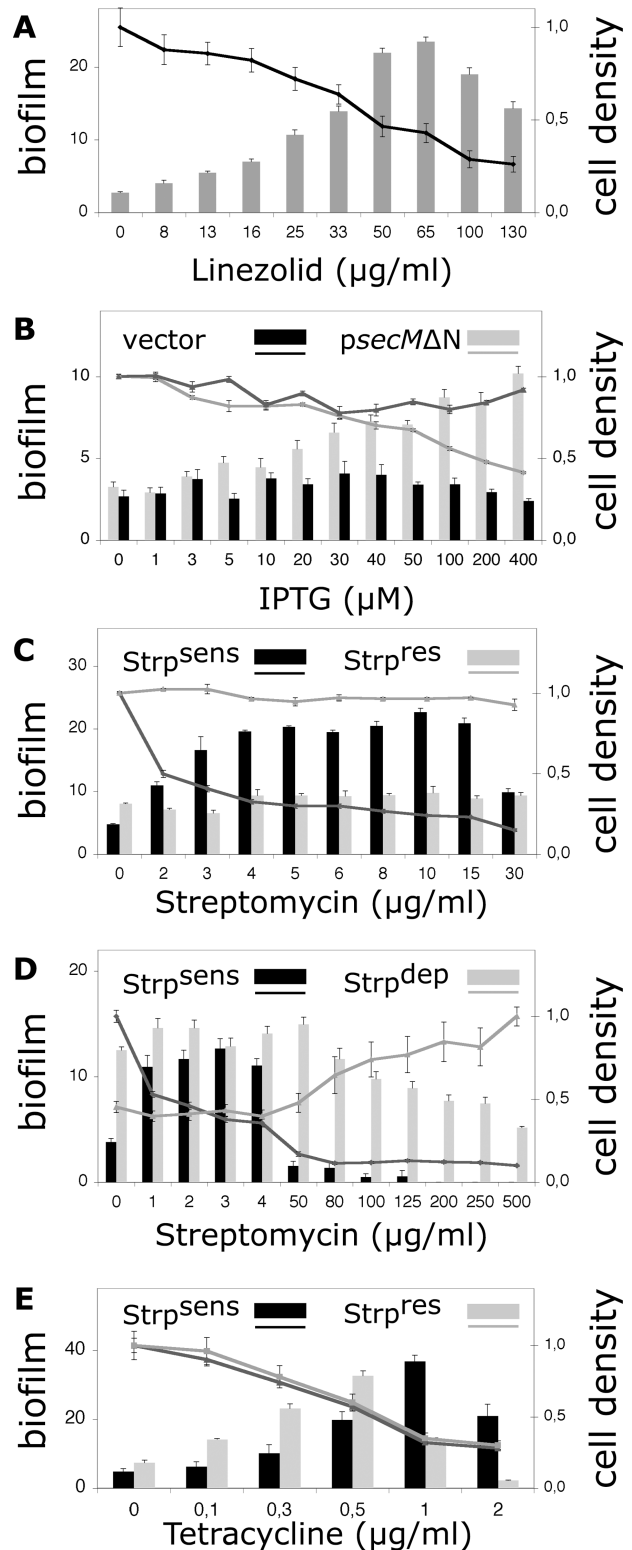
Translation interference induces biofilm formation

Next, we asked how the bacteria sense subinhibitory drug concentrations to induce biofilm formation. In principle, the chemicals *per se* could be perceived by one or several dedicated chemoreceptors. Alternatively, the drugs' effect(s) on ribosome functioning could constitute the signal leading to biofilm induction. The following observations support the latter, indirect mechanism. First, one would expect that potential chemoreceptors would only bind naturally occurring antibiotics (or derivatives thereof), but would not be able to sense artificial compounds that have been introduced only recently. However, the fully synthetic oxazolidinone antibiotic linezolid (Clemett and Markham, 2000) strongly induced biofilm formation (Fig. 2A). Second, to mimic a drug-induced drop in ribosome performance, we analysed an *E. coli* strain that produced a truncated version of SecM (*secMΔN*), which inhibits translation by jamming elongating ribosomes (Nakatogawa and Ito, 2002). Overexpression of *secMΔN* from a plasmid led to significant induction of biofilm formation, while an empty vector control showed no response (Fig. 2B). Similar effects were observed when different translation-targeting toxins (YoeB, MazE and RelE) were overproduced from plasmids (Fig. S4). Third,

mutant strains with drug-resistant ribosomes showed an altered biofilm induction behavior. A streptomycin-resistant strain with a point mutation in the gene *rpsL*, coding for the S12 protein of the small ribosomal subunit

Fig. 2. Translation interference leads to biofilm induction. In all panels, bars represent biofilm formation (surface-attached biomass divided by optical density of total cells) with standard errors of the mean. Biofilm values are indicated on the left *y*-axis. Curves represent relative optical density of total cells (optical density divided by the value of optical density in the absence of antibiotics) with standard errors. Values for normalized cell density are indicated on the right *y*-axis.

- A. The artificial translation inhibitor linezolid induces biofilm formation of a *csrA*::Tn5 strain.
 B. Jamming the ribosome by overproduction of SecMΔN induces biofilm formation. IPTG-mediated overproduction of a truncated version of SecM (grey) is compared with a vector control (black) in a *csrA*::Tn5 strain.
 C. Streptomycin-resistant mutants do not induce biofilm formation upon exposure to streptomycin. A streptomycin-resistant *csrA*::Tn5 *rpsL*(K43N) mutant (grey) is compared with its streptomycin-sensitive *rpsL*^{wt} ancestor (black).
 D. A streptomycin-dependent mutant displays biofilm induction with decreasing streptomycin concentrations. A streptomycin-dependent *csrA*::Tn5 *rpsL*(R54C P91L) mutant (grey) is compared with its streptomycin-sensitive *rpsL*^{wt} ancestor (black).
 E. A streptomycin-resistant mutant displays 'hypersensitive' biofilm induction in response to tetracycline. Normalized biofilm values of a streptomycin-resistant *csrA*::Tn5 *rpsL*(K43N) mutant (grey) and its streptomycin-sensitive *rpsL*^{wt} ancestor (black) are compared.



(Ozaki *et al.*, 1969), displayed no growth inhibition and showed no biofilm induction, even in the presence of high concentrations of streptomycin (Fig. 2C). In marked contrast, an *rpsL* mutant that *requires* the presence of high concentrations of streptomycin for optimal ribosome functioning (Timms and Bridges, 1993) showed induction of biofilm with *decreasing* concentrations of the drug (Fig. 2D). Thus, both classes of *rpsL* mutants showed a strict correlation between decreased ribosomal performance and increased biofilm formation. We also tested biofilm induction of the streptomycin-resistant *rpsL* mutant in response to tetracycline, which targets the ribosome in an RpsL-independent manner (Harms *et al.*, 2003). The *rpsL* mutant was 'hypersensitive' to tetracycline-mediated biofilm induction, with significantly higher induction values at low drug concentrations as compared with the *rpsL* wild-type control (Fig. 2E). Although the molecular details of this 'hypersensitive' induction phenomenon are unclear, the synergistic effects of the *rpsL* mutation and tetracycline argue that at least two features of ribosomal functioning influence biofilm formation. Altogether, these findings strongly link ribosomal performance to biofilm induction and suggest that at sub-MIC concentrations of translation inhibitors, altered translation activity is responsible for biofilm induction.

The diguanylate cyclase YdeH is required for full biofilm upregulation in response to translation inhibition

Next, we investigated how information about the status of the ribosome is communicated to the poly-GlcNAc system in the cell envelope. Recently, an almost ubiquitous bacterial intracellular signalling molecule – bis-(3'-5')-cyclic di-GMP (c-di-GMP) – was identified as a key factor controlling biofilm formation in pathogenic and non-pathogenic bacteria (Jenal and Malone, 2006; Tamayo *et al.*, 2007). The cellular levels of c-di-GMP are controlled by two antagonistic enzyme families, diguanylate cyclases (DGCs) harbouring a GGDEF domain to produce c-di-GMP; and phosphodiesterases harbouring an EAL domain to degrade the compound (Jenal and Malone, 2006). To test if biofilm formation in our model system responds to perturbations of the cellular c-di-GMP pool, c-di-GMP signalling proteins were overproduced. Ectopic expression of the *Caulobacter crescentus* DGC *dgcA* induced biofilm formation and led to a marked increase of both number and size of the knob-like poly-GlcNAc surface structures (Fig. 3A and B). A strain lacking the poly-GlcNAc genes showed no biofilm formation and no poly-GlcNAc-associated surface structures, even when DgcA was overproduced (Fig. 3A and B). Conversely, ectopic expression of either of two predicted c-di-GMP-specific phosphodiesterase genes from *E. coli*, *yliE* and *yjcC*, strongly reduced biofilm formation (Fig. 3A). The latter result is consistent with the

observed reduction of biofilm formation in a *csrA::Tn5* strain upon overexpression of the phosphodiesterase *yjhH* (Suzuki *et al.*, 2006). These findings strongly support a model where c-di-GMP signalling controls poly-GlcNAc production and thereby biofilm formation in *E. coli*.

According to the SMART database *E. coli* K-12 possesses 29 potential c-di-GMP-specific diguanylate cyclases or phosphodiesterases (Letunic *et al.*, 2006). To identify components involved in poly-GlcNAc regulation, 29 mutant strains were constructed, each carrying a deletion of one of the respective genes. Analysis of this mutant pool identified a single strain with significantly altered biofilm formation (Fig. S5). This mutant had a deletion in the *ydeH* gene, which encodes a soluble GGDEF domain protein with a short 117-residue N-terminal domain of unknown function. The $\Delta ydeH$ mutant not only showed a significant reduction in surface attachment (see also Fig. S3C at zero $\mu\text{g ml}^{-1}$ streptomycin) but also a very weak signal when probed with anti-poly-GlcNAc antibodies (Fig. S2). A similar phenotype was observed for a strain harbouring a YdeH active site mutant protein (GGEEF \rightarrow GGQEF) (Fig. 4A). The attachment defect of the $\Delta ydeH$ strain was fully restored upon expression of the heterologous DGC DgcA (Fig. 4B).

The *ydeH* gene was recently identified as a member of the CsrA regulon (Jonas *et al.*, 2008). Consistent with this, YdeH protein levels were higher in a *csrA::Tn5* mutant compared with a *csrA*⁺ control (Fig. 3D). Jonas *et al.* (2008) also provided genetic data indicating that YdeH is a DGC. To test if YdeH possesses DGC activity *in vitro*, a hexahistidine-tagged version of the protein was purified by Ni-affinity and subsequent size exclusion chromatography. Based on static light scattering measurements the protein eluted from the gel filtration column as a stable dimer at a concentration of 2 μM (not shown). Biochemical characterization of YdeH revealed kinetic properties similar to other bona fide DGCs. GTP was converted into c-di-GMP (Fig. S6) with a specific activity of approximately 1.6 ± 0.2 ($\mu\text{M c-di-GMP}$) min^{-1} ($\mu\text{M YdeH}$)⁻¹ and a K_m for GTP of about 17 ± 3 μM (Fig. 4C). The enzyme was subject to product inhibition with a relatively large K_i for c-di-GMP of about 44 ± 9 μM , but exhibited residual activity even at high c-di-GMP concentrations (Fig. 4D). Together, these data strongly argue that YdeH is a DGC and that the *ydeH* mutant biofilm phenotype is caused by a reduction of cellular c-di-GMP levels.

Importantly, exposure to aminoglycosides, including streptomycin (Fig. 3C), kanamycin (Fig. S7), tobramycin, dihydrostreptomycin, apramycin, gentamicin, sisomicin or amikacin (data not shown), completely failed to induce biofilm of the $\Delta ydeH$ mutant strain. This suggested that YdeH is not only required for basal level surface attachment, but is also involved in aminoglycoside-mediated induction of biofilm formation. This response is not medi-

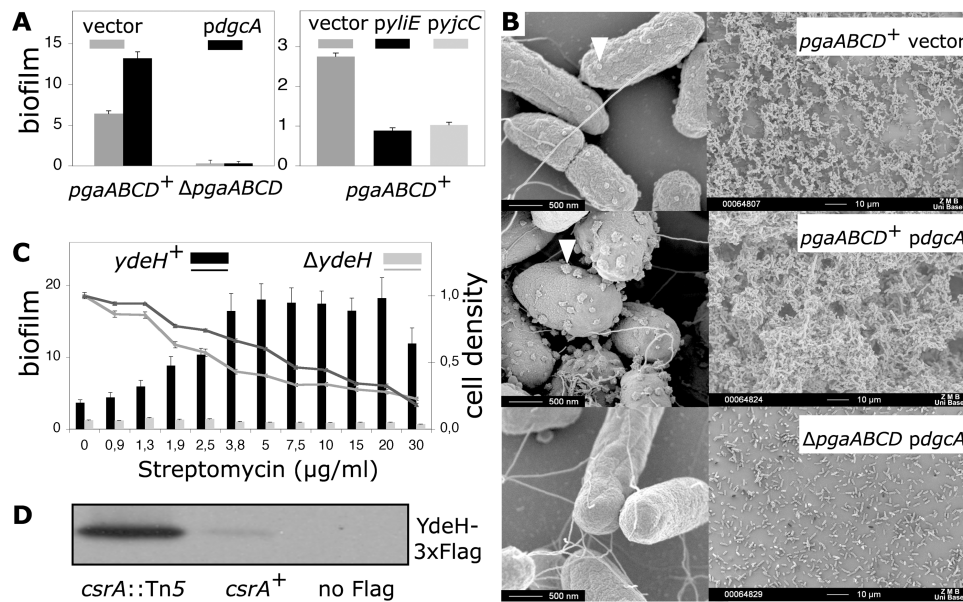


Fig. 3. Poly-GlcNAc-mediated biofilm formation is modulated by c-di-GMP.

A. Left: Biofilm formation upon plasmid-mediated overexpression of the foreign DGC *dgcA* (black bars) is compared with a vector control (grey bars) in the indicated *csrA*::Tn5 strain backgrounds. Error bars are standard errors of the mean. Right: Biofilm formation upon plasmid-mediated overproduction of two different c-di-GMP-specific phosphodiesterases (*yliE* and *yjcC*) is compared with a vector control in a *csrA*::Tn5 background. Error bars are standard errors of the mean.

B. Scanning electron micrographs of biofilms. A *csrA*::Tn5 strain overexpressing the foreign DGC *dgcA* (middle) is compared with a vector control (top) and to a strain overexpressing *dgcA* but lacking the *pga* genes (bottom). Two different magnifications are shown. Scale bars are indicated. Arrows indicate characteristic poly-GlcNAc-associated surface structures. Such structures were never observed on the surface of cells lacking the *pgaABCD* genes (see also Fig. S3).

C. The GGDEF domain protein YdeH is essential for aminoglycoside-mediated induction of biofilm formation. A *csrA*::Tn5 $\Delta ydeH$ mutant (grey) is compared with its *ydeH*⁺ ancestor (black). Bars represent biofilm formation (surface-attached biomass divided by optical density of total cells) with standard errors of the mean. Biofilm values are indicated on the left y-axis. Curves represent relative optical density of total cells (optical density divided by the value of optical density in the absence of antibiotics) with standard errors. Values for normalized cell density are indicated on the right y-axis.

D. YdeH protein levels are controlled by CsrA. Western blots of strains carrying a C-terminal 3xFlag-tagged version of YdeH are shown. Relevant genotypes are indicated. Please note the presence of a faint band for the *csrA*⁺ sample as compared with a control lacking the 3xFlag epitope.

ated through upregulation of *ydeH* expression, as YdeH protein levels were unaltered in the presence of sub-MIC concentrations of streptomycin or other antibiotics (data not shown). In contrast to aminoglycosides, addition of tetracycline or chloramphenicol still led to biofilm induction of the $\Delta ydeH$ mutant, although at a much lower level compared with the *ydeH*⁺ strain (Fig. S7). Thus, YdeH is essential for biofilm induction by aminoglycosides and contributes to the response to other classes of translation inhibitors. Although the molecular details underlying the differential requirement of YdeH for the response to different drugs are not clear, aminoglycosides are known to evoke a different adaptational response from ribosomes as compared with tetracycline or chloramphenicol (VanBogelen and Neidhardt, 1990).

SpoT-mediated reduction of ppGpp triggers biofilm upregulation in response to translation inhibition

Because the $\Delta ydeH$ mutant showed residual biofilm induction in response to tetracycline or chloramphenicol,

we reasoned that an additional signal transduction mechanism must exist to respond to non-aminoglycoside inhibitors. A candidate for such a redundant function is the signalling molecule guanosine-bis 3', 5'(diphosphate) (ppGpp). ppGpp is involved in the response to nutrient starvation-induced translational stress in bacteria (Cashel *et al.*, 1996) and has been previously linked to biofilm formation in *E. coli* and *Campylobacter jejuni* (Balzer and McLean, 2002; McLennan *et al.*, 2008). In *E. coli*, the cellular ppGpp concentration is controlled by two enzymes, RelA and SpoT (Ramagopal and Davis, 1974; Xiao *et al.*, 1991). RelA has GDP diphosphokinase activity and uses ATP and GDP to produce ppGpp. SpoT is bifunctional and comprises both diphosphokinase and ppGpp hydrolase activity. To test whether RelA or SpoT are involved in biofilm formation mutants lacking either RelA ($\Delta relA$) or RelA and SpoT ($\Delta relA \Delta spoT$) were analysed. Whereas the $\Delta relA$ single mutant exhibits (SpoT-derived) residual levels of ppGpp, the double mutant is completely devoid of the signalling compound and is therefore also referred to as ppGpp⁰ mutant (Xiao

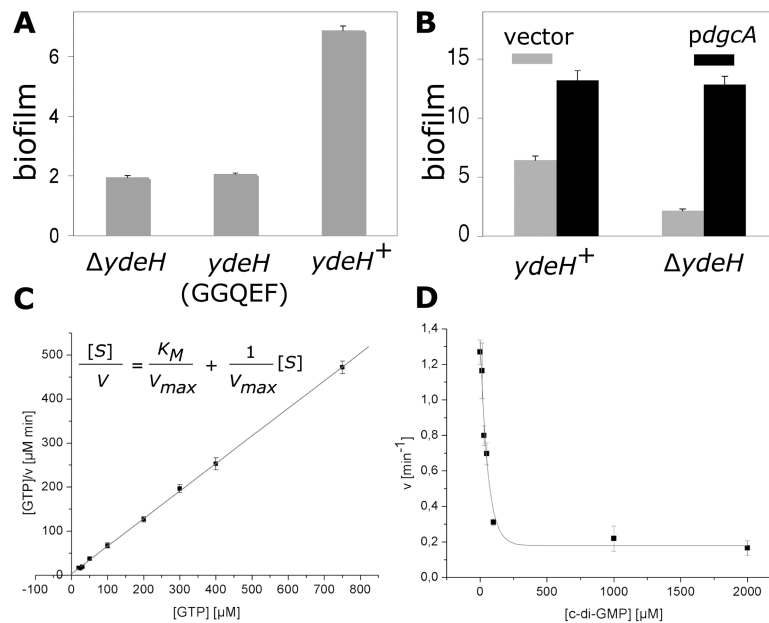


Fig. 4. YdeH is a DGC.

A. A *ydeH* active site mutation behaves like a null allele. Biofilm formation of a *csrA::Tn5 ydeH⁺* strain is compared with a *csrA::Tn5 ydeH* mutant and a *csrA::Tn5* mutant harbouring a point mutation in *ydeH*, leading to a defective active site motif (GGEEF to GGQEF).

B. A foreign DGC can compensate the biofilm defect of a *ydeH* mutant. Biofilm formation of a *csrA::Tn5 ydeH⁺* ancestor in the presence (black) or absence (grey) of a plasmid encoding for the foreign DGC DgcA.

C. YdeH is a bona fide DGC. Rate of c-di-GMP formation as a function of substrate (GTP) concentration fitted with a simple Michaelis–Menten model (see equation) in a Hanes representation. YdeH was present at 2 μM . Error bars are standard deviations.

D. The DGC activity of YdeH is product-inhibited. V_0 of c-di-GMP production is plotted over the c-di-GMP concentration present at the start of the experiment. YdeH was present at 2 μM . Error bars are standard deviations. Please note that product inhibition was found to be independent of the substrate (GTP) concentration and must therefore be allosteric (data not shown).

et al., 1991). As shown in Fig. 5A, the $\Delta relA$ mutant displayed slightly higher relative surface attachment as compared with the isogenic *relA⁺* strain. In contrast, biofilm formation was strongly increased in the $\Delta relA \Delta spoT$ double mutant, with biofilm values reaching levels similar to those observed upon antibiotic induction of a *relA⁺ spoT⁺* strain. Increased attachment of the $\Delta relA \Delta spoT$ mutant was accompanied by an upregulation of poly-GlcNAc-associated surface structures (Fig. 5C, Fig. S2) and was entirely dependent on the genes encoding the poly-GlcNAc synthesis machinery (data not shown). Strikingly, increased biofilm formation of the ppGpp⁰ mutant was also fully dependent on the presence of YdeH (Fig. 5A), arguing that c-di-GMP and ppGpp together control biofilm formation through poly-GlcNAc synthesis. This notion is further supported by the finding that the increased biofilm formation of a ppGpp⁰ strain was diminished by overproduction of either of two c-di-GMP-specific phosphodiesterases (Fig. 5B). YdeH protein levels were not altered in a ppGpp⁰ strain, indicating that ppGpp does not influence biofilm formation by modulating *ydeH* expression (Fig. 5D).

To determine whether SpoT-derived ppGpp synthase or hydrolase activity is responsible for biofilm control, we

introduced mutations in *spoT* that specifically affected one of the two enzymatic activities by replacing invariant residues in the enzyme's ppGpp synthase (Asp259) or hydrolase (Asp73) active centres (Hogg *et al.*, 2004). The $\Delta relA spoT(D259N)$ synthase mutant showed strongly increased biofilm formation, similar to the $\Delta relA \Delta spoT$ strain (Fig. 5A). In contrast, the $\Delta relA spoT(D73N)$ hydrolase mutant, which constitutively produces ppGpp, showed moderate biofilm formation, comparable to the *relA⁺ spoT⁺* ancestor. Importantly, both the ppGpp⁰ and the *spoT* hydrolase mutants were severely impaired in biofilm induction in response to chloramphenicol, tetracycline or streptomycin. The already very high biofilm level of the $\Delta relA \Delta spoT$ (ppGpp⁰) mutant was only weakly induced with translation inhibitors (Fig. 5E, Fig. S8A). This weak induction was accompanied by a marginal increase of the attached biomass (biofilm values not normalized to cell density) and is thus mainly based on a decreased antibiotic susceptibility of the cells in the biofilm compared with the cells in the planktonic phase (Fig. S9A, see also *Experimental procedures*). Likewise, the $\Delta relA spoT(D73N)$ hydrolase mutant was unable to respond to translation inhibitors with full biofilm induction (Fig. S9B). Importantly, *relA* does not appear to play a role in the

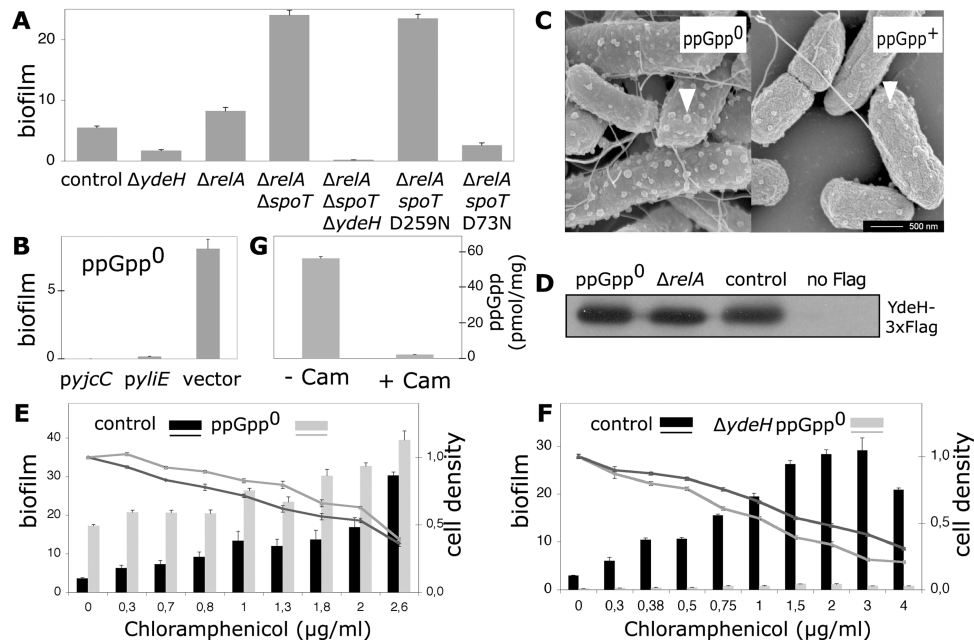


Fig. 5. ppGpp controls biofilm formation in a c-di-GMP- and poly-GlcNAc-dependent fashion.

A. Bars represent biofilm values with standard errors of the mean. All strains are *csrA::Tn5*. Relevant genotypes are indicated. The *spoT(D259N)* allele confers a ppGpp synthase-negative, ppGpp hydrolase-positive phenotype. The *spoT(D73N)* allele confers a ppGpp synthase-positive, ppGpp hydrolase-negative phenotype. Note that in the presence of a wt *relA* allele, *spoT* cannot be deleted because accumulation of ppGpp is toxic (Cashel *et al.*, 1996).

B. Bars represent normalized biofilm values. A *csrA::Tn5* $\Delta relA$ $\Delta spoT$ (ppGpp⁰) strain harbouring plasmids encoding for c-di-GMP-specific phosphodiesterases (YliE, YjC) or a control plasmid are shown in comparison.

C. Scanning electron micrographs of a *csrA::Tn5* $\Delta relA$ $\Delta spoT$ (ppGpp⁰) strain (left) and a *relA*⁺ *spoT*⁺ control (right) are compared. Arrows indicate surface structures associated with poly-GlcNAc.

D. ppGpp does not influence YdeH protein levels. Western blot of strains harbouring a 3xFlag-tagged version of YdeH are shown. All strains are *csrA::Tn5*. Relevant genotypes are indicated.

E. A ppGpp⁰ strain shows aberrant biofilm induction in response to chloramphenicol. A *csrA::Tn5* $\Delta relA$ $\Delta spoT$ strain (grey) is compared with its *relA*⁺ *spoT*⁺ ancestor (black). Bars represent biofilm formation with standard errors of the mean. Biofilm values are indicated on the left y-axis. Curves represent relative optical density of total cells with standard errors. Values for normalized cell density are indicated on the right y-axis.

F. Biofilm formation of a ppGpp⁰ $\Delta ydeH$ strain is diminished and cannot be induced by chloramphenicol. A *csrA::Tn5* $\Delta relA$ $\Delta spoT$ $\Delta ydeH$ strain (grey) is compared with its *relA*⁺ *spoT*⁺ *ydeH*⁺ ancestor (black). Bars represent biofilm formation with standard errors of the mean. Biofilm values are indicated on the left y-axis. Curves represent relative optical density of total cells with standard errors. Values for normalized cell density are indicated on the right y-axis.

G. Treatment with chloramphenicol leads to reduction of the cellular ppGpp pool. Bars indicate cellular ppGpp levels (pmol mg⁻¹ dry weight) of a *csrA::Tn5* strain that has been grown in the presence or absence of chloramphenicol (1.5 $\mu\text{g ml}^{-1}$). Values are derived from HPLC measurements of ppGpp in cell extracts (see *Experimental procedures*).

antibiotic induction phenomenon: a $\Delta relA$ strain shows slightly higher basal biofilm values compared with the *relA*⁺ control strain and is not impaired in biofilm induction when challenged with translation inhibitors (Fig. S10). Altogether, these findings suggest that ppGpp inhibits biofilm and that the SpoT hydrolase activity is critical for induction of *E. coli* surface attachment. The data also support a model where sub-MIC concentrations of translation inhibitors cause a SpoT-dependent decrease of the cellular ppGpp pool, leading to the derepression of poly-GlcNAc production and biofilm induction. This was confirmed by the finding that cellular levels of ppGpp were indeed strongly reduced in the presence of chloramphenicol (Fig. 5G). This result is fully consistent with a series of reports demonstrating that cells exposed to translation

inhibitors display markedly decreased levels of ppGpp, even under conditions that would normally lead to a stringent response (Gallant *et al.*, 1972; Muto *et al.*, 1975; Baracchini and Bremer, 1988; Hernandez and Bremer, 1990; Murray and Bremer, 1996). Together, this suggests that SpoT-mediated reduction of ppGpp is necessary for maximal biofilm induction. However, drug-induced biofilm formation was not completely abolished in a ppGpp⁰ mutant (Fig. 5E), arguing that translation inhibition does not influence biofilm formation solely through ppGpp reduction. In agreement with this, a strain lacking *relA*, *spoT* and *ydeH* showed no significant biofilm formation, even when challenged with optimal concentrations of chloramphenicol or tetracycline (Fig. 5F, Fig. S8B). In summary, these data suggest that the guanosine-based

second messengers c-di-GMP and ppGpp together control biofilm formation in response to translational stress.

ppGpp and c-di-GMP post-transcriptionally regulate the levels of PgaA and PgaD

To address the molecular basis of c-di-GMP- and ppGpp-mediated control of poly-GlcNAc synthesis, we sought to test if either of these factors influences the expression of the *pga* genes. To be able to monitor Pga components, we constructed 3xFlag-tagged versions of PgaA and PgaD, which are encoded by the most proximal and most distal genes of the *pga* operon. Surprisingly, levels of PgaD, but not PgaA, were controlled by c-di-GMP. Deletion of the DGC coding gene *ydeH* or overproduction of the phosphodiesterase YjcC reduced PgaD levels (Fig. 6A), while ectopic expression of the heterologous DGC *dgcA* led to strongly elevated levels of PgaD, both in the presence or absence of *ydeH* (Fig. 6A). In contrast to PgaD, PgaA levels were not altered in a mutant lacking the DGC YdeH (Fig. 6A). Conversely, cellular levels of PgaA, but not PgaD, were controlled by ppGpp. Whereas PgaA levels were strongly increased in a strain unable to produce ppGpp, PgaD levels were unaltered under these conditions (Fig. 6A). These data argue that ppGpp negatively regulates PgaA levels, while YdeH through its product c-di-GMP stimulates PgaD protein levels. Next, we tested if translation inhibition influences PgaA and PgaD levels. PgaD showed a small but reproducible increase in response to tetracycline (Fig. 6B) or chloramphenicol (data not shown). Surprisingly, this increase was not dependent on YdeH, as PgaD levels still increased under these conditions in a strain lacking YdeH (Fig. 6B). In contrast, PgaA levels were strongly induced in response to tetracycline in the control strain, while they were constitutively upregulated and insensitive to the drug in a mutant unable to produce ppGpp (Fig. 6C). Because *pgaD* and *pgaA* are encoded in one operon, but their cellular levels were influenced differentially by c-di-GMP and ppGpp, it appeared likely that the second messengers influence the PgaA and PgaD levels post-transcriptionally. To test this idea, a translational *lacZ* fusion to the *pga* promoter, including the 5' untranslated region of the *pga* operon, was used to measure *pga* promoter activity in response to perturbations of ppGpp or c-di-GMP levels, or in response to translation inhibitors. As expected, β -galactosidase activity of the *pgaA-lacZ* assay strain was dependent on the transcription factor NhaR, known to be essential for *pga* transcription (Goller *et al.*, 2006), and was negatively controlled by CsrA, which is known to inhibit *pga* operon translation (Wang *et al.*, 2005) (Fig. S11). However, neither deletion of *ydeH* nor overexpression of the DGC *dgcA* led to significant

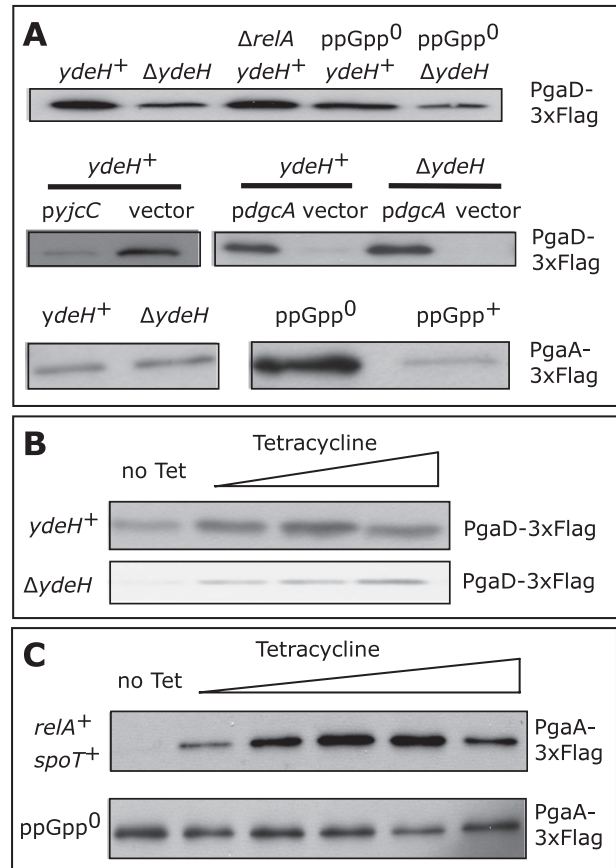


Fig. 6. Control of the PgaA and PgaD protein levels by ppGpp, c-di-GMP and tetracycline.

A. PgaD levels are controlled by c-di-GMP, whereas PgaA levels are controlled by ppGpp. Western blots of strains harbouring a 3xFlag-tagged version of PgaD or PgaA (indicated on the right side of each panel). All strains are *csrA::Tn5*. Relevant genotypes are indicated. *pdgCA* and *pyjC* represent overexpression of a foreign DGC or of a phosphodiesterase from *E. coli* respectively. B. Tetracycline induces PgaD protein levels. PgaD protein levels are compared by Western blotting at increasing tetracycline concentrations in *csrA::Tn5 ydeH⁺* (top) and a *csrA::Tn5 ΔydeH* (bottom) strain. C. Tetracycline induces PgaA protein levels. PgaA protein levels are compared by Western blotting at increasing tetracycline concentrations in a *csrA::Tn5 ppGpp⁺* (top) and a *csrA::Tn5 ppGpp⁰* (bottom) strain.

alteration of the LacZ activity (Fig. S11 and data not shown). Likewise, deletion of *relA* and *spoT* or exposure to subinhibitory concentrations of translation inhibitors did not change the specific LacZ activity (Fig. S11 and data not shown). Thus, none of these parameters has any measurable influence on the *pga* promoter or the *pga* 5' untranslated region. To corroborate the above findings we constructed a complementary strain in which the native *pga* promoter was replaced with the L-arabinose-dependent P_{ara} promoter. The resulting strain harbours an *araB-pgaA* translational fusion with the promoter and the 5' untranslated region of the *pga* operon being replaced

with the corresponding regions of the *araBAD* operon. As expected, biofilm formation of strains harbouring such an *araB-pga* fusion is dependent on the presence of L-arabinose in the medium, but independent of *nhaR* and *csrA* (data not shown). Biofilm formation of an *araB-pga* (*csrA*⁺) strain was induced by tetracycline, chloramphenicol or streptomycin in an L-arabinose-dependent fashion (Fig. S12). This corroborates the above notion that poly-GlcNAc-dependent biofilm induction by translation inhibitors is independent of the *pga* promoter and the 5' untranslated region. Moreover, because the *araB-pga* (*csrA*⁺) strain shows strong biofilm induction in response to translation inhibitors (Fig. S12), it can be ruled out that antibiotic induction depends on the presence of the *csrA::Tn5* mutant allele. Together, these data demonstrate that induction of poly-GlcNAc-dependent biofilm formation by subinhibitory concentrations of ribosome inhibitors involves upregulation of at least two components of the Pga machinery, PgaD and PgaA. Our data further indicate that induction of PgaA is mediated by ppGpp signalling, while c-di-GMP specifically influences cellular levels of PgaD. Because upregulation of both proteins is independent of the promoter and the untranslated leader sequence of the *pga* message, drug-mediated control takes place on the post-transcriptional level.

Discussion

With their potential to withstand antimicrobial therapy and the host immune system, bacterial biofilms represent a major problem for human health. Several reports indicated that the presence of certain antibiotics influences bacterial biofilm formation (Rachid *et al.*, 2000; Hoffman *et al.*, 2005; Linares *et al.*, 2006). However, in these studies only a few selected antibiotics were tested and the mechanistic details remained largely unexplored. To analyse this phenomenon in a more comprehensive way and to decipher the underlying cellular and molecular mechanisms, we used an established *E. coli* laboratory biofilm model system. The model strain harbours a *csrA::Tn5* transposon insertion mutation causing derepression of the primary surface adhesin poly-GlcNAc (Romeo *et al.*, 1993; Wang *et al.*, 2004; Itoh *et al.*, 2008). This system was chosen because it allowed the employment of a commercially available comprehensive chemical library – the Biolog system (Bochner *et al.*, 2001), which is ideally suited for use with *E. coli* K-12. The relevance of our model system is underscored by recent reports demonstrating that uropathogenic *E. coli* form biofilms and express poly-GlcNAc during host colonization (Anderson *et al.*, 2004; Cerca *et al.*, 2007). Also, CsrA homologues from a variety of pathogenic bacteria have been shown to be involved in host–pathogen interaction (Lucchetti-Miganeh *et al.*, 2008).

When grouped according to their mode of action, it became obvious that all translation inhibitors induced biofilm formation. The few exceptions (see Table S1) most likely failed to induce biofilm formation because the screening strain encodes a resistance factor for kanamycin and closely related aminoglycosides, or because the drug concentrations present in the Biolog plates were outside of the effective range. Other classes of antibiotics, e.g. compounds targeting cell wall biosynthesis or gyrase, showed an indistinct picture with some representatives inducing biofilms (e.g. cefotaxime, enoxacin, see Table S1), while others inhibited biofilm (e.g. cefmetazole, novobiocin, see Table S1). In this study, we focused on representatives of the major classes of translation inhibitors because they constitute one of the biggest groups of antibiotics, are of great clinical relevance and, as a group, behaved very homogeneously in our initial screening.

In principle, cells could sense translation inhibitors directly via dedicated receptors or indirectly through their effect on ribosomal function. Several observations make a strong case for the latter, indirect mechanism. First, for all substances tested, biofilm upregulation correlated with a progressive effect on cell growth. Second, linezolid, a fully synthetic translation inhibitor effectively stimulated biofilm formation. Third, experiments with *secMΔN* and ribosome-specific toxins confirmed that interference with ribosome functioning can induce biofilm formation independently of the presence of antibiotics. Fourth, mutations in *rpsL* that lead to streptomycin-insensitive ribosomes completely abolished streptomycin-mediated biofilm induction, while streptomycin-dependent mutants induced biofilm with decreasing streptomycin concentrations. Interestingly, although blind to streptomycin induction, *rpsL* mutants displayed a higher basal level of biofilm formation as compared with the streptomycin-sensitive strains (Fig. 2C and E). Streptomycin-resistant *rpsL* mutants are known to exhibit 'restrictive' or hyperaccurate translation (Bilgin *et al.*, 1992). It is possible that ribosome hyperaccuracy might contribute to biofilm induction. However, because most other conditions that were shown here to induce biofilms are not linked to hyperaccurate ribosomes, the mechanisms involved might be more complex and the exact nature of the signal remains unclear.

Several experiments suggested that the signal emanating from drug-affected ribosomes stimulates biofilm formation through upregulation of the cell surface-exposed poly-GlcNAc adhesin. The presence of the *pga* genes was absolutely essential for biofilm formation under all conditions tested and poly-GlcNAc itself, as well as components of the Pga machinery were upregulated when cells were challenged with translation inhibitors. While scanning EM demonstrated that Pga-associated surface structures increased under inducing conditions, these

experiments failed to provide evidence for the upregulation of other cell surface structures like pili or fimbriae. This does not rule out that additional factors that were not visualized by EM contribute to the observed biofilm induction. Although flagella are involved in biofilm formation in a different *E. coli* strain, they did not play a role in the induction phenomenon (Pratt and Kolter, 1998).

How is the information about translation performance relayed from ribosomes to the Pga machinery? The second messenger c-di-GMP was considered a good candidate because of its implication in biofilm control in a wide range of bacteria (Jenal and Malone, 2006) and because the *pga* operon is linked to and co-regulated with the *ycdT* gene, encoding a DGC (Jonas *et al.*, 2008). While biofilm formation was unaffected in a strain lacking YcdT in the presence and absence of translation inhibitors (Fig. S5 and data not shown) (Wang *et al.*, 2005), a systematic analysis of all potential genes involved in the turnover of c-di-GMP in *E. coli* revealed that the DGC YdeH is essential for aminoglycoside-mediated biofilm induction and is involved in the chloramphenicol- and tetracycline-mediated response. YdeH, via its product c-di-GMP, specifically upregulates poly-GlcNAc and the levels of at least one Pga component, PgaD. The underlying mechanism of this regulation is unclear. However, the observation that upregulation of PgaD in the presence of translation inhibitors is independent of YdeH (Fig. 6B) suggests that c-di-GMP-dependent stimulation of PgaD is merely a precondition for full biofilm induction by antibiotics and that c-di-GMP signalling is not the main inducing principle.

Conversely, the direct involvement of ppGpp signalling in antibiotic-mediated biofilm induction is supported by a number of observations. First, ppGpp inhibits poly-GlcNAc-dependent biofilm formation, and strains with lesions in ppGpp signalling proteins show aberrant biofilm induction. Second, surface-exposed poly-GlcNAc as well as PgaA protein levels are negatively controlled by ppGpp. Third, the already derepressed PgaA levels in a ppGpp⁰ strain cannot be induced further by tetracycline. Fourth, treatment of *E. coli* cells with subinhibitory concentrations of chloramphenicol results in reduced levels of ppGpp. Because basal biofilm formation as well as biofilm induction by antibiotics is similar in a $\Delta relA$ mutant and the *relA*⁺ ancestor, reduction of the ppGpp pool in response to drug-elicited translational stress must be mediated by SpoT. These data support a model where in response to partial inhibition of ribosome functioning, a SpoT-mediated reduction of ppGpp leads to the upregulation of Pga components and increased production of poly-GlcNAc.

It remains unclear which parameters of ribosome function are measured and linked to SpoT activity. Although it is well documented that the ribosome or ribosome-coupled factors can function as sensory devices (VanBogelen and

Neidhardt, 1990), a direct association of SpoT with the ribosome is controversial (Gentry and Cashel, 1995; Potrykus and Cashel, 2008). However, based on recent reports one cannot rule out the possibility that under certain conditions SpoT associates with the ribosome (Wout *et al.*, 2004). Possibly, translation inhibitors influence the GTP hydrolysis rate of ribosome-associated GTPases, which in turn might govern the balance between SpoT-mediated ppGpp synthesis and hydrolysis (Jiang *et al.*, 2007). At first sight, the notion that slow growth of *E. coli* in the presence of antibiotics results in reduced levels of ppGpp appears at odds with a central dogma of ppGpp signalling, which inversely correlates ppGpp concentration with cell division rate (Cashel *et al.*, 1996). Nevertheless, a rapid and strong decrease of the cellular ppGpp pool in response to treatment with translation inhibitors is well documented in the literature (Gallant *et al.*, 1972; Muto *et al.*, 1975; Baracchini and Bremer, 1988; Hernandez and Bremer, 1990; Murray and Bremer, 1996). Furthermore, global transcription analysis of *relA*⁻ or *relA*⁺ cells exposed to subinhibitory concentrations of the translation inhibitor puromycin (a strong inducer of biofilm, see Table S1) revealed a pattern that can be characterized as an inverse stringent response, e.g. repression of RpoS-dependent genes and amino acid biosynthesis genes and induction of ribosomal genes (Sabina *et al.*, 2003). It has been known for a long time that ppGpp⁰ mutants display a very distinctive physiology, but little information is available about environmental conditions that might lead to a reduction of the cellular ppGpp pool (Xiao *et al.*, 1991; Cashel *et al.*, 1996; Traxler *et al.*, 2008). Our data open up the possibility that the physiology of ppGpp⁰ cells represents a specific adaptation to ribosomal stress conditions that do *not* originate from nutritional stress or a shortage of charged tRNA species. We propose that ppGpp signalling is involved in the decision between two mutually exclusive adaptational programmes; nutrient starvation leads to an increase of the cellular ppGpp pool and evokes a stringent response, while ribosomal stress caused by the presence of translation inhibitors diminishes the cellular ppGpp pool and induces poly-GlcNAc-dependent biofilm formation. In this context it should be noted that the formation of a different type of *E. coli* biofilm based on curli fimbriae and cellulose expression might actually require elevated levels of ppGpp. This requirement is based on ppGpp dependence of *rpoS* expression, which in turn is instrumental for curli and cellulose production (Lange *et al.*, 1995; Weber *et al.*, 2006).

The exact molecular mechanism through which ppGpp and c-di-GMP control biofilm formation, in particular the cellular receptors that bind these second messengers, remain to be elucidated. The fact that *pgaA* and *pgaD* are encoded in the same operon, together with the finding that PgaA levels are controlled by ppGpp but not by c-di-GMP,

while PgaD levels are controlled by c-di-GMP but not by ppGpp, argues for post-transcriptional regulation. This idea is strongly supported by the finding that the *pga* promoter and 5' untranslated region are dispensable for antibiotic-mediated biofilm induction (Fig. S12). In addition, neither the *pga* promoter nor the 5' untranslated region of the *pga* message appear to respond to perturbations of c-di-GMP levels, ppGpp levels or to the presence of translation inhibitors (Fig. S11). Further support for a post-transcriptional mechanism comes from the finding that DksA, a factor known to enhance the effects of ppGpp on transcription is not involved in biofilm induction by translation inhibitors (data not shown). Irrespective of the molecular mechanisms, the observation that strong biofilm formation of a ppGpp⁰ strain is fully dependent on the presence of YdeH (Fig. 5A) argues for a model where the effect of the two signalling molecules is not merely additive. Instead, it appears that maximal poly-GlcNAc expression depends on the exact ratio between ppGpp and c-di-GMP. It is noteworthy that c-di-GMP and ppGpp not only influence biofilm formation in an antagonistic fashion, but also virulence properties of pathogenic bacteria: while c-di-GMP is implicated in the downregulation of virulence traits (Cotter and Stibitz, 2007), basal ppGpp levels are required for full virulence of a number of bacterial species (Braeken *et al.*, 2006). Moreover, because both guanosine second messengers are structurally related, it is conceivable that they might compete for some cellular target(s). Thus, it appears possible that the connections between c-di-GMP and ppGpp signalling are even more intricate.

It is well known that antibiotic chemotherapy can cause severe side-effects (Walker, 1996). Besides direct effects on the patients' physiology, unwanted side-effects of antibiotics are also attributed to imbalances of the commensal flora that are brought about by a strong selection for bacterial species (or life styles) that are less susceptible to the growth inhibitory effect of the drug (Dancer, 2004). Our work raises the question whether some side-effects of antimicrobial chemotherapy might be attributed to biofilm formation of host-associated bacteria that experience sub-inhibitory concentrations of translation inhibitors. Finally, our findings imply that pharmacological interference with ppGpp and/or c-di-GMP signalling, possibly in combination with translation inhibitors or antibiotics that have a different mode of action, might represent promising avenues for the development of novel antimicrobial strategies.

Experimental procedures

Biofilm assay

Attachment assays were carried out essentially as described (O'Toole *et al.*, 1999). Freshly grown LB overnight cultures were diluted 1:40 into 200 μ l LB medium in 96-well polysty-

rene microtiter plates (Falcon, ordering number 353072). When necessary, ampicillin was present at 100 μ g ml⁻¹ to select for plasmids. Other antibiotics were present at the indicated concentrations. The 96-well plates were incubated for 24 h at 30°C without shaking and cell density was recorded at 600 nm with the help of a plate reader. Subsequently, medium containing non-attached cells was discarded and the wells of the microtiter plates were washed vigorously with deionized water from a hose. After air-drying, wells were filled with 200 μ l of a crystal violet solution [0.1% in H₂O, 1-propanol, methanol (96.7:1.66:1.66)] and incubated with moderate shaking for at least 30 min at room temperature (RT). The staining solution was discarded and wells were washed and dried as before. Retained crystal violet was redissolved in 200 μ l of 20% acetic acid and quantified at 600 nm in a plate reader. If measurements were outside the dynamic range of the plate reader, crystal violet solutions were diluted in 20% acetic acid. Normalized attachment values are ratios of the optical density of dissolved crystal violet (corresponding to the attached biomass) divided by the cell density. In general, a single data point is derived from at least six replicates. Error bars for normalized attachment values are standard errors of the mean. For antibiotic titration curves, normalized cell density values are displayed. These were calculated by dividing the mean optical density measured for a specific concentration of antibiotic by the mean optical density measured in the absence of antibiotics. Error bars for relative cell densities were calculated as follows: $(X/Y)^2 * ((SE(x)/X)^2 + (SE(y)/Y)^2)$, where X and Y are the mean optical densities with and without antibiotics, and SE(x) and SE(y) are the standard errors of the mean densities. These error bars correspond to the standard errors of the ratios.

Because cells in the biofilm display a decreased susceptibility towards the action of antibiotics and other forms of stress (Costerton *et al.*, 1995), it is possible that certain conditions lead to a selective decrease of the cell density in the planktonic phase, while the attached biomass (crystal violet value) remains unchanged. In these instances, normalized biofilm values suggest that there is a (usually weak) biofilm induction. However, to rule out the possibility that this is a mere artefact of selectively decreasing the cell density in the planktonic phase, a condition or compound can only be scored as biofilm inducing or inhibiting if it has an effect on both, the attached biomass (not normalized to cell density) as well as on the normalized value.

Screening of a chemical compound library

Strain AB400 was grown over night in TB (10 g l⁻¹ Bacto tryptone, 5 g l⁻¹ NaCl). The optical density at 600 nm was adjusted to 0.1 with fresh TB and 150 μ l cells were inoculated in individual wells of Biolog phenotype microarray plates (Bochner *et al.*, 2001), containing the various chemicals in freeze-dried form. Plates were incubated for 24 h at 30°C and attachment was quantified as described above. Antimicrobials and related substances are present at four increasing concentrations. Compounds were scored as growth inhibitory or growth promoting if cell density readings (see above) decreased with increasing antibiotic concentrations (indicated by '–' in Table S1), or if cell density readings increased

with increasing antibiotic concentrations (indicated by '+' in Table S1) respectively. Normalized attachment (biofilm formation) was calculated as outlined in the section above. Compounds were scored as biofilm inducing (indicated by '+' in Table S1) or inhibiting (indicated by '-' in Table S1) if normalized attachment values increased or decreased with increasing antibiotic concentration respectively. Factors for cell density, attached biomass and normalized attachment values are ratios of the highest value for a given chemical divided by the lowest value for the same chemical respectively. If factors were below an arbitrarily chosen threshold of 1.5, the compound was scored as neither inhibiting nor inducing (indicated by '0' in Table S1).

Bacterial strains and plasmids

All strains are derivatives of AB400 (*csrA::Tn5kan*) and are listed in Table S2. AB400 was constructed from *E. coli* K-12 MG1655 by P1 transduction with TR1-5 as donor (Romeo *et al.*, 1993). To obtain a *csrA::Tn5* mutant that harbours no antibiotic resistance cassette, the kanamycin cassette of AB400 was replaced by a chloramphenicol cassette with the help of λ RED-mediated gene replacement and subsequent removal of the chloramphenicol cassette by site-specific recombination according to (Datsenko and Wanner, 2000). The resulting kanamycin- and chloramphenicol-sensitive strain (AB958) harbours a 'guttled' Tn5 (a Tn5 lacking the kan cassette) and was used for all subsequent strain constructions. Deletion mutations of genes coding for c-di-GMP signalling proteins and other genes were moved from a comprehensive gene deletion library [the 'Keio collection' (Baba *et al.*, 2006)] into recipient strains by P1 transduction. In cases where deletion mutants were not present in the Keio collection, they were generated according to Datsenko and Wanner (2000). Resistance cassettes used as selection markers were generally removed by Flp recombinase-mediated site-specific recombination (Datsenko and Wanner, 2000). Strains AB1029 and AB1000 are spontaneous streptomycin-resistant mutants, which were selected on LB plates containing 100 $\mu\text{g ml}^{-1}$ streptomycin and screened for streptomycin dependence on LB plates without antibiotic. Sequencing of the *rpsL* gene confirmed the presence of mutations leading to the indicated amino acid exchanges (see Table S2). To obtain the *spoT*(D259N) and *spoT*(D73N) alleles, *spoT* was first replaced with the help of λ RED technology by a counter-selectable marker (the toxin *ccdB* under control of the L-rhamnose promoter plus a linked kanamycin resistance cassette; kind gift of K. Datsenko and B. Wanner, Purdue University) in a Δ *relA* background. In a second recombineering step, this marker was replaced by splice overlap extension PCR (Higuchi *et al.*, 1988) products encoding for the two *spoT* alleles by selecting for growth on minimal plates containing 0.2% L-rhamnose and 0.1% casamino acids. To confirm the presence of desired mutations and absence of undesired mutations the *spoT* alleles of the final strains AB1132 [*spoT*(D259N)] and AB1134 [*spoT*(D73N)] were sequenced (there is a second unrelated mutation in *spoT* leading to I158N, which was found to be present in our copy of MG1655 and is thus present in all our strains). Due to the constitutive high level of ppGpp in AB1134, this strain has a severe growth deficit (Cashel *et al.*, 1996). Therefore, spon-

taneous fast-growing suppressors (most of which are predicted to be ppGpp⁰) arise with high frequency. To monitor the emergence of these suppressor mutants in liquid cultures of AB1134, aliquots from cultures were routinely plated on LB agar plates. Suppressors are easily distinguishable as larger colonies and data were only considered to be meaningful, if less than approximately 5% suppressors were present at the end of an experiment (e.g. a biofilm assay). To obtain the *ydeH* active site mutant allele in strain AB1299 the same strategy as for the *spoT* active site mutant alleles was employed (see above). The *P_{ara}-pgaA* fusion strain AB1028 was constructed by fusing the first codon of the *araB* open reading frame with the second codon of the *pgaA* open reading frame with the help of λ RED technology at the native *pga* locus. This was carried out in a way that replaces the entire *pga* promoter plus 5' untranslated region of the *pga* message with the corresponding regions of *P_{ara}*. The final strain harbours a copy of *araC* at the *pga* locus, which is transcribed divergently to the *P_{ara}* promoter. A kanamycin cassette that was used for selection during intermediate steps of the construction of AB1028 was removed by Flp-mediated site-specific recombination (Datsenko and Wanner, 2000). Chromosomal 3 \times Flag-tag encoding sequences at the 3' ends of genes were constructed according to (Uzzau *et al.*, 2001) with the help of pSUB11. The translational *pgaA-lacZ* fusion strain was constructed in two steps with the help of λ RED technology. In a first step, a chromosomal region comprising the native *lacZYA* promoter, *lacI* and the upstream genes *mhpR* and a part of *mhpA* was replaced by the same counter-selectable marker as mentioned above. This procedure removes any promoter that could read into *lacZ* and thereby cause undesired basal activity of the *lacZ* fusion. The *mhp* operon is not expressed under laboratory conditions and therefore the removal of the *mhp* genes can be considered a neutral mutation (Torres *et al.*, 2003). In a second step, the counter-selectable element was replaced by the entire *ycdT-pgaA* intergenic region in a way that fuses the 5' untranslated region directly to the start codon of *lacZ*. The kanamycin resistance cassette (which stems from the first recombineering step and reads into the opposite direction relative to *lacZ*) was left intact during this procedure and was used to move this *lacZ* fusion into any desired recipient strain with the help of P1 transduction. The advantage of this method is that it does not involve any molecular cloning and that it is not necessary to remove the native *lac* locus (in a second, time-consuming step) when the fusion is introduced into a *lac*⁺ target strain. In cases where L-arabinose was used to drive gene expression from *P_{ara}* (Guzman *et al.*, 1995), host strains were deleted for the *araB* gene, which yields a strain that allows for uptake but not metabolism of L-arabinose. Plasmid *psecM Δ N* was constructed according to standard PCR-cloning procedures and encodes for SecM lacking the first 40 amino acids. Expression is driven from a *lac* promoter, which is under control of *lacI*^q. Plasmids *pyliE* and *pyjC* were isolated in a parallel study (A.B and U.J., unpublished) from a chromosomal expression library. *pyliE* harbours a 1107 bp fragment (position 873528–874635 of the genome according to the 'Colibri' database: <http://genolist.pasteur.fr/Colibri/>) inserted in the BamH1 site of pCJ30 (see Table S2). The plasmid encodes the C-terminal part of YliE starting from amino acid 443 with the sequence MLQD (derived from the

vector) at the N-terminus. This peptide comprises the entire EAL domain plus a stretch of 83 N-terminal amino acids from the N-terminal domain of YliE. Expression of *yliE* can be induced with IPTG, but basal expression was found to be sufficient to observe the phenotypes described in the results section. *pyjC* harbours a 2443 bp fragment (position 4272495–4274938 of the genome according to the 'Colibri' database: <http://genolist.pasteur.fr/Colibri/>) inserted in the BamHI site of pCJ30 (see Table S2). The insert contains the entire *yjC* gene including the native promoter (same orientation as the plasmid encoded *lac* promoter), plus very short truncated versions of both genes that are adjacent to *yjC* (*yjB* and *soxS*).

Anti-poly-GlcNAc immunoblots

Bacterial cultures were grown as described for biofilm assays in 96-well microtiter plates. Cells from the planktonic phase and surface-associated cells were harvested by scraping them off the surface of individual wells with a pipette tip followed by vigorous up and down pipetting. Cellular material from six wells was pooled and adjusted to the same OD. Sample processing was done according to reference (Cerca *et al.*, 2007). Anti-poly-GlcNAc antibody raised against poly-GlcNAc from *S. epidermidis* was a kind gift from R. Landmann (University of Basel). Blots were quantified by scanning the blots and dividing the signal by the background intensity. The results from five independent experiments were combined and different treatments were compared with an analysis of variance (with the treatment as fixed effect and the experiment as random effects; procedure GLM in SPSS 13.0.0, SPSS, Chicago, IL). Differences between the control strain grown in the absence of antibiotics and other treatments were tested with a Dunnett posthoc analysis that corrects for multiple testing.

Anti-Flag-tag immunoblots

Bacteria were grown as for biofilm assays, total cells of several wells were pooled and adjusted to the same optical density. Samples were boiled for 5 min in SDS sample buffer and gel electrophoresis and blotting onto PVDF membrane, which were carried out according to standard protocols (Laemmli, 1970; Towbin *et al.*, 1979). For immunodetection of 3×Flag-tagged proteins mouse monoclonal α -M2 antibody and HRP-conjugated rabbit α -mouse (DakyoCytomation, Denmark) were used at 1:10000 dilutions. Blots were developed with the ECL Kit and photographic films.

Measurements of ppGpp in total cellular nucleotide extracts

Total cellular nucleotides were extracted according to the procedure by Little and Bremer (1982). Cells were grown in minimal medium A (Miller, 1972) containing 0.4% glycerol and 0.1% casamino acids in the presence or absence of 1.5 μ g ml⁻¹ chloramphenicol under conditions that closely mimic the conditions used for biofilm assays. Biofilm formation in this medium was found to be similar to biofilm forma-

tion in LB and can be induced with translation inhibitors. To rapidly prevent any turnover of nucleotides during cell harvesting, formaldehyde was added to the culture to a final concentration of 0.19% and cells were chilled on ice for 20 min. Forty microlitres of cells were spun down, the pellet was resuspended in ice cold 0.1 M KOH (1 ml), incubated on ice for 30 min and the samples were acidified with 5 μ l of 88% H₃PO₄. Cellular debris was removed by centrifugation (1 h, 20 000 g, 4°C) and supernatants containing total cellular nucleotide extracts were stored at -80°C. Samples were analysed on a Prostar HPLC system (Varian) equipped with a nucleosil-4000 PEI column (Macherey-Nagel) by anion exchange chromatography according to Ochi (Ochi, 1986). To identify ppGpp in elution profiles representative samples were spiked with the authentic compound purchased from Trilink (<http://www.trilinkbiotech.com/>).

Purification and activity tests of YdeH

YdeH was expressed at 37°C from a pET28 vector with a C-terminal 6×His-tag (without intervening linker amino acids) in Rosetta cells (Novagen). Ni-affinity chromatography was carried out according to standard protocols (Novagen) with the help of FPLC equipment. Elution occurred at 300 mM imidazol. YdeH containing fractions were pooled and chromatographed over a Sephadex S75 column. Oligomerization of purified and concentrated YdeH was determined on a Sephadex S200 column in a buffer containing 20 mM Tris pH 7.6 and 150 mM NaCl with the help of an online refractometer (Optilab rEX, Wyatt technology). To test for DGC activity 2 μ M protein was incubated with 100 μ M GTP in 100 μ l at RT for 30 min and the sample was analysed by LC/MS. Detailed protocols are available upon request.

Scanning electron microscopy

Cells were grown essentially as for attachment assays in 2 ml LB in 24-well plates in the presence of a sterile glass slide. After growth, glass slides were removed, rinsed gently with 1×PBS and fixed in 2.5% glutaraldehyde in 1×PBS for 1 h at RT. Glutaraldehyde was washed out with 1×PBS and the sample was dehydrated with an acetone step gradient (30%, 50%, 70%, 90%, 100%; 10 min each). Samples were critical point-dried and sputter-coated with a 3–5 nm Pt layer. Micrographs were recorded on a Hitachi S-4800 field emission scanning electron microscope. Acceleration voltage was generally between 1.5 and 5 kV.

Acknowledgements

We gratefully acknowledge sharing of unpublished material by K. Datsenko and B. Wanner and thank M. Duggelin, D. Mathys and M. Dürrenberger from the ZMB for excellent service, R. Landmann for the gift of anti-poly-GlcNAc antiserum, M. Folcher for assistance with HPLC and R. Hallez for strains and discussion. This work was supported by Swiss National Science Foundation Fellowship 3100A0-108186 to U.J. and a grant from the Werner Siemens-Foundation (Zug) to S.S.

References

- Anderson, G.G., Dodson, K.W., Hooton, T.M., and Hultgren, S.J. (2004) Intracellular bacterial communities of uropathogenic *Escherichia coli* in urinary tract pathogenesis. *Trends Microbiol* **12**: 424–430.
- Baba, T., Ara, T., Hasegawa, M., Takai, Y., Okumura, Y., Baba, M., *et al.* (2006) Construction of *Escherichia coli* K-12 in-frame, single-gene knockout mutants: the Keio collection. *Mol Syst Biol* **2**: 2006, 0008.
- Babitzke, P., and Romeo, T. (2007) CsrB sRNA family: sequestration of RNA-binding regulatory proteins. *Curr Opin Microbiol* **10**: 156–163.
- Balzer, G.J., and McLean, R.J. (2002) The stringent response genes *relA* and *spoT* are important for *Escherichia coli* biofilms under slow-growth conditions. *Can J Microbiol* **48**: 675–680.
- Baracchini, E., and Bremer, H. (1988) Stringent and growth control of rRNA synthesis in *Escherichia coli* are both mediated by ppGpp. *J Biol Chem* **263**: 2597–2602.
- Bilgin, N., Claesens, F., Pahverk, H., and Ehrenberg, M. (1992) Kinetic properties of *Escherichia coli* ribosomes with altered forms of S12. *J Mol Biol* **224**: 1011–1027.
- Bisognano, C., Vaudaux, P.E., Lew, D.P., Ng, E.Y., and Hooper, D.C. (1997) Increased expression of fibronectin-binding proteins by fluoroquinolone-resistant *Staphylococcus aureus* exposed to subinhibitory levels of ciprofloxacin. *Antimicrob Agents Chemother* **41**: 906–913.
- Blickwede, M., Valentin-Weigand, P., and Schwarz, S. (2004) Subinhibitory concentrations of florfenicol enhance the adherence of florfenicol-susceptible and florfenicol-resistant *Staphylococcus aureus*. *J Antimicrob Chemother* **54**: 286–288.
- Bobrov, A.G., Kirillina, O., Forman, S., Mack, D., and Perry, R.D. (2008) Insights into *Yersinia pestis* biofilm development: topology and co interaction of Hms inner membrane proteins involved in exopolysaccharide production. *Environ Microbiol* **10**: 1419–1432.
- Bochner, B.R., Gadzinski, P., and Panomitros, E. (2001) Phenotype microarrays for high-throughput phenotypic testing and assay of gene function. *Genome Res* **11**: 1246–1255.
- Braeken, K., Moris, M., Daniels, R., Vanderleyden, J., and Michiels, J. (2006) New horizons for (p)ppGpp in bacterial and plant physiology. *Trends Microbiol* **14**: 45–54.
- Branda, S.S., Vik, S., Friedman, L., and Kolter, R. (2005) Biofilms: the matrix revisited. *Trends Microbiol* **13**: 20–26.
- Cashel, M., Gentry, D.R., Hernandez, V.J., and Vinella, D. (1996) The stringent response. In *Escherichia coli and Salmonella typhimurium cellular and molecular biology*. Neidhardt, F.C., Curtiss, R., Ingraham, J.L., Lin, E.C.C., Low, K.B., Magasanik, B., *et al.* (eds). Washington, DC: American Society of Microbiology, pp. 1458–1496.
- Cerca, N., Maira-Litran, T., Jefferson, K.K., Grout, M., Goldmann, D.A., and Pier, G.B. (2007) Protection against *Escherichia coli* infection by antibody to the *Staphylococcus aureus* poly-N-acetylglucosamine surface polysaccharide. *Proc Natl Acad Sci USA* **104**: 7528–7533.
- Clemett, D., and Markham, A. (2000) Linezolid. *Drugs* **59**: 815–827; discussion 828.
- Costerton, J.W., Lewandowski, Z., Caldwell, D.E., Korber, D.R., and Lappin-Scott, H.M. (1995) Microbial biofilms. *Annu Rev Microbiol* **49**: 711–745.
- Costerton, J.W., Stewart, P.S., and Greenberg, E.P. (1999) Bacterial biofilms: a common cause of persistent infections. *Science* **284**: 1318–1322.
- Cotter, P.A., and Stibitz, S. (2007) c-di-GMP-mediated regulation of virulence and biofilm formation. *Curr Opin Microbiol* **10**: 17–23.
- Craig, W.A. (1998) Pharmacokinetic/pharmacodynamic parameters: rationale for antibacterial dosing of mice and men. *Clin Infect Dis* **26**: 1–10; quiz 11–12.
- Daley, D.O., Rapp, M., Granseth, E., Melen, K., Drew, D., and von Heijne, G. (2005) Global topology analysis of the *Escherichia coli* inner membrane proteome. *Science* **308**: 1321–1323.
- Dancer, S.J. (2004) How antibiotics can make us sick: the less obvious adverse effects of antimicrobial chemotherapy. *Lancet Infect Dis* **4**: 611–619.
- Datsenko, K.A., and Wanner, B.L. (2000) One-step inactivation of chromosomal genes in *Escherichia coli* K-12 using PCR products. *Proc Natl Acad Sci USA* **97**: 6640–6645.
- Erickson, D.L., Jarrett, C.O., Callison, J.A., Fischer, E.R., and Hinnebusch, B.J. (2008) Loss of a biofilm-inhibiting glycosyl hydrolase during the emergence of *Yersinia pestis*. *J Bacteriol* **190**: 8163–8170.
- Fajardo, A., and Martinez, J.L. (2008) Antibiotics as signals that trigger specific bacterial responses. *Curr Opin Microbiol* **11**: 161–167.
- Furukawa, S., Kuchma, S.L., and O'Toole, G.A. (2006) Keeping their options open: acute versus persistent infections. *J Bacteriol* **188**: 1211–1217.
- Fux, C.A., Costerton, J.W., Stewart, P.S., and Stoodley, P. (2005) Survival strategies of infectious biofilms. *Trends Microbiol* **13**: 34–40.
- Gallant, J., Margason, G., and Finch, B. (1972) On the turnover of ppGpp in *Escherichia coli*. *J Biol Chem* **247**: 6055–6058.
- Gentry, D.R., and Cashel, M. (1995) Cellular localization of the *Escherichia coli* SpoT protein. *J Bacteriol* **177**: 3890–3893.
- Goh, E.B., Yim, G., Tsui, W., McClure, J., Surette, M.G., and Davies, J. (2002) Transcriptional modulation of bacterial gene expression by subinhibitory concentrations of antibiotics. *Proc Natl Acad Sci USA* **99**: 17025–17030.
- Goller, C., Wang, X., Itoh, Y., and Romeo, T. (2006) The cation-responsive protein NhaR of *Escherichia coli* activates *pgaABCD* transcription, required for production of the biofilm adhesin poly-beta-1,6-N-acetyl-D-glucosamine. *J Bacteriol* **188**: 8022–8032.
- Gotz, F. (2002) *Staphylococcus* and biofilms. *Mol Microbiol* **43**: 1367–1378.
- Guzman, L.M., Belin, D., Carson, M.J., and Beckwith, J. (1995) Tight regulation, modulation, and high-level expression by vectors containing the arabinose PBAD promoter. *J Bacteriol* **177**: 4121–4130.
- Harms, J.M., Bartels, H., Schlunzen, F., and Yonath, A. (2003) Antibiotics acting on the translational machinery. *J Cell Sci* **116**: 1391–1393.
- Hernandez, V.J., and Bremer, H. (1990) Guanosine tetraphosphate (ppGpp) dependence of the growth rate control

- of *rrnB* P1 promoter activity in *Escherichia coli*. *J Biol Chem* **265**: 11605–11614.
- Higuchi, R., Krummel, B., and Saiki, R.K. (1988) A general method of *in vitro* preparation and specific mutagenesis of DNA fragments: study of protein and DNA interactions. *Nucl Acids Res* **16**: 7351–7367.
- Hoffman, L.R., D'Argenio, D.A., MacCoss, M.J., Zhang, Z., Jones, R.A., and Miller, S.I. (2005) Aminoglycoside antibiotics induce bacterial biofilm formation. *Nature* **436**: 1171–1175.
- Hogg, T., Mechold, U., Malke, H., Cashel, M., and Hilgenfeld, R. (2004) Conformational antagonism between opposing active sites in a bifunctional RelA/SpoT homolog modulates (p)ppGpp metabolism during the stringent response [corrected]. *Cell* **117**: 57–68.
- Itoh, Y., Rice, J.D., Goller, C., Pannuri, A., Taylor, J., Meisner, J., *et al.* (2008) Roles of *pgaABCD* genes in synthesis, modification, and export of the *Escherichia coli* biofilm adhesin poly-beta-1,6-N-acetyl-D-glucosamine. *J Bacteriol* **190**: 3670–3680.
- Jenal, U., and Malone, J. (2006) Mechanisms of cyclic-di-GMP signaling in bacteria. *Annu Rev Genet* **40**: 385–407.
- Jiang, M., Sullivan, S.M., Wout, P.K., and Maddock, J.R. (2007) G-protein control of the ribosome-associated stress response protein SpoT. *J Bacteriol* **189**: 6140–6147.
- Jonas, K., Edwards, A.N., Simm, R., Romeo, T., Romling, U., and Melefors, O., (2008) The RNA binding protein CsrA controls c-di-GMP metabolism by directly regulating the expression of GGDEF proteins. *Mol Microbiol* **70**: 236–257.
- Laemmli, U.K. (1970) Cleavage of structural proteins during the assembly of the head of bacteriophage T4. *Nature* **227**: 680–685.
- Lange, R., Fischer, D., and Hengge-Aronis, R. (1995) Identification of transcriptional start sites and the role of ppGpp in the expression of *rpoS*, the structural gene for the sigma S subunit of RNA polymerase in *Escherichia coli*. *J Bacteriol* **177**: 4676–4680.
- Letunic, I., Copley, R.R., Pils, B., Pinkert, S., Schultz, J., and Bork, P. (2006) SMART 5: domains in the context of genomes and networks. *Nucl Acids Res* **34**: D257–D260.
- Lewis, K. (2007) Persister cells, dormancy and infectious disease. *Nature Rev* **5**: 48–56.
- Linares, J.F., Gustafsson, I., Baquero, F., and Martinez, J.L. (2006) Antibiotics as intermicrobial signaling agents instead of weapons. *Proc Natl Acad Sci USA* **103**: 19484–19489.
- Little, R., and Bremer, H. (1982) Quantitation of guanosine 5',3'-bisdiphosphate in extracts from bacterial cells by ion-pair reverse-phase high-performance liquid chromatography. *Anal Biochem* **126**: 381–388.
- Lucchetti-Miganeh, C., Burrowes, E., Baysse, C., and Ermel, G. (2008) The post-transcriptional regulator CsrA plays a central role in the adaptation of bacterial pathogens to different stages of infection in animal hosts. *Microbiology* **154**: 16–29.
- McLennan, M.K., Ringoir, D.D., Fridrich, E., Svensson, S.L., Wells, D.H., Jarrell, H., *et al.* (2008) *Campylobacter jejuni* biofilms up-regulated in the absence of the stringent response utilize a calcofluor white-reactive polysaccharide. *J Bacteriol* **190**: 1097–1107.
- Mah, T.F., and O'Toole, G.A. (2001) Mechanisms of biofilm resistance to antimicrobial agents. *Trends Microbiol* **9**: 34–39.
- Miller, J.H. (1972) *Experiments in Molecular Genetics*. Cold Spring Harbor, NY: Cold Spring Harbor Laboratory Press.
- Murray, K.D., and Bremer, H. (1996) Control of *spoT*-dependent ppGpp synthesis and degradation in *Escherichia coli*. *J Mol Biol* **259**: 41–57.
- Muto, A., Kimura, A., and Osawa, S. (1975) Effects of some antibiotics on the stringent control of RNA synthesis in *Escherichia coli*. *Mol Gen Genet* **139**: 321–327.
- Nakatogawa, H., and Ito, K. (2002) The ribosomal exit tunnel functions as a discriminating gate. *Cell* **108**: 629–636.
- O'Toole, G.A., Pratt, L.A., Watnick, P.I., Newman, D.K., Weaver, V.B., and Kolter, R. (1999) Genetic approaches to study of biofilms. *Meth Enzymol* **310**: 91–109.
- Ochi, K. (1986) Occurrence of the stringent response in *Streptomyces* sp. and its significance for the initiation of morphological and physiological differentiation. *J Gen Microbiol* **132**: 2621–2631.
- Ozaki, M., Mizushima, S., and Nomura, M. (1969) Identification and functional characterization of the protein controlled by the streptomycin-resistant locus in *E. coli*. *Nature* **222**: 333–339.
- Parise, G., Mishra, M., Itoh, Y., Romeo, T., and Deora, R. (2007) Role of a putative polysaccharide locus in *Bordetella* biofilm development. *J Bacteriol* **189**: 750–760.
- Potrykus, K., and Cashel, M. (2008) (p)ppGpp: still magical? *Annu Rev Microbiol* **62**: 35–51.
- Pratt, L.A., and Kolter, R. (1998) Genetic analysis of *Escherichia coli* biofilm formation: roles of flagella, motility, chemotaxis and type I pili. *Mol Microbiol* **30**: 285–293.
- Rachid, S., Ohlsen, K., Witte, W., Hacker, J., and Ziebuhr, W. (2000) Effect of subinhibitory antibiotic concentrations on polysaccharide intercellular adhesin expression in biofilm-forming *Staphylococcus epidermidis*. *Antimicrob Agents Chemother* **44**: 3357–3363.
- Ramagopal, S., and Davis, B.D. (1974) Localization of the stringent protein of *Escherichia coli* on the 50S ribosomal subunit. *Proc Natl Acad Sci USA* **71**: 820–824.
- Romeo, T., Gong, M., Liu, M.Y., and Brunzinkernagel, A.M. (1993) Identification and molecular characterization of *csrA*, a pleiotropic gene from *Escherichia coli* that affects glycogen biosynthesis, gluconeogenesis, cell size, and surface properties. *J Bacteriol* **175**: 4744–4755.
- Sabina, J., Dover, N., Templeton, L.J., Smulski, D.R., Soll, D., and LaRossa, R.A. (2003) Interfering with different steps of protein synthesis explored by transcriptional profiling of *Escherichia coli* K-12. *J Bacteriol* **185**: 6158–6170.
- Smith, D.L.A.D., Harris, J.A., Johnson, E.K., Silbergeld and Morris, Jr (2002) Animal antibiotic use has an early but important impact on the emergence of antibiotic resistance in human commensal bacteria. *Proc Natl Acad Sci USA* **99**: 6434–6439.
- Suzuki, K., Babitzke, P., Kushner, S.R., and Romeo, T. (2006) Identification of a novel regulatory protein (CsrD) that targets the global regulatory RNAs CsrB and CsrC for degradation by RNase E. *Gen Dev* **20**: 2605–2617.
- Tamayo, R., Pratt, J.T., and Camilli, A. (2007) Roles of cyclic diguanylate in the regulation of bacterial pathogenesis. *Annu Rev Microbiol* **61**: 131–148.

- Timmermans, J., and Van Melderen, L. (2008) Conditional essentiality of the *csrA* gene in *E. coli*. *J Bacteriol* **191**: 1722–1724.
- Timms, A.R., and Bridges, B.A. (1993) Double, independent mutational events in the *rpsL* gene of *Escherichia coli*: an example of hypermutability? *Mol Microbiol* **9**: 335–342.
- Tomenius, H., Pernestig, A.K., Jonas, K., Georgellis, D., Mollby, R., Normark, S., and Melefors, O. (2006) The *Escherichia coli* BarA-UvrY two-component system is a virulence determinant in the urinary tract. *BMC Microbiol* **6**: 27.
- Torres, B., Porras, G., Garcia, J.L., and Diaz, E. (2003) Regulation of the *mhp* cluster responsible for 3-(3-hydroxyphenyl) propionic acid degradation in *Escherichia coli*. *J Biol Chem* **278**: 27575–27585.
- Towbin, H., Staehelin, T., and Gordon, J. (1979) Electrophoretic transfer of proteins from polyacrylamide gels to nitrocellulose sheets: procedure and some applications. *Proc Natl Acad Sci USA* **76**: 4350–4354.
- Traxler, M.F., Summers, S.M., Nguyen, H.T., Zacharia, V.M., Hightower, G.A., Smith, J.T., and Conway, T. (2008) The global, ppGpp-mediated stringent response to amino acid starvation in *Escherichia coli*. *Mol Microbiol* **68**: 1128–1148.
- Tsui, W.H., Yim, G., Wang, H.H., McClure, J.E., Surette, M.G., and Davies, J. (2004) Dual effects of MLS antibiotics: transcriptional modulation and interactions on the ribosome. *Chem Biol* **11**: 1307–1316.
- Uzzau, S., Figueroa-Bossi, N., Rubino, S., and Bossi, L. (2001) Epitope tagging of chromosomal genes in *Salmonella*. *Proc Natl Acad Sci USA* **98**: 15264–15269.
- VanBogelen, R.A., and Neidhardt, F.C. (1990) Ribosomes as sensors of heat and cold shock in *Escherichia coli*. *Proc Natl Acad Sci USA* **87**: 5589–5593.
- Vuong, C., Kocianova, S., Voyich, J.M., Yao, Y., Fischer, E.R., DeLeo, F.R., and Otto, M. (2004) A crucial role for exopolysaccharide modification in bacterial biofilm formation, immune evasion, and virulence. *J Biol Chem* **279**: 54881–54886.
- Walker, C.B. (1996) Selected antimicrobial agents: mechanisms of action, side effects and drug interactions. *Periodontol* **10**: 12–28.
- Wang, X., Preston, 3rd, J.F., and Romeo, T. (2004) The *pgaABCD* locus of *Escherichia coli* promotes the synthesis of a polysaccharide adhesin required for biofilm formation. *J Bacteriol* **186**: 2724–2734.
- Wang, X., Dubey, A.K., Suzuki, K., Baker, C.S., Babitzke, P., and Romeo, T. (2005) *CsrA* post-transcriptionally represses *pgaABCD*, responsible for synthesis of a biofilm polysaccharide adhesin of *Escherichia coli*. *Mol Microbiol* **56**: 1648–1663.
- Weber, H., Pesavento, C., Possling, A., Tischendorf, G., and Hengge, R. (2006) Cyclic-di-GMP-mediated signalling within the sigma network of *Escherichia coli*. *Mol Microbiol* **62**: 1014–1034.
- Wout, P., Pu, K., Sullivan, S.M., Reese, V., Zhou, S., Lin, B., and Maddock, J.R. (2004) The *Escherichia coli* GTPase CgtAE cofractionates with the 50S ribosomal subunit and interacts with SpoT, a ppGpp synthetase/hydrolase. *J Bacteriol* **186**: 5249–5257.
- Xiao, H., Kalman, M., Ikehara, K., Zemel, S., Glaser, G., and Cashel, M. (1991) Residual guanosine 3',5'-bispyrophosphate synthetic activity of *relA* null mutants can be eliminated by *spoT* null mutations. *J Biol Chem* **266**: 5980–5990.
- Yim, G., de la Cruz, F., Spiegelman, G.B., and Davies, J. (2006) Transcription modulation of *Salmonella enterica* serovar Typhimurium promoters by sub-MIC levels of rifampin. *J Bacteriol* **188**: 7988–7991.
- Yim, G., Wang, H.H., and Davies, J. (2007) Antibiotics as signalling molecules. *Philos Trans R Soc Lond B Biol Sci* **362**: 1195–1200.

Supporting information

Additional supporting information may be found in the online version of this article.

Please note: Wiley-Blackwell are not responsible for the content or functionality of any supporting materials supplied by the authors. Any queries (other than missing material) should be directed to the corresponding author for the article.

Table S1. Comprehensive screening of antimicrobials and related substances for effects on biofilm formation.

Substances are grouped according to their cellular target/mode of action. Effects on cell density, surface attached biomass and normalized attachment (biofilm formation) are indicated (see material and methods). “+”, “-“ and “0” indicate induction, inhibition or no effect (above a threshold of 1,5) on a given parameter, respectively. Factors indicate ratios between highest and lowest values for a given parameter (see material and methods). Please note that absence of effects for a given substance might indicate that the employed concentrations were outside the active range. Substances marked with a “*” did not elicit any response, most likely because the screening strain carried an aminoglycoside phosphotransferase gene, conferring resistance to kanamycin and closely related substances.

Table S1		cell density		surface attached biomass		normalized attachment (biofilm)	
substance	target/mode of action	FAC TOR	+/-	FAC TOR	+/-	FAC TOR	+/-
Chloramphenicol	protein synthesis	2,11	-	1,98	+	3,55	+
Thiamphenicol	protein synthesis	1,86	-	1,95	+	3,16	+
Chloramphenicol	protein synthesis	2,03	-	1,97	+	3,09	+
Blasticidin S	protein synthesis	1,78	-	1,62	+	2,89	+
Capreomycin	protein synthesis	1,25	0	1,28	0	1,56	+
Streptomycin	protein synthesis, 30S subunit, aminoglycoside	1,90	-	2,20	+	3,61	+
Sisomicin	protein synthesis, 30S subunit, aminoglycoside	2,26	-	2,07	+	3,48	+
Dihydro streptomycin	protein synthesis, 30S subunit, aminoglycoside	1,83	-	2,15	+	3,46	+
Tobramycin	protein synthesis, 30S subunit, aminoglycoside	2,22	-	1,96	+	3,26	+
Amikacin	protein synthesis, 30S subunit, aminoglycoside	1,84	-	1,78	+	2,94	+
Apramycin	protein synthesis, 30S subunit, aminoglycoside	1,48	0	1,42	0	2,08	+
Neomycin*	protein synthesis, 30S subunit, aminoglycoside	1,01	0	1,48	0	1,50	0
Gentamicin	protein synthesis, 30S subunit, aminoglycoside	1,18	0	1,20	0	1,40	0
Kanamycin*	protein synthesis, 30S subunit, aminoglycoside	1,07	0	1,32	0	1,37	0
Paromomycin*	protein synthesis, 30S subunit, aminoglycoside	1,06	0	1,05	0	1,10	0
Puromycin	protein synthesis, 30S subunit, protein synthesis, 30S subunit, tetracycline	1,74	-	1,78	+	2,40	+
Penimepicycline	protein synthesis, 30S subunit, tetracycline	2,82	-	2,89	+	7,20	+
Minocycline	protein synthesis, 30S subunit, tetracycline	3,21	-	2,63	+	5,46	+
Tetracycline	protein synthesis, 30S subunit, protein synthesis, 30S subunit, tetracycline	2,23	-	2,30	+	4,98	+
Demeclocycline	protein synthesis, 30S subunit, tetracycline	2,22	-	2,26	+	4,92	+
Chlortetracycline	protein synthesis, 30S subunit, tetracycline	2,19	-	2,15	+	4,26	+
Rolitetraacycline	protein synthesis, 30S subunit, tetracycline	2,21	-	2,05	+	2,79	+

Rolitetraacycline	protein synthesis, 30S subunit, tetracycline	2,21	-	2,05	+	2,79	+
Oxytetraacycline	protein synthesis, 30S subunit, tetracycline	1,16	0	1,89	+	2,01	+
Josamycin	protein synthesis, 50S subunit, macrolide	2,27	-	3,60	+	7,03	+
Erythromycin	protein synthesis, 50S subunit, macrolide	2,00	-	2,36	+	4,72	+
Spiramycin	protein synthesis, 50S subunit, macrolide	1,85	-	2,07	+	3,59	+
Oleandomycin	protein synthesis, 50S subunit, macrolide	1,58	-	1,50	+	2,20	+
Oleandomycin	protein synthesis, 50S subunit, macrolide	1,30	0	1,26	0	1,56	+
Tylosin	protein synthesis, 50S subunit, macrolide	1,21	0	1,32	0	1,17	0
Hygromycin B	protein synthesis, aminoglycoside	1,22	0	1,12	0	1,27	0
Geneticin (G418)	protein synthesis, aminoglycoside	1,03	0	1,05	0	1,06	0
Fusidic acid	protein synthesis, elongation factor	1,35	0	1,21	0	1,34	+
Lincomycin	protein synthesis, lincosamide	1,80	-	2,43	-	2,51	+
Spectinomycin	protein synthesis, ribosome, aminoglycoside	1,81	-	1,78	+	2,65	+
Doxycycline	protein synthesis, tetracycline	2,22	-	2,66	+	5,33	+
Atropine	acetylcholine receptor, antagonist	1,83	-	2,54	+	4,01	+
Ketoprofen	anti-capsule	1,93	+	1,33	0	2,44	-
Thiosalicylate	anti-capsule	1,33	0	2,87	-	2,43	-
Ethionamide	anti-tuberculositic	1,20	0	1,97	-	1,74	-
Sanguinarine	ATPase, Na ⁺ /K ⁺ and Mg ⁺⁺	1,25	0	7,14	-	5,72	-
Chlorpromazine	calmodulin-dependent cyclic nucleotide phosphodiesterase	1,78	-	6,58	-	5,14	-
Compound 48/80	Calmodulin inhibitor phospholipase C, ADP ribosylation	1,86	-	2,08	+	3,45	+
Trifluoperazine	cell cycle modulation, DNA synthesis, Ca(2 ⁺)	1,45	0	2,73	-	3,39	-
4-Aminopyridine	channel blocker, K ⁺	1,07	0	1,48	0	1,38	0
Pyrophosphate	chelating agent	1,15	0	1,47	0	1,61	-
EGTA	chelator, Ca ⁺⁺	1,40	0	1,41	0	1,89	+
Fusaric acid	chelator, Fe, lipophilic, deplete Fe in yeast	1,67	-	1,43	0	2,02	+
2,2'-Dipyridyl	chelator, Fe ⁺⁺	1,30	0	2,37	+	2,82	+
1,10-Phenanthroline	chelator, Fe ⁺⁺ , Zn ⁺⁺ , divalent metal ions	2,37	-	1,83	+	4,29	+
EDTA	chelator, hydrophilic	1,59	-	2,02	-	1,27	0
5,7-Dichloro-8-hydroxyquinoline	chelator, lipophilic	2,53	-	2,42	+	5,36	+
5,7-Dichloro-8-hydroxy-quinaldine	chelator, lipophilic	1,55	-	1,40	0	2,00	+
5-Chloro-7-iodo-8-hydroxyquinoline	chelator, lipophilic	1,54	-	1,95	-	1,38	0
8-Hydroxy	chelator, lipophilic, RNA						

Orphenadrine	cholinergic antagonist	1,75	-	2,36	+	4,07	+
Caffeine	cyclic AMP phosphodiesterase	1,14	0	2,16	-	2,01	-
Promethazine	cyclic nucleotide phosphodiesterase	2,08	-	2,55	-	1,81	+
2,4-Diamino-6,7-diisopropylpteridine	dihydrofolate reductase inhibitor	1,13	0	1,17	0	1,18	0
Myricetin	DNA & RNA synthesis, polymerase inhibitor	1,32	0	3,49	-	4,60	-
Nitrofurazone	DNA damage, multiple sites, nitrofurane analog	1,14	0	1,46	0	1,32	0
Furaltadone	DNA damage, multiple sites, nitrofurane analog	1,08	0	1,11	0	1,17	0
Nitrofurantoin	DNA damage, multiple sites, nitrofurane analog	1,10	0	1,11	0	1,02	0
Hydroxylamine	DNA damage, mutagen, antifolate	1,10	0	2,43	-	2,68	-
Phleomycin	DNA damage, oxidative, ionizing radiation	2,11	-	2,13	+	3,73	+
Bleomycin	DNA damage, oxidative, ionizing radiation	1,57	-	1,75	+	2,51	+
2-Phenylphenol	DNA intercalator	2,18	-	2,21	-	4,71	+
9-Aminoacridine	DNA intercalator	2,58	-	2,25	+	4,41	+
Acridine	DNA intercalator	2,22	-	1,93	+	4,28	+
Coumarin	DNA intercalator	2,56	-	9,11	-	3,57	-
4-Hydroxycoumarin	DNA intercalator	1,45	0	2,27	+	2,86	+
Umbelliferone	DNA intercalator	1,17	0	1,11	0	1,28	0
5-Azacytidine	DNA methylation, methyltransferase inhib.	1,07	0	1,08	0	1,05	0
Hexammincobalt (III) Chloride	DNA synthesis	1,72	-	1,78	+	2,67	+
Enoxacin	DNA unwinding, gyrase, fluoroquinolone	2,40	-	2,47	+	5,05	+
Norfloxacin	DNA unwinding, gyrase, fluoroquinolone	2,18	-	1,86	+	4,03	+
Lomefloxacin	DNA unwinding, gyrase, fluoroquinolone	2,29	-	5,68	-	2,53	-
Ciprofloxacin	DNA unwinding, gyrase, fluoroquinolone	1,29	0	2,33	+	2,12	+
Ofloxacin	DNA unwinding, gyrase, fluoroquinolone	2,16	-	2,11	-	1,46	0
Pipemidic Acid	DNA unwinding, gyrase, quinolone	2,39	-	2,42	+	5,70	+
Cinoxacin	DNA unwinding, gyrase, fluoroquinolone	2,21	-	3,03	-	2,91	-
Novobiocin	DNA unwinding, gyrase, fluoroquinolone	1,23	0	3,51	-	2,84	-
Nalidixic acid	DNA unwinding, gyrase, quinolone	2,22	-	4,48	-	2,02	-
Oxolinic acid	DNA unwinding, gyrase, fluoroquinolone	1,05	0	1,47	0	1,52	-
Proflavine	flavone, antibacterial	1,74	-	2,01	+	2,86	+
Sulfamono methoxine	folate antagonist	1,55	-	1,25	0	1,88	+
Trimethoprim	folate synthesis, dihydrofolate reductase inhibitor	1,27	0	3,25	-	2,56	-

Sulfachloro pyridazine	folate synthesis, PABA analog	1,84	-	1,84	+	2,75	+
Sulfanilamide	folate synthesis, PABA analog	1,69	-	1,76	+	2,56	+
Sulfamethazine	folate synthesis, PABA analog	1,58	-	1,87	+	2,46	+
Sulfadiazine	folate synthesis, PABA analog	1,45	0	1,62	+	2,14	+
Sulfisoxazole	folate synthesis, PABA analog	1,05	0	1,84	+	1,90	+
Sulfamethoxazole	folate synthesis, PABA analog	1,31	0	1,51	+	1,83	+
Sulfathiazole	folate synthesis, PABA analog	1,30	0	1,42	0	1,76	+
Chloroxylenol	fungicide	2,45	-	2,99	+	6,36	+
Dichlofluanid	fungicide, phenylsulphamide	1,51	-	1,71	+	2,43	+
Tolyfluanid	fungicide, phenylsulphamide	1,10	0	1,20	0	1,24	0
Harmane	imidazoline binding sites, agonist	2,05	-	2,02	+	3,62	+
D-Serine	inhibits 3PGA dehydrogenase (L-serine and pantothenate synt.)	1,38	0	1,59	-	2,10	-
Dequalinium	ion channel inhibitor, K ⁺ (m)	1,09	0	1,01	0	1,08	0
Procaine	ion channel inhibitor, Na ⁺ (m)	2,20	-	1,79	+	2,79	+
Triclosan	lipid synthesis, fatty acid inhibitor	1,13	0	1,12	0	1,15	0
Nordihydro guaiaretic acid	lipoxygenase, fungicide	1,38	0	3,65	-	4,91	-
Dodine	membrane permeability, guanidine, fungicide	1,26	0	1,91	+	2,23	+
Alexidine	membrane, biguanide, electron transport	1,17	0	1,03	0	1,21	0
Guanidine hydrochloride	membrane, chaotropic agent	1,90	-	2,54	+	3,86	+
Niaproof	membrane, detergent, anionic	1,29	0	1,29	0	1,34	0
Dodecyltrimethyl ammonium bromide	membrane, detergent, cationic	2,37	-	8,71	-	4,91	-
Benzethonium chloride	membrane, detergent, cationic	1,55	-	6,17	-	4,24	-
Cetylpyridinium chloride	membrane, detergent, cationic	2,33	-	7,62	-	3,27	-
Poly-L-lysine	membrane, detergent, cationic	1,14	0	2,22	-	2,31	-
Methyltrioctyl Ammonium chloride	membrane, detergent, cationic	1,38	0	1,34	0	1,61	+
Domiphen bromide	membrane, detergent, cationic, fungicide	1,79	-	2,21	+	3,96	+
Lauryl sulfobetaine	membrane, detergent, zwitterionic	1,78	-	1,86	+	3,30	+
Polymyxin B	membrane, disorganize structure	3,03	-	9,73	-	3,27	-
Polymyxin B	membrane, disorganize structure	1,15	0	2,39	-	2,66	-
Hexachlorophene	membrane, electron transport	2,01	-	4,95	-	2,69	-
Chlorhexidine	membrane, electron transport	1,11	0	1,03	0	1,14	0
Protamine sulfate	membrane, nonspecific binding	1,81	-	1,85	-	2,73	+
Amitriptyline	membrane, transport	2,41	-	2,48	+	5,85	+
Colistin	membrane, transport	1,07	0	1,16	0	1,23	0
Patulin	microtubulin polymerization	1,52	-	1,70	+	2,59	+

Patulin	microtubulin polymerization inhibitor	1,52	-	1,70	+	2,59	+
Captan	multisite, carbamate, fungicide	1,06	0	1,15	0	1,12	0
Tinidazole	Mutagen, nitroimidazole	1,47	0	1,77	-	1,46	0
6-Mercaptopurine	nucleic acid analog, purine	1,38	0	1,67	+	2,30	+
Azathioprine	nucleic acid analog, purine	1,21	0	2,25	-	1,87	-
5-Fluoro-5'-deoxyuridine	nucleic acid analog, pyrimidine	1,34	0	1,31	0	1,58	+
5-Fluoroorotic acid	nucleic acid analog, pyrimidine	1,88	-	1,31	0	1,48	0
Cytosine arabinoside	nucleic acid analog, pyrimidine	1,08	0	1,23	0	1,30	0
5-Fluorouracil	nucleic acid analog, pyrimidine	1,12	0	1,20	0	1,08	0
1-Chloro-2,4-dinitrobenzene	oxidation, glutathione	1,81	+	1,49	0	2,66	-
Iodoacetate	oxidation, sulfhydryl	2,18	-	2,08	+	4,54	+
Lawsone	oxidizing agent	1,59	-	7,01	-	9,92	-
Plumbagin	oxidizing agent	1,68	-	7,40	-	4,48	-
Methyl viologen	oxidizing agent	1,53	-	1,47	0	1,36	0
D,L-Thioctic acid	oxidizing agent	1,47	0	1,88	-	1,35	0
3, 4-Dimethoxy benzyl alcohol	oxidizing agent, free radical- peroxidase subst.	2,24	-	2,53	+	4,99	+
Phenyl-methyl sulfonyl-fluoride	protease inhibitor, serine	1,03	0	2,05	-	2,02	-
Ornidazole	protein glycosylation	2,21	-	6,44	-	2,97	-
Chelerythrine	protein kinase C inhibitor	2,56	-	2,41	+	3,85	+
Thioglycerol	reducing agent, adenosyl methionine antagonist	1,82	-	1,77	+	3,20	+
Gallic acid	respiration ionophore H+	2,89	+	3,33	-	9,60	-
CCCP	respiration ionophore H+	2,89	-	3,28	+	9,51	+
Cinnamic acid	respiration ionophore H+	1,17	0	5,71	-	5,06	-
FCCP	respiration ionophore H+	2,45	-	2,38	-	4,99	+
18-Crown-6 ether	respiration ionophore H+	2,83	-	6,63	-	4,23	-
3,5-Dinitrobenzene	respiration ionophore H+	1,54	-	2,53	-	3,74	+
Pentachlorophenol	respiration ionophore H+	2,27	-	6,93	-	3,15	-
Sodium caprylate	respiration ionophore H+	2,31	-	5,02	-	3,04	-
2,4-Dinitrophenol	respiration ionophore H+	2,39	-	5,61	-	2,35	-
Sorbic Acid	respiration ionophore H+	1,16	0	1,48	0	1,71	-
Ruthenium red	respiration ionophore H+	1,07	0	1,36	0	1,28	0
Sodium azide	respiration, uncoupler	3,33	-	2,89	+	8,84	+
Thioridazine	respiration, uncoupler	2,49	+	3,17	-	6,39	-
Menadione	respiration, uncoupler	1,13	0	4,14	-	3,66	-
Oxycarboxin	respiratory enzymes, carboxamide, fungicide	1,63	-	1,32	0	1,23	0
2-Nitroimidazole	ribonucleotide DP reductase	3,12	-	3,74	+	10,58	+
Guanazole	ribonucleotide DP reductase	1,61	-	1,56	-	2,03	+
Hydroxyurea	ribonucleotide DP reductase, antifolate	1,61	-	1,77	+	2,86	+
Rifampicin	RNA polymerase	1,48	0	1,48	0	1,93	+
Rifamycin SV	RNA polymerase	1,12	0	1,49	0	1,46	0
Sodium cyanate	toxic anion	1,17	0	12,03	-	12,53	-
Potassium chromate	toxic anion	1,80	-	11,07	-	6,27	-
Sodium metaborate	toxic anion	1,48	0	8,72	-	5,91	-

Sodium m-arsenite	toxic anion	1,46	0	2,36	+	3,45	+
Potassium tellurite	toxic anion	2,85	-	6,97	-	2,68	-
Nitrite	toxic anion	2,64	-	6,00	-	2,27	-
Boric Acid	toxic anion	1,71	-	1,69	+	2,26	+
Sodium metasilicate	toxic anion	1,61	-	1,61	-	2,08	+
Sodium selenite	toxic anion	1,15	0	1,59	+	1,74	+
Sodium bromate	toxic anion	1,58	-	1,48	0	1,52	+
Sodium tungstate	toxic anion, molybdate analog	1,73	-	8,69	-	5,02	-
Sodium periodate	toxic anion, oxidizing agent	2,55	-	2,19	-	3,85	+
Sodium metavanadate	toxic anion, PO4 analog	1,23	0	9,82	-	12,11	-
Sodium orthovanadate	toxic anion, PO4 analog	1,25	0	7,64	-	9,17	-
Sodium arsenate	toxic anion, PO4 analog	1,60	-	7,86	-	8,51	-
Sodium dichromate	toxic anion, SO4 analog	1,05	0	3,28	-	3,39	-
Aluminum sulfate	toxic cation	2,41	+	7,35	-	15,30	-
Zinc chloride	toxic cation	1,14	0	9,45	-	8,76	-
Cadmium chloride	toxic cation	3,03	-	2,53	+	7,65	+
Nickel chloride	toxic cation	1,48	0	9,52	-	6,90	-
Ferric chloride	toxic cation	2,33	+	2,37	-	4,57	-
Lithium chloride	toxic cation	1,92	-	2,44	+	4,52	+
Cobalt chloride	toxic cation	1,78	-	2,10	+	3,64	+
Antimony (III) chloride	toxic cation	1,30	0	4,38	-	3,38	-
Thallium (I) acetate	toxic cation	2,41	-	4,73	-	2,73	-
Chromium chloride	toxic cation	1,67	+	1,52	+	2,29	-
Cupric chloride	toxic cation	1,19	0	1,32	0	1,53	-
Manganese (II) chloride	toxic cation	1,29	0	1,08	0	1,40	0
Cesium chloride	toxic cation	1,11	0	1,11	0	1,14	0
Glycine hydroxamate	tRNA synthetase	4,22	-	2,78	+	11,71	+
L- Aspartic-hydroxamate	tRNA synthetase	2,19	-	1,79	-	1,94	+
D,L-Methionine hydroxamate	tRNA synthetase	1,33	0	1,36	0	1,73	+
L-Glutamic acid g-hydroxamate	tRNA synthetase	1,14	0	1,55	-	1,70	-
D,L-Serine hydroxamate	tRNA synthetase	1,96	-	2,96	-	1,52	-
Phenylarsine oxide	tyrosine phosphatase inhibitor	2,96	-	3,33	-	2,32	-
Vancomycin	wall	1,60	-	1,67	+	2,47	+
Phosphomycin	wall	1,14	0	1,11	0	1,22	0
Glycine	wall	1,05	0	1,14	0	1,17	0
Cefsulodin	wall, cephalosporin	1,22	0	1,18	0	1,33	0
Cephalothin	wall, cephalosporin first generation	1,29	0	1,29	0	1,42	0
Cefazolin	wall, cephalosporin first generation	1,12	0	1,15	0	1,14	0

Cefmetazole	wall, cephalosporin second generation	1,10	0	4,87	-	4,62	-
Cefuroxime	wall, cephalosporin second generation	2,39	-	1,92	+	4,54	+
Cefamandole	wall, cephalosporin second generation	2,00	-	2,13	+	4,01	+
Cefoxitin	wall, cephalosporin second generation	1,98	-	1,95	+	3,42	+
Cefotaxime	wall, cephalosporin third generation	2,55	-	2,60	+	6,26	+
Ceftriaxone	wall, cephalosporin third generation	1,78	-	1,78	+	3,07	+
Cefoperazone	wall, cephalosporin third generation	2,35	-	1,67	-	2,02	+
Phenethicillin	wall, lactam	1,89	-	3,12	+	5,61	+
Carbenicillin	wall, lactam	2,06	-	7,61	-	4,26	-
Carbenicillin	wall, lactam	1,79	-	2,59	+	4,17	+
Amoxicillin	wall, lactam	2,10	-	1,96	+	3,68	+
Cloxacillin	wall, lactam	1,59	-	2,20	+	3,45	+
Ampicillin	wall, lactam	1,95	-	1,84	+	3,35	+
Oxacillin	wall, lactam	1,73	-	2,14	+	3,34	+
Penicillin G	wall, lactam	1,73	-	1,61	+	2,50	+
Nafcillin	wall, lactam	1,85	-	2,44	-	1,91	-
Aztreonam	wall, lactam	2,05	-	1,49	0	1,77	+
Azlocillin	wall, lactam	1,85	-	2,62	-	1,67	-
Piperacillin	wall, lactam	1,14	0	1,15	0	1,19	0
Moxalactam	wall, lactam	1,01	0	1,01	0	1,01	0
D-Cycloserine	wall, sphingolipid synthesis	1,09	0	1,11	0	1,20	0
1-Hydroxy-pyridine-2-thione		2,32	-	2,67	+	5,60	+
Lidocaine		2,14	-	6,70	-	3,13	-
Semicarbazide hydrochloride		1,56	-	2,03	+	2,90	+
Aminotriazole		1,22	0	1,95	+	2,35	+
Chlorambucil		1,62	+	1,50	0	2,19	-
Trifluorothymidine		1,19	0	1,10	0	1,29	0
Diamide		1,07	0	1,14	0	1,19	0

Table S2 Bacterial strains and plasmids.

Strain	Relevant Genotype	Ancestor/ comments	Source or reference
MG1655	wt	K-12 wildtype	(Blattner <i>et al.</i> , 1997)
Tr1-5	<i>csrA::Tn5(kan)</i>	kan ^R	(Romeo <i>et al.</i> , 1993)
AB400	<i>csrA::Tn5(kan)</i>	MG1655 kan ^R	This work
AB955	<i>csrA::Tn5Δ(kan)::Frt ΔpgaABCD::Frt</i>	AB958 kan ^S	This work
AB957	<i>csrA::Tn5Δ(kan)::cat</i>	AB400 kan ^S , cam ^R	This work
AB958	<i>csrA::Tn5Δ(kan)::Frt</i>	AB957 kan ^S , cam ^S	This work
AB959	<i>csrA::Tn5Δ(kan)::Frt ΔydeH::Frt</i>	AB958	This work
AB1000	<i>csrA::Tn5Δ(kan)::Frt rpsL-3(R54C; P91L)</i>	AB958 strp ^D	This work
AB1024	<i>csrA::Tn5Δ(kan)::Frt ΔaraB::Frt</i>	AB958	This work
AB1028	<i>ΔaraB::Frt Para::pgaA</i> (translat. <i>araB-pgaA</i> fusion) <i>csrA</i> ⁺	MG1655	This work
AB1029	<i>csrA::Tn5Δ(kan)::Frt rpsL-1(K43N)</i>	AB958 strp ^R	This work
AB1032	<i>csrA::Tn5Δ(kan)::Frt ΔaraB::Frt ΔpgaABCD::Frt</i>	AB955	This work
AB1035	<i>csrA::Tn5Δ(kan)::Frt rpsL-1(K43N) ΔydeH::Frt</i>	AB1029	This work
AB1041	<i>csrA::Tn5Δ(kan)::Frt ΔfliC::Frt</i>	AB958	This work
AB1056	<i>csrA::Tn5Δ(kan)::Frt ΔrelA::Frt</i>	AB958	This work
AB1057	<i>csrA::Tn5Δ(kan)::Frt ΔrelA::Frt ΔspoT::Frt</i>	AB1056	This work
AB1061	<i>csrA::Tn5Δ(kan)::Frt ΔydeH::Frt ΔaraB::Frt</i>	AB959	This work
AB1062	<i>csrA::Tn5Δ(kan)::Frt pgaD-3xFlag-kan</i>	AB958	This work
AB1063	<i>csrA::Tn5Δ(kan)::Frt ΔydeH::Frt pgaD-3xFlag-kan</i>	AB959	This work
AB1089	<i>csrA::Tn5Δ(kan)::Frt ΔrelA::Frt ΔspoT::Frt ΔydeH::Frt</i>	AB1057	This work
AB1090	<i>csrA::Tn5Δ(kan)::Frt ΔrelA::Frt pgaD-3xFlag-kan</i>	AB1056	This work
AB1091	<i>csrA::Tn5Δ(kan)::Frt ΔrelA::Frt ΔspoT::Frt pgaD-3xFlag-kan</i>	AB1057	This work
AB1092	<i>csrA::Tn5Δ(kan)::Frt ΔrelA::Frt ΔspoT::Frt ΔydeH::Frt pgaD-3xFlag-kan</i>	AB1089	This work
AB1129	<i>csrA::Tn5Δ(kan)::Frt ydeH-3xFlag-kan</i>	AB958	This work
AB1639	<i>csrA::Tn5Δ(kan)::Frt ΔpgaABCD::Frt ΔmhpA-lacI PpgaA-lacZYA</i>	AB955	This work
AB1640	<i>csrA::Tn5Δ(kan)::Frt ΔpgaABCD::Frt ΔmhpA-lacI PpgaA-lacZYA ΔydeH::Frt</i>	AB959	This work
AB1119	<i>csrA::Tn5Δ(kan)::Frt ΔpgaABCD::cat ΔmhpA-lacI PpgaA-lacZYA ΔrelA::Frt</i>	AB1056	This work
AB1120	<i>csrA::Tn5Δ(kan)::Frt ΔpgaABCD::cat ΔmhpA-lacI PpgaA-lacZYA ΔrelA::Frt ΔspoT::Frt</i>	AB1057	This work
AB1594	<i>csrA</i> ⁺ <i>ΔpgaABCD::cat ΔmhpA-lacI::kan PpgaA-lacZYA</i>	MG1655	This work
AB1596	<i>csrA::Tn5Δ(kan)::Frt ΔpgaABCD::cat ΔmhpA-lacI PpgaA-lacZYA ΔnhaR::Frt</i>	AB958	This work
AB1130	<i>csrA::Tn5Δ(kan)::Frt ydeH-3xFlag-kan ΔrelA::Frt</i>	AB1056	This work
AB1131	<i>csrA::Tn5Δ(kan)::Frt ydeH-3xFlag-kan ΔrelA::Frt ΔspoT::Frt</i>	AB1057	This work
AB1132	<i>csrA::Tn5Δ(kan)::Frt ΔrelA::Frt spoT(D259N)</i>	AB1056 SpoT synt	This work
AB1134	<i>csrA::Tn5Δ(kan)::Frt ΔrelA::Frt spoT(D73N)</i>	AB1056 SpoT hyd	This work
AB1212	<i>ydeH-3xFlag-kan</i>	MG1655	This work
AB1299	<i>csrA::Tn5Δ(kan)::Frt ydeH(E208Q)</i>	AB958	This work
AB1417	<i>csrA::Tn5Δ(kan)::Frt pgaA-3xFlag-kan ΔpgaB-D</i>	AB958	This work
AB1419	<i>csrA::Tn5Δ(kan)::Frt ΔydeH::Frt pgaA-3xFlag-kan ΔpgaB-D</i>	AB959	This work
AB1470	<i>csrA::Tn5Δ(kan)::Frt ΔrelA::Frt ΔspoT::Frt pgaA-3xFlag-kan ΔpgaB-D</i>	AB1057	This work

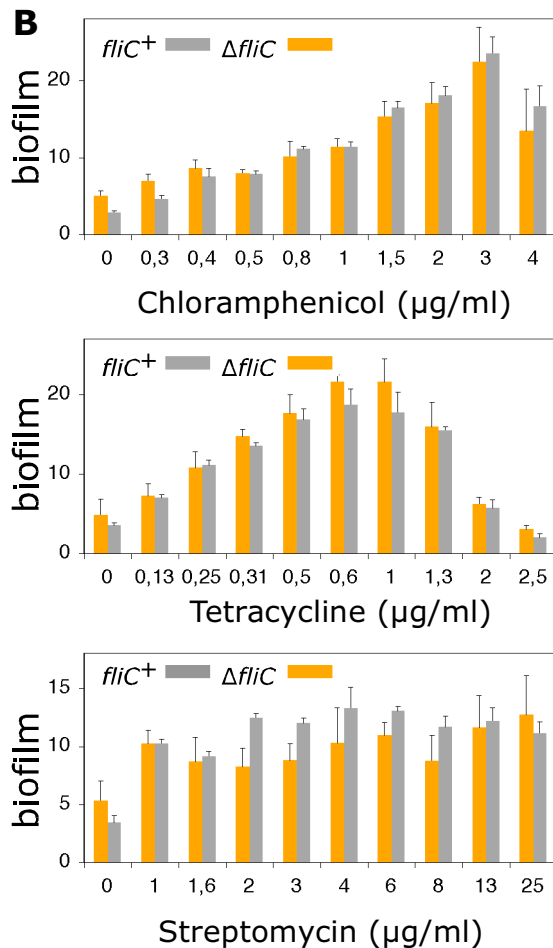
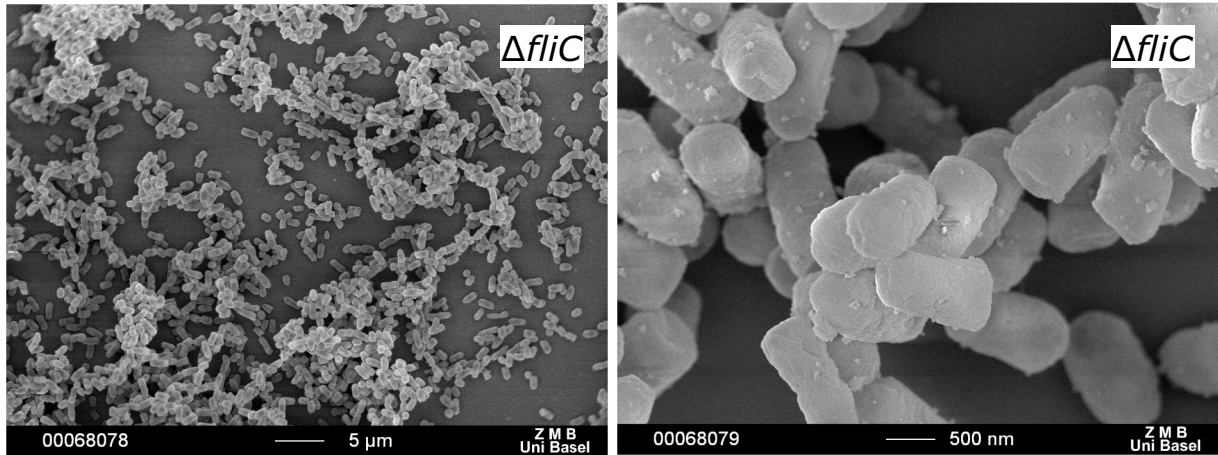
Plasmids

pBAD18	<i>araC⁺ bla⁺ P_{araBAD}</i> (amp ^R)	arabinose inducible expression vector	(Guzman <i>et al.</i> , 1995)
pCJ30	<i>lacI^q bla⁺</i> (amp ^R)	IPTG inducible expression vector	(Bibikov <i>et al.</i> , 1997)
pydeH	pET28:: <i>ydeH</i> -6xHis (kan ^R)	IPTG inducible expression vector	This work
pAB551	pBAD18:: <i>dgcA</i> (amp ^R)	<i>dgcA</i> (cc3285) from <i>C. crescentus</i>	This work; see also (Christen <i>et al.</i> , 2006)
pyliE	pCJ30:: <i>yliE</i> (amp ^R)	<i>yliE</i> from <i>E. coli</i>	This work
pyjcC	pCJ30:: <i>yjcC</i> (amp ^R)	<i>yjcC</i> from <i>E. coli</i>	This work
psecMΔN	pCJ30:: <i>secMΔN</i> (amp ^R)	SecM lacking amino acids 1-40	This work
pmazE	pBAD18:: <i>mazE</i> (amp ^R)	Translation targeting toxin	R. Hallez
pyoeB	pBAD18:: <i>yoeB</i> (amp ^R)	Translation targeting toxin	R. Hallez
preIE	pBAD18:: <i>relE</i> (amp ^R)	Translation targeting toxin	R. Hallez

Table S3 Primer list.

Name	Sequence 5'→3'	Function/reference
86	AGGGTTTTCCCAGTCACGACG	sequencing <i>lacZ</i> fusions
1545	GTGCAGAGCCCAGGCGAACCGGGCTTTGTTTTGGGTGTTTATGCC CGTCACATATGAATATCCTCCTTAG	<i>ΔpgaABCD</i> mutant according to (Datsenko & Wanner, 2000)
1546	TAATTAGATACAGAGAGAGATTTTGGCAATACATGGAGTAATAC AGGTGTGTAGGCTGGAGCTGCTTC	
1651	GCCGGACCAGATGATCAACATTAGTGG	<i>ydeH</i> E208Q point mutant fwd primer in SOE PCR
1652	TGACTAATGAACGGAGATAATCCCTCACC	<i>ydeH</i> E208Q point mutant rev primer in SOE PCR
1655	GAAATCGCTGCATGTTTTATTGACGAACAAAATGTGATTAACCGAG TTTTCGACTACAAAGATGACGAC	constructing 3xFlag-tag <i>ydeH</i> according to (Uzzau <i>et al.</i> , 2001)
2225	AATCGCTGCATGTTTTATTGACGAACAAAATGTGATTAACCGAGTT TTCGACTACAAAGACCATGACGG	
1665	AACAATTTAATTATTACGACCCGACAATCACC	sequencing <i>pgaD-3xF</i>
1938	CCGGGAGCTGCATGTGTGACAGG	sequencing pCJ30 inserts
1939	ATACCGCGAAAGGTTTTGCGCC	sequencing pCJ30 inserts
1975	GAGCCATATTCAACGGGAAACGTCTTGCTCGAGGCCGCGATTAAT GTAGGCTGGAGCTGCTTCG	exchanging kan cassette in AB400 for cat cassette
1976	AAAACATCGAGCATCAAATGAAACTGCAATTTATTCATATCAC ATATGAATATCCTCCTTAG	
2035	ATAGTTCCCATCATCAGCCCAACCGGGCCGGCACCAGCTCATT CGAACCCAGAGTCCCGC	inserting a counter-selectable marker in front of the <i>lac</i> locus according to (Datsenko & Wanner, 2000)
2037	CCACACAACATACGAGCCGGAAGCATAAAGTGTAAGCCTACCC GGATATTATCGTGAGGATGCG	
2041	TTTGGTTTTCGGGCACCTTTTTCTGCTACTTGAATACATCGTTTCA CTCCATCCAAAAAACGG	constructing a translational <i>araB-pgaA</i> fusion according to (Datsenko & Wanner, 2000)
2042	TAACAATTAATCCGTGAGTGCCGTAGCGCAGCCTTTCACATATG AATATCCTCCTTAGTTCCTATTCCG	
2051	TCGCTTGCTGCTCCGGAAGTAGTCGAGGCCATGGTGGCCGCTAC ACCAATCTGTAGGTTGTAGATCCC	replacing counter-selectable marker in front of <i>lac</i> with <i>pga</i> promoter to create <i>PpgaA-lacZ</i> fusion according to (Datsenko & Wanner, 2000)
2053	CGTTGTAACGACGGCCAGTGAATCCGTAATCATGGTCATCCTG TATACTCCATGTATTGCC	
2055	CCGAATAGCCTCTCCACCCAAGC	sequencing <i>araB-pgaA</i> fusion, <i>PpgaA-lacZ</i> fusion, <i>pgaA-3xF</i> and <i>pgaD-3xF</i>
2056	AACTGCAGAACGCGCCCGCAAAGCGACAAC	<i>secMΔN</i> cloning (PstI fwd)
2057	GGGGTACCTTAGGTGAGGCGTTGAGGGCCAGC	<i>secMΔN</i> cloning (KpnI rev)
2062	GGACTCGCTGCTAAAAATGCGGC	sequencing <i>araB-pgaA</i> fusion
2107	CTAAAATTCGGCGTCCATATTG	sequencing <i>rpsL</i>
2108	TGTTAATTCAGGATTGTCCAAAACCTC	sequencing <i>rpsL</i>
2125	TGCTGAAGGTCGTCGTTAATCACAAGCGGGTCGCCCTTGATCT GTTTTGTAGGCTGGAGCTGCTTCG	<i>spoT</i> deletion according to (Datsenko & Wanner, 2000)
2126	GTTGGGTTCAAAAACATTAATTTCCGGTTTCGGGTGACTTTAATC ACATATGAATATCCTCCTTAG	
2141	ACGTTCCGGCACTTTGCCAACGTACGCTGCATGCCTACAGTTAAGT GTTACATATGAATATCCTCCTTAG	constructing of 3xFlag-tag <i>pgaD</i> according to (Uzzau <i>et al.</i> , 2001)
2142	CCAGGGGCAAATAAAAATGGTTGTTTCAGAAAAAGCGCTAGTCC GGGCATTCGACTACAAAGACCATGAC	
2143	GCGCTGCGCGAAATCGAAGAAG	<i>spoT</i> upstream fwd (sequencing, confirming deletion, SOE-PCR fwd)
2144	TACGCCAACGGCATCTGCGGTAC	<i>spoT</i> downstream rev (sequencing, confirming deletion)
2178	CATGCCATGGCTATCAAGAAGACAACGGAAATTGATGCCATC	cloning <i>ydeH</i> into pET28 (NcoI fwd)
2179	AACCGCTCGAGAACTCGGTTAATCACATTTTGTTCGTCAATAAAC	cloning <i>ydeH</i> into pET28 (XhoI rev)

2200	CACCACATTA AAAACCGAACTCG	sequencing <i>spoT</i>
2201	TCGAGAGCGTTAAATCCGATCTC	sequencing <i>spoT</i>
2211	GTTGCCTGCATTCTGGCCGAGATGAACTCGACTATGAAACGCTG TCATTTCGAACCCAGAGTCCCGC	replacing <i>spoT</i> with a counter-selectable marker according to (Datsenko & Wanner, 2000)
2212	CAGGCTGTGCATCTGGCCCAGCACGCGATAACAGGTGTCAGAAT CACCCGATATTATCGTGAGGATGCG	
2213	GCGCTGCTGCATAACGTGATTGAAGATAC	<i>spoT</i> point mutant D73N
2214	GTATCTCAATCACGTTATGCAGCAGCGC	<i>spoT</i> point mutant D73N
2215	CACTCGATCATGAACATCTACGCTTTCCG	<i>spoT</i> point mutant D259N
2216	CGGAAAGCGTAGATGTTTCATGATCGAGTG	<i>spoT</i> point mutant D259N
2217	ATAAGCGAAGTCGACGGGCGTTGC	<i>spoT</i> rev (sequencing, SOE-PCR rev)
2221	GACAGAGAACAACAATTATACGTTGAATTCGATATGACATTCAGA TTTTTCGACTACAAAGACCATGAC	constructing of 3xFlag-tag <i>pgaA</i> according to (Uzzau et al., 2001)
2224	GTGCAGAGCCCGGGCGAACC GGGCTTTGTTTTGGGTGTTTATGCC CGTACATATGAATATCCTCCTTAG	
2269	GATCAAGAAGACAACGAAATTGATGCCATCTTGTTAAATCTCAA TTCATTTCGAACCCAGAGTCCCGC	replacing <i>ydeH</i> with a counter-selectable marker according to (Datsenko & Wanner, 2000)
2270	TTCTGACACCTGCACGACATGCTTCTTCATCATTAGCCGCTTTGAA CCCGGATATTATCGTGAGGATGCG	
2271	CGCTACGGGGGCAAGAATTTATC	<i>ydeH</i> point mutant E208Q (SOE-PCR)
2272	GATAAATCTTGGCCCCCGTAGCG	

A**Figure S1**

Flagella are not relevant for biofilm induction by translation inhibitors.

A. Scanning electron micrographs of a biofilm formed by a flagellar mutant (*csrA*::Tn5 *ΔfliC*). Please note the absence of any filamentous structures. Scale bars are indicated.

B. Translation inhibitor-mediated biofilm induction of a flagellar mutant (*csrA*::Tn5 *ΔfliC*, orange) is compared to the ancestral strain (*csrA*::Tn5 *fliC*⁺, grey). Bars represent normalized biofilm values with standard errors of the mean. Representative antibiotics and their concentrations are indicated.

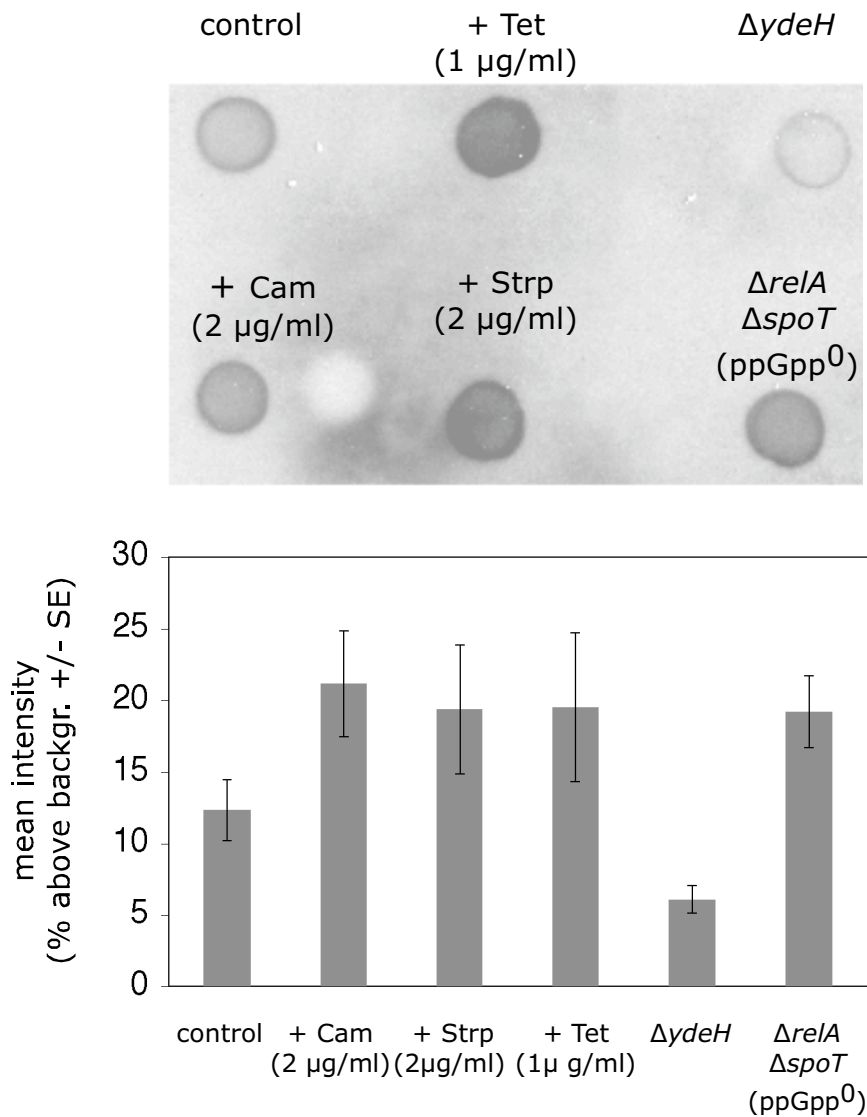


Figure S2

Poly-GlcNAc production is controlled by ppGpp, c-di-GMP and antibiotics.

Top: A representative immuno dot-blot is shown. Bottom: Bars show mean intensities (normalized to background) of six independent experiments (see material and methods). All strains are *csrA::Tn5*. Relevant genotypes and the presence of antibiotics are indicated. The *csrA::Tn5* strain grown in the absence of antibiotics is significantly different from all other treatments (general linear model with Dunnett post-hoc analysis, $p < 0,002$ for all comparisons; see material and methods).

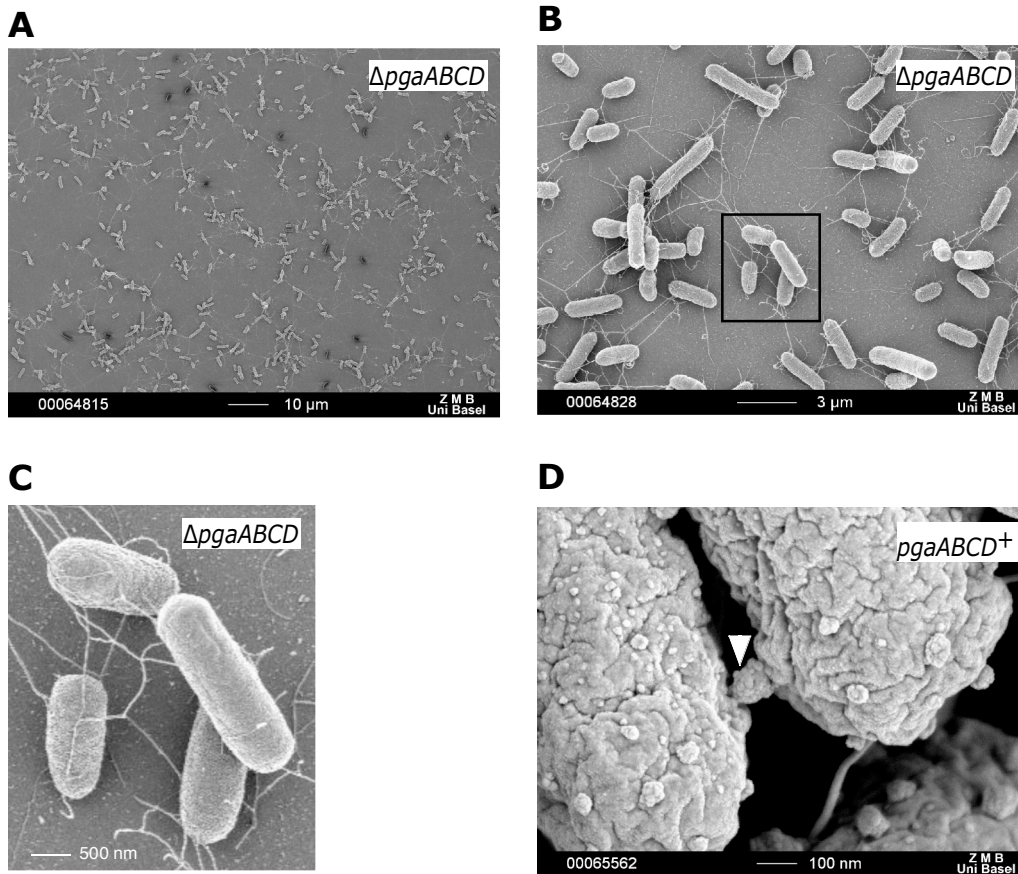


Figure S3

Cell surface-associated spheres depend on the presence of the *pgaABCD* genes.

A, B and C. Scanning electron micrographs of a *csrA::Tn5 ΔpgaABCD* strain at different magnifications. The boxed area in B is reproduced at higher magnification in C. Note the absence of any poly-GlcNAc spheres on cell surfaces in B and C and the absence of any biofilm formation in A.

D. Scanning electron micrograph at high magnification of a typical poly-GlcNAc sphere (indicated by an arrow) bridging two cells of a *csrA::Tn5* strain exposed to 2 μg/ml chloramphenicol.

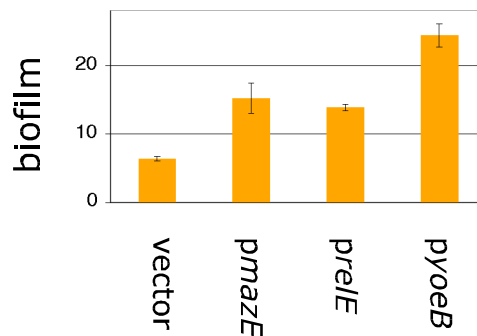


Figure S4

Plasmid-mediated overproduction of three different ribosome targeting toxins leads to biofilm induction.

Normalized biofilm values are indicated. Toxins were overproduced from pBAD18-derived plasmids in a *csrA::Tn5* strain. 0,2% L-arabinose was present in the culture medium. Error bars are SEM.

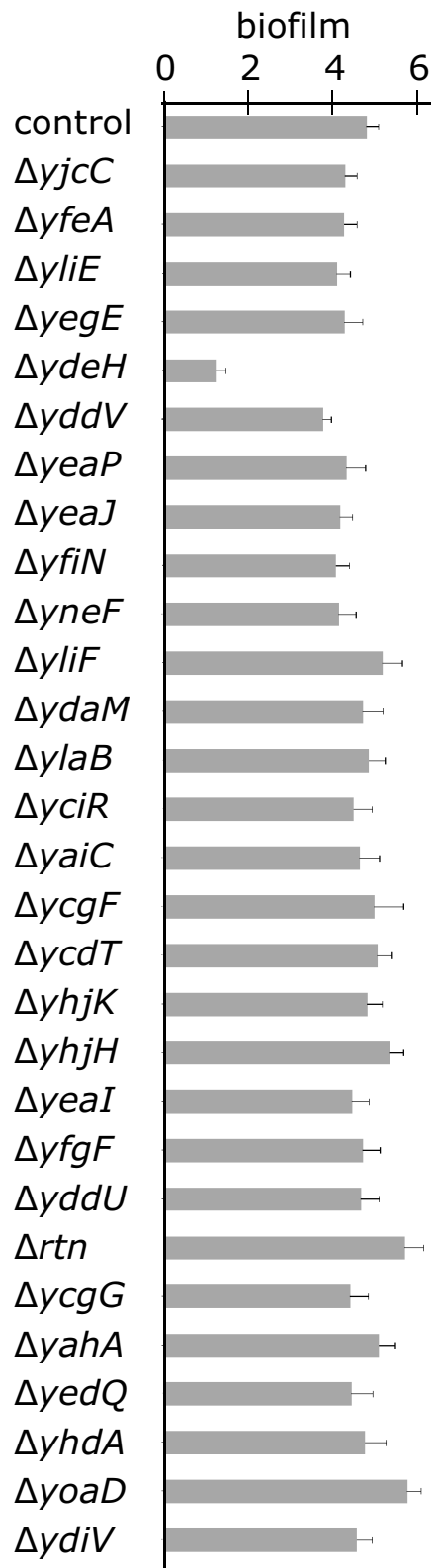


Figure S5

The $\Delta ydeH$ mutant displays a biofilm phenotype.

Normalized biofilm values for 29 in frame deletion mutants, representing all predicted GGDEF and/or EAL domain proteins, are displayed. All strains are *csrA::Tn5*. Error bars are standard deviations.

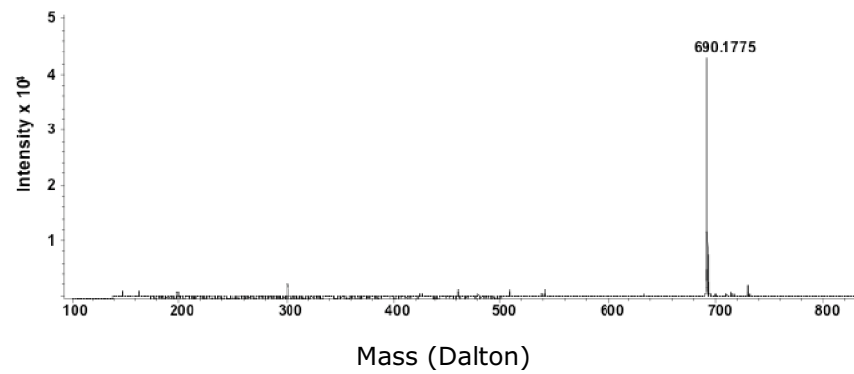


Figure S6

YdeH possesses diguanylate cyclase activity.

Mass spectrogram of solute after incubation of purified YdeH with GTP for 30 min. The single peak corresponds to the molecular mass of c-di-GMP.

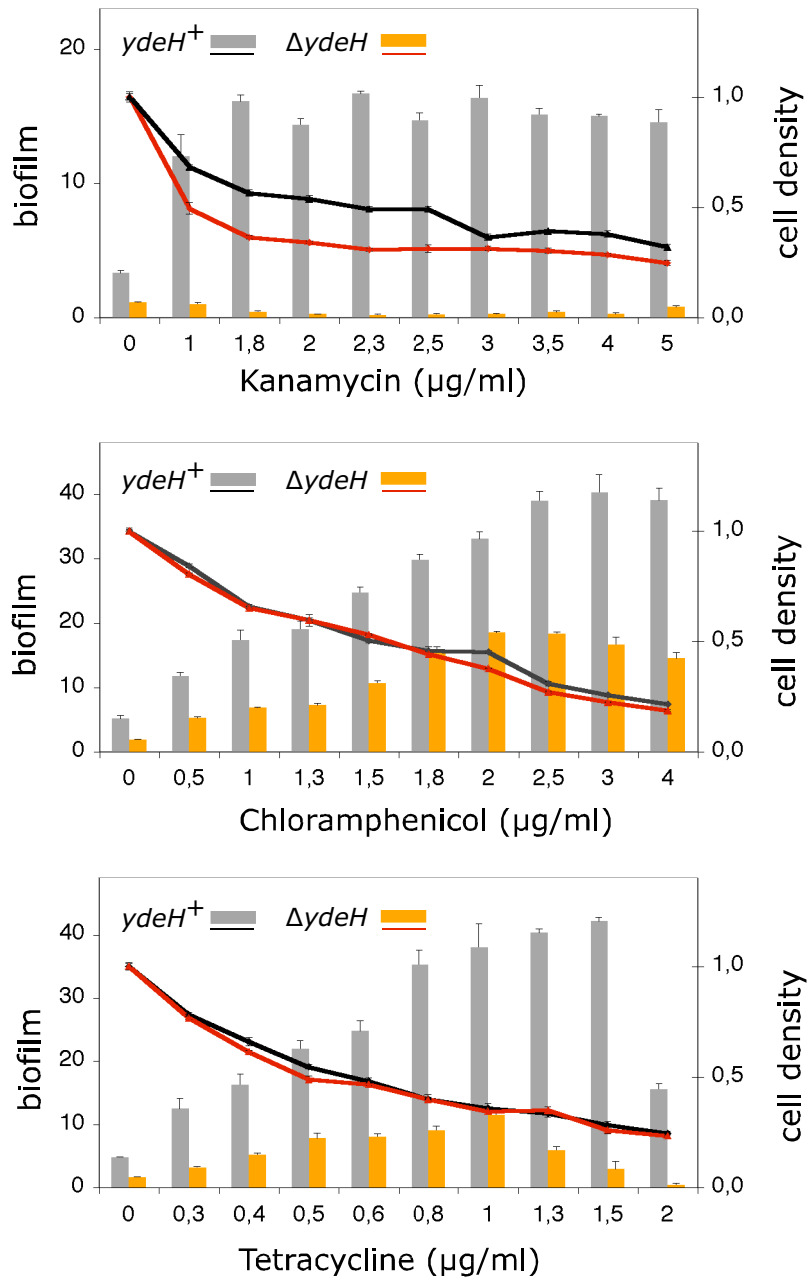


Figure S7

YdeH is essential for aminoglycoside-mediated biofilm induction and involved in tetracycline- and chloramphenicol-mediated biofilm induction. Biofilm formation of a *csrA*::Tn5 $\Delta ydeH$ strain (orange bars, red curves) is compared to the isogenic *ydeH*⁺ ancestor (grey bars, black curves) in the presence of the indicated antibiotics. Bars represent biofilm formation (surface attached biomass divided by optical density of total cells) with standard errors of the mean (SEM). Biofilm values are indicated on the left Y-axis. Curves represent relative optical density of total cells (optical density divided by the value of optical density in the absence of antibiotics) with standard errors. Values for normalized cell density are indicated on the right Y-axis.

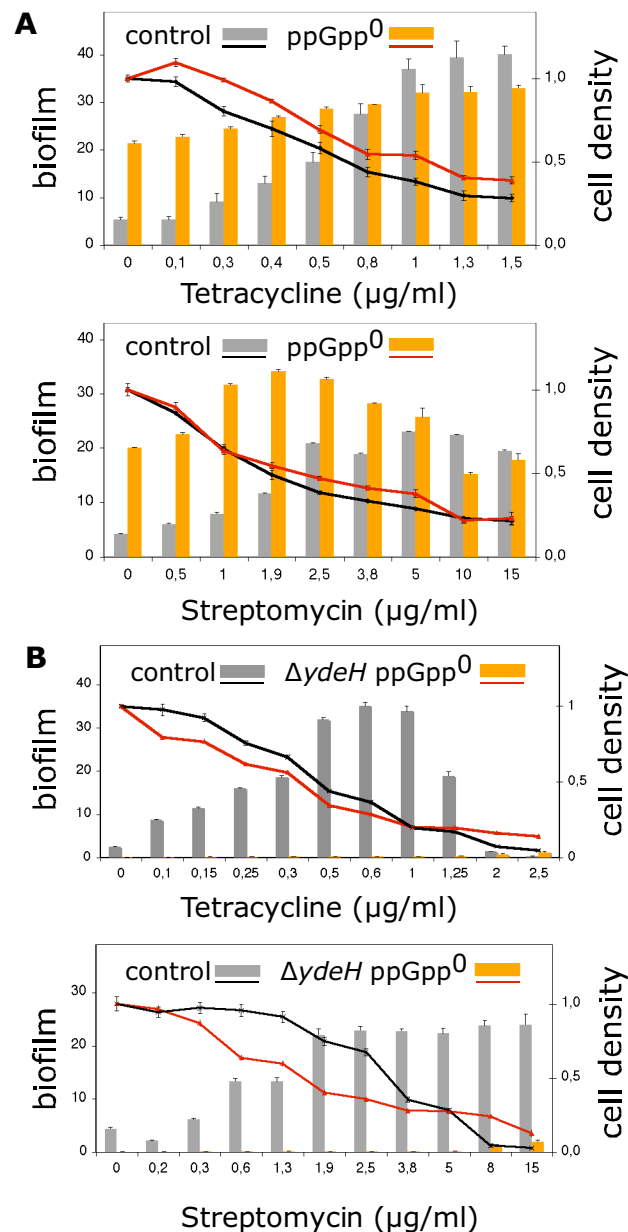


Figure S8

A. A *ppGpp⁰* strain shows aberrant biofilm induction upon treatment with translation inhibitors. Biofilm formation of a *csrA::Tn5 ΔrelA ΔspoT* strain (orange bars, red curves) is compared to the isogenic *relA⁺ spoT⁺* ancestor (grey bars, black curves) in the presence of the indicated antibiotics. Bars represent biofilm formation (surface attached biomass divided by optical density of total cells) with standard errors of the mean (SEM). Biofilm values are indicated on the left Y-axis. Curves represent relative optical density of total cells (optical density divided by the value of optical density in the absence of antibiotics) with standard errors. Values for normalized cell density are indicated on the right Y-axis.

B. Biofilm formation of a *ppGpp⁰ ΔydeH* mutant is diminished and cannot be induced by tetracycline or streptomycin.

Biofilm formation of a *csrA::Tn5 ΔrelA ΔspoT ΔydeH* strain (orange bars, red curves) is compared to the isogenic *relA⁺ spoT⁺ ydeH⁺* ancestor (grey bars, black curves) in the presence of the indicated antibiotics. Bars represent biofilm formation (surface attached biomass divided by optical density of total cells) with standard errors of the mean (SEM). Biofilm values are indicated on the left Y-axis. Curves represent relative optical density of total cells (optical density divided by the value of optical density in the absence of antibiotics) with standard errors. Values for normalized cell density are indicated on the right Y-axis.

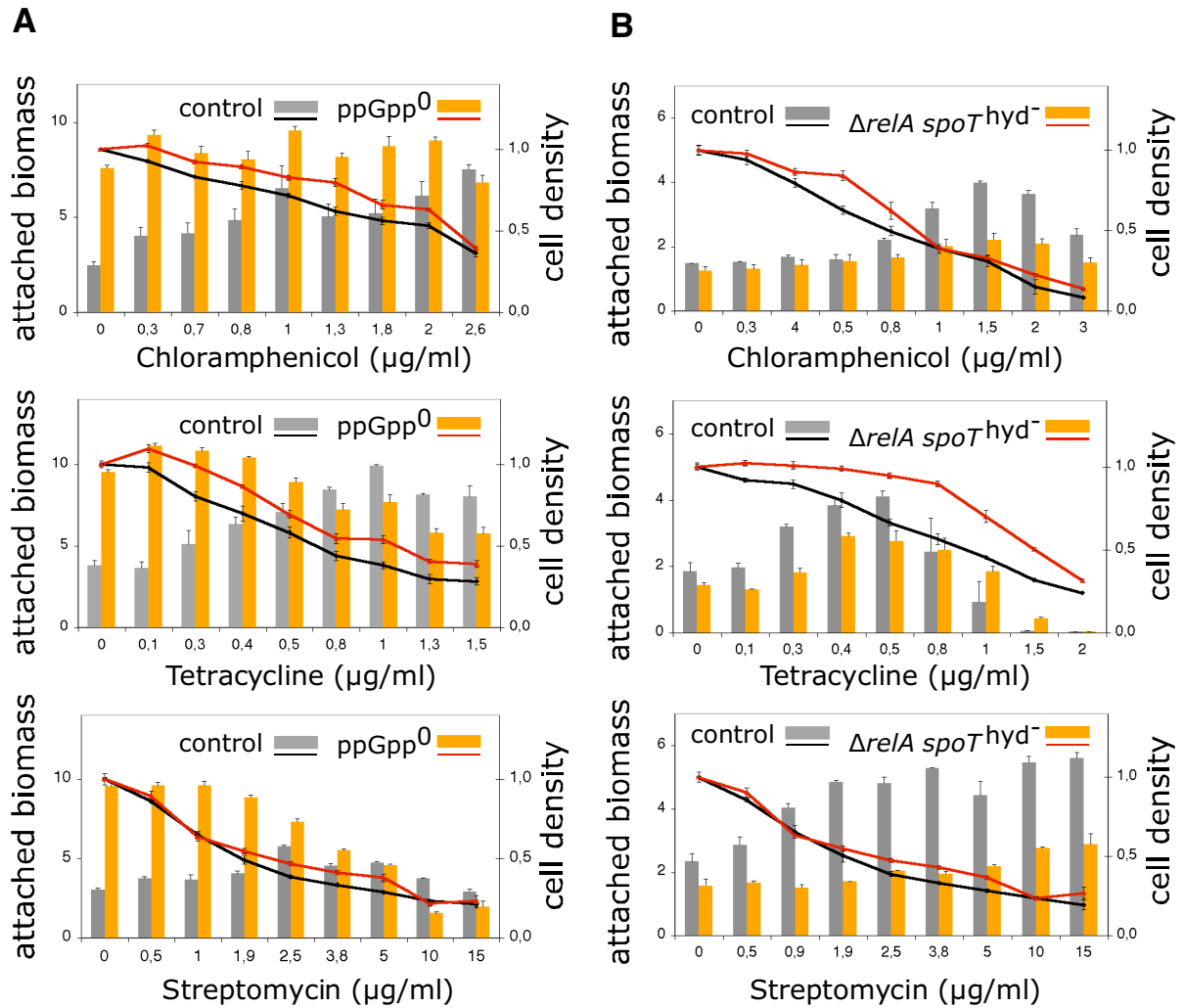


Figure S9

A. The attached biomass of a *ppGpp⁰* strain shows marginal increases upon treatment with translation inhibitors.

Attached biomass of a *csrA::Tn5 ΔrelA ΔspoT* mutant (orange bars, red curves) is compared to its isogenic *relA⁺ spoT⁺* ancestor (grey bars, black curves) in the presence of the indicated antibiotics. Bars represent surface attached biomass (not divided by optical density of the cells) with standard errors of the mean. Attached biomass values are indicated on the left Y-axis. Curves represent relative optical density of total cells (optical density divided by the value of optical density in the absence of antibiotics) with standard errors. Values for normalized cell density are indicated on the right Y-axis.

B. *SpoT* *ppGpp* hydrolase activity is required for full induction of surface attached biomass upon treatment with translation inhibitors.

Attached biomass of a *csrA::Tn5 ΔrelA spoT(D73N) ppGpp* hydrolase mutant (orange bars, red curves) is compared to its isogenic *spoT^{WT}* ancestor (grey bars, black curves) in the presence of the indicated antibiotics. Bars represent surface attached biomass (not divided by optical density of the cells) with standard errors of the mean. Attached biomass values are indicated on the left Y-axis. Curves represent relative optical density of total cells (optical density divided by the value of optical density in the absence of antibiotics) with standard errors. Values for normalized cell density are indicated on the right Y-axis. Please note that the biofilm data in Figure S9 are not normalized to cell density. For an explanation see the section biofilm assay in material and methods.

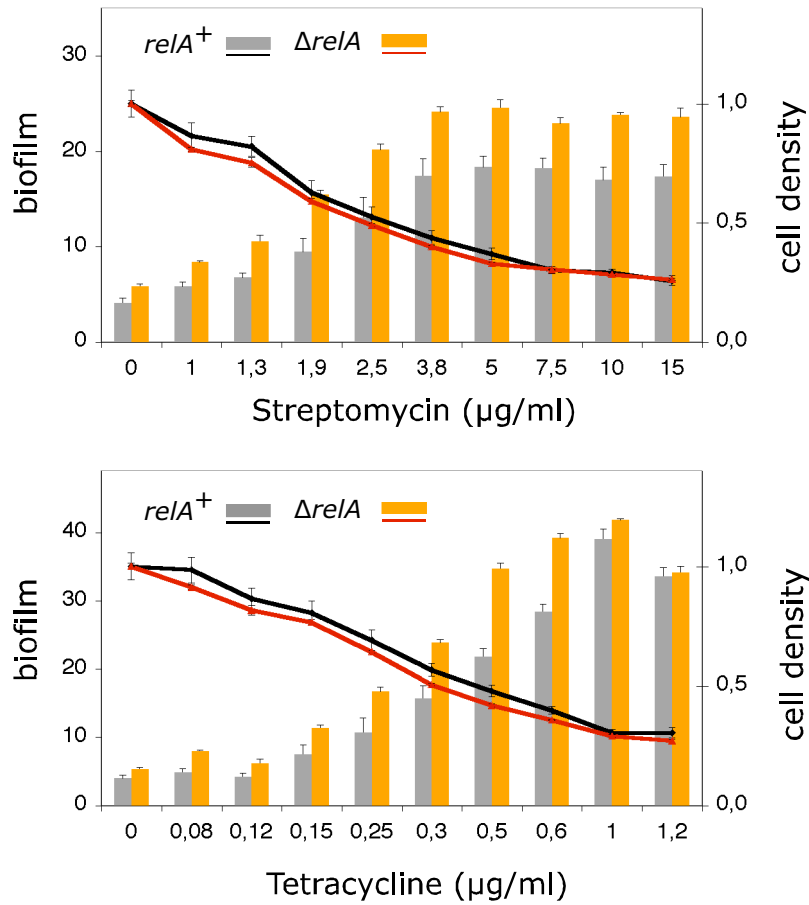


Figure S10

RelA is not required for antibiotic-mediated biofilm induction.

Biofilm formation of a *csrA*::Tn5 *ΔrelA* strain (orange bars, red curves) challenged with two different translation inhibitors is compared to a *relA*⁺ control (grey bars, black curves).

Bars represent biofilm formation (surface attached biomass divided by optical density of total cells) with standard errors of the mean (SEM). Biofilm values are indicated on the left Y-axis. Curves represent relative optical density of total cells (optical density divided by the value of optical density in the absence of antibiotics) with standard errors. Values for normalized cell density are indicated on the right Y-axis.

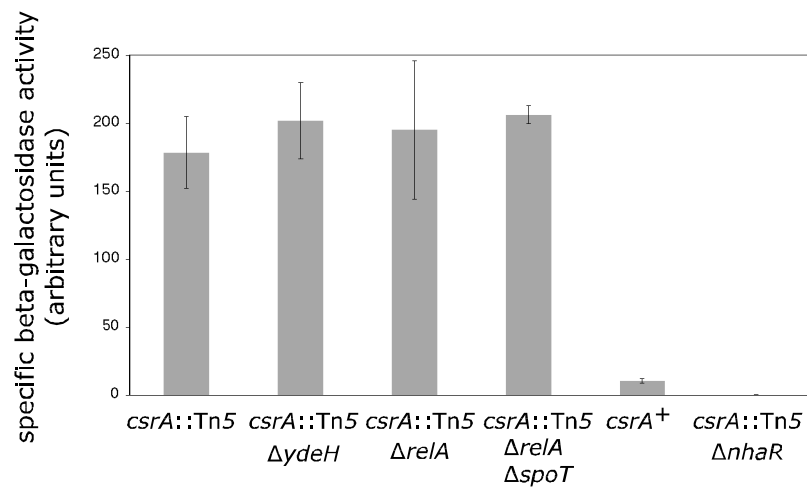


Figure S11

The activity of a translational *pgaA-lacZ* fusion is controlled by NhaR and CsrA but not by c-di-GMP or ppGpp.

Specific beta-galactosidase activity of a single copy translational *pgaA-lacZ* fusion that is integrated at the *lac* locus is shown. Relevant genotypes are indicated. Beta-galactosidase assays were carried out in microtiter plates according to (Slauch & Silhavy, 1991).

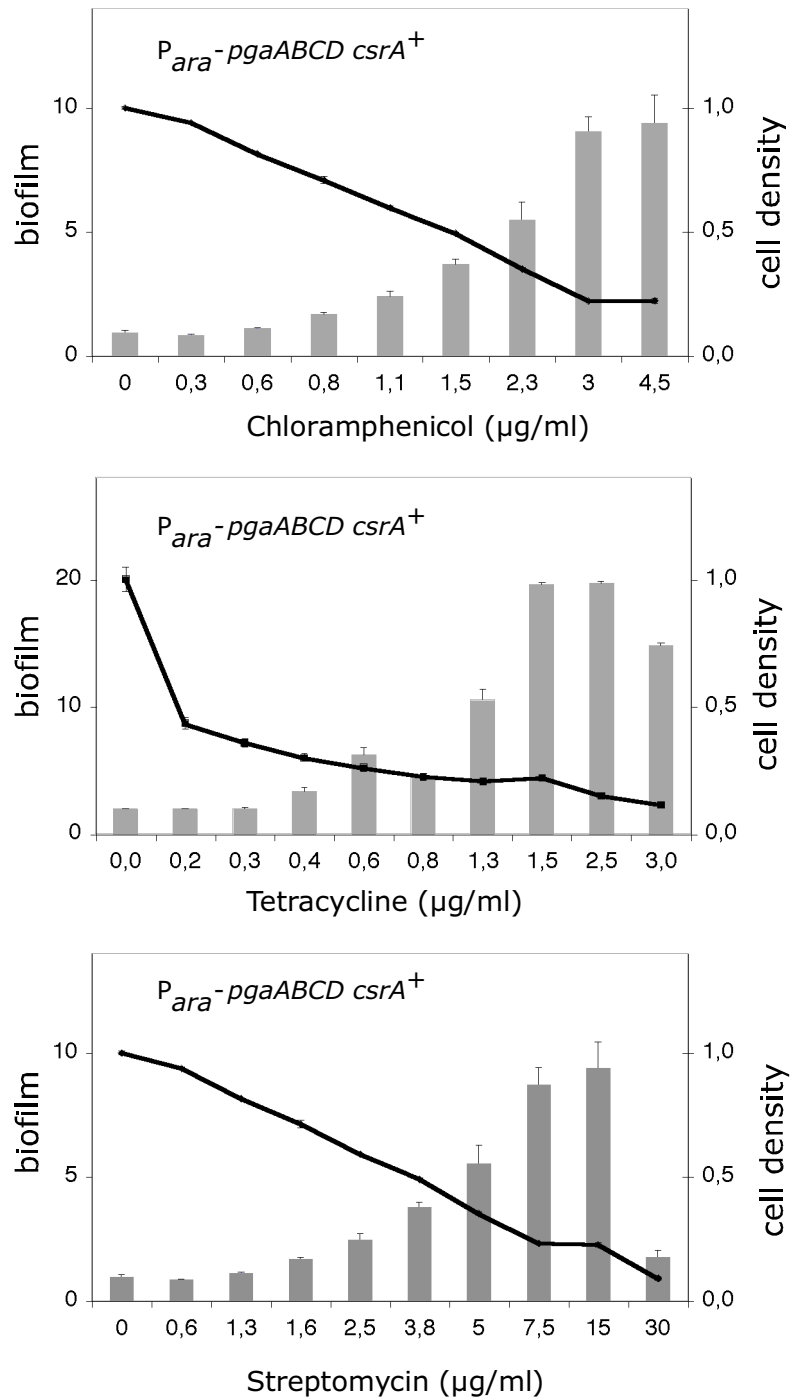


Figure S12

Antibiotic-mediated induction of poly-GlcNAc-dependent biofilm formation is independent of the *csrA::Tn5* allele and independent of the *pgaA* promoter and 5' untranslated region.

Biofilm formation of a *csrA*⁺ strain that allows ectopic *pgaABCD* expression from a L-arabinose-dependent *Para* promoter is shown in response to challenges with three different translation inhibitors. 0,02% L-arabinose was present. Bars represent biofilm formation (surface attached biomass divided by optical density of total cells) with standard errors of the mean (SEM). Biofilm values are indicated on the left Y-axis. Curves represent relative optical density of total cells (optical density divided by the value of optical density in the absence of antibiotics) with standard errors. Values for normalized cell density are indicated on the right Y-axis.

Supplemental references

- Bibikov, S. I., R. Biran, K. E. Rudd & J. S. Parkinson, (1997) A signal transducer for aerotaxis in *Escherichia coli*. *J. Bacteriol.* 179: 4075-4079.
- Blattner, F. R., G. Plunkett, C. A. Bloch, N. T. Perna, V. Burland, R. M., J. Collado-Vides, J. D. Glasner, C. K. Rode, G. F. Mayhew, J. Gregor, N. W. Davis, H. A. Kirkpatrick, M. A. Goeden, D. J. Rose, B. Mau & Y. Shao, (1997) The complete genome sequence of *Escherichia coli* K-12. *Science* 277: 1453-1462.
- Christen, B., M. Christen, R. Paul, F. Schmid, M. Folcher, P. Jenoe, M. Meuwly & U. Jenal, (2006) Allosteric control of cyclic di-GMP signaling. *J Biol Chem* 281: 32015-32024.
- Guzman, L. M., D. Belin, M. J. Carson & J. Beckwith, (1995) Tight regulation, modulation, and high-level expression by vectors containing the arabinose PBAD promoter. *J. Bacteriol.* 177: 4121-4130.
- Romeo, T., M. Gong, M. Y. Liu & A. M. Brunzinkernagel, (1993) Identification and Molecular Characterization of *csrA*, a Pleiotropic Gene from *Escherichia-Coli* That Affects Glycogen Biosynthesis, Gluconeogenesis, Cell Size, and Surface Properties. *Journal of Bacteriology* 175: 4744-4755.
- Slauch, J. M. & T. J. Silhavy, (1991) *cis*-Acting *ompF* Mutations That Result in *OmpR*-Dependent Constitutive Expression. *Journal of Bacteriology* 173: 4039-4048.

3.2 *Allosteric activation of exopolysaccharide synthesis through cyclic di-GMP-mediated protein-protein interplay in Escherichia coli*

Samuel Steiner, Christian Lori, Alex Boehm and Urs Jenal

In preparation for submission.

Statement of my work: Most of the experiments of this manuscript were performed by myself, while some were done by or in collaboration with Christian Lori, a Master student under my supervision.

Allosteric activation of exopolysaccharide synthesis through cyclic di-GMP-mediated protein-protein interplay in *Escherichia coli*

Samuel Steiner¹, Christian Lori¹, Alex Boehm² and Urs Jenal¹

Affiliations:

¹Biozentrum, University of Basel, Klingelbergstrasse 50/70, CH-4056 Basel, Switzerland

²Institut für Molekulare Infektionsbiologie, Universität Würzburg, Josef-Schneider-Str. 2/D15, D-97080 Würzburg, Germany

For correspondence: urs.jenal@unibas.ch

Abstract

Poly- β -1,6-*N*-acetylglucosamine (poly-GlcNAc) is a major component of the extracellular matrix of *Escherichia coli* biofilms and is known to contribute to bacterial survival in the animal host. Expression of the Pga machinery that promotes the synthesis and secretion of poly-GlcNAc is regulated via the global Csr cascade in response to metabolic signals. Here, we show how the nucleotide second messenger cyclic di-GMP (c-di-GMP) allosterically controls poly-GlcNAc-dependent biofilm formation. C-di-GMP mediates the formation of a tight complex between PgaC and PgaD, the two inner membrane components of the Pga machinery. We report that c-di-GMP directly binds to the PgaCD complex and allosterically stimulates its glycosyltransferase activity. We present biochemical and genetic data to suggest that the PgaCD machinery is a novel type c-di-GMP receptor, where ligand binding to two individual proteins stabilizes their interaction and subsequently promotes enzyme activation. PgaD fails to interact with PgaC at low cellular c-di-GMP concentrations and, as a result, is rapidly degraded. Based on this, we propose that the Pga machinery is irreversibly switched off through the accessory protein PgaD in response to c-di-GMP fluctuations, thereby temporarily uncoupling it from c-di-GMP signalling. These data not only unravel the mechanism of c-di-GMP-mediated poly-GlcNAc biosynthesis control, but also provide a frame for the molecular basis of specificity of c-di-GMP signalling systems.

Introduction

Most bacteria can switch from a motile planktonic 'lifestyle' to growth in surface-associated multicellular communities known as biofilms. Within these structures, cells are encased in a self-produced extracellular polymeric matrix that is typically composed of proteinaceous adhesin factors, DNA and exopolysaccharides (EPS) (Branda *et al.*, 2005; Flemming & Wingender, 2010). This complex biofilm structure is known to protect bacteria from antimicrobials, physical stresses and the predation by the host immune system. Bacterial biofilms are often associated with chronic infections and infection relapses causing health problems of growing importance (Costerton *et al.*, 1999; Mah & O'Toole, 2001; Davies, 2003; Hall-Stoodley *et al.*, 2004; Fux *et al.*, 2005; Lewis, 2010).

The bacterial second messenger bis-(3'-5')-cyclic dimeric GMP (c-di-GMP) is well known for its central role in integrating environmental and cellular cues to control the 'lifestyle' transition by disfavoring motility and single cell behavior and by promoting biofilm formation. The small molecule c-di-GMP is synthesized from GTP by diguanylate cyclases (DGCs) that harbor a conserved GGDEF domain (Paul *et al.*, 2004) and is degraded to pGpG by specific phosphodiesterases (PDEs) that typically harbor a conserved EAL domain (Christen *et al.*, 2005; Hengge, 2009; Schirmer & Jenal, 2009). While DGCs and PDEs have been analyzed in detail, both structurally and functionally, little is known about how c-di-GMP acts on downstream targets. Only a few c-di-GMP-specific receptor protein families have been described up to now, for most of which no mechanistic details are available (Sondermann *et al.*, 2011).

In *Escherichia coli*, c-di-GMP regulates several cellular processes including EPS production, fimbriae biogenesis, flagellar-based motility and RNA degradation (Pesavento *et al.*, 2008; Monteiro *et al.*, 2009; Boehm *et al.*, 2009; Tagliabue *et al.*, 2010; Boehm *et al.*, 2010; Paul *et al.*, 2010; Fang & Gomelsky, 2010; Tuckerman *et al.*, 2011; Povolotsky & Hengge, 2012). To colonize surfaces, *E. coli* produces the EPS poly- β -1,6-*N*-acetylglucosamine (poly-GlcNAc) (Wang *et al.*, 2004). This linear homopolymer was recently implicated in biofilm formation in a wide variety of pathogenic bacteria including *Staphylococcus epidermidis* and *S. aureus* (Mack *et al.*, 1996; O'Gara, 2007), *Yersinia pestis* (Hinnebusch *et al.*, 1996; Bobrov *et al.*, 2008), *Actinobacillus pleuropneumoniae* (Izano *et al.*, 2007), *Aggregatibacter actinomycetemcomitans* (Izano *et al.*, 2008), *Acinetobacter baumannii* (Choi *et al.*, 2009), *Bordetella* spp. (Parise *et al.*, 2007; Conover *et al.*, 2010), *Pectobacterium atrosepticum* (Pérez-Mendoza *et al.*, 2011), *Chromobacterium violaceum* (Becker *et al.*, 2009) and *Burkholderia* spp. (Yakandawala *et al.*, 2011). In many of these species, poly-GlcNAc promotes virulence and contributes to survival in the animal host (Maira-Litrán *et al.*, 2005; Cerca *et al.*, 2007; Bentancor *et al.*, 2012; Skurnik *et al.*, 2012).

In *E. coli*, poly-GlcNAc is synthesized and secreted by the cell envelope-spanning Pga machinery, which is encoded by the *pgaABCD* operon (Wang *et al.*, 2004). While PgaA and PgaB are required for poly-GlcNAc export, PgaC and PgaD are necessary for poly-GlcNAc synthesis (Itoh *et al.*, 2008). PgaA is an outer membrane porin that serves to translocate growing poly-GlcNAc chains to the cell surface (Itoh *et al.*, 2008). PgaB is a putative outer membrane lipoprotein that harbors a deacetylase domain, which deacetylates about 3% of the GlcNAc residues during poly-GlcNAc export (Wang *et al.*, 2004; Itoh *et al.*, 2008). PgaC is a putative inner membrane processive β -glycosyltransferase (GT) of the GT-2 family with a conserved 'D, D, D35QXXRW' motif that polymerizes poly-GlcNAc from activated UDP-GlcNAc precursor (Saxena & Brown, 1997; Wang *et al.*, 2004; Itoh *et al.*, 2008). The catalytic domain of GT-2 family members is exposed to the cytoplasm (Heldermon *et al.*, 2001; Ciocchini *et al.*, 2006; Bobrov *et al.*, 2008) and sugar transfer through the cytoplasmic membrane is thought to function independently of an undecaprenyl phosphate lipid carrier (Gerke *et al.*, 1998). Finally, PgaD is a small protein with two predicted N-terminal transmembrane helices. Its function is unknown and it does not show any obvious similarity to other protein families or domains. However, because PgaD is essential for poly-GlcNAc synthesis (Wang *et al.*, 2004), it was suggested to assist the GT in polymerizing poly-GlcNAc (Itoh *et al.*, 2008). The small protein IcaD of *S. epidermidis* is required to fully activate the IcaA GT *in vitro* (Gerke *et al.*, 1998). Even though PgaD and IcaD are not related in sequence, these proteins may function similarly.

The expression of the *E. coli pgaABCD* operon is tightly regulated on multiple levels. Most importantly, *pgaABCD* translation is repressed by the action of the RNA binding protein CsrA (carbon storage regulator A) (Wang *et al.*, 2005). CsrA is a global regulator that controls numerous cellular pathways including carbon metabolism, virulence, motility and EPS production. Its activity is firmly regulated via a complex signal transduction cascade (Romeo *et al.*, 1993; Suzuki *et al.*, 2006; Babitzke & Romeo, 2007; Timmermans & Van Melderren, 2010). Apart from repressing the *pga* operon, CsrA represses the two genes *ydeH* and *ycdT* that encode DGCs (Jonas *et al.*, 2008). The observation that YdeH stimulates poly-GlcNAc-dependent biofilm formation (Boehm *et al.*, 2009) argued that the expression of this DGC and its target, the Pga machinery, is coupled via CsrA. Although it was shown that YdeH and c-di-GMP control poly-GlcNAc biogenesis on a post-transcriptional level (Boehm *et al.*, 2009), the mechanism responsible for this induction is unknown.

In this paper, we unravel a novel allosteric mechanism through which c-di-GMP stimulates poly-GlcNAc-dependent biofilm formation in *E. coli*. We show that c-di-GMP allosterically activates the PgaCD GT complex. We present genetic and biochemical evidence arguing that c-di-

GMP binds to both components of the Pga machinery, thereby mediating their tight interaction and GT activation. Finally, we demonstrate that in the absence of c-di-GMP PgaD is rapidly degraded, offering the means to shut-off the Pga machinery in response to c-di-GMP fluctuations and temporarily uncouple it from c-di-GMP signalling. These studies provide the molecular basis of specificity of c-di-GMP signalling systems.

Results

PgaD *in vivo* stability depends on c-di-GMP

It has previously been reported that PgaD steady state protein levels are positively controlled by c-di-GMP on a post-transcriptional level (Boehm *et al*, 2009). This observation was used as an entry point to address the molecular mechanism of c-di-GMP-regulated poly-GlcNAc biogenesis. To mimic the induced state of the Csr regulon, all assays were done in a partial loss-of-function *csrA::Tn5* mutant strain background (*csrA* mutant) (Romeo *et al*, 1993). In order to monitor all Pga complex components individually, 3xFlag-tagged versions of PgaA, PgaB, PgaC and PgaD were constructed. Deletion of the DGC-encoding gene *ydeH* specifically affected the steady state protein level of PgaD, while the levels of the other three Pga proteins remained constant, regardless of whether the *pga* operon was expressed from its native promoter including the 5' untranslated region of *pgaA* or from the L-arabinose-dependent P_{ara} promoter with the 5' untranslated leader sequence from *araB* (Figure 1A and Supplementary Figure 1A). Moreover, PgaD levels were almost absent in $\Delta pgaC$ and $\Delta pgaABC$ mutants, but were restored in a c-di-GMP-dependent manner when *pgaC* was expressed *in trans* and were further increased upon overexpression of *pgaC* (Figure 1B). The expression of *dgcA* encoding a heterologous DGC from *Caulobacter crescentus* (Christen *et al*, 2006) strongly elevated PgaD levels of a $\Delta ydeH$ mutant in an active site-dependent manner, but only when *pgaC* was present (Figure 1B). Finally, PgaC glycosyltransferase activity is not required to stabilize PgaD in a c-di-GMP-dependent manner, as a *pgaC* active site mutant (D256N) behaved similarly to the wildtype (Supplementary Figure 1B).

The data above indicated that PgaC and c-di-GMP together control PgaD levels post-translationally. To substantiate this and to demonstrate that the effect is specific for PgaD, *pgaD* was replaced with *yfiR*, an unrelated gene from *Pseudomonas aeruginosa*. The observation that YfiR levels failed to fluctuate in response to c-di-GMP availability excludes the possibility that PgaD levels respond to a c-di-GMP-controlled promoter or to translation initiation control elements within *pgaABC* (Supplementary Figure 1C). Next, the overall *in vivo* protein stability of PgaD-3xFlag was determined under different c-di-GMP concentrations by blocking translation of exponentially growing cells with translation inhibitors. While PgaD remained stable over time in strains with increased c-di-GMP levels (*ydeH*⁺ strain and $\Delta ydeH$ mutant expressing *dgcA*), the protein was rapidly degraded in strains with low cellular c-di-GMP concentrations ($\Delta ydeH$ mutant and $\Delta ydeH$ mutant expressing an active site mutant of *dgcA*) (Figure 1C).

In summary, these data suggest that c-di-GMP positively modulates PgaD *in vivo* protein stability in a PgaC-dependent manner.

C-di-GMP and PgaD together promote poly-GlcNAc-dependent biofilm formation

The *E. coli csrA* mutant strain forms biofilms under laboratory conditions that fully depend on the EPS adhesin poly-GlcNAc (Wang *et al.*, 2004), the formation of which is modulated by c-di-GMP that is produced by YdeH (Boehm *et al.*, 2009). To test if c-di-GMP is essential for poly-GlcNAc-dependent biofilm formation, multiple genes coding for potential DGCs (each containing a GGDEF domain) were consecutively deleted in the *csrA* mutant background. Deletions of the two CsrA-controlled genes *ydeH* and *ycdT* (Jonas *et al.*, 2008) in combination with *yegE* resulted in a drastic reduction of biofilm formation, while a strain carrying a total of seven deletions (*ydeH*, *yegE*, *ycdT*, *yfiN*, *yhjK*, *ydaM*, *yneF*) completely lost the ability to form biofilms (Figure 1D). This strain will be referred to as $\Delta 7$ or c-di-GMP^{low} strain throughout this work. Importantly, the biofilm deficiency could be complemented by reintroducing only *ydeH* into the bacterial genome (data not shown), supporting the idea that YdeH represents the major DGC responsible for poly-GlcNAc induction under these conditions (Boehm *et al.*, 2009). Moreover, these findings indicate that low levels of c-di-GMP are responsible for the failure of the $\Delta 7$ strain to form biofilms. In line with the data described above, PgaD protein was not detectable in the $\Delta 7$ mutant (Figure 1D). While PgaD levels are dependent on c-di-GMP, overexpression of *pgaD* resulted in a biofilm induction both in the presence and in the absence of YdeH (Supplementary Figure 1D). However, the $\Delta ydeH$ mutant never reached the same level of biofilm formation as the control strain, arguing that PgaD and c-di-GMP are synergistically needed for optimal biofilm formation.

C-di-GMP mediates PgaC-PgaD interaction

One scenario that could explain PgaC-dependent PgaD stability is a direct interaction of the two membrane proteins. In fact, HmsR and HmsS, homologues of PgaC and PgaD in *Y. pestis*, were shown to interact (Bobrov *et al.*, 2008). Co-immunoprecipitation experiments using detergent-solubilized membranes revealed that PgaC and PgaD indeed form a stable complex that proved to be resistant to high salt concentrations and up to 2 M urea (Figure 2A). When overexpressed, PgaC and PgaD could be co-purified even from membranes of a c-di-GMP^{low} strain (Figure 2B), arguing that under these conditions c-di-GMP is no longer required for PgaD stability. Together, this opened up the possibility that PgaC and PgaD form a stable complex in the cytoplasmic membrane, which under physiological conditions is mediated by c-di-GMP.

To test if c-di-GMP is involved in PgaC-PgaD interaction, a bacterial two-hybrid assay was used that is based on the interaction-mediated reconstitution of the split cAMP signalling pathway in *E. coli* (Karimova *et al.*, 1998). In this assay, full-length PgaC and PgaD showed a robust interaction (Figure 2C), while all truncated variants (e.g. predicted cytosolic parts) were negative

(Supplementary Table 2). This interaction was stimulated by the ectopic expression of the heterologous DGC *dgcA* from *C. crescentus* (Figure 2D). Conversely, a step-wise reduction of the cellular c-di-GMP pool gradually lowered the interaction strength. PgaC-PgaD interaction was weakened upon deletion of *ydeH* and almost completely lost in the c-di-GMP^{low} strain (Figure 2D). These data further support the idea that c-di-GMP stimulates PgaC-PgaD interaction or complex stability.

The above results can be interpreted in two different ways. C-di-GMP could regulate poly-GlcNAc production by determining PgaD stability and availability. Alternatively, c-di-GMP could mediate PgaC-PgaD interaction with PgaD instability and degradation being a consequence of complex disintegration at low c-di-GMP concentrations. To be able to distinguish between these two possibilities, PgaD was attempted to be stabilized under low c-di-GMP conditions by directly fusing the C-terminus of PgaC to the N-terminus of PgaD. Surprisingly, the resulting *pgaCD* fusion construct (*pgaCDf*) was fully functional and able to complement biofilm formation of a Δ *pgaCD* mutant in a c-di-GMP-dependent manner (Figure 2E). But in contrast to PgaD, the level of the PgaCD fusion protein (PgaCDf) was unaltered in a strain with lower c-di-GMP concentrations (Figure 2E). These findings not only reinforce the notion of a direct interplay between PgaC and PgaD, but furthermore imply that PgaD instability at low c-di-GMP levels is not the cause of Pga machinery control, but may simply result from weak protein interactions under these conditions. The data also raise the question why PgaC and PgaD exist as two separate proteins in all bacteria harboring this EPS biogenesis system.

c-di-GMP acts as an allosteric activator of PgaCD glycosyltransferase activity

In order to test whether c-di-GMP acts as an allosteric activator for the PgaCD glycosyltransferase (GT) complex, an *in vitro* activity assay was developed based on crude membranes containing PgaCD. Activities were indirectly determined using a modified enzyme-coupled spectrophotometric assay (Baykov *et al.*, 1988) or directly by measuring UDP-GlcNAc consumption. In agreement with earlier data demonstrating that both PgaC and PgaD are needed for poly-GlcNAc synthesis *in vivo* (Wang *et al.*, 2004; Itoh *et al.*, 2008), UDP-GlcNAc was only turned over to poly-GlcNAc and UDP by membranes of cells expressing *pgaC* and *pgaD* (Figure 3A). Following incubation of active membranes with substrate for several hours, a slimy and viscous reaction product was visualized by light microscopy (Figure 3B). Immunoblot analysis with an anti-poly-GlcNAc antibody confirmed the identity of the reaction product (Supplementary Figure 2A). Experiments to determine the substrate affinity of the PgaCD GT complex revealed a K_m for UDP-GlcNAc of $270.5 \pm 37.2 \mu\text{M}$ (Figure 3C). To test if PgaCD GT activity is stimulated by c-di-GMP,

initial reaction velocities were measured at varying c-di-GMP concentrations in the presence of a constant UDP-GlcNAc concentration of 50 μ M. Under these conditions, c-di-GMP stimulated GT activity more than 20-fold and curve fitting indicated a c-di-GMP concentration for half-maximal initial velocity (K_{act}) of 62.2 ± 7.2 nM (Figure 3D). The addition of GTP failed to activate the enzyme and c-di-GMP-mediated activity was fully dependent on the PgaCD machinery (Supplementary Figure 2B). The basal enzymatic GT activity in the absence of exogenously added c-di-GMP correlated with the cellular c-di-GMP concentration of the strain used for *pgaCD* overexpression and membrane preparation. Almost no basal activity was detected for membranes originating from the $\Delta 7$ mutant (Supplementary Figure 2B).

In summary, these data strongly suggest that c-di-GMP acts as a direct allosteric activator of the PgaCD glycosyltransferase.

Concomitant binding of c-di-GMP to both PgaC and PgaD

The above *in vitro* assays argued for a direct role of c-di-GMP as an allosteric activator of PgaCD GT activity. To corroborate these findings, c-di-GMP binding to the PgaCD complex was tested by using a c-di-GMP capture compound (c-di-GMP-cc, Nesper *et al.*, submitted) and by performing UV light-induced crosslinking experiments with radiolabeled c-di-GMP (Christen *et al.*, 2006). The PgaCD complex was specifically and competitively captured by the c-di-GMP-cc from membrane preparations (Figure 4A). An excess of c-di-GMP, but not GTP, gradually competed with c-di-GMP-cc binding. While the PgaCD complex and the PgaCD fusion protein were specifically pulled-down, no specific binding could be observed when membranes were used that only contained PgaC or PgaD (Figure 4B). The residual captured protein binds non-specifically to the c-di-GMP-cc as it cannot be competed by an excess of c-di-GMP. When membranes were used that contained 3xFlag-tagged variants of both PgaC and PgaD, both proteins showed specific binding to the c-di-GMP-cc. A fraction of the PgaC-PgaD heterodimers withstood boiling in SDS sample buffer and appeared as a distinct band on the immunoblot, emphasizing the remarkable stability of these complexes (Figure 4B). Probing c-di-GMP-cc samples with an anti-biotin antibody revealed that the c-di-GMP-cc was covalently crosslinked to both PgaC and PgaD in a competitive way, suggesting that c-di-GMP is able to directly interact with both components of the complex (Supplementary Figure 3A).

To corroborate the above findings, a different binding assay based on UV light-induced crosslinking with radiolabeled c-di-GMP was performed. In good agreement with the data obtained with the capture compound, PgaC and PgaD were specifically and competitively labeled with [33 P]c-di-GMP when both proteins were present in the membrane fraction (Figure 4C). An

excess of c-di-GMP, but not GTP, strongly competed with crosslinking of [³³P]c-di-GMP to both proteins. It is interesting to note that PgaC labeling was generally much stronger than PgaD labeling. Again, specific c-di-GMP binding and radiolabeling of PgaC and PgaD was only observed in membranes containing both proteins, but was lost for PgaC when PgaD was not present (Figure 4D). Interestingly, the presence of UDP-GlcNAc substrate was tendentially increasing the specific binding of c-di-GMP (with the exception of one experiment), indicating some form of communication between the GT active site and the allosteric pocket within the PgaCD complex (Supplementary Figure 3B).

Altogether, these data suggest that the PgaCD GT complex represents a novel type of c-di-GMP receptor, where a tight interplay between two proteins is needed for ligand binding.

Gain-of-function mutants in *pgaD* uncouple the PgaCD complex from c-di-GMP

To get a better understanding of the c-di-GMP-dependent regulatory mechanisms within the PgaCD complex, a gain-of-function (GOF) screen was set up that allowed the identification of *pgaC* and *pgaD* mutants, which cause biofilm formation in a c-di-GMP^{low} Δ7 strain background. Following error-prone PCR mutagenesis and screening for biofilm-forming colonies using Congo Red agar plates, several different GOF mutants were isolated (Supplementary Table 3). Most interestingly, all (with the exception of one) isolated PgaD GOF mutations cluster within the most conserved region of the protein that has initially been described in *Y. pestis* (Forman *et al.*, 2006) and that is located at the C-terminal end of the second predicted transmembrane helix (Figure 5A). Two of the activating *pgaD* alleles (N75D, K76E and L73Q, K76E, R78C) not only caused biofilm formation in a c-di-GMP^{low} strain, but furthermore locked biofilm formation at an intermediate level in a c-di-GMP-independent way, thus abolished the difference in biofilm formation between a Δ7 mutant and the wildtype (Figure 5B). These specific c-di-GMP-‘blind’ GOF phenotypes were found to be due to the presence of all mutations within each allele. While the *pgaD* (N75D, K76E) allele proved to be fully c-di-GMP-independent, the *pgaD* (L73Q, K76E, R78C) allele retained some residual c-di-GMP inducibility upon ectopic expression of the heterologous DGC *wspR* from *P. aeruginosa* (Supplementary Figure 4A). The two residues W71 and Y74 that are also located within the conserved region have previously been shown to be important for the function of HmsS, the PgaD homologue of *Y. pestis* (Forman *et al.*, 2006). However, alanine mutagenesis only resulted in an almost complete loss-of-function (LOF) phenotype for W71A, while the Y74A mutation did not affect PgaD function (Figure 5B). The LOF phenotype caused by the W71A mutation could also not be rescued by the GOF mutations N75D and K76E, as the triple mutant totally abolished biofilm formation (Supplementary Figure 4B).

Most interestingly, the GOF phenotypes of *pgaD* (N75D, K76E) and *pgaD* (L73Q, K76E, R78C), which enabled these two alleles to trigger biofilm formation in a $\Delta 7$ mutant, were reflected in the mutant's PgaD steady state protein levels. Both GOF mutants showed an increased PgaD level in the c-di-GMP^{low} strain and in addition c-di-GMP-dependent PgaD level fluctuations were absent or strongly reduced (Figure 5C). Unexpectedly, the protein levels of the PgaD (W71A) LOF mutant showed a similar pattern, strongly suggesting that PgaD stabilization is not sufficient to activate the PgaCD complex (Supplementary Figure 4C).

Since the above data suggest that *pgaD* GOF mutants are able to uncouple the PgaCD complex from c-di-GMP signalling, this raises the question of whether these mutants fail to bind the allosteric ligand and withstand the allosteric activation *in vitro*. To circumvent the problem of having different PgaC-PgaD ratios when comparing the wildtype and the mutants, c-di-GMP binding was assayed using the c-di-GMP capture compound in the context of the PgaCD fusion protein. The PgaCDf (PgaD: N75D, K76E) mutant protein was found to be strongly impaired in ligand binding (Figure 5D). In contrast, PgaCDf (PgaD: L73Q, K76E, R78C) and PgaCDf (PgaD: W71A) were pulled-down by c-di-GMP-cc, albeit to a lesser extent, suggesting a reduced c-di-GMP affinity for these alleles in comparison to the wildtype. These findings corroborate biofilm formation and protein level data for both GOF mutants described above and imply that the LOF phenotype caused by the W71A mutation is not (solely) linked to a ligand binding deficiency.

When the behavior of the two PgaD GOF alleles was addressed in the *in vitro* GT activity assay, both mutant proteins showed a more than 3-fold increased basal enzymatic GT activity in the absence of exogenously added c-di-GMP (Figure 5E). Since these activities are directly proportional to the amount of protein within the reaction, protein input was adjusted beforehand and controlled during the experiment on an immunoblot (Supplementary Figure 4D). In addition to the increased basal activity, both alleles were not allosterically stimulated by the addition of 100 nM c-di-GMP, a concentration that causes approximately half-maximal activation of the wildtype enzyme (Figure 5E).

In summary, the data discussed above demonstrate that certain GOF mutants in *pgaD* mimic a c-di-GMP-bound state that activates the PgaCD GT complex and furthermore uncouples the machinery from c-di-GMP signalling. This again implies a close interplay between PgaC and PgaD in forming an active enzyme complex.

The C-terminus of PgaD is dispensable for c-di-GMP-controllable biofilm formation

The fact that the GOF mutants described above almost entirely lie within the PgaD protein family's most conserved region, which is located just C-terminally to the second transmembrane

helix (Figure 5A), argued for a very central role of these amino acid residues in c-di-GMP-dependent PgaCD complex activation. Following the gradual C-terminal truncation of wildtype PgaD, it was evident that most of the C-terminal cytosolic domain is not absolutely required for the maintenance of c-di-GMP-controllable poly-GlcNAc-dependent biofilm formation as judged by the reaction to *wspR* overexpression (Figures 5F and 5A). Even *pgaD* alleles that encode for proteins that end either after amino acid P92, Q80 or R78 caused the formation of some residual c-di-GMP-controlled biofilm. However, the overall biofilm amount was clearly reduced, the shorter the protein got.

Since c-di-GMP binding to the PgaCD complex is a requirement for poly-GlcNAc-dependent biofilm formation, it can be concluded that the potential site of contact between c-di-GMP and PgaD resides within the protein's first 78 residues. Furthermore, such a short PgaD allele basically consists of only two transmembrane helices that are connected via a periplasmic loop, thus suggesting a role for PgaD in the c-di-GMP-dependent interplay with PgaC in the vicinity of the cytoplasmic membrane.

Gain-of-function mutants in *pgaC* positively influence PgaD protein levels

In contrast to some *pgaD* GOF mutants, all GOF mutants isolated in *pgaC* retained the stimulating response to c-di-GMP as monitored when comparing biofilm formation in a $\Delta 7$ mutant and a wildtype background (Figure 6A and Supplementary Table 3). In addition, they all still depended on the presence of *pgaD* for biofilm formation (data not shown). In case of the *pgaC* (S7P, M44T, W60R) allele, all three mutations were found to contribute to the high level of biofilm formation observed in a c-di-GMP^{low} $\Delta 7$ strain. The V227L mutation had an interesting phenotype, as it strongly upregulated biofilm formation in the c-di-GMP^{low} strain as well as in the wildtype. Co-expression of this *pgaC* allele together with the c-di-GMP-independent *pgaD* (N75D, K76E) GOF mutant resulted in an additive biofilm phenotype in the c-di-GMP^{low} strain. However, the effect of the *pgaD* GOF allele proved to be dominant in terms of c-di-GMP inducibility, as the allele combination caused c-di-GMP-independent biofilm formation (Supplementary Figure 5A).

Because PgaD stability was shown to be controlled by c-di-GMP in a PgaC-dependent manner (Figure 1), it was hypothesized that *pgaC* GOF alleles may lead to an enhanced PgaD protein level. This was indeed the case. Immunoblot analysis revealed increased PgaD levels in response to the two activating *pgaC* alleles (S7P, M44T, W60R and V227L) in a c-di-GMP^{low} strain background (Figure 6B). This further substantiates the idea that PgaD stabilization is mainly a secondary effect caused by the allosteric activation of the Pga machinery.

R222 of PgaC plays an essential role in c-di-GMP-dependent PgaCD activation

As discussed above, UV light-induced crosslinking experiments resulted in a strong specific and competitive labeling of PgaC (Figure 4C). In order to get an idea about potential amino acid residues that may be involved in the formation of the c-di-GMP binding pocket within PgaC, a loss-of-function (LOF) approach was chosen. Arginines have been shown to play a critical role in c-di-GMP binding sites, e.g. in the PilZ domain (Ryjenkov *et al*, 2006; Christen *et al*, 2007). From a total of 29 arginine residues within PgaC, the most interesting ones were selected based on a bioinformatical analysis. PgaC sequences from c-di-GMP signalling-containing bacterial species were compared with sequences from species that lack c-di-GMP signalling proteins (no GGDEF domain proteins). Only gram-negative species that encode for an entire *pgaABCD* operon were considered in the analysis. *Actinobacillus pleuropneumoniae* (Izano *et al*, 2007; Bossé *et al*, 2010), *Aggregatibacter actinomycetemcomitans* (Izano *et al*, 2008), *Mannheimia succiniciproducens* and *Haemophilus parainfluenzae* were among the gram-negative species found with an intact Pga system and no c-di-GMP signalling. A total of 6 arginines were selected as interesting candidates. Because they are conserved in PgaC sequences from c-di-GMP signalling-containing species, but not in sequences from species that lack c-di-GMP signalling (Supplementary Figure 6), arginines R56, R58, R133, R222, R428 and R430 were individually or in combination mutated to alanines. The two mutant alleles *pgaCDf* (*pgaC*: R222A) and *pgaCDf* (*pgaC*: R428A, R430A) almost completely failed to complement biofilm formation (Figure 6C) without showing an aberrant PgaCDf protein level in comparison to the wildtype (Supplementary Figure 5B). Testing the c-di-GMP binding capacity of these mutant proteins using the c-di-GMP-cc revealed a strong binding defect for PgaCDf (*PgaC*: R222A), but not for PgaCDf (*PgaC*: R428A, R430A) (Figure 6D). In agreement with being c-di-GMP-‘blind’, PgaC (R222A) was unable to stabilize PgaD in the wildtype. In contrast, PgaD was still partially stabilized by a biofilm complementation-deficient PgaC (D256N) active site mutant in a c-di-GMP-dependent way (Supplementary Figure 5C).

Interestingly, the *pgaD* (N75D, K76E) GOF allele was able to rescue the LOF phenotype caused by the *pgaC* (R222A) mutant. C-di-GMP-independent biofilm formation was restored at an intermediate level (Figure 6E), thus strongly indicating that PgaC (R222A) states an enzyme that can principally be active, but misses its allosteric activation signal. Overall, the data suggest a critical role for R222 of PgaC in the c-di-GMP-dependent PgaCD GT complex activation and may imply that R222 is directly involved in forming the c-di-GMP binding pocket.

Within the PgaCD complex, PgaC and PgaD both participate in c-di-GMP binding

Finally, the impact on ligand binding caused by mutations, which render the PgaCD complex insensitive to c-di-GMP fluctuations, was tested side by side in an UV light-induced crosslinking experiment. In case of crude membranes containing wildtype PgaCD complexes, PgaC and PgaD both specifically and competitively incorporated radiolabeled c-di-GMP (Figure 7). On the other hand, PgaCD complexes composed of either wildtype PgaC and PgaD (N75D, K76E) or PgaC (R222A) and wildtype PgaD were strongly impaired in c-di-GMP binding. In both cases, this was reflected by the total amount of radiolabeled c-di-GMP associated with PgaC as well as PgaD (Figure 7). Hence, UV light-induced crosslinking experiments back up c-di-GMP-cc experiment findings and further corroborate the tight interplay between PgaC and PgaD to form a c-di-GMP receptor.

Discussion

The transition from a planktonic to a biofilm-associated bacterial lifestyle is a complex and highly regulated process (O'Toole *et al.*, 2000; Karatan & Watnick, 2009). Over the recent years, the ubiquitous bacterial second messenger c-di-GMP has emerged as a central controller of surface-associated traits in many different bacterial species (Schirmer & Jenal, 2009; Hengge, 2009; Povolotsky & Hengge, 2012; Sondermann *et al.*, 2011) and several mechanisms by which this molecule exerts its stimulating effects on biofilm formation were elucidated. One of these mechanisms is the direct allosteric regulation of EPS synthesis and secretion machineries through binding of c-di-GMP to machinery-associated PilZ domains (*G. xylinus* cellulose synthase complex (Ross *et al.*, 1987, 1990) and *P. aeruginosa* alginate synthesis and secretion machinery (Merighi *et al.*, 2007)) or degenerate GGDEF or EAL domains (*P. aeruginosa* PEL polysaccharide synthesis complex (Lee *et al.*, 2007)).

The secretion of poly-GlcNAc, another relevant biofilm-associated EPS that is used as an adhesin by several bacterial species, was repetitively linked to c-di-GMP signalling (Kirillina *et al.*, 2004; Boehm *et al.*, 2009; Tagliabue *et al.*, 2010; Pérez-Mendoza *et al.*, 2011). Transcriptional as well as post-transcriptional regulation has been proposed. However, the molecular mechanisms how c-di-GMP stimulates poly-GlcNAc-dependent biofilm formation have not been clarified yet. Despite obvious analogies to other EPS secretion systems, none of the canonical c-di-GMP receptor domains is found as an inherent part of the Pga system.

Previously, we suggested that c-di-GMP post-transcriptionally (in respect to *pga* operon transcription) controls poly-GlcNAc-dependent biofilm formation (Boehm *et al.*, 2009). In this study, we close the gap by demonstrating that the PgaCD glycosyltransferase complex, which forms the inner membrane part of the Pga system, states a novel type of c-di-GMP receptor, in which two membrane-bound proteins have to interact in order to form a ligand binding pocket. Binding of the allosteric activator c-di-GMP enhances the PgaC-PgaD interaction and causes PgaC-dependent PgaD stabilization. Using an *in vitro* GT activity assay, we determined the c-di-GMP concentration needed for half-maximal enzyme activation (K_{act}) to be 62.2 ± 7.2 nM, strongly suggesting a high c-di-GMP binding affinity of the PgaCD complex. In the presence of a saturating c-di-GMP concentration, the enzyme's K_m for UDP-GlcNAc was found to be 270.5 ± 37.2 μ M, a value that lies within the range of reported cellular UDP-GlcNAc concentrations in *E. coli* (Mengin-Lecreulx *et al.*, 1989; Namboori & Graham, 2008). In the same line with c-di-GMP being a direct stimulator of GT velocity, our *in vivo* and *in vitro* data suggest that c-di-GMP furthermore is absolutely essential for poly-GlcNAc synthesis. The gradual deletion of DGC-encoding genes finally resulted in the loss of biofilm formation. On the other hand, *in vitro* GT reactions using

membranes from a c-di-GMP^{low} $\Delta 7$ strain essentially showed no basal activity in the absence of exogenously added c-di-GMP. It is noteworthy that the basal GT activity measured *in vitro* correlated with the c-di-GMP concentration of the strain that was used for membrane preparation. This likely resulted from impurities of the membrane fraction that were not removed during the preparation procedure or from c-di-GMP-preloaded PgaCD complexes.

According to our results from the c-di-GMP binding experiments, we propose that the PgaCD GT complex is the first example of a c-di-GMP receptor that relies on protein-protein interaction. Only a membrane-bound PgaCD complex, but not PgaC or PgaD alone, showed specific and competitive ligand binding and is thus thought to function as a c-di-GMP receptor. Upon UV light-induced crosslinking with radiolabeled c-di-GMP, PgaC and PgaD were both specifically and competitively labeled. Because of the close proximity that is needed for covalent zero-length crosslink formation, this implies that amino acid residues from both proteins might participate in the formation of the PgaCD complex ligand binding pocket. The fact that PgaC was incorporating more radioactivity than PgaD can readily be explained by the nature of the c-di-GMP binding pocket, since not all amino acid residues show the same propensity to get covalently crosslinked to a nucleotide ligand upon UV light irradiation (Meisenheimer & Koch, 1997).

Besides the fact that PgaC and PgaD have to interact to form a c-di-GMP receptor, several other results from our study suggest a tight interplay between PgaC and PgaD. A genetic error-prone PCR-based gain-of-function (GOF) screen enabled us to identify *pgaC* and *pgaD* mutant alleles that cause biofilm formation independently of c-di-GMP. To our knowledge, this is the first study that describes such GOF mutations in a c-di-GMP receptor protein. Most interestingly, the two activating *pgaD* alleles (N75D, K76E and L73Q, K76E, R78C) not only allowed biofilm formation in a c-di-GMP^{low} strain, but furthermore fully or at least partially uncoupled the PgaCD complex from c-di-GMP signalling in terms of c-di-GMP binding, allosteric GT activation and biofilm formation. In contrast, none of the activating *pgaC* alleles showed completely c-di-GMP-‘blind’ phenotypes, indicating that PgaD plays an important role in c-di-GMP-mediated PgaC GT activation. Even though we have found several mutations multiple times and in different combinations, the fact that certain combinations of mutations, e.g. the *pgaC* (S7P, W60R) allele, which clearly allowed biofilm formation in a c-di-GMP^{low} strain, were not found in our GOF screen is highly suggestive that our genetic screen was not fully saturated. Especially combinations of multiple mutations, which are anyway more difficult to be isolated due to the increased probability of picking up deleterious mutations, were likely to be missed with our approach.

Our results showed that an alanine substitution of R222 of PgaC results in a PgaCD complex with a heavily reduced c-di-GMP binding affinity, leading to a strong loss-of-function (LOF)

phenotype in terms of poly-GlcNAc-dependent biofilm formation. The finding that the activating *pgaD* (N75D, K76E) GOF allele rescued the LOF phenotype caused by the R222A mutation, underlines the tight interplay between PgaC and PgaD and proves that the LOF phenotype is not due to a broken *pgaC* allele. R222 of PgaC is rather a residue, which may be directly involved in the formation of the c-di-GMP binding pocket.

The bioinformatical approach that led to the identification of R222 is based on two assumptions. First, arginines have repetitively been described to be important in c-di-GMP coordination within different families of binding sites (Christen *et al.*, 2007; Wassmann *et al.*, 2007; Krasteva *et al.*, 2010). Therefore, we assumed that this would most likely also be true for the PgaCD complex. The second assumption was that those arginines involved in ligand binding are fully conserved in gram-negative bacterial species that contain c-di-GMP signalling, but not conserved in PgaC sequences of gram-negative bacterial species that are devoid of c-di-GMP signalling as judged by the absence of GGDEF domain-encoding genes (Galperin *et al.*, 2010). It was very interesting to note that all gram-negative strains devoid of c-di-GMP signalling harbor a *S. epidermidis* IcaD-like (Gerke *et al.*, 1998) fourth protein instead of a PgaD/HmsS-like protein. This is striking since more and more evidence is accumulating that *Staphylococcus* spp. are unable to synthesize c-di-GMP (Holland *et al.*, 2008). It can thus be speculated that a PgaD/HmsS-like fourth protein within a poly-GlcNAc secretion system goes along with a c-di-GMP-controlled machinery. In line with this, it remains unknown whether poly-GlcNAc synthesis and secretion is also allosterically controlled by c-di-GMP in *Burkholderia* spp. and *Bordetella* spp. (Parise *et al.*, 2007; Yakandawala *et al.*, 2011). Since these two species both encode c-di-GMP signalling proteins, but miss R222 in PgaC and harbor a fourth protein that shows low or no significant similarity to the PgaD/HmsS protein family, it may even be possible that a different allosteric ligand controls the GT activity in these species. Clearly, further and more profound genetic, biochemical and bioinformatical studies are needed to get a better understanding about similarities and differences between c-di-GMP-mediated regulation mechanisms of poly-GlcNAc secretion systems in different bacterial species.

Generally, the minimal functional unit of processive (inverting) GT-2 β -glycosyltransferases is thought to be a monomer, which uses the active site-containing domains A and B for the sugar polymerization reaction (Saxena & Brown, 1997; Tlapak-Simmons *et al.*, 1998; Ciocchini *et al.*, 2006). However, the question remains how a growing polysaccharide chain is efficiently transferred across the hydrophobic lipid barrier of the plasma membrane with as little as four true transmembrane helices (e.g. in case of PgaC). The interaction of the GT with several

cardiolipin molecules has been suggested as a solution to this dilemma for the *Streptococcus* hyaluronan synthase (Tlapak-Simmons *et al.*, 1999).

In our model for the allosteric c-di-GMP-dependent PgaCD GT activation (Figures 8A and 8B), we propose a central role for PgaD in turning the GT PgaC into a secretion-compatible state upon binding of c-di-GMP to a loosely associated PgaC-PgaD heterodimer. Second messenger binding induces a conformational change that is predicted to trigger the integration of the two N-terminal transmembrane helices of PgaD into the core of transmembrane helices formed by PgaC, thus turning the heterodimeric GT complex into a stable, active and secretion-compatible state by opening up a pore for poly-GlcNAc translocation across the cytoplasmic membrane (Figure 8B). We suggest that this activation mechanism is the reason for the strong c-di-GMP-dependent induction of the PgaCD GT velocity measured in our *in vitro* experiments. The formation of a heterodimeric complex as a functional unit within the membrane is the easiest possible model and is supported by our findings that a PgaCD fusion protein is fully functional and that both proteins are absolutely required for poly-GlcNAc synthesis *in vivo* and *in vitro*. The association of the GT with a second inner membrane protein that is essential for activity seems to be a general phenomenon of homopolymeric EPS secretion systems (Keiski *et al.*, 2010).

The allosteric ligand likely interacts with amino acid residues of both subunits of the PgaCD complex in the vicinity of the cytoplasmic face of the inner membrane. This is supported by the following findings: On the PgaC side, the critical residue R222 just precedes helix 3, the first of the two membrane-associated helices, while the strong V227L GOF mutation lies inside helix 3. On the PgaD side accordingly, GOF mutations that render the complex c-di-GMP-insensitive unexceptionally clustered within the most conserved region of the PgaD/HmsS protein family that is located at the C-terminal end of the second transmembrane helix (Figure 8A) (Forman *et al.*, 2006). Finally, our results from the analysis of C-terminally truncated PgaD alleles imply that the main function of PgaD in contributing to a c-di-GMP-controllable PgaCD complex is linked to its two transmembrane helices, since the truncation of PgaD just C-terminally of the most conserved region still allowed residual c-di-GMP-controlled biofilm formation.

It is an obvious question why PgaC and PgaD exist as two separate proteins in the *E. coli* Pga system and in all other homologous systems that have been identified, although the PgaCD complex behaves as one protein in many respects. We postulate that the answer to this question is based on the at first sight meaningless instability of PgaD as a secondary effect in response to low cellular c-di-GMP levels. In agreement with previously published data and results from this work, it is conceivable that besides the central role of PgaD in the formation of a secretion-compatible GT complex, its instability is a way to shut-off the Pga machinery and to temporarily

uncouple poly-GlcNAc synthesis and secretion from cellular c-di-GMP levels (Figure 8C). This states a new concept for the c-di-GMP-dependent regulation of EPS secretion machineries. Briefly, following an input signal into the Csr cascade, e.g. via the BarA-UvrY two-component system (Chavez *et al.*, 2010; Timmermans & Van Melderen, 2010), PgaC and PgaD get co-translationally inserted into the cytoplasmic membrane (Wang *et al.*, 2005) and the two DGCs *ydeH* and *ycdT* are translated (Jonas *et al.*, 2008). Under high cellular c-di-GMP concentrations, the PgaCD complex gets allosterically activated and stabilized, thus promoting poly-GlcNAc-dependent biofilm formation. Conversely, if c-di-GMP levels are low when the PgaCD complex is inserted into the membrane (because the expressed DGCs are either inactive and/or certain PDEs are very active) or if c-di-GMP levels strongly decrease after having been high in the first place (e.g. if the Csr input signal disappears, the expressed DGCs are inactivated and/or certain PDEs are very active), PgaD is or turns highly unstable and is removed by an unknown protease. In the course of this study, all attempts to find the protease(s) involved in PgaD degradation under low c-di-GMP conditions were not successful. A Pga machinery devoid of PgaD is temporarily shut-off and unresponsive to c-di-GMP signalling. In this situation, a sudden increase in the c-di-GMP concentration (e.g. caused by DGCs that are not part of the CsrA regulon) would not result in poly-GlcNAc synthesis. Only a new Csr input signal allows the resynthesis of PgaD and thus resets the whole system (Figure 8C). This thus implies a novel model for the molecular basis of specificity of c-di-GMP signalling systems.

The c-di-GMP-dependent regulation of the *E. coli* Pga system seems to differ in some aspects from the mechanisms that have been proposed for the *Y. pestis* Hms system. While all our data are consistent with a model in which a 'global pool' of c-di-GMP controls the Pga machinery, the existence of an inner membrane complex composed of HmsR, HmsS (the homologues of PgaC and PgaD), the membrane-bound DGC HmsT and the membrane-bound PDE HmsP was suggested to generate a physically isolated c-di-GMP signalling entity in *Y. pestis* (Kirillina *et al.*, 2004; Bobrov *et al.*, 2008). Even though we have absolutely no experimental evidence (e.g. from MS-analyzed co-immunoprecipitation experiments), it cannot be fully ruled out that in *E. coli* the soluble DGC YdeH and/or the membrane-bound DGC YcdT, which is encoded by a divergently transcribed gene in respect to the *pga* operon (just like HmsT in *Y. pestis*), co-localize with the Pga machinery. On the other hand, while in *E. coli* the expression of the *pga* operon, *ydeH* and *ycdT* is negatively controlled by the global regulator CsrA (Wang *et al.*, 2005; Jonas *et al.*, 2008), a Csr-type regulatory system has only recently been described in *Yersinia* spp. (Heroven *et al.*, 2008) and has not been linked to the Hms system. It is thus conceivable that the coupling of c-di-GMP signalling proteins

and the poly-GlcNAc secretion machinery is achieved in a variety of ways in different bacterial species, e.g. via expression in *E. coli* or via co-localization in *Y. pestis*.

In conclusion, this work shows that in *E. coli*, poly-GlcNAc-dependent biofilm formation is allosterically controlled through c-di-GMP binding to the membrane-anchored PgaCD complex. Since two proteins have to interact in order to form a ligand binding pocket, the PgaCD complex states novel type of c-di-GMP receptor. Whether indeed amino acids residues of both proteins within the PgaCD complex participate in the coordination of the second messenger, as we suggest in our model, has to be carefully addressed with biochemical and/or structural approaches in the future.

Materials and methods

Strains, plasmids, growth conditions and genetic constructions

Strains and plasmids used in this study are listed in Supplementary Table 1. Unless otherwise stated, *E. coli* strains were grown at 30°C or 37°C in Luria Bertani (LB) medium (Miller, 1972) or on LB agar plates. When appropriate, antibiotics were used at the following concentrations: 50 µg/ml or 100 µg/ml ampicillin, 50 µg/ml kanamycin, 20 µg/ml or 30 µg/ml chloramphenicol, 12.5 µg/ml tetracycline. Plasmids were transformed into electro-, chemo- (Inoue *et al.*, 1990) or TSS-competent (Chung *et al.*, 1989) *E. coli* cells.

Most strains are derivatives of AB958 (Boehm *et al.*, 2009), an *E. coli* K-12 MG1655 strain that encodes for a truncated partial loss-of-function *csrA* allele (*csrA::Tn5*) (Romeo *et al.*, 1993). Deletion mutants were generally constructed by moving the deletion construct from a comprehensive gene deletion library (the Keio collection (Baba *et al.*, 2006)) into the recipient strains by P1 transduction (Miller, 1972). Deletions that were not present in the Keio collection and all other chromosomal constructs were done using the λRED technology (Datsenko & Wanner, 2000; Yu *et al.*, 2000). Resistance cassettes used as selection markers were generally removed by Flp recombinase-mediated site-specific recombination (Cherepanov & Wackernagel, 1995). C-terminally 3xFlag-tagged chromosomal constructs were constructed with the help of pSUB11 (Uzzau *et al.*, 2001). When the selection for two co-transducible markers was required, the kanamycin cassette linked to the 3xFlag tag was replaced by a chloramphenicol resistance cassette using the λRED technology. The *araB-pgaA* translational fusion construct was done by fusing the first codon of the *araB* ORF with the second codon of the *pgaA* ORF at the native *pga* locus with the help of λRED technology. The entire *pga* promoter including the 5' untranslated region is replaced with the corresponding regions of the *araBAD* operon (amplified from strain TB55 (Bernhardt & de Boer, 2004)). A kanamycin cassette was used for selection. The final strains harbor a copy of *araC* at the *pga* locus, which is divergently transcribed in respect to the P_{ara} promoter. In cases where L-arabinose was used to drive the expression from chromosomal P_{ara}, strains were generally deleted for the *araB* gene, yielding strains that allow for uptake but not metabolism of L-arabinose. λRED-mediated gene replacement was used to construct the bacterial two-hybrid strains that express the *pgaC-T18* fusion from the *pga* locus. *T18* linked to an ampicillin resistance cassette was amplified from pUT18 (Karimova *et al.*, 1998). In the resulting strain, the ampicillin cassette was replaced by a kanamycin resistance cassette, which was subsequently removed by Flp recombinase-mediated site-specific recombination (Cherepanov & Wackernagel, 1995), using the λRED technology (Datsenko & Wanner, 2000; Yu *et al.*, 2000).

Cloning was carried out in accordance with standard molecular biology techniques. Strain DH5 α was used for general cloning purposes. All derivatives of pUT18, pUT18C and pKT25 were produced by ligation of PCR products between the *Xba*I and *Kpn*I sites. All pBAD18 derivatives (with the exception of pAC551) were generated by ligation of PCR products or SOE-PCR (Higuchi *et al.*, 1988) products in case of site-directed mutagenesis between the *Nhe*I and *Kpn*I sites. pCDfusion, p2-3xF and pC-His-D-3xF were produced by ligation of SOE-PCR products. The two 3xFlag tags on p2-3xF are encoded by a slightly different DNA sequence to prevent homologous recombination. pAC551 is a derivative of pAB551 that has been generated according to the method of QuikChange site-directed mutagenesis (Papworth *et al.*, 1996).

Error-prone PCR mutagenesis-based gain-of-function (GOF) screen

Plasmids p5a (*pgaC*), pins1 (*pgaD*) and pCD-3xF (*pgaCD*) were used as templates for error-prone PCR following the previously described method (Rasila *et al.*, 2009). A standard 50 μ l Taq polymerase-based PCR was supplemented with mutagenesis buffer (4 mM dTTP, 4 mM dCTP, 27.5 mM MgCl₂ and 2.5 mM MnCl₂). To adjust the mutation frequency to approximately 1-3 mutations per 1'000 bp, reactions were run using different template concentrations in the presence of 0.5-4 μ l mutagenesis buffer. Pools of mutated alleles were then cloned into pBAD18 between the *Nhe*I and *Kpn*I sites. Following ligation, plasmid libraries were directly transformed into the corresponding electro-competent non-attaching c-di-GMP^{low} screening strain (AB2021, AB2134 or AB2022).

Production of poly-GlcNAc by *E. coli* cells could previously be visualized using Congo Red agar plates (Amini *et al.*, 2009). Therefore, transformants exhibiting a red colony phenotype on selective Congo Red agar plates (very dark LB agar plates with a final Congo Red concentration of 0.1%) were isolated by visual screening as potentially carrying a plasmid-encoded *pga* GOF allele. Only if the isolated plasmid allowed the corresponding screening strain to form biofilm in a standard biofilm assay upon plasmid re-transformation (secondary screen), the plasmid-encoded allele was sequenced to identify the GOF mutations.

Biofilm assay

Biofilm assays were essentially performed as previously described (Boehm *et al.*, 2009). Briefly, overnight cultures were diluted 1:40 into 200 μ l LB medium in 96-well polystyrene microtiter plates (BD Falcon). Plates were incubated for 24 h at 30°C without shaking and optical cell density was recorded, before non-attached cells were discarded and plates were vigorously washed with deionized water from a hose. Attached biomass was stained with a 0.1% crystal violet solution

(H₂O:isopropanol:methanol 96.7:1.66:1.66, v/v). Following the removal of excess dye, retained crystal violet was dissolved in 200 µl 20% acetic acid and quantified by measuring absorbance at 600 nm. Normalized biofilm formation values (biofilm) are ratios of the optical density of dissolved crystal violet (corresponding to the attached biomass) divided by the optical cell density (measured before discarding non-attached cells). Background values were subtracted. Generally, a single data point is derived from 3-6 wells per strain and condition. Error bars are standard deviations. Experiments were repeated multiple times.

Immunoblots

For the determination of *in vivo* steady state protein levels, cells were grown as for biofilm assays, total cells of several wells were pooled and adjusted to the same optical density. Proteins were generally separated on 7.5-15% SDS-PAGE gels and blotted onto PVDF membranes (Millipore) according to standard protocols (Laemmli, 1970; Towbin *et al.*, 1979). After overnight incubation in blocking solution (1x PBS pH 7.4, 0.1% Tween 20, 5% milk powder), immunodetection of proteins was carried out using mouse monoclonal α-Flag M2 (1:10'000; Sigma), rabbit polyclonal α-His (1:3'000; GenScript) or rabbit α-FliC (1:5'000; kind gift of John S. Parkinson) antibody. The biotin moiety of the c-di-GMP-cc was detected with goat polyclonal α-biotin (1:3'000; XXX) antibody or HRP-coupled Streptavidin (1:4'000; XXX). HRP-conjugated rabbit α-mouse, swine α-rabbit (1:10'000; DakoCytomation, Denmark) or rabbit α-goat (1:10'000; Invitrogen) secondary antibodies were used. Blots were developed with the ECL chemiluminescent substrate (PerkinElmer, USA) and photographic films (Fujifilm, Japan). If needed, band intensities were quantified from scanned X-ray films using the ImageJ software 'Integrated Density' tool.

Translation block experiment

To assess the *in vivo* stability of PgaD-3xF, overnight cultures of strains AB1062 (or AB1569 harboring pins1), AB1063 (or AB1570 harboring pins1) and AB1063 harboring either pAB551 or pAC551 were diluted 1:100 into fresh LB medium and cultures were grown to exponential phase (OD₆₀₀ between 0.8 and 1.8) at 30°C, before protein synthesis was inhibited at time point zero by the addition of 100-200 µg/ml chloramphenicol or 300 µg/ml erythromycin, respectively. *dgca* alleles encoded on pAB551 and pAC551 were not induced, because of leaky expression. Samples were harvested at indicated time points after translation inhibition and PgaD levels were analyzed by immunoblots. Band intensities were quantified using the ImageJ software 'Integrated Density' tool and normalized to levels present 5 min after translation inhibition for each strain.

Co-immunoprecipitation

Crude membranes containing overexpressed proteins of interest from strain AB2043 harboring pC-His-D-3xF (experiment A) or from strains AB1638 harboring pCD-3xF and AB2043 harboring pCD-3xF (experiment B) were used for anti-Flag co-immunoprecipitation experiments. In experiment A, crude membrane fraction (approximately 4 mg/ml total protein) was solubilized in IP Solubilization Buffer A (50 mM Tris HCl pH 7.5, 1 mM EDTA, 1 M NaCl, 0.5% DDM) for 4 h at 4°C with end-over-end agitation. Thereafter, sample was ultracentrifuged (100'000 g, 1 h, 4°C) and supernatant with solubilized proteins was collected. Supernatant was split in three parts and either incubated with 20 µl prewashed anti-Flag M2 affinity gel (Sigma) (with or without 2 M urea) or with the same amount of prewashed Protein A agarose (Roche) (mock IP) for 45 min at 4°C with end-over-end agitation. Aliquots of the protein fraction that did not bind to the beads (1st supernatant) were harvested, before beads were washed multiple times with IP Wash Buffer A (50 mM Tris HCl pH 7.5, 1 mM EDTA, 1 M NaCl, 0.1% DDM, ± 2 M urea). Immunoprecipitated proteins and 1st supernatant controls were analyzed by immunoblots. In experiment B, crude membrane fractions (approximately 3-5 mg/ml total protein) were solubilized in IP Solubilization Buffer B (50 mM Tris HCl pH 7.5, 1 M NaCl, 5% glycerol, 1 mM DTT, 0.5% DDM) overnight at 4°C with end-over-end agitation. After ultracentrifugation (100'000 g, 1 h, 4°C), supernatants were collected and incubated with 40 µl prewashed anti-Flag M2 affinity gel (Sigma) overnight at 4°C with end-over-end agitation. Beads were washed multiple times with IP Wash Buffer B (50 mM Tris HCl pH 7.5, 1 M NaCl, 5% glycerol, 0.1% DDM), before immunoprecipitated proteins were analyzed by Coomassie staining.

Bacterial two-hybrid

Bacterial two-hybrid experiments were performed according to the previously described method (Karimova *et al*, 1998). Full-length *pgaC* and *pgaD* ORFs or gene fragments were fused to the 3' end of the *T18* (pUT18C), the 5' end of the *T18* (pUT18) or the 3' end of the *T25* (pKT25) fragment of the *Bordetella pertussis* adenylate cyclase. AB1768 (Δ *cyaA*) transformants containing the relevant plasmids were analyzed on MacConkey agar base plates supplemented with 1% maltose, kanamycin and ampicillin. Plates were incubated overnight at 30°C and positive interactions were scored based on red coloration of colonies.

A slightly modified bacterial two-hybrid setup was used to measure interaction of full-length PgaC with full-length PgaD in response to different cellular c-di-GMP concentrations. In order to lower the expression level, the *pgaC-T18* fusion was expressed from the chromosomal *pga* locus (see above for details about the strain construction) instead of from the high copy number

plasmid pUT18, while the *T25-pgaD* fusion was expressed from pKT25. MacConkey agar base plates supplemented with 1% maltose and kanamycin were incubated overnight at 30°C.

Crude membrane preparation

Crude *E. coli* crude membranes, which were used for co-IP experiments, glycosyltransferase assays and c-di-GMP binding experiments, were prepared according to the following protocol: Overnight pre-cultures of strains AB1638 or AB2043 harboring the desired plasmid for protein overexpression (or strains AB1775, AB1776 and AB1777) were diluted 1:100 into 1 L LB medium and cultures were grown at 30°C to OD₆₀₀ of 0.2, before expression of plasmid-encoded genes was induced with 0.2% L-arabinose for 5 h. Cells were harvested by centrifugation, resuspended in 5-10 ml ice-cold French Press Buffer (50 mM HEPES pH 7, 5 mM CaCl₂, 1 mM DTT, Complete Mini EDTA-free protease inhibitors (Roche)) and lysed by passage three times through a French pressure cell (Vanderheiden *et al.*, 1970). Lysate was first clarified by centrifugation (27'000 g, 70 min, 4°C), before membranes were pelleted by ultracentrifugation (120'000 g, 90 min, 4°C). Crude membranes were generally resuspended in ~250 µl French Press Buffer and stored at -80°C.

Glycosyltransferase activity assays

Modified enzyme-coupled spectrophotometric assay. PgaCD GT activity was indirectly determined by monitoring the production of phosphate (released from UDP) using a modified enzyme-coupled spectrophotometric assay (Baykov *et al.*, 1988). Briefly, 50 µl reaction mixtures containing crude membranes from strains AB1775, AB1776 or AB1777 (approximately 10 mg/ml total protein) in GT Activity Buffer (50 mM HEPES pH 7, 5 mM CaCl₂, 5 mM MgCl₂) were incubated for 5 h at 30°C in a PCR machine with or without 2 mM UDP-GlcNAc. The pH of the reactions was increased to 8-8.5 by adding 0.1 M NaOH and taking them up in SAP Buffer (50 mM Tris HCl pH 9, 10 mM MgCl₂), before reactions were incubated with 1.5 µl shrimp alkaline phosphatase (SAP) (Promega) for 80 min at 37°C in a PCR machine. Phosphate content, an indirect measure for PgaCD GT activity, was spectrophotometrically measured at 630 nm by diluting reactions 1:10 into color reagent containing molybdate and malachite green (Baykov *et al.*, 1988). Color reagent background value was subtracted.

FPLC anion exchange column assay. Standard 100 µl reaction mixtures contained crude membranes from strain AB2043 harboring the desired plasmid for protein overexpression (approximately 0.3-0.6 mg/ml total protein), varying UDP-GlcNAc concentrations (between 50 µM and 2 mM) and different c-di-GMP concentrations (between 0 µM and 2 µM) in GT Activity Buffer (50 mM HEPES pH 7, 5 mM CaCl₂, 5 mM MgCl₂). Whenever different mutant alleles were

compared to each other in the same experiment, crude membrane inputs were adjusted with an immunoblot beforehand. The reactions were kept at 30°C in a PCR machine for different incubation times (between 0 min and 180 min), before they were stopped by boiling for 5 min at 98°C. Samples were cleared by centrifugation (16'100 g, 1 min, 25°C) and supernatants were taken up in 900 µl 1 mM sodium acetate. Nucleotides UDP and UDP-GlcNAc were separated on an anion exchange column (1 ml Resource Q, GE Healthcare) mounted on an ÄKTA Purifier FPLC unit (GE Healthcare) with a linear gradient of sodium acetate from 1 mM to 1 M and monitored with Unicorn software. Initial linear PgaCD GT reaction velocities were determined by plotting integrated peak areas against reaction incubation times using GraphPad Prism.

c-di-GMP capture compound binding assay

The capture experiments using the c-di-GMP capture compound (c-di-GMP-cc) (Caprotec Bioanalytics, Germany) were essentially carried out as previously described (Nesper *et al*, submitted) with some modifications and performed in 200 µl 12-tube PCR strips (Thermo Scientific). 100 µl samples generally contained crude membranes from strain AB1638 harboring the desired plasmid (approximately 3-4 mg/ml total protein) and 20 mM UDP-GlcNAc in Binding Buffer (20 mM HEPES pH 7.5, 50 mM potassium acetate, 10 mM magnesium acetate, 10% glycerol, 5 mM MgCl₂, 1.5 mM CaCl₂). Whenever different mutant alleles were compared to each other in the same experiment, experiments were performed in the context of the PgaCD fusion protein (PgaCDf) and crude membrane inputs were adjusted with an immunoblot beforehand. A 12.5- or 125-fold molar excess of c-di-GMP or GTP was added to competition experiments and strips were preincubated for 30 min at 30°C with end-over-end agitation. After the addition of 0.8 µM or 8 µM c-di-GMP-cc, the strips were wrapped in aluminum foil and incubated for 2 h at 30°C with end-over-end agitation. The samples were UV-irradiated at 310 nm for 4 min at 4°C using a caproBox (Caprotec Bioanalytics, Germany), before they were removed from the strips, taken up in a final volume of 200 µl Capture Solubilization Buffer (50 mM Tris HCl pH 7.5, 1 mM EDTA, 1 M NaCl, 0.5% DDM) and solubilized for 4 h at 4°C with end-over-end agitation. After ultracentrifugation (100'000 g, 1 h, 4°C), an aliquot of the supernatants was saved and the rest of the supernatants was incubated with 35 µl magnetic streptavidin beads (Dynabeads MyOne Streptavidin C1, Invitrogen) in PCR strips (Thermo Scientific) for 40 min at 4°C with end-over-end agitation. Beads were then collected with a magnet (caproMag, Caprotec Bioanalytics, Germany) and washed 9x with 200 µl Capture Wash Buffer (50 mM Tris HCl pH 7.5, 1 mM EDTA, 1 M NaCl, 0.1% DDM), before captured proteins were analyzed by immunoblots. If different mutant alleles were compared to each other, band intensities were quantified using the ImageJ software

'Integrated Density' tool and band intensities were normalized to the total solubilized protein amount of each sample.

Synthesis of radiolabeled [^{32/33}P]c-di-GMP

For the synthesis of radiolabeled [^{32/33}P]c-di-GMP, ³²P- or ³³P-labeled GTP ([α -³²P]GTP (100 μ Ci, 3000 Ci/mmol) (Hartmann Analytics, Germany) or [α -³³P]GTP (100 μ Ci, 3000 Ci/mmol) (PerkinElmer, USA)) was incubated with 2 μ M DGC YdeH (purified according to (Zähringer *et al.*, 2011)) in YdeH Reaction Buffer (50 mM Tris HCl pH 7.5, 50 mM NaCl, 5 mM MgCl₂) overnight at 30°C. The completeness of GTP turnover (>98%) was estimated by running a reaction aliquot on a polyethyleneimine cellulose TLC plate (Macherey-Nagel, Germany) as previously described (Christen *et al.*, 2005). Thereafter, the reaction was stopped by boiling 10 min at 98°C and precipitated YdeH was removed by centrifugation (16'100 g, 5 min, 25°C). Radiolabeled [^{32/33}P]c-di-GMP was mixed with an aqueous solution of unlabeled c-di-GMP (synthesized and purified according to (Zähringer *et al.*, 2011)) in a negligible small ratio of between 1:160 and 1:100 to give final concentrations of 12.5 μ M, 25 μ M or 50 μ M.

UV-crosslinking with [^{32/33}P]c-di-GMP

UV light-induced crosslinking experiments were performed according to the previously described method (Christen *et al.*, 2005, 2006) in conical 96-well plates (Greiner Bio-One). 25 μ l samples generally contained crude membranes from strain AB1638 harboring either p2-3xF or p6a (approximately 30 mg/ml total protein) and 20 mM UDP-GlcNAc in Binding Buffer (20 mM HEPES pH 7.5, 50 mM potassium acetate, 10 mM magnesium acetate, 10% glycerol, 5 mM MgCl₂, 1.5 mM CaCl₂). Whenever different mutant alleles were compared to each other in the same experiment, crude membrane inputs were adjusted with an immunoblot beforehand. Each sample was done in triplicates. For competition experiments, a 100-fold molar excess of c-di-GMP or GTP was added. Plates were preincubated sealed with a foil for 35 min at 30°C on a rocking platform, before the addition of 1 μ M or 2 μ M radiolabeled [^{32/33}P]c-di-GMP. After a second incubation for 2 h at 30°C, plate sealing foils were removed and 96-well plates were placed on a cooling plate and UV-irradiated at 254 nm for 20 min using a Bio-Link crosslinker (Vilber Lourmat, France). Thereafter, samples were taken up in a final volume of 200 μ l Crosslinking Solubilization Buffer (50 mM Tris HCl pH 7.5, 200 mM NaCl, 5% glycerol, 1 mM DTT, 0.5% DDM) and solubilized overnight at 4°C with end-over-end agitation. After ultracentrifugation (100'000 g, 1 h, 4°C), supernatants of triplicates were collected, pooled and incubated with 40 μ l anti-Flag M2 magnetic beads (Sigma) overnight at 4°C with end-over-end agitation. Beads were washed multiple times

with IP Wash Buffer B (50 mM Tris HCl pH 7.5, 1 M NaCl, 5% glycerol, 0.1% DDM) and the help of a magnet, before immunoprecipitated proteins were analyzed by Coomassie staining and autoradiography. If needed, band intensities were quantified using the ImageJ software 'Integrated Density' tool and autoradiography band intensities were normalized to protein amounts on Coomassie-stained gels.

Acknowledgements

We thank Jacob G. Malone for assistance with error-prone PCR, Alain Casanova for the construction of strain AB1313 and plasmid pAC551, XXX XXX and John S. Parkinson for the generous gifts of anti-poly-GlcNAc and α -FliC antiserum, respectively, and Régis Hallez for helpful advice and discussions. This work was supported by Swiss National Science Foundation Fellowship XXX to UJ and a fellowship from the Werner Siemens Foundation (Zug) to SS.

Author Contributions

SS, CL, AB and UJ conceived and designed the experiments. SS and CL performed the experiments. SS, CL, AB and UJ analyzed the data. SS and UJ wrote the paper.

Conflict of Interest

The authors declare that they have no conflict of interest.

References

- Amini S, Goodarzi H & Tavazoie S (2009) Genetic dissection of an exogenously induced biofilm in laboratory and clinical isolates of *E. coli*. *PLoS Pathog* **5**: e1000432
- Baba T, Ara T, Hasegawa M, Takai Y, Okumura Y, Baba M, Datsenko KA, Tomita M, Wanner BL & Mori H (2006) Construction of *Escherichia coli* K-12 in-frame, single-gene knockout mutants: the Keio collection. *Mol Syst Biol* **2**: 2006.0008
- Babitzke P & Romeo T (2007) CsrB sRNA family: sequestration of RNA-binding regulatory proteins. *Curr Opin Microbiol* **10**: 156-163
- Baykov AA, Evtushenko OA & Avaeva SM (1988) A malachite green procedure for orthophosphate determination and its use in alkaline phosphatase-based enzyme immunoassay. *Anal Biochem* **171**: 266-270
- Becker S, Soares C & Porto LM (2009) Computational analysis suggests that virulence of *Chromobacterium violaceum* might be linked to biofilm formation and poly-NAG biosynthesis. *Genet Mol Biol* **32**: 640-644
- Bentancor LV, O'Malley JM, Bozkurt-Guzel C, Pier GB & Maira-Litrán T (2012) Poly-N-acetyl-beta-(1-6)-glucosamine is a target for protective immunity against *Acinetobacter baumannii* infections. *Infect Immun* **80**: 651-656
- Bernhardt TG & de Boer PAJ (2004) Screening for synthetic lethal mutants in *Escherichia coli* and identification of EnvC (YibP) as a periplasmic septal ring factor with murein hydrolase activity. *Mol Microbiol* **52**: 1255-1269
- Bobrov AG, Kirillina O, Forman S, Mack D & Perry RD (2008) Insights into *Yersinia pestis* biofilm development: topology and co-interaction of Hms inner membrane proteins involved in exopolysaccharide production. *Environ Microbiol* **10**: 1419-1432
- Boehm A, Kaiser M, Li H, Spangler C, Kasper CA, Ackermann M, Kaever V, Sourjik V, Roth V & Jenal U (2010) Second messenger-mediated adjustment of bacterial swimming velocity. *Cell* **141**: 107-116
- Boehm A, Steiner S, Zaehring F, Casanova A, Hamburger F, Ritz D, Keck W, Ackermann M, Schirmer T & Jenal U (2009) Second messenger signalling governs *Escherichia coli* biofilm induction upon ribosomal stress. *Mol Microbiol* **72**: 1500-1516
- Bossé JT, Sinha S, Li M-S, O'Dwyer CA, Nash JHE, Rycroft AN, Kroll JS & Langford PR (2010) Regulation of *pga* operon expression and biofilm formation in *Actinobacillus pleuropneumoniae* by sigmaE and H-NS. *J Bacteriol* **192**: 2414-2423
- Branda SS, Vik A, Friedman L & Kolter R (2005) Biofilms: the matrix revisited. *Trends Microbiol* **13**: 20-26
- Cerca N, Maira-Litrán T, Jefferson KK, Grout M, Goldmann DA & Pier GB (2007) Protection against *Escherichia coli* infection by antibody to the *Staphylococcus aureus* poly-N-acetylglucosamine surface polysaccharide. *Proc Natl Acad Sci USA* **104**: 7528-7533
- Chavez RG, Alvarez AF, Romeo T & Georgellis D (2010) The physiological stimulus for the BarA sensor kinase. *J Bacteriol* **192**: 2009-2012
- Cherepanov PP & Wackernagel W (1995) Gene disruption in *Escherichia coli*: TcR and KmR cassettes with the option of Flp-catalyzed excision of the antibiotic-resistance determinant. *Gene* **158**: 9-14
- Choi AHK, Slamti L, Avci FY, Pier GB & Maira-Litrán T (2009) The *pga*ABCD locus of *Acinetobacter baumannii* encodes the production of poly-beta-1-6-N-acetylglucosamine, which is critical for biofilm formation. *J Bacteriol* **191**: 5953-5963
- Christen B, Christen M, Paul R, Schmid F, Folcher M, Jenoe P, Meuwly M & Jenal U (2006) Allosteric control of cyclic di-GMP signaling. *J Biol Chem* **281**: 32015-32024
- Christen M, Christen B, Allan MG, Folcher M, Jenö P, Grzesiek S & Jenal U (2007) DgrA is a member of a new family of cyclic diguanosine monophosphate receptors and controls flagellar motor function in *Caulobacter crescentus*. *Proc Natl Acad Sci USA* **104**: 4112-4117

- Christen M, Christen B, Folcher M, Schauerte A & Jenal U (2005) Identification and characterization of a cyclic di-GMP-specific phosphodiesterase and its allosteric control by GTP. *J Biol Chem* **280**: 30829-30837
- Chung CT, Niemela SL & Miller RH (1989) One-step preparation of competent Escherichia coli: transformation and storage of bacterial cells in the same solution. *Proc Natl Acad Sci USA* **86**: 2172-2175
- Ciocchini AE, Roset MS, Briones G, Iñón de Iannino N & Ugalde RA (2006) Identification of active site residues of the inverting glycosyltransferase Cgs required for the synthesis of cyclic beta-1,2-glucan, a Brucella abortus virulence factor. *Glycobiology* **16**: 679-691
- Conover MS, Sloan GP, Love CF, Sukumar N & Deora R (2010) The Bps polysaccharide of Bordetella pertussis promotes colonization and biofilm formation in the nose by functioning as an adhesin. *Mol Microbiol* **77**: 1439-1455
- Costerton JW, Stewart PS & Greenberg EP (1999) Bacterial biofilms: a common cause of persistent infections. *Science* **284**: 1318-1322
- Datsenko KA & Wanner BL (2000) One-step inactivation of chromosomal genes in Escherichia coli K-12 using PCR products. *Proc Natl Acad Sci USA* **97**: 6640-6645
- Davies D (2003) Understanding biofilm resistance to antibacterial agents. *Nat Rev Drug Discov* **2**: 114-122
- Fang X & Gomelsky M (2010) A post-translational, c-di-GMP-dependent mechanism regulating flagellar motility. *Mol Microbiol* **76**: 1295-1305
- Flemming H-C & Wingender J (2010) The biofilm matrix. *Nat Rev Microbiol* **8**: 623-633
- Forman S, Bobrov AG, Kirillina O, Craig SK, Abney J, Fetherston JD & Perry RD (2006) Identification of critical amino acid residues in the plague biofilm Hms proteins. *Microbiology* **152**: 3399-3410
- Fux CA, Costerton JW, Stewart PS & Stoodley P (2005) Survival strategies of infectious biofilms. *Trends Microbiol* **13**: 34-40
- Galperin MY, Higdon R & Kolker E (2010) Interplay of heritage and habitat in the distribution of bacterial signal transduction systems. *Mol BioSyst* **6**: 721-728
- Gerke C, Kraft A, Süßmuth R, Schweitzer O & Götz F (1998) Characterization of the N-acetylglucosaminyltransferase activity involved in the biosynthesis of the Staphylococcus epidermidis polysaccharide intercellular adhesin. *J Biol Chem* **273**: 18586-18593
- Hall-Stoodley L, Costerton JW & Stoodley P (2004) Bacterial biofilms: from the natural environment to infectious diseases. *Nat Rev Microbiol* **2**: 95-108
- Heldermon C, DeAngelis PL & Weigel PH (2001) Topological organization of the hyaluronan synthase from Streptococcus pyogenes. *J Biol Chem* **276**: 2037-2046
- Hengge R (2009) Principles of c-di-GMP signalling in bacteria. *Nat Rev Microbiol* **7**: 263-273
- Heroven AK, Böhme K, Rohde M & Dersch P (2008) A Csr-type regulatory system, including small non-coding RNAs, regulates the global virulence regulator RovA of Yersinia pseudotuberculosis through RovM. *Mol Microbiol* **68**: 1179-1195
- Higuchi R, Krummel B & Saiki R (1988) A general method of in vitro preparation and specific mutagenesis of DNA fragments: study of protein and DNA interactions. *Nucleic Acids Res* **16**: 7351-7367
- Hinnebusch BJ, Perry RD & Schwan TG (1996) Role of the Yersinia pestis hemin storage (hms) locus in the transmission of plague by fleas. *Science* **273**: 367-370
- Holland LM, O'Donnell ST, Ryjenkov DA, Gomelsky L, Slater SR, Fey PD, Gomelsky M & O'Gara JP (2008) A staphylococcal GGDEF domain protein regulates biofilm formation independently of cyclic dimeric GMP. *J Bacteriol* **190**: 5178-5189
- Inoue H, Nojima H & Okayama H (1990) High efficiency transformation of Escherichia coli with plasmids. *Gene* **96**: 2172-2175
- Itoh Y, Rice JD, Goller C, Pannuri A, Taylor J, Meisner J, Beveridge TJ, Preston JF & Romeo T (2008) Roles of pgaABCD genes in synthesis, modification, and export of the Escherichia coli biofilm adhesin poly-beta-1,6-N-acetyl-D-glucosamine. *J Bacteriol* **190**: 3670-3680

- Izano E a, Sadovskaya I, Vinogradov E, Mulks MH, Velliyagounder K, Ragunath C, Kher WB, Ramasubbu N, Jabbouri S, Perry MB & Kaplan JB (2007) Poly-N-acetylglucosamine mediates biofilm formation and antibiotic resistance in *Actinobacillus pleuropneumoniae*. *Microb Pathog* **43**: 1-9
- Izano EA, Sadovskaya I, Wang H, Vinogradov E, Ragunath C, Ramasubbu N, Jabbouri S, Perry MB & Kaplan JB (2008) Poly-N-acetylglucosamine mediates biofilm formation and detergent resistance in *Aggregatibacter actinomycetemcomitans*. *Microb Pathog* **44**: 52-60
- Jonas K, Edwards AN, Simm R, Romeo T, Römling U & Melefors O (2008) The RNA binding protein CsrA controls cyclic di-GMP metabolism by directly regulating the expression of GGDEF proteins. *Mol Microbiol* **70**: 236-257
- Karatan E & Watnick P (2009) Signals, regulatory networks, and materials that build and break bacterial biofilms. *Microbiol Mol Biol Rev* **73**: 310-347
- Karimova G, Pidoux J, Ullmann A & Ladant D (1998) A bacterial two-hybrid system based on a reconstituted signal transduction pathway. *Proc Natl Acad Sci USA* **95**: 5752-5756
- Keiski C-L, Harwich M, Jain S, Neculai AM, Yip P, Robinson H, Whitney JC, Riley L, Burrows LL, Ohman DE & Howell PL (2010) AlgK is a TPR-containing protein and the periplasmic component of a novel exopolysaccharide secretin. *Structure* **18**: 265-273
- Kirillina O, Fetherston JD, Bobrov AG, Abney J & Perry RD (2004) HmsP, a putative phosphodiesterase, and HmsT, a putative diguanylate cyclase, control Hms-dependent biofilm formation in *Yersinia pestis*. *Mol Microbiol* **54**: 75-88
- Krasteva PV, Fong JCN, Shikuma NJ, Beyhan S, Navarro MVA, Yildiz FH & Sondermann H (2010) *Vibrio cholerae* VpsT regulates matrix production and motility by directly sensing cyclic di-GMP. *Science* **327**: 866-868
- Laemmli UK (1970) Cleavage of structural proteins during the assembly of the head of bacteriophage T4. *Nature* **227**: 680-685
- Lee VT, Matewish JM, Kessler JL, Hyodo M, Hayakawa Y & Lory S (2007) A cyclic-di-GMP receptor required for bacterial exopolysaccharide production. *Mol Microbiol* **65**: 1474-1484
- Lewis K (2010) Persister cells. *Annu Rev Microbiol* **64**: 357-372
- Mack D, Fischer W, Krokotsch A, Leopold K, Hartmann R, Egge H & Laufs R (1996) The intercellular adhesin involved in biofilm accumulation of *Staphylococcus epidermidis* is a linear beta-1,6-linked glucosaminoglycan: purification and structural analysis. *J Bacteriol* **178**: 175-183
- Mah TF & O'Toole GA (2001) Mechanisms of biofilm resistance to antimicrobial agents. *Trends Microbiol* **9**: 34-39
- Maira-Litrán T, Kropec A, Goldmann DA & Pier GB (2005) Comparative opsonic and protective activities of *Staphylococcus aureus* conjugate vaccines containing native or deacetylated *Staphylococcal* poly-N-acetyl-beta-(1-6)-glucosamine. *Infect Immun* **73**: 6752-6762
- Meisenheimer KM & Koch TH (1997) Photocross-linking of nucleic acids to associated proteins. *Crit Rev Biochem Mol* **32**: 101-140
- Mengin-Lecreux D, Siegel E & van Heijenoort J (1989) Variations in UDP-N-acetylglucosamine and UDP-N-acetylmuramyl-pentapeptide pools in *Escherichia coli* after inhibition of protein synthesis. *J Bacteriol* **171**: 3282-3287
- Merighi M, Lee VT, Hyodo M, Hayakawa Y & Lory S (2007) The second messenger bis-(3'-5')-cyclic-GMP and its PilZ domain-containing receptor Alg44 are required for alginate biosynthesis in *Pseudomonas aeruginosa*. *Mol Microbiol* **65**: 876-895
- Miller JH (1972) Experiments in molecular genetics. Cold Spring Harbor Laboratory (Cold Spring Harbor, N.Y)
- Monteiro C, Saxena I, Wang X, Kader A, Bokranz W, Simm R, Nobles D, Chromek M, Brauner A, Brown RMJ & Römling U (2009) Characterization of cellulose production in *Escherichia coli* Nissle 1917 and its biological consequences. *Environ Microbiol* **11**: 1105-1116
- Namboori SC & Graham DE (2008) Enzymatic analysis of uridine diphosphate N-acetyl-D-glucosamine. *Anal Biochem* **381**: 94-100

- O’Gara JP (2007) *ica* and beyond: biofilm mechanisms and regulation in *Staphylococcus epidermidis* and *Staphylococcus aureus*. *FEMS Microbiol Lett* **270**: 179-188
- O’Toole G, Kaplan HB & Kolter R (2000) Biofilm formation as microbial development. *Annu Rev Microbiol* **54**: 49-79
- Papworth C, Bauer JC, Braman J & Wright D (1996) Site-directed mutagenesis in one day with >80% efficiency. *Strategies* **9**: 3-4
- Parise G, Mishra M, Itoh Y, Romeo T & Deora R (2007) Role of a putative polysaccharide locus in *Bordetella* biofilm development. *J Bacteriol* **189**: 750-760
- Paul K, Nieto V, Carlquist WC, Blair DF & Harshey RM (2010) The c-di-GMP binding protein YcgR controls flagellar motor direction and speed to affect chemotaxis by a “backstop brake” mechanism. *Mol Cell* **38**: 128-139
- Paul R, Weiser S, Amiot NC, Chan C, Schirmer T, Giese B & Jenal U (2004) Cell cycle-dependent dynamic localization of a bacterial response regulator with a novel di-guanylate cyclase output domain. *Genes Dev* **18**: 715-727
- Pesavento C, Becker G, Sommerfeldt N, Possling A, Tschowri N, Mehliis A & Hengge R (2008) Inverse regulatory coordination of motility and curli-mediated adhesion in *Escherichia coli*. *Genes Dev* **22**: 2434-2446
- Povolotsky TL & Hengge R (2012) “Life-style” control networks in *Escherichia coli*: Signaling by the second messenger c-di-GMP. *J Biotechnol*: 1-7
- Pérez-Mendoza D, Coulthurst SJ, Sanjuán J & Salmond GPC (2011) N-acetyl-glucosamine-dependent biofilm formation in *Pectobacterium atrosepticum* is cryptic and activated by elevated c-di-GMP levels. *Microbiology* **157**: 3340-3348
- Rasila TS, Pajunen MI & Savilahti H (2009) Critical evaluation of random mutagenesis by error-prone polymerase chain reaction protocols, *Escherichia coli* mutator strain, and hydroxylamine treatment. *Anal Biochem* **388**: 71-80
- Romeo T, Gong M, Liu MY & Brun-Zinkernagel A (1993) Identification and molecular characterization of *csrA*, a pleiotropic gene from *Escherichia coli* that affects glycogen biosynthesis, gluconeogenesis, cell size, and surface properties. *J Bacteriol* **175**: 4744-4755
- Ross P, Mayer R, Weinhouse H, Amikam D, Huggirat Y & Benziman M (1990) The cyclic diguanylic acid regulatory system of cellulose synthesis in *Acetobacter xylinum*. *J Biol Chem* **265**: 18933-18943
- Ross P, Weinhouse H, Aloni Y, Michaeli D, Weinberger-Ohana P, Mayer R, Braun S, Vroom E de, Van der Marel GA, Van Broom JH & Benziman M (1987) Regulation of cellulose synthesis in *Acetobacter xylinum* by cyclic diguanylic acid. *Nature* **325**: 279-281
- Ryjenkov DA, Simm R, Römling U & Gomelsky M (2006) The PilZ domain is a receptor for the second messenger c-di-GMP: the PilZ domain protein YcgR controls motility in enterobacteria. *J Biol Chem* **281**: 30310-30314
- Saxena IM & Brown RM (1997) Identification of cellulose synthase(s) in higher plants: sequence analysis of processive beta-glycosyltransferases with the common motif “D, D, D35Q(R,Q)XRW”. *Cellulose* **4**: 33-49
- Saxena IM, Brown RM & Dandekar T (2001) Structure-function characterization of cellulose synthase: relationship to other glycosyltransferases. *Phytochemistry* **57**: 1135-1148
- Schirmer T & Jenal U (2009) Structural and mechanistic determinants of c-di-GMP signalling. *Nat Rev Microbiol* **7**: 724-735
- Skurnik D, Davis MRJ, Benedetti D, Moravec KL, Cywes-Bentley C, Roux D, Traficante DC, Walsh RL, Maria-Litràn T, Cassidy SK, Hermos CR, Martin TR, Thakkallapalli EL, Vargas SO, McAdam AJ, Lieberman TD, Kishony R, LiPuma JJ, Pier GB, Goldberg JB, *et al* (2012) Targeting pan-resistant bacteria with antibodies to a broadly conserved surface polysaccharide expressed during infection. *J Infect Dis*
- Sondermann H, Shikuma NJ & Yildiz FH (2011) You’ve come a long way: c-di-GMP signaling. *Curr Opin Microbiol* **15**: 140-146

- Sonnhammer EL, von Heijne G & Krogh A (1998) A hidden Markov model for predicting transmembrane helices in protein sequences. *Proceedings International Conference on Intelligent Systems for Molecular Biology* **6**: 175-182
- Suzuki K, Babitzke P, Kushner SR & Romeo T (2006) Identification of a novel regulatory protein (CsrD) that targets the global regulatory RNAs CsrB and CsrC for degradation by RNase E. *Genes Dev* **20**: 2605-2617
- Tagliabue L, Antoniani D, Maciag A, Bocci P, Raffaelli N & Landini P (2010) The diguanylate cyclase YddV controls production of the exopolysaccharide poly-N-acetylglucosamine (PNAG) through regulation of the PNAG biosynthetic pgaABCD operon. *Microbiology* **156**: 2901-2911
- Timmermans J & Van Melderen L (2010) Post-transcriptional global regulation by CsrA in bacteria. *Cell Mol Life Sci* **67**: 2897-2908
- Tlapak-Simmons VL, Baggenstoss BA, Clyne T & Weigel PH (1999) Purification and lipid dependence of the recombinant hyaluronan synthases from *Streptococcus pyogenes* and *Streptococcus equisimilis*. *J Biol Chem* **274**: 4239-4245
- Tlapak-Simmons VL, Kempner ES, Baggenstoss BA & Weigel PH (1998) The active Streptococcal hyaluronan synthases (HASs) contain a single HAS monomer and multiple cardiolipin molecules. *J Biol Chem* **273**: 26100-26109
- Towbin H, Staehelin T & Gordon J (1979) Electrophoretic transfer of proteins from polyacrylamide gels to nitrocellulose sheets: procedure and some applications. *Proc Natl Acad Sci USA* **76**: 4350-4354
- Tuckerman JR, Gonzalez G & Gilles-Gonzalez M-A (2011) Cyclic di-GMP activation of polynucleotide phosphorylase signal-dependent RNA processing. *J Mol Biol* **407**: 633-639
- Uzzau S, Figueroa-Bossi N, Rubino S & Bossi L (2001) Epitope tagging of chromosomal genes in *Salmonella*. *Proc Natl Acad Sci USA* **98**: 15264-15269
- Vanderheiden GJ, Fairchild AC & Jago GR (1970) Construction of a laboratory press for use with the French pressure cell. *Appl Microbiol* **19**: 875-877
- Wang X, Dubey AK, Suzuki K, Baker CS, Babitzke P & Romeo T (2005) CsrA post-transcriptionally represses pgaABCD, responsible for synthesis of a biofilm polysaccharide adhesin of *Escherichia coli*. *Mol Microbiol* **56**: 1648-1663
- Wang X, Preston JF & Romeo T (2004) The pgaABCD locus of *Escherichia coli* promotes the synthesis of a polysaccharide adhesin required for biofilm formation. *J Bacteriol* **186**: 2724-2734
- Wassmann P, Chan C, Paul R, Beck A, Heerklotz H, Jenal U & Schirmer T (2007) Structure of BeF₃-modified response regulator PleD: implications for diguanylate cyclase activation, catalysis, and feedback inhibition. *Structure* **15**: 915-927
- Weigel PH & DeAngelis PL (2007) Hyaluronan synthases: a decade-plus of novel glycosyltransferases. *J Biol Chem* **282**: 36777-36781
- Yakandawala N, Gawande PV, LoVetri K, Cardona ST, Romeo T, Nitz M & Madhyastha S (2011) Characterization of the poly-beta-1,6-N-acetylglucosamine polysaccharide component of *Burkholderia* biofilms. *Appl Environ Microbiol* **77**: 8303-8309
- Yu D, Ellis HM, Lee EC, Jenkins NA, Copeland NG & Court DL (2000) An efficient recombination system for chromosome engineering in *Escherichia coli*. *Proc Natl Acad Sci USA* **97**: 5978-5983
- Zähringer F, Massa C & Schirmer T (2011) Efficient enzymatic production of the bacterial second messenger c-di-GMP by the diguanylate cyclase YdeH from *E. coli*. *Appl Biochem Biotechnol* **163**: 71-79

Figure legends

Figure 1 c-di-GMP controls PgaD stability in a PgaC-dependent manner. (A) Immunoblot analysis of 3xFlag-tagged Pga proteins in the *E. coli* wildtype and $\Delta ydeH$ mutant. In the right panel, the native *pga* promoter was replaced with the P_{ara} promoter. Expression of the *araB-pgaA* translational fusion was induced with 0.0002% arabinose. (B) PgaD levels depend on PgaC and on c-di-GMP. Immunoblots of 3xFlag-tagged PgaD are shown for the indicated mutant strains. Expression of *pgaC* was induced with 0.0002% arabinose (upper panel) and with 0.0002% and 0.2% arabinose (lower left panel). Expression of the heterologous DGC *dgcA* from *C. crescentus* and its active site mutant *dgcA^{mut}* (D164N) was not induced (basal level) (lower right panel). (C) C-di-GMP determines *in vivo* PgaD stability. Levels of 3xFlag-tagged PgaD were analyzed by immunoblot over time after the addition of translation inhibitor to exponentially growing cells. Left: The graph shows an average of two independent experiments with standard deviations. Right: Two representative sets of immunoblots are shown. Time after translation inhibition (min) is indicated. Expression of *dgcA* and its active site mutant *dgcA^{mut}* (D164N) was not induced (basal level). (D) Biofilm formation of strains carrying multiple deletions in genes predicted to encode DGCs. The strain with a total of seven deletions ($\Delta ydeH$, $\Delta yegE$, $\Delta ycdT$, $\Delta yfiN$, $\Delta yhjK$, $\Delta ydaM$, $\Delta yneF$) is referred to as $\Delta 7$ strain. Error bars are standard deviations. Inset: PgaD is absent in a c-di-GMP^{low} strain.

Figure 2 C-di-GMP mediates tight PgaC-PgaD interaction. (A) PgaC-6xHis and PgaD-3xFlag co-immunoprecipitate from detergent-solubilized membranes. Resulting samples of Flag and Protein A (mock) IPs were analyzed by immunoblots using antibodies against the specific tags. 1st supernatant represents the protein fraction that did not bind to the beads. 2 M urea was present during the IP procedure as indicated. (B) Co-immunoprecipitation of PgaC and PgaD-3xFlag from detergent-solubilized membranes of wildtype and $\Delta 7$ mutant cells overexpressing *pgaC* and *pgaD*. Resulting IP samples were analyzed by Coomassie staining. HC and LC indicate heavy and light chains of IgG. (C) Bacterial two-hybrid analysis of PgaC-PgaD interaction. Plasmid-born T18 and T25 fusions were expressed in an adenylate cyclase mutant ($\Delta cyaA$) and transformants were analyzed on MacConkey indicator plates. Zip indicates the leucine zipper positive control. (D) Bacterial two-hybrid analysis of c-di-GMP-mediated PgaC-PgaD interaction. The *pgaC-T18* fusion was expressed from the chromosomal *pga* locus in an adenylate cyclase and cAMP phosphodiesterase mutant background ($\Delta cyaA \Delta cpdA$). Left: PgaC-PgaD interaction in the presence of a plasmid-born copy of *dgcA* wildtype or *dgcA* active site mutant (*dgcA^{mut}* (D164N)). Alleles were induced with 0.2% arabinose. Right: PgaC-PgaD interaction in strains lacking the DGC

YdeH or multiple DGCs ($\Delta 7$). (E) A PgaCD fusion protein is fully functional. Biofilm formation and protein levels of 3xFlag-tagged PgaD or PgaCD fusion protein (CDf) are indicated for a *ydeH*⁺ strain (black bars) and a $\Delta ydeH$ mutant (grey bars). Error bars are standard deviations. Expression of plasmid constructs was not induced (basal level).

Figure 3 C-di-GMP allosterically stimulates PgaCD glycosyltransferase activity *in vitro*. (A) GT activity depends on an intact PgaCD complex as measured with an enzyme-coupled spectrophotometric assay. Membranes of *csrA* mutant strains expressing *pgaC* and *pgaD* together or individually were used. 2 mM of the substrate UDP-GlcNAc was added as indicated. A representative dataset is shown. (B) Microscopic analysis of viscous poly-GlcNAc reaction product. PgaCD GT reaction was incubated with 30 mM UDP-GlcNAc for 5 h at 30°C. (C) Determination of K_m for UDP-GlcNAc of PgaCD. Membranes of a $\Delta 7$ mutant containing PgaC and PgaD were incubated with increasing concentrations of UDP-GlcNAc in the presence of 1 μ M c-di-GMP. GraphPad Prism was used to fit the curve to Michaelis-Menten kinetics. Data represent an average of two independent experiments with standard deviations. (D) Stimulatory effect of c-di-GMP on PgaCD GT activity (K_{act}). Membranes of a $\Delta 7$ mutant containing PgaC and PgaD were incubated with increasing concentrations of c-di-GMP in the presence of 50 μ M UDP-GlcNAc. GraphPad Prism was used for curve fitting. A representative dataset is shown.

Figure 4 Specific and competitive c-di-GMP binding requires PgaC and PgaD. (A) Immunoblot of captured PgaD from membranes containing PgaC and PgaD-3xFlag. The concentrations of c-di-GMP-cc and competing nucleotides are indicated. (B) Immunoblots of captured PgaC, PgaD and PgaCD fusion protein (PgaCDf) from membranes containing PgaC and PgaD-3xFlag (1st panel), PgaCDf-3xFlag (2nd panel), PgaC-3xFlag (3rd panel), PgaD-3xFlag (4th panel) or PgaC-3xFlag and PgaD-3xFlag (5th panel). The concentrations of c-di-GMP-cc and competing nucleotides are indicated. SDS-resistant heterodimeric PgaCD complexes are indicated (PgaC + PgaD). (C) Both PgaC and PgaD are specifically and competitively labeled with [³³P]c-di-GMP. Membranes containing PgaC-3xFlag and PgaD-3xFlag were UV-crosslinked in the presence of [³³P]c-di-GMP. The concentrations of [³³P]c-di-GMP and competing nucleotides are indicated. Following Flag IP, samples were analyzed by Coomassie staining (left panel) and autoradiography (right panel). Light (LC) and heavy (HC) chains of IgG and SDS-resistant PgaCD complexes (PgaC + PgaD) are indicated. (D) Absence of PgaD abolishes c-di-GMP binding. [³²P]c-di-GMP UV-crosslinking of membranes containing PgaC-3xFlag and PgaD-3xFlag (upper panels) or PgaC-3xFlag (lower panel). The

concentrations of [³²P]c-di-GMP and competing nucleotides are indicated. Following Flag IP, samples were analyzed by autoradiography.

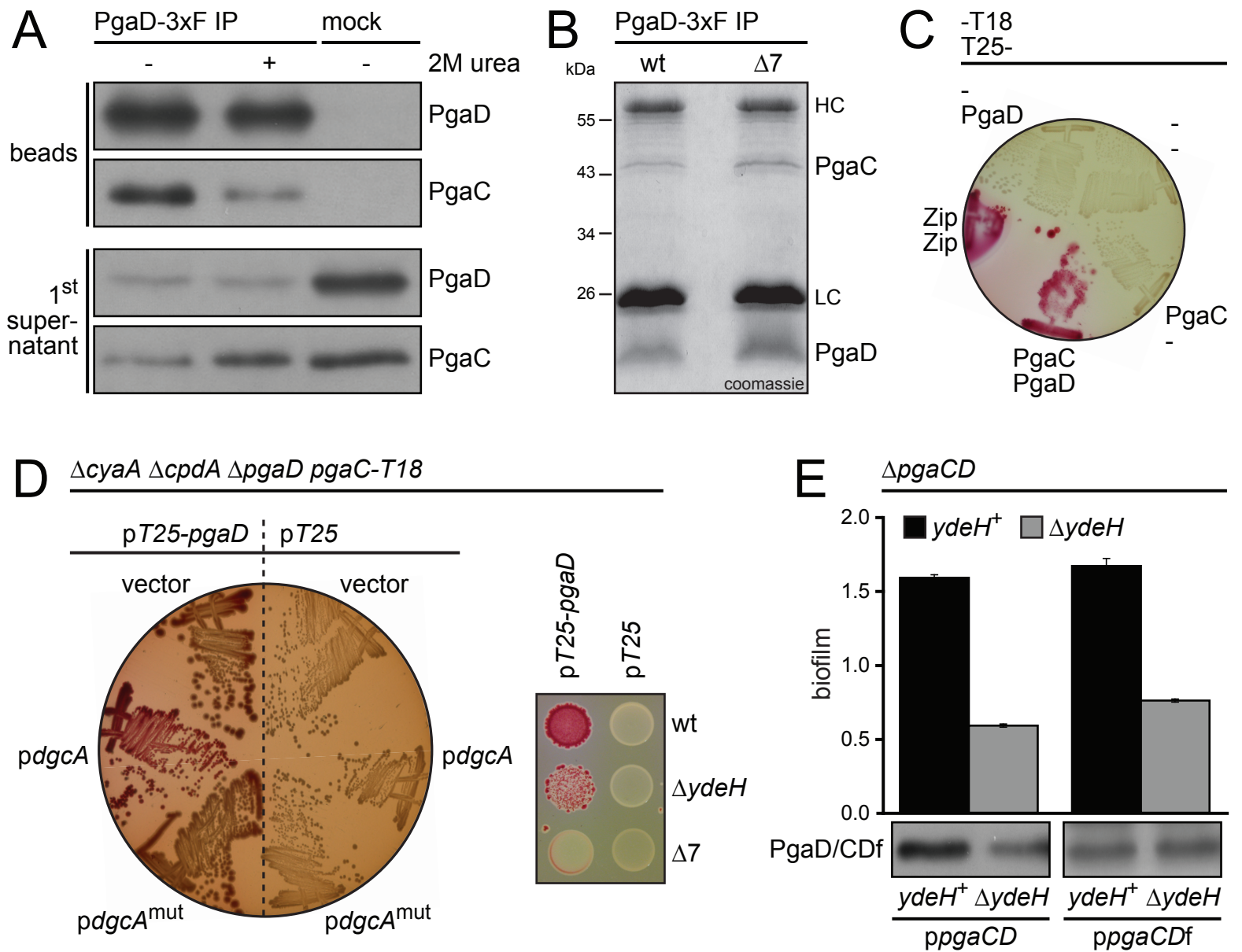
Figure 5 *pgaD* gain-of-function mutants render the PgaCD complex insensitive to c-di-GMP. (A) PgaD GOF mutations cluster within the most conserved region of the protein (highlighted in grey) that has previously been described (Forman *et al*, 2006). Transmembrane helices were predicted using the TMHMM server (Sonnhammer *et al*, 1998). Isolated PgaD GOF mutations are colored in orange. The previously described W71 that is important for PgaD function is shown in red (Forman *et al*, 2006). Triangles depict the sites of C-terminal PgaD truncations that still allowed c-di-GMP-controlled biofilm formation (see Figure 5F). Model was drawn using the TOPO2 software (S. J. Johns, <http://www.sacs.ucsf.edu/TOPO2/>). N and C denote the N- and C-termini of the protein. IM = inner membrane. (B) Biofilm formation in response to different *pgaD* alleles. Wildtype (black bars) is compared to a $\Delta 7$ mutant background (grey bars). Isolated GOF alleles are underlined. Error bars are standard deviations. Expression of plasmid constructs was not induced (basal level). (C) Immunoblot analysis of PgaD steady state protein levels in response to c-di-GMP ($\Delta 7$ mutant/wildtype). A C-terminally 3xFlag-tagged construct was used for PgaD detection. Expression of plasmid constructs was not induced (basal level). (D) The PgaCDf (PgaD: N75D, K76E) is strongly impaired in c-di-GMP binding. The quantification of pulled-down protein amounts relative to wildtype is an average of two independent experiments with standard deviations. 0.8 μ M c-di-GMP-cc was used for pull-downs (grey bars). In competition experiments, samples were preincubated with a 125-fold molar excess of c-di-GMP (black bars). (PgaD) indicates that mutations lie within the PgaD part of PgaCDf with amino acid numbering according to unfused PgaD. (E) *In vitro* PgaCD GT activity in response to c-di-GMP. Initial reaction velocities were measured using three $\Delta 7$ mutant membrane fractions, each expressing a different *pgaCDf* allele (see Supplementary Figure 4D), in the presence of 300 μ M UDP-GlcNAc and with (black bars) or without (grey bars) the addition of 100 nM c-di-GMP. Error bars are standard errors. (PgaD) indicates that mutations lie within the PgaD part of PgaCDf with amino acid numbering according to unfused PgaD. A representative dataset is shown. (F) Biofilm formation in response to C-terminally truncated *pgaD* alleles and cellular c-di-GMP concentrations (*wspR* overexpression). The last amino acid of each allele is stated in brackets (see Figure 5A). Vector controls (white and black bars) are compared to *wspR* overexpressions (light and dark grey bars) in a $\Delta 7$ background. Error bars are standard deviations. Expression of *pgaD* alleles was induced with 0.2% (left graph) and 0.02% arabinose (right graph), respectively.

Figure 6 The *pgaD* (N75D, K76E) GOF allele rescues biofilm formation of a *pgaC* (R222A) LOF mutant. (A) Isolated *pgaC* GOF mutants are not c-di-GMP-independent. Biofilm formation in response to different *pgaC* alleles. Wildtype (black bars) is compared to a $\Delta 7$ mutant background (grey bars). Isolated GOF alleles are underlined. Error bars are standard deviations. Expression of plasmid constructs was not induced (basal level). (B) Immunoblot analysis of PgaD steady state protein levels in response to different *pgaC* GOF alleles and c-di-GMP ($\Delta 7$ mutant/wildtype). A C-terminally 3xFlag-tagged construct was used for PgaD detection. Expression of plasmid constructs was not induced (basal level). (C) Analysis of arginine residues in PgaC that are not conserved between c-di-GMP signalling-containing and non-containing species (see Supplementary Figure 6). Biofilm formation relative to wildtype in response to different *pgaCDf* alleles. (*pgaC*) indicates that mutations lie within the PgaC part of PgaCDf with amino acid numbering according to unfused PgaC. R198D was included as a control as this arginine is also conserved in PgaC homologues of species that lack c-di-GMP signalling. Error bars are standard deviations. Expression of plasmid constructs was not induced (basal level). (D) The PgaCDf (PgaC: R222A) is strongly impaired in c-di-GMP binding. A quantification of pulled-down protein amounts relative to wildtype with standard deviations is shown. 0.8 μ M c-di-GMP-cc was used for pull-downs (grey bars). In competition experiments, samples were preincubated with a 125-fold molar excess of c-di-GMP (black bars). (PgaC) indicates that mutations lie within the PgaC part of PgaCDf with amino acid numbering according to unfused PgaC. (E) PgaD (N75D, K76E) rescues PgaC (R222A). Biofilm formation relative to wildtype in response to different *pgaCD* alleles. Wildtype (black bars) is compared to a $\Delta 7$ mutant background (grey bars). Error bars are standard deviations. Expression of plasmid constructs was not induced (basal level).

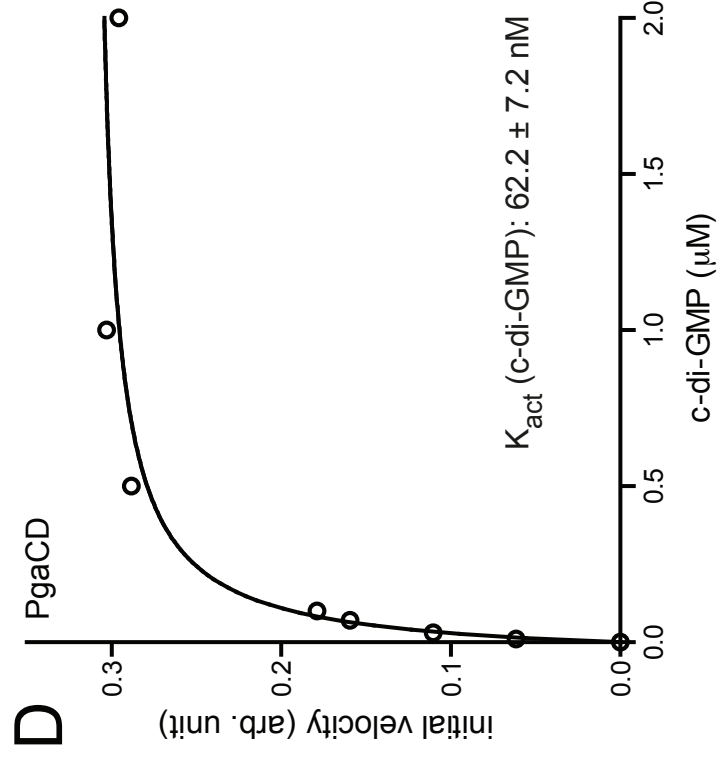
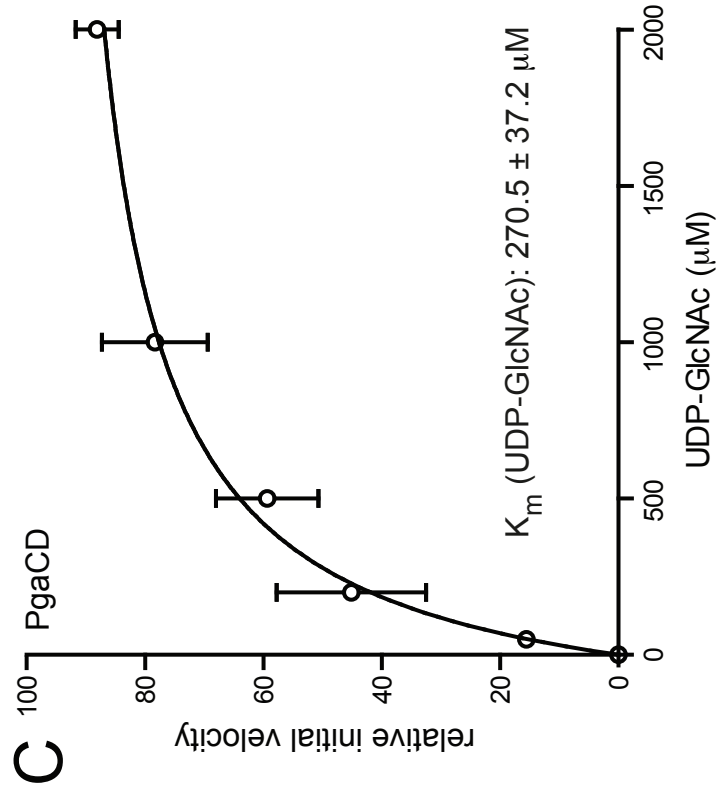
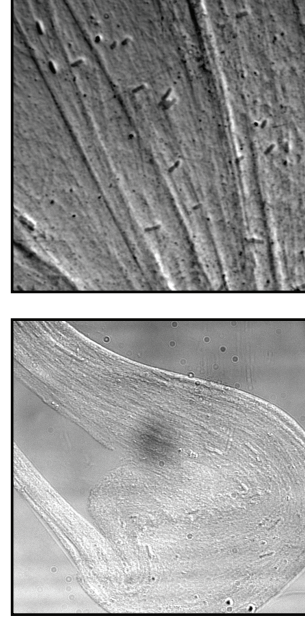
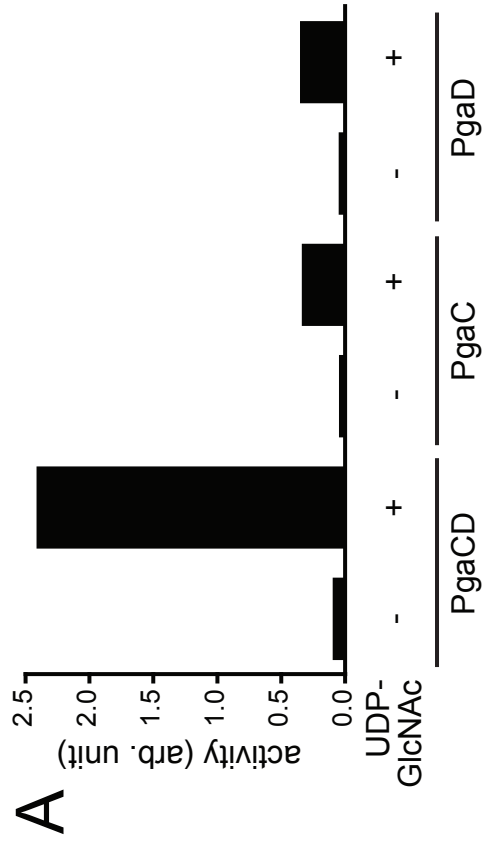
Figure 7 PgaC and PgaD both participate in c-di-GMP binding within the PgaCD complex. (A) PgaD GOF mutations N75D and K76E and PgaC LOF mutation R222A abolish competitive labeling of PgaC and PgaD with [³²P]c-di-GMP. 1 μ M [³²P]c-di-GMP was used for UV light-induced crosslinking of membranes expressing different *pgaC*-3xF *pgaD*-3xF alleles as well as *pgaC*-3xF-expressing membranes. In competition experiments, samples were preincubated with a 100-fold molar excess of c-di-GMP as indicated. Following Flag IP, samples were analyzed by Coomassie staining and autoradiography. (B) Quantification of normalized PgaC (upper graph) and PgaD (lower graph) band intensities from A relative to wildtype as an average of two independent experiments with standard deviations. UV light-induced crosslinking experiments (grey bars) are compared to competition experiments (black bars).

Figure 8 A model for allosteric c-di-GMP-dependent PgaCD glycosyltransferase activation. (A) Topology models for PgaC and PgaD in the inner membrane. Orientations of PgaC transmembrane helices is based on the integration of results of this study, TMHMM server predictions (Sonnhammer *et al*, 1998), previous results from a study on the PgaC homologue HmsR from *Y. pestis* (Bobrov *et al*, 2008), and analogies to the hyaluronan synthase from *Streptococcus pyogenes* (Heldermon *et al*, 2001; Weigel & DeAngelis, 2007). Helices 1, 2, 4 and 5 are true transmembrane helices, while helices 3 and 6 are membrane-associated helices. The two domains containing the two active sites of processive GT-2 β -glycosyltransferases are indicated (Saxena & Brown, 1997; Saxena *et al*, 2001). Position of R222 that is critical for c-di-GMP binding is highlighted in red, while the strong V227L GOF mutation is shown in green. Transmembrane helices of PgaD were predicted using the TMHMM server (Sonnhammer *et al*, 1998). NKLR as part of the conserved region likely to be involved in c-di-GMP binding is highlighted in red. N and C denote the N- and C-termini of the proteins. IM = inner membrane, PP = periplasm and CP = cytoplasm. (B) c-di-GMP binding to the PgaCD complex stabilizes the heterodimeric complex and induces a poly-GlcNAc secretion-compatible conformation within the membrane. Left: Top-view of a secretion-incompatible state with loosely associated and highly unstable PgaD. Right: Top-view of a poly-GlcNAc secretion-compatible state following c-di-GMP binding. (C) A model for a shut-off mechanism: PgaD instability temporarily uncouples the Pga machinery from c-di-GMP signalling. Following a Csr cascade input signal, the Pga machinery and DGCs get expressed (a) (Wang *et al*, 2005; Jonas *et al*, 2008). PgaC and PgaD are co-translationally synthesized into the membrane side by side and loosely interact with each other (b). Under a high c-di-GMP concentration, c-di-GMP binds the PgaCD GT complex, causing a conformational change, PgaD stabilization and allosteric GT activation (c), to promote biofilm formation. Under a low c-di-GMP concentration (e.g. DGCs are inactive), PgaD gets prone to protease-mediated degradation (d). The Pga machinery is thus temporarily uncoupled from c-di-GMP signalling. High c-di-GMP concentrations do not cause poly-GlcNAc-dependent biofilm formation since PgaD is absent (e). Only a new Csr input signal will allow any given cell to reset the system (f).

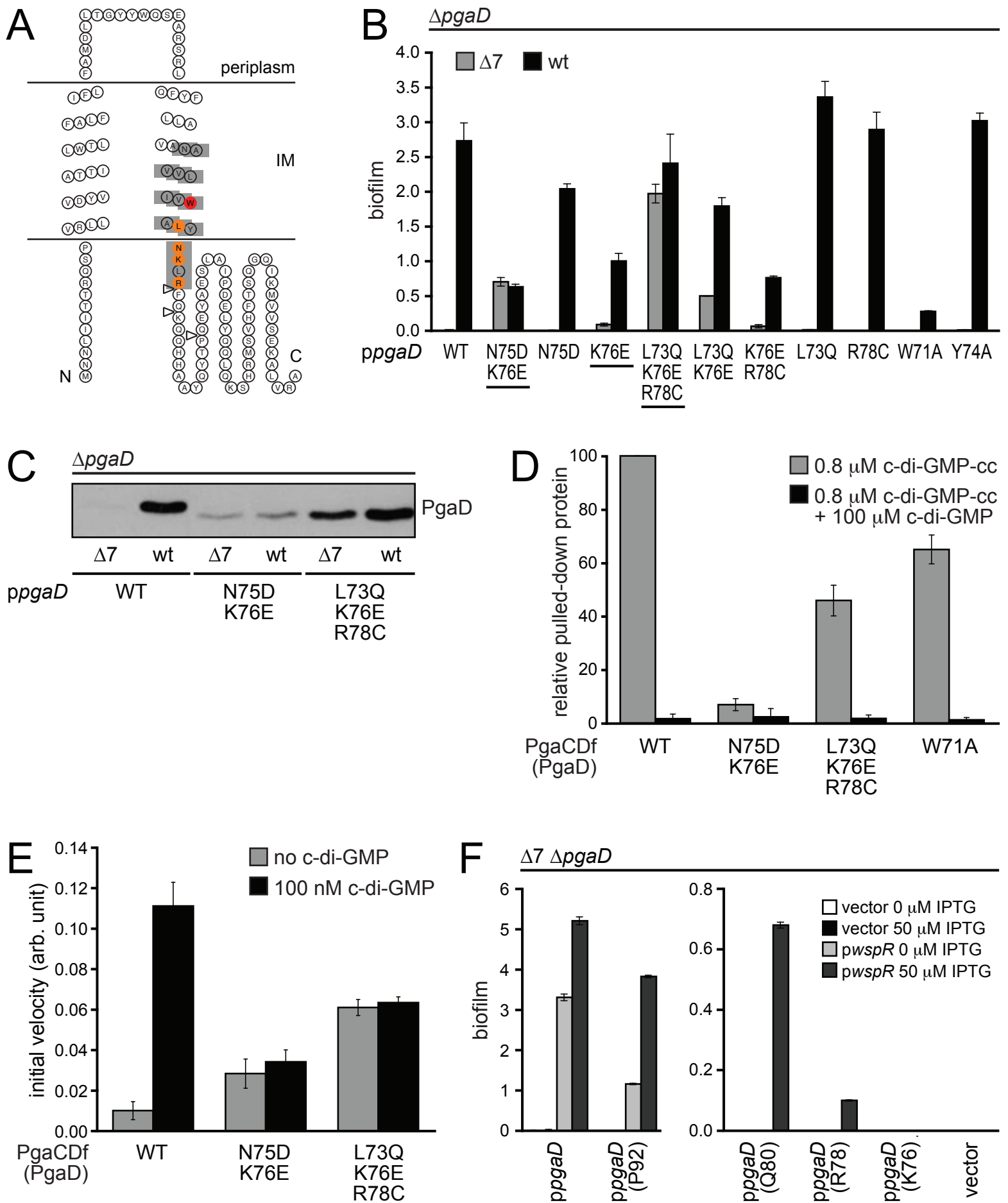
Steiner et al. Figure 2



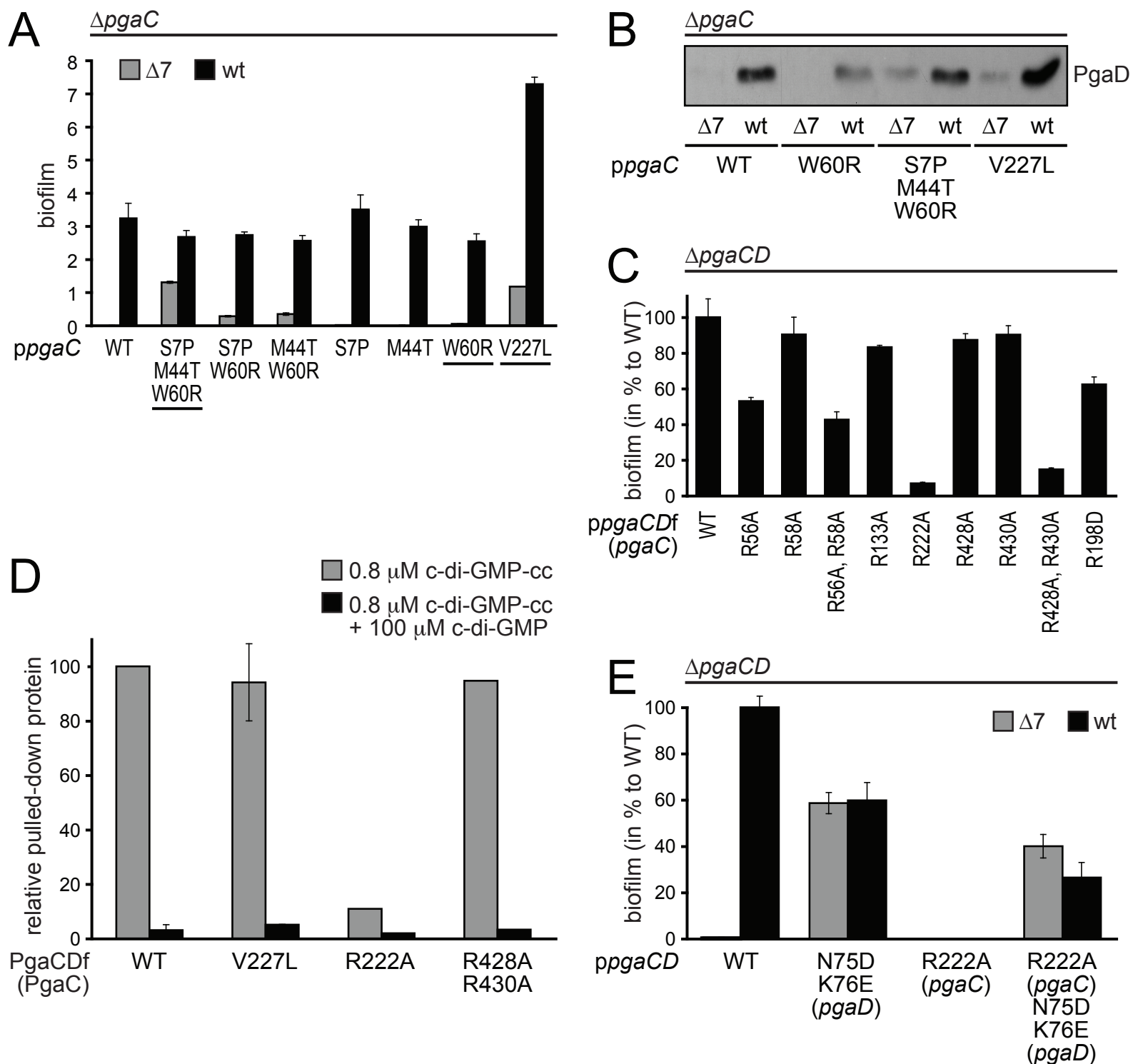
Steiner et al. Figure 3



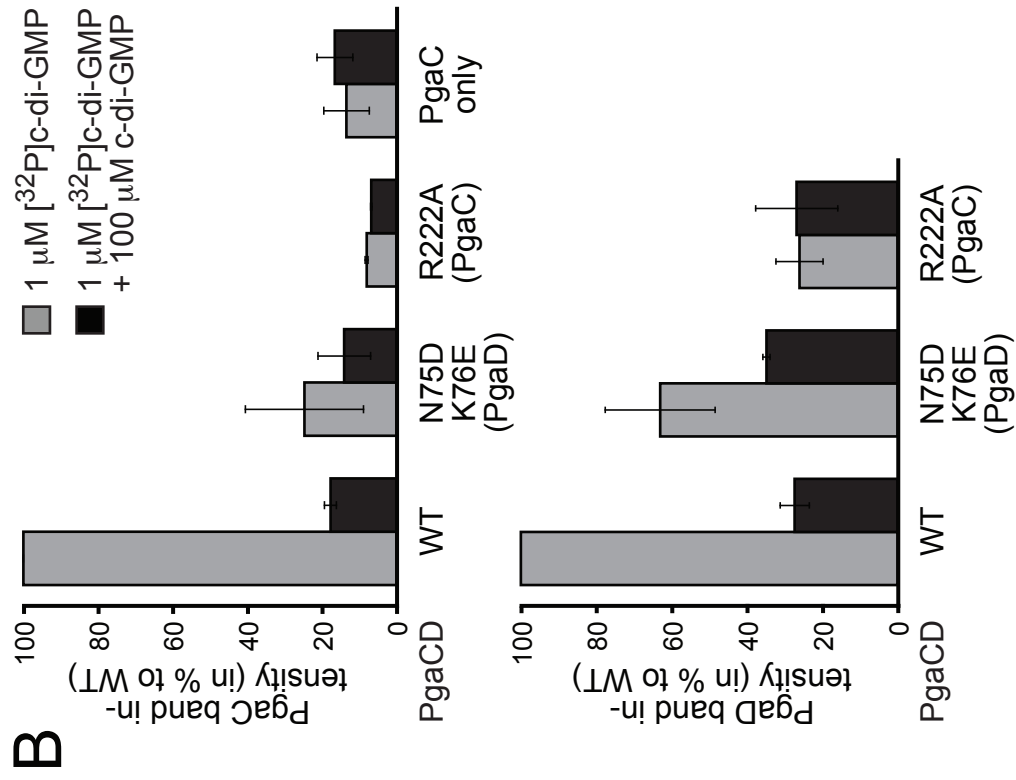
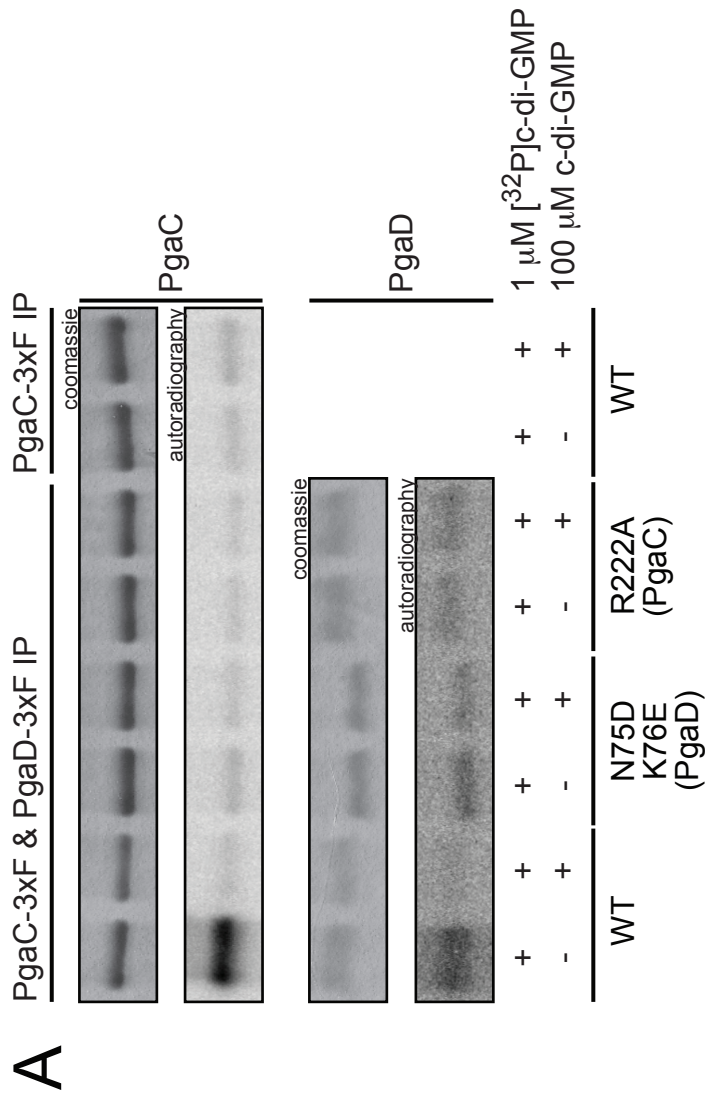
Steiner et al. Figure 5



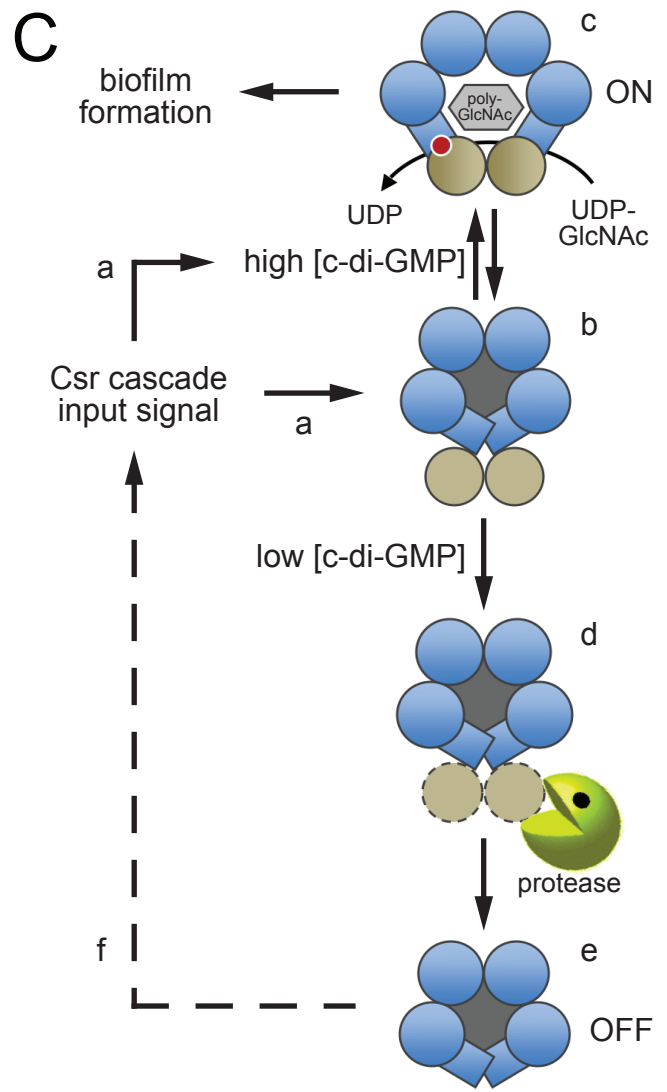
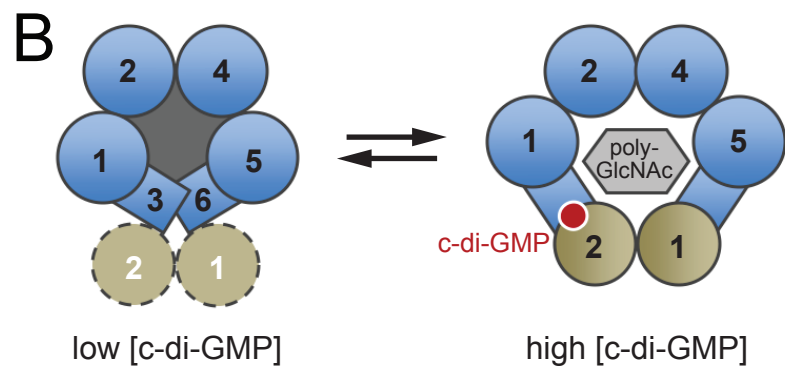
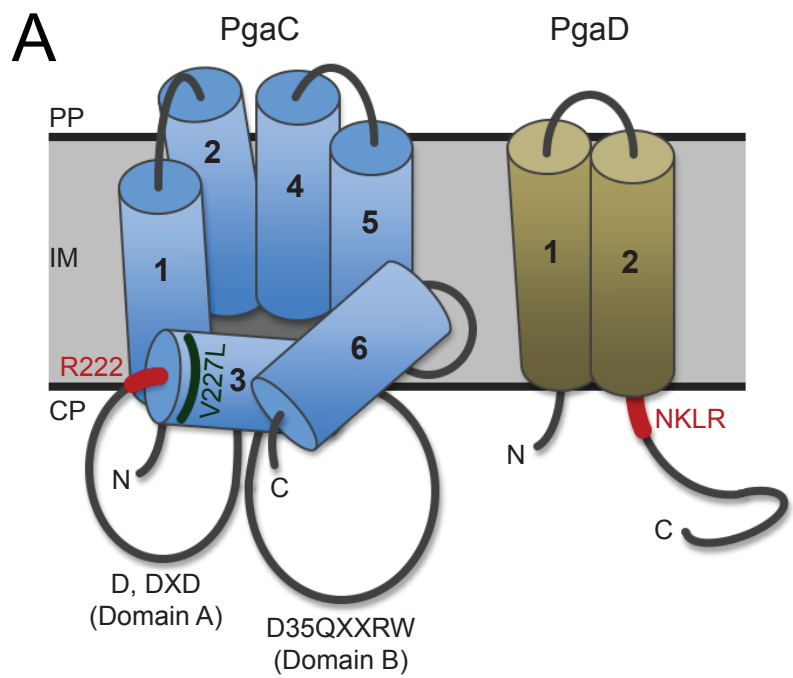
Steiner et al. Figure 6



Steiner et al. Figure 7



Steiner et al. Figure 8



Supplementary information**Supplementary Figure legends**

Supplementary Figure 1 Additional findings and controls related to Figure 1. (A) Immunoblots demonstrating that PgaC levels are not affected by a $\Delta ydeH$ deletion, neither in the presence nor in the absence of PgaD. C-terminal 3xFlag fusions were used for PgaC and PgaD detection. Expression of *pgaD* was induced as indicated. (B) Both PgaC wildtype and a PgaC active site mutant (D256N) stabilize PgaD in a *ydeH*-dependent manner. A C-terminal 3xFlag fusion was used for PgaD detection. (C) YfiR levels are not controlled by c-di-GMP (*ydeH*⁺/ $\Delta ydeH$). The chromosomal *pgaD* copy was replaced with 3xFlag-tagged *yfiR* from *P. aeruginosa* (Malone *et al*, 2010). *YfiR* (ΔN) encodes for a truncated YfiR that lacks the first 35 amino acids including the export signal sequence. FliC levels are shown as a loading control. (D) *PgaD* overexpression stimulates biofilm formation. The *pgaD* gene was replaced by an *araB-pgaD* translational fusion that was integrated downstream of *pgaC* in a *ydeH*⁺ strain (black bars) and a $\Delta ydeH$ mutant (grey bars). Expression of *pgaD* was induced as indicated. Error bars are standard deviations.

Supplementary Figure 2 C-di-GMP stimulates poly-GlcNAc biogenesis. (A) Immunoblot analysis of PgaCD GT reaction products using an anti-poly-GlcNAc antiserum. Membranes of *csrA* mutant strains harboring PgaC and PgaD (upper part) or PgaD (lower part) were incubated with 2 mM UDP-GlcNAc and increasing concentrations of c-di-GMP. The basal PgaCD GT activity in the absence of exogenously added c-di-GMP is due to increased concentrations of c-di-GMP in the *csrA* mutant strain used for membrane preparation. (B) Kinetic data for c-di-GMP K_{act} determination. Membranes of a $\Delta 7$ mutant containing PgaC and PgaD were incubated with increasing concentrations of c-di-GMP in the presence of 50 μ M UDP-GlcNAc. The GTP control is shown in green. Red lines depict vector control membranes. GraphPad Prism was used for linear regression. A representative dataset is shown.

Supplementary Figure 3 Additional findings and controls related to Figure 4. (A) Left: Anti-Biotin immunoblots showing captured PgaCDf from *pgaCDf*-expressing membranes and captured PgaC and PgaD from *pgaCD*-expressing membranes. 8 μ M c-di-GMP-cc was used for pull-downs. In competition experiments, samples were preincubated with a 125-fold molar excess of c-di-GMP as indicated. Right: Anti-Biotin immunoblots from 7.5% SDS-PAGE gels showing captured PgaC of slightly different molecular masses from *pgaCD*-expressing membranes harboring untagged (~43 kDa), His-tagged (~46 kDa) or 3xFlag-tagged PgaC (~49 kDa). 0.8 μ M c-di-GMP-cc was used for pull-downs. (B) Effect of UDP-GlcNAc on competitive c-di-GMP binding. Left and middle:

Immunoblots showing captured PgaD from *pgaCD*-expressing membranes, PgaCDf from *pgaCDf*-expressing membranes and PgaC and PgaD from *pgaC-3xF pgaD-3xF*-expressing membranes in the presence or absence of 20 mM UDP-GlcNAc. 8 μ M (left panel) and 0.8 μ M (middle panel) c-di-GMP-cc were used for pull-downs. In competition experiments, samples were preincubated with a 125-fold molar excess of c-di-GMP as indicated. The middle panel shows the experimental exception where the absence of UDP-GlcNAc did not have a negative impact on c-di-GMP binding. C-terminally 3xFlag-tagged constructs were used for protein detection. PgaC + PgaD indicates heterodimeric PgaCD complexes that withstood boiling in SDS sample buffer (middle panel). Right: 1 μ M [³²P]c-di-GMP was used for UV light-induced crosslinking of *pgaC-3xF pgaD-3xF*-expressing membranes in the presence or absence of 20 mM UDP-GlcNAc. In competition experiments, samples were preincubated with a 100-fold molar excess of c-di-GMP as indicated. Following Flag IP, samples were analyzed by autoradiography.

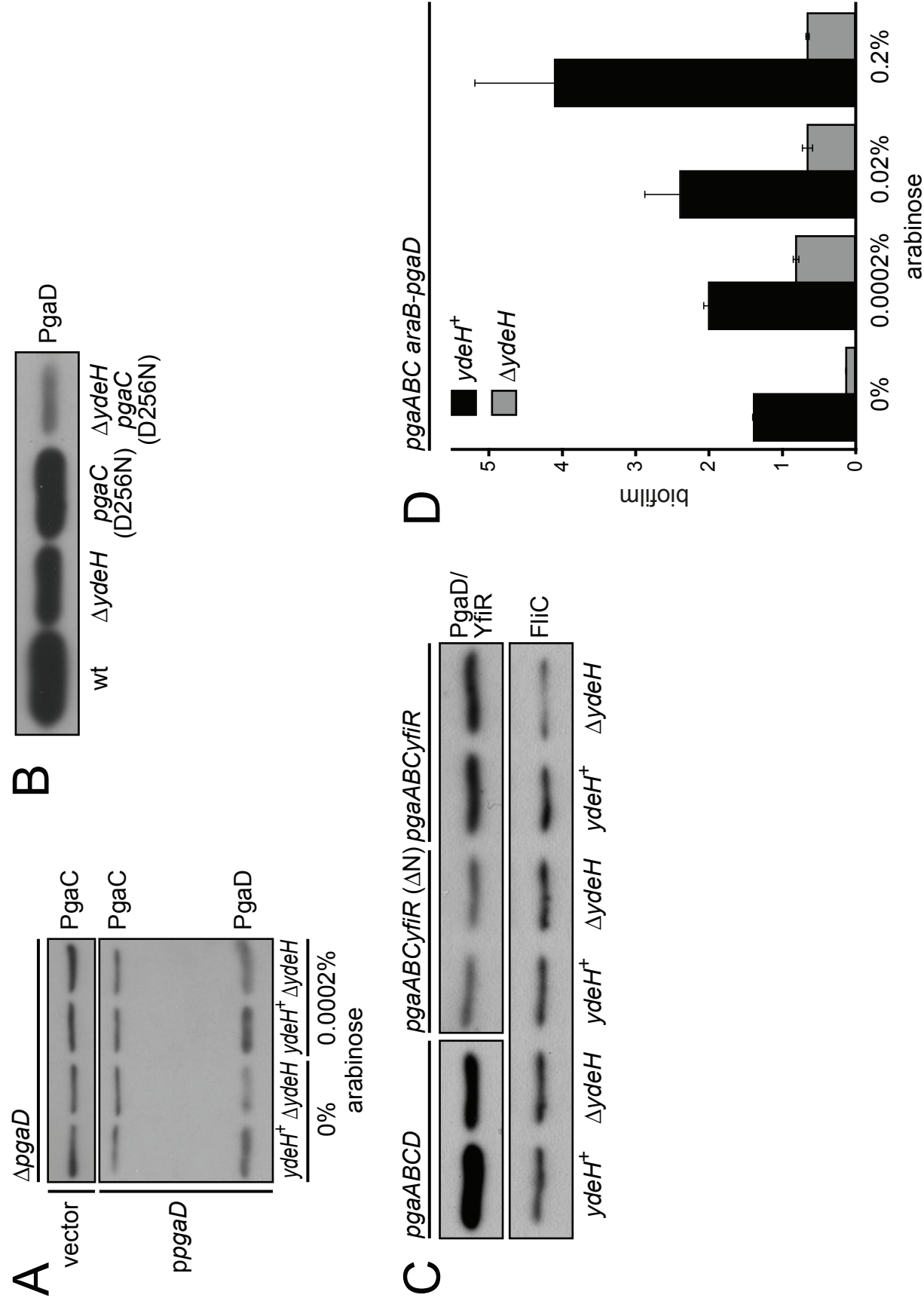
Supplementary Figure 4 Additional findings and controls related to Figure 5. (A) Biofilm formation in response to different *pgaD* alleles and cellular c-di-GMP concentrations (*wspR* overexpression). Vector controls (bars without colors) are compared to *wspR* overexpressions (colored bars) in a $\Delta 7$ background. Error bars are standard deviations. Expression of *pgaD* alleles was not induced (basal level). (B) W71A LOF mutation is dominant over N75D, K76E GOF mutations. Biofilm formation in response to different *pgaD* alleles. Wildtype (black bars) is compared to a $\Delta 7$ mutant background (grey bars). Error bars are standard deviations. Expression of plasmid constructs was not induced (basal level). (C) Immunoblot analysis of PgaD steady state protein levels in response to c-di-GMP ($\Delta 7$ mutant/wildtype). Cells were grown as for biofilm assays. A C-terminally 3xFlag-tagged construct was used for PgaD detection. Expression of plasmid constructs was not induced (basal level). (D) Immunoblot analysis of protein input used for *in vitro* GT activity assay of PgaD GOF alleles (see Figure 5E). A C-terminally 3xFlag-tagged construct was used for PgaCDf detection. (PgaD) indicates that mutations lie within the PgaD part of PgaCDf with amino acid numbering according to unfused PgaD.

Supplementary Figure 5 Additional findings and controls related to Figure 6. (A) Effects of GOF mutations can be additive. Biofilm formation in response to different *pgaCD* alleles. Wildtype (black bars) is compared to a $\Delta 7$ mutant background (grey bars). Error bars are standard deviations. Expression of plasmid constructs was not induced (basal level). (B) Immunoblot analysis of PgaCDf steady state protein levels of arginine mutants. (*pgaC*) indicates that mutations lie within the PgaC part of PgaCDf with amino acid numbering according to unfused PgaC. Cells

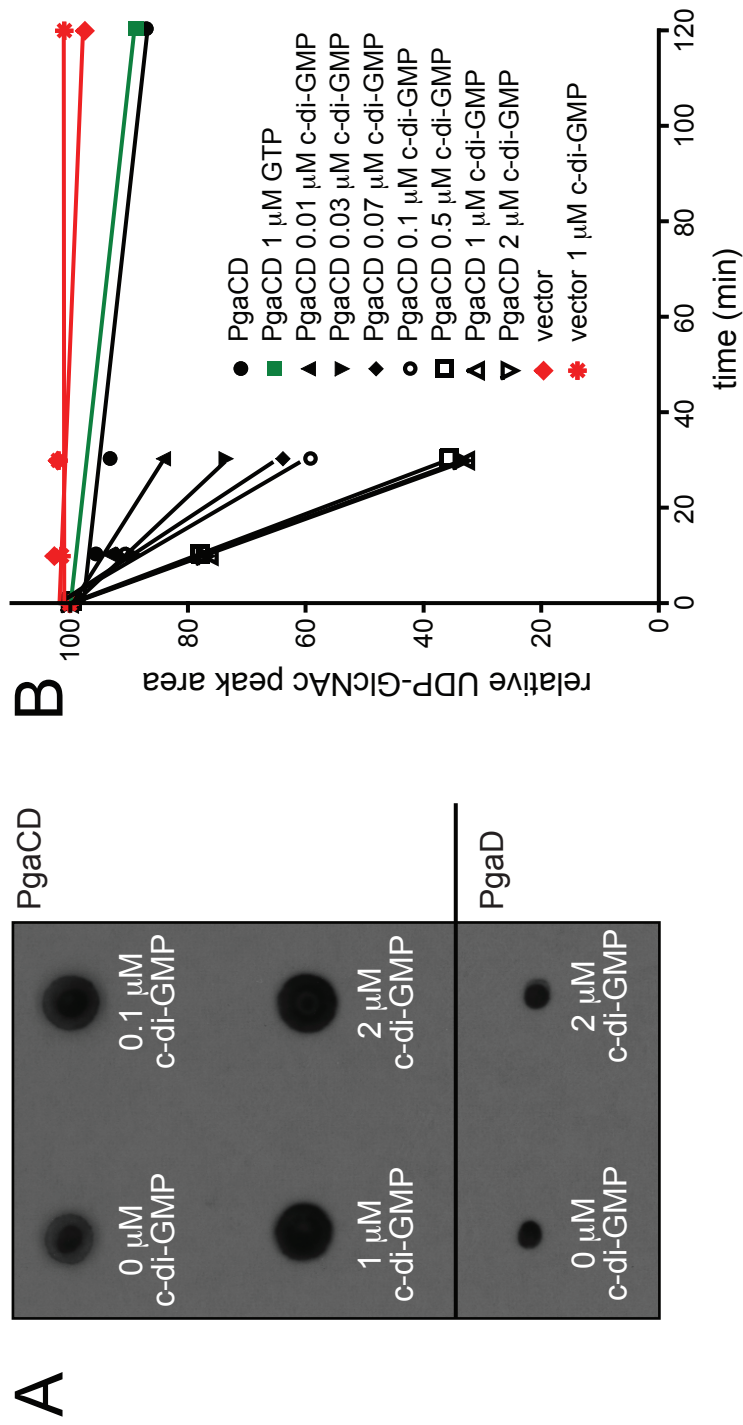
were grown as for biofilm assays. A C-terminally 3xFlag-tagged construct was used for PgaCDf detection. Expression of plasmid constructs was not induced (basal level). (C) PgaC (R222A) cannot stabilize PgaD. Immunoblot analysis of PgaD steady state protein levels in response to different *pgaC* alleles and c-di-GMP ($\Delta 7$ mutant/wildtype). Cells were grown as for biofilm assays. A C-terminally 3xFlag-tagged construct was used for PgaD detection. Expression of plasmid constructs was not induced (basal level).

Supplementary Figure 6 Alignment of PgaC homologues reveals several non-conserved arginines in gram-negative species without c-di-GMP signalling. PgaC amino acid sequences of seven gram-negative species that harbor c-di-GMP signalling (a-g) are shown in comparison to PgaC amino acid sequences of three gram-negative species that lack c-di-GMP signalling (h-j). Alignment was done using ClustalW2 at the EBI (Larkin *et al*, 2007). Amino acid coloring according to Clustal X default coloring. Amino acid numbering is according to *E. coli* PgaC sequence (a). Boxes with continuous lines indicate transmembrane helices, while boxes with dashed lines indicate membrane-associated helices. Classification into transmembrane and membrane-associated helices is based on the integration of results from this study, TMHMM server predictions (Sonnhammer *et al*, 1998), previous results from a study on the PgaC homologue HmsR from *Y. pestis* (Bobrov *et al*, 2008) and analogies to the hyaluronan synthase from *Streptococcus pyogenes*, another well-characterized membrane-bound processive glycosyltransferase of the GT-2 family (Heldermon *et al*, 2001; Weigel & DeAngelis, 2007). White letters on a black background indicate conserved motifs and residues of the active site of processive β -glycosyltransferase GT-2 family proteins. D112, D163 and D165 are part of domain A, while D256 and the QXXRW motif belong to domain B (Saxena & Brown, 1997; Saxena *et al*, 2001). Green arrows mark GOF mutations isolated in this study (accompanying mutations that did not cause a GOF phenotype themselves are not indicated). Black and red arrows mark arginines that are not conserved between c-di-GMP signalling-containing and non-containing species. LOF mutation R222A is highlighted with a red arrow.

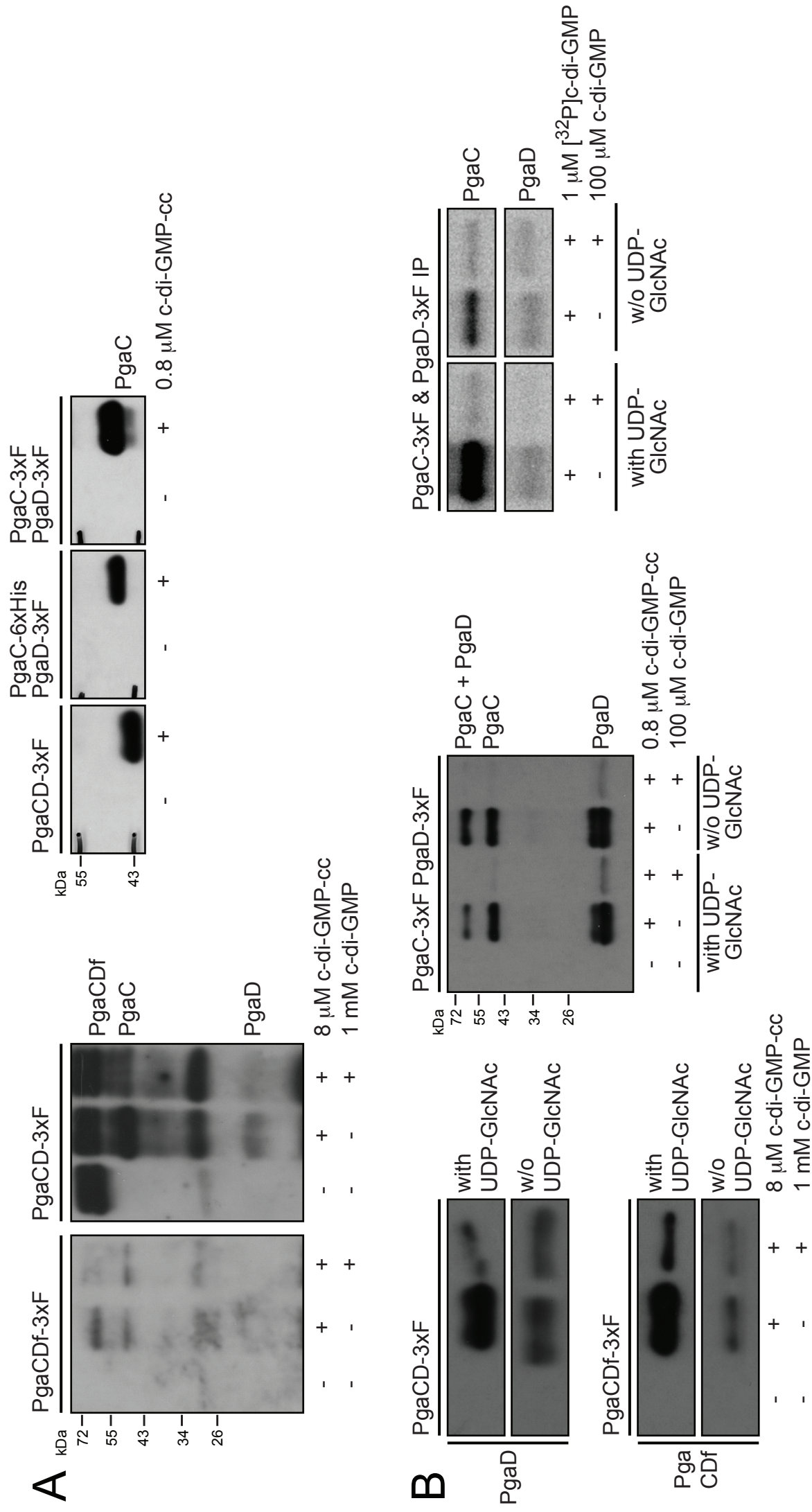
Steiner et al. Supplementary Figure 1



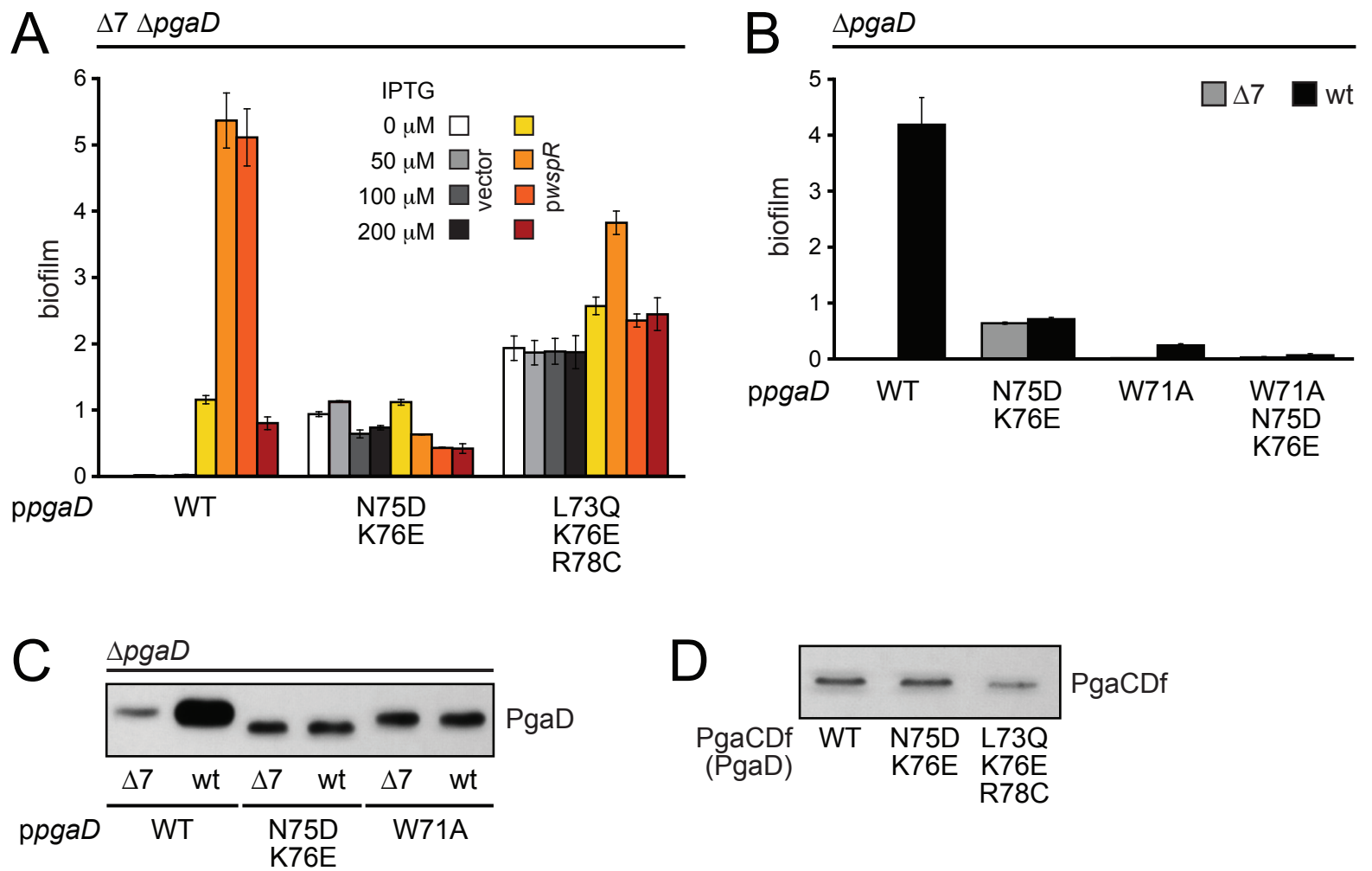
Steiner et al. Supplementary Figure 2



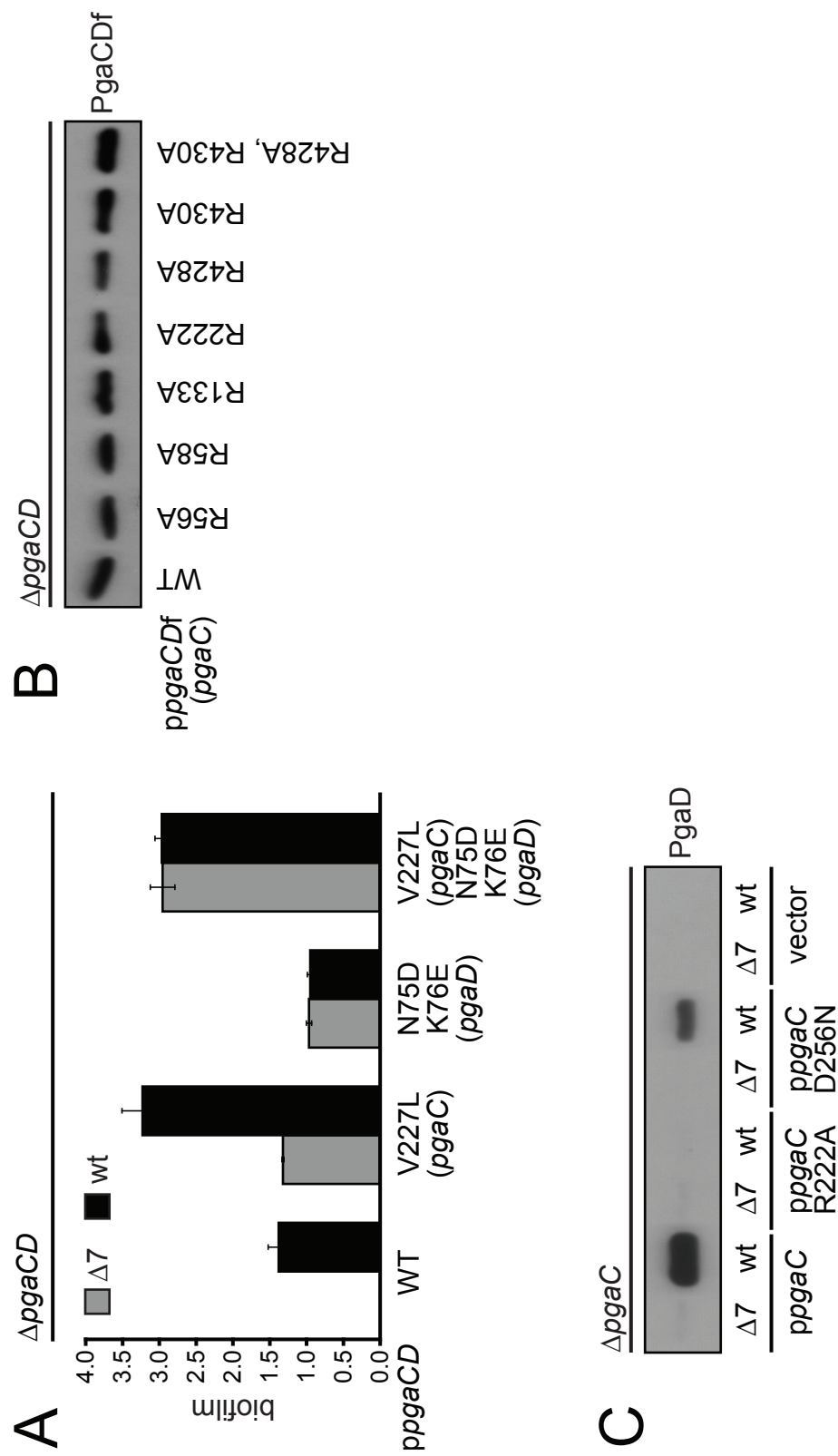
Steiner et al. Supplementary Figure 3

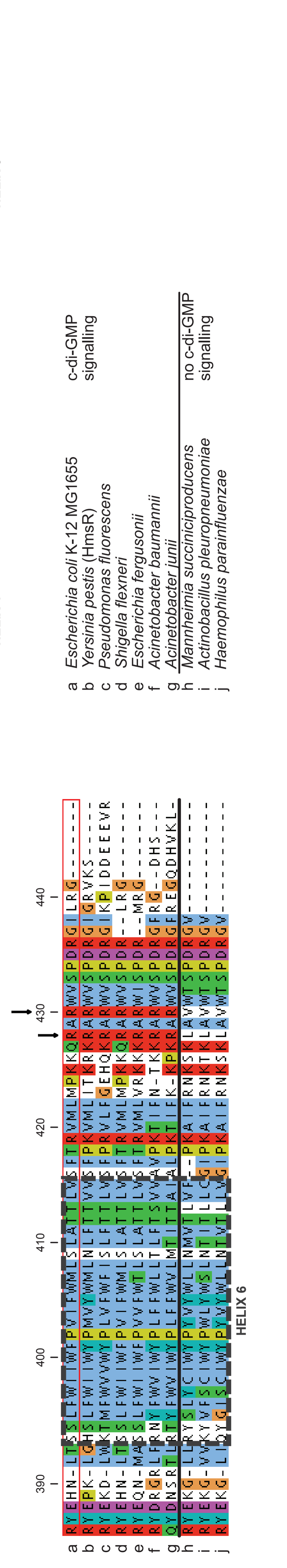
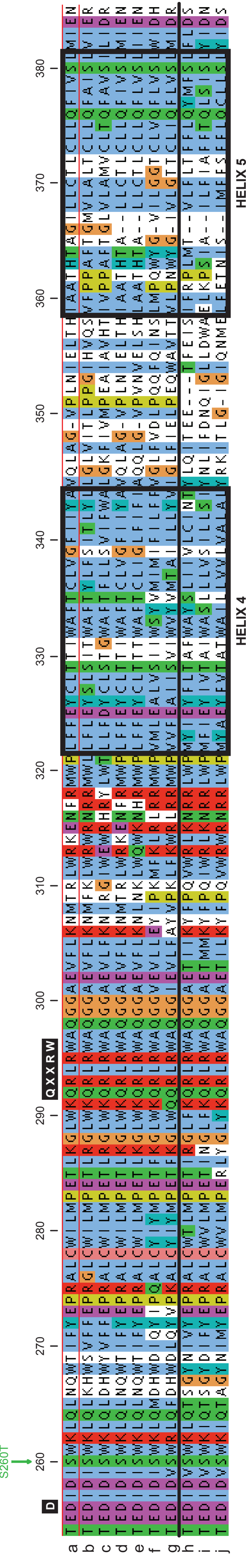
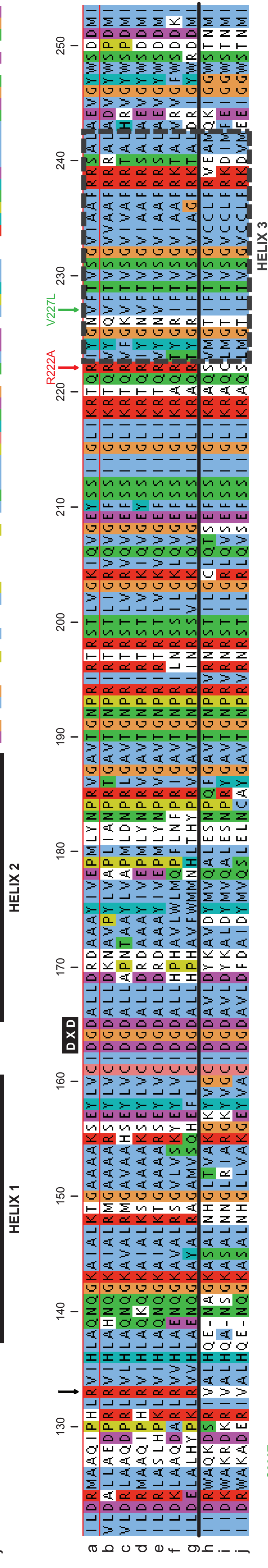
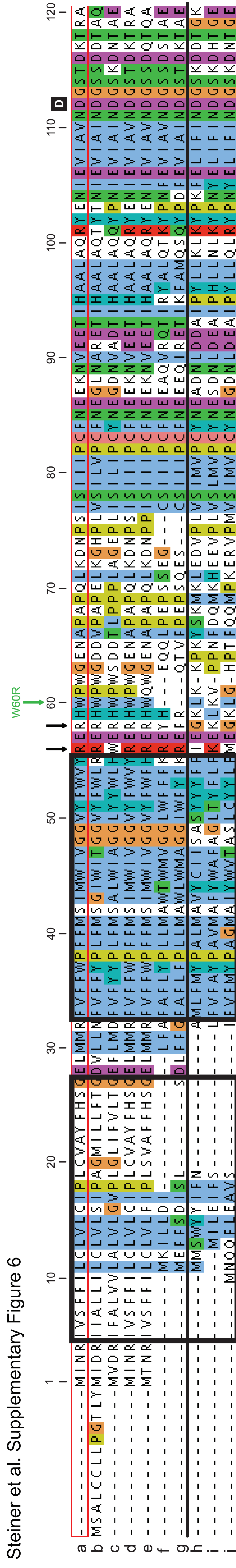


Steiner et al. Supplementary Figure 4



Steiner et al. Supplementary Figure 5





- a *Escherichia coli* K-12 MG1655
- b *Yersinia pestis* (HmsR)
- c *Pseudomonas fluorescens*
- d *Shigella flexneri*
- e *Escherichia fergusonii*
- f *Acinetobacter baumannii*
- g *Acinetobacter junii*
- h *Mannheimia succiniciproducens*
- i *Actinobacillus pleuropneumoniae*
- j *Haemophilus parainfluenzae*

- a c-di-GMP signalling
- b c-di-GMP signalling
- c c-di-GMP signalling
- d c-di-GMP signalling
- e c-di-GMP signalling
- f c-di-GMP signalling
- g c-di-GMP signalling
- h no c-di-GMP signalling
- i no c-di-GMP signalling
- j no c-di-GMP signalling

Steiner et al. Supplementary Table 1

Supplementary Table 1 Strains and plasmids used in this study.

<i>E. coli</i> strains			
Name	Relevant genotype	Description/comments	Source/reference
MG1655	wildtype	<i>E. coli</i> K-12 wildtype	(Blattner <i>et al.</i> , 1997)
AB330	DY330 λ cI ^{B57} Δ (<i>cro-bioA</i>)	temperature sensitive, λ RED system	(Yu <i>et al.</i> , 2000)
AB958	<i>csrA</i> ::Tn5 Δ (<i>kan</i>)::Frt	ancestor of most strains used in this study	(Boehm <i>et al.</i> , 2009)
AB959	<i>csrA</i> ::Tn5 Δ (<i>kan</i>)::Frt Δ <i>yeH</i> ::Frt		(Boehm <i>et al.</i> , 2009)
AB1062	<i>csrA</i> ::Tn5 Δ (<i>kan</i>)::Frt <i>pgaD</i> -3xFlag- <i>kan</i>		(Boehm <i>et al.</i> , 2009)
AB1063	<i>csrA</i> ::Tn5 Δ (<i>kan</i>)::Frt Δ <i>yeH</i> ::Frt <i>pgaD</i> -3xFlag- <i>kan</i>		(Boehm <i>et al.</i> , 2009)
AB1094	<i>csrA</i> ::Tn5 Δ (<i>kan</i>)::Frt Frt- <i>araC</i> - <i>araB</i> <i>pgaA</i> (tl.) <i>pgaD</i> -3xFlag-Frt Δ <i>araBC</i> ::Frt	translational <i>araB</i> - <i>pgaA</i> fusion, <i>kan</i> - <i>araC</i> -P _{<i>ara</i>} amplified from TB55	This work
AB1152	<i>csrA</i> ::Tn5 Δ (<i>kan</i>)::Frt Δ <i>yeH</i> ::Frt Δ <i>yegE</i> ::Frt		This work
AB1197	<i>csrA</i> ::Tn5 Δ (<i>kan</i>)::Frt Δ <i>yeH</i> ::Frt Δ <i>yegE</i> ::Frt Δ <i>ycdT</i> ::Frt		This work
AB1313 *	<i>csrA</i> ::Tn5 Δ (<i>kan</i>)::Frt Δ <i>yeH</i> ::Frt Δ <i>yegE</i> ::Frt Δ <i>ycdT</i> ::Frt Δ <i>yfiN</i> ::Frt Δ <i>yhjK</i> ::Frt Δ <i>ydaM</i> ::Frt Δ <i>yneF</i> ::Frt *	c-di-GMP ^{low} Δ 7 mutant	This work
AB1412	<i>csrA</i> ::Tn5 Δ (<i>kan</i>)::Frt <i>pgaC</i> -3xFlag Δ <i>pgaD</i> ::Frt		This work
AB1413	<i>csrA</i> ::Tn5 Δ (<i>kan</i>)::Frt <i>pgaC</i> -3xFlag Δ <i>pgaD</i> ::Frt Δ <i>yeH</i> ::Frt		This work
AB1416	<i>csrA</i> ::Tn5 Δ (<i>kan</i>)::Frt Frt- <i>araC</i> - <i>araB</i> <i>pgaA</i> (tl.) <i>pgaD</i> -3xFlag-Frt Δ <i>araBC</i> ::Frt Δ <i>yeH</i> ::Frt	translational <i>araB</i> - <i>pgaA</i> fusion, <i>kan</i> - <i>araC</i> -P _{<i>ara</i>} amplified from TB55	This work
AB1417	<i>csrA</i> ::Tn5 Δ (<i>kan</i>)::Frt <i>pgaA</i> -3xFlag Δ <i>pgaBCD</i> :: <i>kan</i>		(Boehm <i>et al.</i> , 2009)
AB1418	<i>csrA</i> ::Tn5 Δ (<i>kan</i>)::Frt <i>pgaB</i> -3xFlag Δ <i>pgaCD</i> :: <i>kan</i>		This work
AB1419	<i>csrA</i> ::Tn5 Δ (<i>kan</i>)::Frt Δ <i>yeH</i> ::Frt <i>pgaA</i> -3xFlag Δ <i>pgaBCD</i> :: <i>kan</i>		(Boehm <i>et al.</i> , 2009)
AB1420	<i>csrA</i> ::Tn5 Δ (<i>kan</i>)::Frt Δ <i>yeH</i> ::Frt <i>pgaB</i> -3xFlag Δ <i>pgaCD</i> :: <i>kan</i>		This work
AB1433	<i>csrA</i> ::Tn5 Δ (<i>kan</i>)::Frt Δ <i>araBC</i> ::Frt Frt- <i>kan</i> -Frt- <i>araC</i> - <i>araB</i> <i>pgaA</i> -3xFlag (tl.) Δ <i>pgaBCD</i> :: <i>cat</i>	translational <i>araB</i> - <i>pgaA</i> fusion, <i>kan</i> - <i>araC</i> -P _{<i>ara</i>} amplified from TB55	This work
AB1434	<i>csrA</i> ::Tn5 Δ (<i>kan</i>)::Frt Δ <i>araBC</i> ::Frt Frt- <i>kan</i> -Frt- <i>araC</i> - <i>araB</i> <i>pgaA</i> -3xFlag (tl.) Δ <i>pgaCD</i> :: <i>cat</i>	translational <i>araB</i> - <i>pgaA</i> fusion, <i>kan</i> - <i>araC</i> -P _{<i>ara</i>} amplified from TB55	This work
AB1435	<i>csrA</i> ::Tn5 Δ (<i>kan</i>)::Frt Δ <i>araBC</i> ::Frt Frt- <i>kan</i> -Frt- <i>araC</i> - <i>araB</i> <i>pgaABC</i> -3xFlag (tl.) Δ <i>pgaD</i> :: <i>cat</i>	translational <i>araB</i> - <i>pgaA</i> fusion, <i>kan</i> - <i>araC</i> -P _{<i>ara</i>} amplified from TB55	This work
AB1514	<i>csrA</i> ::Tn5 Δ (<i>kan</i>)::Frt Δ <i>yeH</i> ::Frt Δ <i>araBC</i> ::Frt Frt- <i>kan</i> -Frt- <i>araC</i> - <i>araB</i> <i>pgaA</i> -3xFlag (tl.) Δ <i>pgaBCD</i> :: <i>cat</i>	translational <i>araB</i> - <i>pgaA</i> fusion, <i>kan</i> - <i>araC</i> -P _{<i>ara</i>} amplified from TB55	This work
AB1515	<i>csrA</i> ::Tn5 Δ (<i>kan</i>)::Frt Δ <i>yeH</i> ::Frt Δ <i>araBC</i> ::Frt Frt- <i>kan</i> - <i>araC</i> - <i>araB</i> <i>pgaAB</i> -3xFlag (tl.) Δ <i>pgaCD</i> :: <i>cat</i>	translational <i>araB</i> - <i>pgaA</i> fusion, <i>kan</i> - <i>araC</i> -P _{<i>ara</i>} amplified from TB55	This work
AB1516	<i>csrA</i> ::Tn5 Δ (<i>kan</i>)::Frt Δ <i>yeH</i> ::Frt Δ <i>araBC</i> ::Frt Frt- <i>kan</i> - <i>araC</i> - <i>araB</i> <i>pgaABC</i> -3xFlag (tl.) Δ <i>pgaD</i> :: <i>cat</i>	translational <i>araB</i> - <i>pgaA</i> fusion, <i>kan</i> - <i>araC</i> -P _{<i>ara</i>} amplified from TB55	This work
AB1537	<i>csrA</i> ::Tn5 Δ (<i>kan</i>)::Frt Δ <i>pgaD</i> :: <i>yfiR</i> (Δ N)-3xFlag- <i>kan</i>	<i>yfiR</i> (Δ N)-3xF amplified from pMR20- <i>yfiR</i> -M2 (Malone <i>et al.</i> , 2010)	This work
AB1538	<i>csrA</i> ::Tn5 Δ (<i>kan</i>)::Frt Δ <i>pgaD</i> :: <i>yfiR</i> -3xFlag- <i>kan</i>	<i>yfiR</i> -3xF amplified from pMR20- <i>yfiR</i> -M2 (Malone <i>et al.</i> , 2010)	This work
AB1539	<i>csrA</i> ::Tn5 Δ (<i>kan</i>)::Frt Δ <i>yeH</i> ::Frt Δ <i>pgaD</i> :: <i>yfiR</i> (Δ N)-3xFlag- <i>kan</i>	<i>yfiR</i> (Δ N)-3xF amplified from pMR20- <i>yfiR</i> -M2 (Malone <i>et al.</i> , 2010)	This work
AB1540	<i>csrA</i> ::Tn5 Δ (<i>kan</i>)::Frt Δ <i>yeH</i> ::Frt Δ <i>pgaD</i> :: <i>yfiR</i> -3xFlag- <i>kan</i>	<i>yfiR</i> -3xF amplified from pMR20- <i>yfiR</i> -M2 (Malone <i>et al.</i> , 2010)	This work
AB1569	<i>csrA</i> ::Tn5 Δ (<i>kan</i>)::Frt Δ <i>pgaD</i> ::Frt		This work
AB1570	<i>csrA</i> ::Tn5 Δ (<i>kan</i>)::Frt Δ <i>yeH</i> ::Frt Δ <i>pgaD</i> ::Frt		This work
AB1572	<i>csrA</i> ::Tn5 Δ (<i>kan</i>)::Frt Δ <i>araBC</i> ::Frt Frt- <i>kan</i> -Frt- <i>araC</i> - <i>araB</i> <i>pgaD</i> (tl.)	translational <i>araB</i> - <i>pgaD</i> fusion, <i>kan</i> - <i>araC</i> -P _{<i>ara</i>} amplified from TB55	This work

Steiner et al. Supplementary Table 1

Name	Relevant genotype	Description/comments	Source/reference
AB1574	<i>csrA::Tn5Δ(kan)::Frt ΔydeH::Frt ΔaraBC::Frt Frt-kan-Frt-araC-araBtpgaD</i> (tl.)	translational <i>araB-pgaD</i> fusion, <i>kan-araC-P_{ara}</i> amplified from TB55	This work
AB1638	<i>csrA::Tn5Δ(kan)::Frt ΔaraBC::Frt ΔpgaABCD::Frt</i>	strain used for overexpressions (c-di-GMP binding assays)	This work
AB1645	<i>csrA::Tn5Δ(kan)::Frt ΔpgaABC::Frt pgaD-3xFlag-kan</i>		This work
AB1647	<i>csrA::Tn5Δ(kan)::Frt ΔydeH::Frt ΔpgaABC::Frt pgaD-3xFlag-kan</i>		This work
AB1747	<i>csrA::Tn5Δ(kan)::Frt ΔpgaC::Frt pgaD-3xFlag-kan</i>		This work
AB1768	<i>ΔcyaA::Frt</i>	standard strain for bacterial two-hybrid analysis	This work
AB1775	<i>csrA::Tn5Δ(kan)::Frt ΔaraBC::Frt Frt-kan-Frt-araC-araBtpgaA</i> (tl.)	translational <i>araB-pgaA</i> fusion, <i>kan-araC-P_{ara}</i> amplified from TB55	This work
AB1776	<i>csrA::Tn5Δ(kan)::Frt ΔaraBC::Frt Frt-kan-Frt-araC-araBtpgaA</i> (tl.) <i>ΔpgaC::Frt</i>	translational <i>araB-pgaA</i> fusion, <i>kan-araC-P_{ara}</i> amplified from TB55	This work
AB1777	<i>csrA::Tn5Δ(kan)::Frt ΔaraBC::Frt Frt-kan-Frt-araC-araBtpgaA</i> (tl.) <i>ΔpgaD::Frt</i>	translational <i>araB-pgaA</i> fusion, <i>kan-araC-P_{ara}</i> amplified from TB55	This work
AB1789	<i>csrA::Tn5Δ(kan)::Frt pgaC</i> (D256N) <i>pgaD-3xFlag-Frt</i>	PgaC active site mutant, secondary mutation Q70R present in <i>pgaC</i>	This work
AB1803	<i>csrA::Tn5Δ(kan)::Frt pgaC</i> (D256N) <i>pgaD-3xFlag-Frt ΔydeH::Frt</i>	PgaC active site mutant, secondary mutation Q70R present in <i>pgaC</i>	This work
AB1880	<i>csrA::Tn5Δ(kan)::Frt ΔcyaA::Frt pgaC-T18 ΔpgaD::Δbla::Frt ΔaraBC::Frt ΔcpdA::Frt</i>	strain for bacterial two-hybrid, <i>T18</i> amplified from pUT18	This work
AB1885	<i>csrA::Tn5Δ(kan)::Frt ΔydeH::Frt ΔyegE::Frt ΔycdT::Frt ΔyfiN::Frt ΔyhjK::Frt ΔydaM::Frt ΔyneF::Frt pgaD-3xFlag-kan</i>	c-di-GMP ^{low} Δ7 mutant	This work
AB1911	<i>csrA::Tn5Δ(kan)::Frt ΔydeH::Frt ΔyegE::Frt ΔyfiN::Frt ΔyhjK::Frt ΔydaM::Frt ΔyneF::Frt pgaC-T18 ΔpgaD::Δbla::Frt ΔcyaA::Frt ΔcpdA::Frt</i>	strain for bacterial two-hybrid, <i>T18</i> amplified from pUT18	This work
AB1936	<i>csrA::Tn5Δ(kan)::Frt ΔcyaA::Frt pgaC-T18 ΔpgaD::Δbla::Frt ΔcpdA::Frt</i>	strain for bacterial two-hybrid, <i>T18</i> amplified from pUT18	This work
AB1937	<i>csrA::Tn5Δ(kan)::Frt ΔydeH::Frt ΔcyaA::Frt pgaC-T18 ΔpgaD::Δbla::Frt ΔcpdA::Frt</i>	strain for bacterial two-hybrid, <i>T18</i> amplified from pUT18	This work
AB2020	<i>csrA::Tn5Δ(kan)::Frt ΔpgaC::kan</i>		This work
AB2021	<i>csrA::Tn5Δ(kan)::Frt ΔydeH::Frt ΔyegE::Frt ΔycdT::Frt ΔyfiN::Frt ΔyhjK::Frt ΔydaM::Frt ΔyneF::Frt ΔpgaC::kan</i>	GOF screening strain, c-di-GMP ^{low} Δ7 mutant	This work
AB2022	<i>csrA::Tn5Δ(kan)::Frt ΔydeH::Frt ΔyegE::Frt ΔycdT::Frt ΔyfiN::Frt ΔyhjK::Frt ΔydaM::Frt ΔyneF::Frt pgaB-3xFlag ΔpgaCD::kan</i>	GOF screening strain, c-di-GMP ^{low} Δ7 mutant	This work
AB2043	<i>csrA::Tn5Δ(kan)::Frt ΔydeH::Frt ΔyegE::Frt ΔycdT::Frt ΔyfiN::Frt ΔyhjK::Frt ΔydaM::Frt ΔyneF::Frt ΔpgaABCD::Frt ΔaraBC::Frt</i>	strain used for overexpressions (c-di-GMP binding assays; GT activity assays), c-di-GMP ^{low} Δ7 mutant	This work
AB2134	<i>csrA::Tn5Δ(kan)::Frt ΔydeH::Frt ΔyegE::Frt ΔycdT::Frt ΔyfiN::Frt ΔyhjK::Frt ΔydaM::Frt ΔyneF::Frt ΔpgaD::kan</i>	GOF screening strain, c-di-GMP ^{low} Δ7 mutant	This work
AB2135	<i>csrA::Tn5Δ(kan)::Frt ΔpgaD::kan</i>		This work
AB2166	<i>csrA::Tn5Δ(kan)::Frt ΔydeH::Frt ΔyegE::Frt ΔycdT::Frt ΔyfiN::Frt ΔyhjK::Frt ΔydaM::Frt ΔyneF::Frt pgaC::Frt pgaD-3xFlag-kan</i>	c-di-GMP ^{low} Δ7 mutant	This work
TB55	DY329 P _{minC} <>(kan-araC-P _{ara})	used for amplification of <i>kan-araC-P_{ara}</i> to construct translational <i>araB</i> fusions	(Bernhardt & de Boer, 2004)
DH5α	(F-) F' <i>endA1 hsdR17</i> (rK-mK plus) <i>glnV44 thi1 recA1 gyr Δ(Nal^R) relA1 Δ(lacZYA-argF)U169 deoR</i> (Φ80d/lac Δ(lacZ) M15)	used for general cloning purposes	(Woodcock <i>et al.</i> , 1989)

Steiner et al. Supplementary Table 1

Plasmids			
Name	Relevant genotype	Description/comments	Source/reference
pKD3	Amp ^R Cm ^R	Frt-flanked Cm ^R gene, for chromosomal gene disruptions	(Datsenko & Wanner, 2000)
pKD4	Amp ^R Km ^R	Frt-flanked Km ^R gene, for chromosomal gene disruptions	(Datsenko & Wanner, 2000)
pKD46	λRED ⁺ Amp ^R	arabinose-inducible expression of λRED system	(Datsenko & Wanner, 2000)
pCP20	FLP ⁺ Amp ^R Cm ^R	temperature-sensitive replication and thermal induction of FLP synthesis	(Cherepanov & Wackernagel, 1995)
pSUB11	3xFlag Km ^R	3xFlag-tagging of chromosomal genes	(Uzzau <i>et al</i> , 2001)
pME6032	<i>lac</i> ^q -P _{tac} (Tet ^R)	IPTG-inducible expression vector, used as vector control for <i>pwspR</i>	(Heeb <i>et al</i> , 2002)
<i>pwspR</i>	pME6010:: <i>wspR</i> (Tet ^R)	<i>wspR</i> from <i>P. aeruginosa</i>	(Malone <i>et al</i> , 2007)
pUT18	P _{lac} T18 Amp ^R	pUC19 derivative, used for fusions to the N-terminus of the T18 fragment of CyaA	(Karimova <i>et al</i> , 1998)
pUT18C	P _{lac} T18 Amp ^R	pUC19 derivative, used for fusions to the C-terminus of the T18 fragment of CyaA	(Karimova <i>et al</i> , 1998)
pKT25	P _{lac} T25 Km ^R	pSU40 derivative, used for fusions to the C-terminus of the T25 fragment of CyaA	(Karimova <i>et al</i> , 1998)
pUT18C- <i>zip</i>	pUT18C:: <i>zip</i>	pUT18C derivative with T18 fused to leucine zipper of GCN4	(Karimova <i>et al</i> , 1998)
pKT25- <i>zip</i>	pKT25:: <i>zip</i>	pKT25 derivative with T25 fused to leucine zipper of GCN4	(Karimova <i>et al</i> , 1998)
pD2	pUT18:: <i>pgaC</i>		This work
pF	pUT18:: <i>pgaC</i> (G63-R318)		This work
pD	pUT18:: <i>pgaC</i> (E384-G441)		This work
pΔGT	pUT18:: <i>pgaC</i> (ΔP75-K314)		This work
pV	pUT18C:: <i>pgaC</i> (G63-R318)		This work
pX	pUT18C:: <i>pgaC</i> (E384-G441)		This work
pG2	pKT25:: <i>pgaD</i>		This work
pB	pKT25:: <i>pgaD</i> (Y74-A137)		This work
pBAD18	<i>araC</i> ⁺ <i>bla</i> ⁺ <i>ParaBAD</i> (Amp ^R)	arabinose-inducible expression vector	(Guzman <i>et al</i> , 1995)
pAB551	pBAD18:: <i>dgcA</i>	<i>dgcA</i> (cc3285) from <i>C. crescentus</i>	(Boehm <i>et al</i> , 2009)
pAC551	pBAD18:: <i>dgcA</i> (D164N)	active site mutant of <i>dgcA</i> (cc3285) from <i>C. crescentus</i>	This work
p5a	pBAD18:: <i>pgaC</i>		This work
p6a	pBAD18:: <i>pgaC</i> -3xF	<i>pgaC</i> -3xF amplified from AB1412	This work
pins1	pBAD18:: <i>pgaD</i> -3xF	<i>pgaD</i> -3xF amplified from AB1062	This work
pCD-3xF	pBAD18:: <i>pgaC pgaD</i> -3xF	<i>pgaCD</i> -3xF amplified from AB1062	This work
pCDfusion	pBAD18:: <i>pgaCDf</i> -3xF	PgaCD fusion protein, C-terminus of PgaC fused to N-terminus of PgaD	This work
p2-3xF	pBAD18:: <i>pgaC</i> -3xF <i>pgaD</i> -3xF		This work
p2-3xF-DE	pBAD18:: <i>pgaC</i> -3xF <i>pgaD</i> -3xF (N75D, K76E)		This work
p2-3xF-R222	pBAD18:: <i>pgaC</i> -3xF (R222A) <i>pgaD</i> -3xF		This work
pC-His-D-3xF	pBAD18:: <i>pgaC</i> -6xHis <i>pgaD</i> -3xF		This work
pD-P92	pBAD18:: <i>pgaD</i> (-P92 trunc.)	truncated PgaD, last amino acid P92	This work
pD-Q80	pBAD18:: <i>pgaD</i> (-Q80 trunc.)	truncated PgaD, last amino acid Q80	This work

Steiner et al. Supplementary Table 1

Name	Relevant genotype	Description/comments	Source/reference
pD-R78	pBAD18:: <i>pgaD</i> (-R78 trunc.)	truncated PgaD, last amino acid R78	This work
pD-K76	pBAD18:: <i>pgaD</i> (-K76 trunc.)	truncated PgaD, last amino acid K76	This work
pCL2	pBAD18:: <i>pgaC</i> (W60R)	isolated GOF allele	This work
pCL3	pBAD18:: <i>pgaC</i> (S7P, M44T, W60R)	isolated GOF allele	This work
pCL5	pBAD18:: <i>pgaC</i> (R222A)		This work
pCL6	pBAD18:: <i>pgaC</i> (D256N)	<i>pgaC</i> active site mutant	This work
pCL7	pBAD18:: <i>pgaC</i> -3xF (S7P)		This work
pCL8	pBAD18:: <i>pgaC</i> -3xF (M44T)		This work
pCL9	pBAD18:: <i>pgaC</i> -3xF (W60R)		This work
pCL10	pBAD18:: <i>pgaC</i> -3xF (S7P, W60R)		This work
pCL11	pBAD18:: <i>pgaC</i> -3xF (M44T, W60R)		This work
pCL12	pBAD18:: <i>pgaC</i> -3xF (S7P, M44T, W60R)		This work
pCL13	pBAD18:: <i>pgaC</i> -3xF (V227L)		This work
pCL20	pBAD18:: <i>pgaD</i> -3xF (L73Q, K76E, R78C)	isolated GOF allele	This work
pCL22	pBAD18:: <i>pgaD</i> -3xF (K76E)	isolated GOF allele	This work
pCL23	pBAD18:: <i>pgaD</i> -3xF (N75D)		This work
pCL25	pBAD18:: <i>pgaD</i> -3xF (N75D, K76E)	isolated GOF allele	This work
pCL28	pBAD18:: <i>pgaD</i> -3xF (L73Q)		This work
pCL29	pBAD18:: <i>pgaD</i> -3xF (R78C)		This work
pCL30	pBAD18:: <i>pgaD</i> -3xF (L73Q, K76E)		This work
pCL31	pBAD18:: <i>pgaD</i> -3xF (K76E, R78C)		This work
pCL32	pBAD18:: <i>pgaD</i> -3xF (W71A)		This work
pCL33	pBAD18:: <i>pgaD</i> -3xF (Y74A)		This work
pCL34	pBAD18:: <i>pgaD</i> -3xF (W71A, N75D, K76E)		This work
pCL42	pBAD18:: <i>pgaC</i> (V227L) <i>pgaD</i> -3xF		This work
pCL43	pBAD18:: <i>pgaC</i> <i>pgaD</i> -3xF (N75D, K76E)		This work
pCL44	pBAD18:: <i>pgaC</i> (V227L) <i>pgaD</i> -3xF (N75D, K76E)		This work
pCL45	pBAD18:: <i>pgaC</i> (R222A) <i>pgaD</i> -3xF		This work
pCL46	pBAD18:: <i>pgaC</i> (R222A) <i>pgaD</i> -3xF (N75D, K76E)		This work
pCL54	pBAD18:: <i>pgaC</i> (V227L) <i>Df</i> -3xF	PgaCD fusion protein, C-terminus of PgaC fused to N-terminus of PgaD	This work
pCL55	pBAD18:: <i>pgaCD</i> (N75D, K76E) f-3xF	PgaCD fusion protein, C-terminus of PgaC fused to N-terminus of PgaD	This work
pCL56	pBAD18:: <i>pgaCD</i> (L73Q, K76E, R78C) f-3xF	PgaCD fusion protein, C-terminus of PgaC fused to N-terminus of PgaD	This work
pCL58	pBAD18:: <i>pgaCD</i> (W71A) f-3xF	PgaCD fusion protein, C-terminus of PgaC fused to N-terminus of PgaD	This work
pCL59	pBAD18:: <i>pgaC</i> (R56A) <i>Df</i> -3xF	PgaCD fusion protein, C-terminus of PgaC fused to N-terminus of PgaD	This work
pCL60	pBAD18:: <i>pgaC</i> (R58A) <i>Df</i> -3xF	PgaCD fusion protein, C-terminus of PgaC fused to N-terminus of PgaD	This work
pCL61	pBAD18:: <i>pgaC</i> (R56A, R58A) <i>Df</i> -3xF	PgaCD fusion protein, C-terminus of PgaC fused to N-terminus of PgaD	This work
pCL62	pBAD18:: <i>pgaC</i> (R133A) <i>Df</i> -3xF	PgaCD fusion protein, C-terminus of PgaC fused to N-terminus of PgaD	This work

Steiner et al. Supplementary Table 1

Name	Relevant genotype	Description/comments	Source/reference
pCL63	pBAD18:: <i>pgaC</i> (R222A) <i>Df</i> -3xF	PgaCD fusion protein, C-terminus of PgaC fused to N-terminus of PgaD	This work
pCL64	pBAD18:: <i>pgaC</i> (R428A) <i>Df</i> -3xF	PgaCD fusion protein, C-terminus of PgaC fused to N-terminus of PgaD	This work
pCL65	pBAD18:: <i>pgaC</i> (R430A) <i>Df</i> -3xF	PgaCD fusion protein, C-terminus of PgaC fused to N-terminus of PgaD	This work
pCL66	pBAD18:: <i>pgaC</i> (R428A, R430A) <i>Df</i> -3xF	PgaCD fusion protein, C-terminus of PgaC fused to N-terminus of PgaD	This work
pCL68	pBAD18:: <i>pgaC</i> (R198D) <i>Df</i> -3xF	PgaCD fusion protein, C-terminus of PgaC fused to N-terminus of PgaD	This work
pCL72	pBAD18:: <i>pgaC</i> (V227L)	isolated GOF allele	This work

* AB1313, the ancestor of all *csrA* $\Delta 7$ c-di-GMP^{low} strains, harbors an approximately 11 kb deletion of the entire region between *ydeH* and *yneF*. The deletion, which arose during the last gene deletion event and the subsequent Flp recombinase-mediated marker removal, does not account for the biofilm formation phenotype of AB1313, since the immediate ancestor of AB1313 (*yneF*⁺, *csrA* $\Delta 6$, no deletion) showed comparable c-di-GMP- and/or GOF allele-mediated biofilm formation (data not shown). Detailed protocols of strain and plasmid constructions are available on request.

Steiner et al. Supplementary Table 2

Supplementary Table 2 Overview of bacterial two-hybrid analysis.

T18-	expression	-T18	expression	T25-	expression	interaction
PgaC (G63-R318)	yes	-	-	PgaD	n.a.	no
PgaC (E384-G441)	no	-	-	PgaD	n.a.	no
-	-	PgaC	n.a.	PgaD	n.a.	YES
-	-	PgaC	n.a.	PgaD (Y74-A137)	no	no
-	-	PgaC (G63-R318)	yes	PgaD	n.a.	no
-	-	PgaC (E384-G441)	no	PgaD	n.a.	no
-	-	PgaC (Δ P75-K314)	n.a.	PgaD	n.a.	no

T18-X on pUT18C, X-T18 on pUT18, T25-X on pKT25. Some constructs were 1xFlag-tagged to check for expression by immunoblot. n.a. = expression not tested. See also Supplementary Figure 6 and Figure 5A.

Steiner et al. Supplementary Table 3

Supplementary Table 3 Isolated gain-of-function (GOF) mutants in *pgaC* and *pgaD*.

<i>pgaC</i>		<i>pgaD</i>		<i>pgaCD</i>	
DNA	AA	DNA	AA	DNA	AA
t178a	W60R	a226g	K76E	g509a	R170H (<i>pgaC</i>)
		a421g	K141E *	g679a	V227I (<i>pgaC</i>)
t19c	S7P			t1001a	F334Y (<i>pgaC</i>)
t131c	M44T	a97g	I33V		
t168c	silent	a223g	N75D	c600g	silent (<i>pgaC</i>)
t178a	W60R	a226g	K76E	a151g	R51G (<i>pgaD</i>)
		a300g	silent		
g679t	V227L			g779c	S260T (<i>pgaC</i>)
t696c	silent	a226g	K76E		
a903g	silent				
a1254t	silent	a223g	N75D		
		a226g	K76E		
a512g	D171G				
g679t	V227L	t218a	L73Q		
a1021g	I341V	a226g	K76E		
		c232t	R78C		
t378c	silent				
g679c	V227L				
g1173c	silent				
a7g	N3D				
g779c	S260T				
t1047a	silent				

In the first two columns, either *pgaC* or *pgaD* was mutagenized. The third column shows mutants found when *pgaCD* were simultaneously mutagenized. Mutations on the DNA level as well as resulting amino acid exchanges are indicated. * Mutation lies within the C-terminal 3xFlag tag of *pgaD*.

Supplementary Materials and methods

Strain constructions

The chromosomal *pgaC* (D256N) allele was constructed with the help of the λ RED technology and a counter-selectable marker essentially as previously described (Boehm *et al.*, 2009). A SOE-PCR product (Higuchi *et al.*, 1988) was used in the second recombineering step. To confirm the presence of the desired mutation, *pgaC* was sequenced in the final strain. A secondary mutation (Q70R) was found to be present. λ RED-mediated gene replacement was used to construct the strains in which *pgaD* is replaced with C-terminally 3x-Flag-tagged *yfiR* from *P. aeruginosa*. *yfiR* and *yfiR* (Δ N) linked to a kanamycin resistance cassette were amplified from pMR20-*yfiR*-M2 (Malone *et al.*, 2010). The *araB-pgaD* translational fusion construct was done by fusing the first codon of the *araB* ORF with the second codon of the *pgaD* ORF at the native *pga* locus with the help of λ RED technology. The L-arabinose-dependent P_{ara} promoter and 5' untranslated region of *araB* (amplified from strain TB55 (Bernhardt & de Boer, 2004)) have been integrated directly upstream of *pgaD*, not disrupting *pgaC*. A kanamycin cassette was used for selection. The final strains harbor a copy of *araC* at the *pga* locus, which is divergently transcribed in respect to the P_{ara} promoter. In cases where L-arabinose was used to drive the expression from chromosomal P_{ara} , strains were generally deleted for the *araB* gene, yielding strains that allow for uptake but not metabolism of L-arabinose.

Anti-poly-GlcNAc immunoblot

Reaction mixtures containing crude membranes from strain AB1638 harboring either pCD-3xF or pins1 were set up essentially as described for the modified enzyme-coupled spectrophotometric GT activity assay and incubated in the presence of different c-di-GMP concentrations for 1 h at 30°C in a PCR machine. 1 μ l per sample was spotted on a nitrocellulose membrane (Hybond-C Extra, Amersham Biosciences). Poly-GlcNAc was detected using a rabbit anti-poly-GlcNAc antiserum (1:2'000; kind gift of XXX XXX) and an HRP-conjugated swine α -rabbit (1:10'000; DakoCytomation, Denmark) secondary antibody. Immunoblots were developed with the ECL chemiluminescent substrate (PerkinElmer, USA) and photographic films (Fujifilm, Japan).

Supplementary References

- Bernhardt TG & de Boer PAJ (2004) Screening for synthetic lethal mutants in *Escherichia coli* and identification of EnvC (YibP) as a periplasmic septal ring factor with murein hydrolase activity. *Mol Microbiol* **52**: 1255-1269
- Blattner FR, Plunkett IG, Bloch CA, Perna NT, Burland V, Riley M, Collado-Vides J, Glasner JD, Rode CK, Mayhew GF, Gregor J, Davis NW, Kirkpatrick HA, Goeden MA, Rose DJ, Mau B & Shao Y (1997) The complete genome sequence of *Escherichia coli* K-12. *Science* **277**: 1453-1462
- Bobrov AG, Kirillina O, Forman S, Mack D & Perry RD (2008) Insights into *Yersinia pestis* biofilm development: topology and co-interaction of Hms inner membrane proteins involved in exopolysaccharide production. *Environ Microbiol* **10**: 1419-1432
- Boehm A, Steiner S, Zaehring F, Casanova A, Hamburger F, Ritz D, Keck W, Ackermann M, Schirmer T & Jenal U (2009) Second messenger signalling governs *Escherichia coli* biofilm induction upon ribosomal stress. *Mol Microbiol* **72**: 1500-1516
- Cherepanov PP & Wackernagel W (1995) Gene disruption in *Escherichia coli*: TcR and KmR cassettes with the option of Flp-catalyzed excision of the antibiotic-resistance determinant. *Gene* **158**: 9-14
- Datsenko KA & Wanner BL (2000) One-step inactivation of chromosomal genes in *Escherichia coli* K-12 using PCR products. *Proc Natl Acad Sci USA* **97**: 6640-6645
- Guzman L-M, Belin D, Carson MJ & Beckwith J (1995) Tight regulation, modulation, and high-level expression by vectors containing the arabinose PBAD promoter. *J Bacteriol* **177**: 4121-4130
- Heeb S, Blumer C & Haas D (2002) Regulatory RNA as mediator in GacA/RsmA-dependent global control of exoproduct formation in *Pseudomonas fluorescens* CHA0. *J Bacteriol* **184**: 1046-1056
- Heldermon C, DeAngelis PL & Weigel PH (2001) Topological organization of the hyaluronan synthase from *Streptococcus pyogenes*. *J Biol Chem* **276**: 2037-2046
- Higuchi R, Krummel B & Saiki R (1988) A general method of in vitro preparation and specific mutagenesis of DNA fragments: study of protein and DNA interactions. *Nucleic Acids Res* **16**: 7351-7367
- Karimova G, Pidoux J, Ullmann A & Ladant D (1998) A bacterial two-hybrid system based on a reconstituted signal transduction pathway. *Proc Natl Acad Sci USA* **95**: 5752-5756
- Larkin MA, Blackshields G, Brown NP, Chenna R, McGettigan PA, McWilliam H, Valentin F, Wallace IM, Wilm A, Lopez R, Thompson JD, Gibson TJ & Higgins DG (2007) Clustal W and Clustal X version 2.0. *Bioinformatics* **23**: 2947-2948
- Malone JG, Jaeger T, Spangler C, Ritz D, Spang A, Arrieumerlou C, Kaefer V, Landmann R & Jenal U (2010) YfiBNR mediates cyclic di-GMP dependent small colony variant formation and persistence in *Pseudomonas aeruginosa*. *PLoS Pathog* **6**: e1000804
- Malone JG, Williams R, Christen M, Jenal U, Spiers AJ & Rainey PB (2007) The structure-function relationship of WspR, a *Pseudomonas fluorescens* response regulator with a GGDEF output domain. *Microbiology* **153**: 980-994
- Saxena IM & Brown RM (1997) Identification of cellulose synthase(s) in higher plants: sequence analysis of processive beta-glycosyltransferases with the common motif "D, D, D35Q(R,Q)XRW". *Cellulose* **4**: 33-49
- Saxena IM, Brown RM & Dandekar T (2001) Structure-function characterization of cellulose synthase: relationship to other glycosyltransferases. *Phytochemistry* **57**: 1135-1148
- Sonnhammer EL, von Heijne G & Krogh A (1998) A hidden Markov model for predicting transmembrane helices in protein sequences. *Proceedings International Conference on Intelligent Systems for Molecular Biology* **6**: 175-182
- Uzzau S, Figueroa-Bossi N, Rubino S & Bossi L (2001) Epitope tagging of chromosomal genes in *Salmonella*. *Proc Natl Acad Sci USA* **98**: 15264-15269

- Weigel PH & DeAngelis PL (2007) Hyaluronan synthases: a decade-plus of novel glycosyltransferases. *J Biol Chem* **282**: 36777-36781
- Woodcock DM, Crowther PJ, Doherty J, Jefferson S, DeCruz E, Noyer-Weidner N, Smith SS, Michael MZ & Graham MW (1989) Quantitative evaluation of Escherichia coli host strains for tolerance to cytosine methylation in plasmid and phage recombinants. *Nucleic Acids Res* **17**: 3469-3478
- Yu D, Ellis HM, Lee EC, Jenkins NA, Copeland NG & Court DL (2000) An efficient recombination system for chromosome engineering in Escherichia coli. *Proc Natl Acad Sci USA* **97**: 5978-5983

3.3 Additional results

3.3.1 Results and interpretations

Probing the c-di-GMP binding site within the PgaCD complex by mass spectrometry (in collaboration with Paul Jenö & Suzette Moes)

As described in detail in chapter 3.2, PgaC as well as PgaD were both specifically and competitively labeled with [³²P]c-di-GMP upon UV light-induced crosslinking. As close proximity is a prerequisite for covalent zero-length crosslink formation, the ligand binding pocket within the PgaCD complex might be formed by amino acid residues from both proteins. The finding that PgaC was always incorporating more radioactivity than PgaD could easily be explained by the fact that not all amino acid residues show the same propensity to get covalently crosslinked to a nucleotide ligand upon UV light irradiation (Meisenheimer & Koch, 1997).

In order to identify the site to which [³²P]c-di-GMP gets covalently crosslinked (the much stronger signal for PgaC may only allow the analysis of the PgaC side), a mass spectrometry (MS) approach was chosen, which has previously been used to map ligand binding sites in different proteins (Lewis *et al*, 1992; Shivanna *et al*, 1993; Cheng *et al*, 1993). It is based on the isolation and identification of radioactive peptides following tryptic digestion of the radiolabeled protein. It is worth mentioning that the use of native nucleotide ligands in UV light-induced crosslinking experiments bares some disadvantages. The crosslinking yield can be very low and photocleavage or oxidation of the interaction partners are often observed. The rather long irradiation times at a wavelength of 254 nm that also excites chromophores within the peptide may cause photodamage. Furthermore, as the UV light-induced mechanisms of covalent crosslink formation are not fully understood and generally hard to predict, MS analysis may be complicated (Steen & Jensen, 2002). Therefore, the use of a wide variety of photoactivatable nucleotide analogs (e.g. azido-substituted nucleobases) proved to be beneficial (Zhou *et al*, 1993; Kotzyba-Hibert *et al*, 1995; Chatterji *et al*, 1998; Steen & Jensen, 2002; Robinette *et al*, 2006).

Whatsoever, native, but radiolabeled [³²P]c-di-GMP was used for UV light-induced crosslinking of *pgaC*-3xF and *pgaD*-3xF-expressing membranes in this approach. The control experiment showed competitive c-di-GMP binding to PgaC and PgaD as previously observed (Additional Figure 1A). Immunoprecipitated PgaCD complexes were eluted from the beads, digested with endoproteinase Lys-C and trypsin, before the peptides were separated by C18 reverse phase HPLC (Additional Figure 1B). A total of 80 15 µl fractions were collected and spotted onto a silica gel plate. Autoradiography analysis revealed the strongest radioactive signal for fraction B6,

indicating the presence of a [³²P]c-di-GMP-modified peptide (Additional Figure 1C). Slightly weaker radioactive signals were observed for the few fractions directly following fraction B6. MS analysis of fraction B6 resulted in the identification of peptides from about 100 different *E. coli* proteins. Moreover, an interesting low abundant precursor ion was found, which eluted at about 37 min and that liberated two c-di-GMP-specific fragment ions (m/z 248.1 and m/z 540.0) (Additional Figure 1D) (Simm *et al*, 2004). Unfortunately, due to the rather bad quality of the MS spectra, further characterization and sequence analysis of this interesting precursor ion candidate was not successful.

Clearly, further optimization of this experimental approach is needed in the future. Upscaling of the entire experiment may generally be helpful to counteract the low yield of UV light-induced crosslink formation. The fact that peptides from almost 100 different proteins could be identified in fraction B6 shows that the immunoprecipitation of PgaCD complexes was rather dirty. Further wash and/or purification steps may therefore be beneficial. Alternatively or in addition, a second enrichment step of the radiolabeled peptide should be performed prior to MS analysis to reduce the sample complexity (e.g. second HPLC fractionation using a different type of column or enrichment of phosphate-containing peptides using either TiO₂ or IMAC methods (Richter *et al*, 2009; Leitner *et al*, 2011)). Peptides that are covalently modified with a c-di-GMP molecule might also be enriched using a c-di-GMP binding protein (e.g. the PilZ domain-containing protein DgrA from *C. crescentus*) that is immobilized on an affinity column.

Which protease degrades PgaD under low c-di-GMP conditions?

As shown in chapter 3.2, PgaD is highly unstable under conditions of low cellular c-di-GMP concentrations. Several experiments were performed in order to identify the protease(s) involved in PgaD degradation. The three proteases ClpP, Lon and FtsH were considered as good candidates, since they are known to be the main proteases involved in processive energy-dependent protein degradation in *E. coli*. The two serine proteases ClpP and Lon are especially involved in the removal of un- or misfolded and damaged proteins (protein quality control), while the essential membrane-bound metalloprotease FtsH has been linked to the turnover of unassembled membrane proteins (Gottesman, 1996; Ito & Akiyama, 2005; Kirstein *et al*, 2009; Akiyama, 2009).

It was hypothesized that in the ideal case, the deletion of the protease involved in PgaD degradation would lead to an increased PgaD steady state level that does not show c-di-GMP-dependent fluctuations. However, deletions of *lon*, *clpP* or *lon* and *clpP* together gave counterintuitive results as PgaD levels were reduced in the *csrA* as well as the *csrA ΔydeH* background (Additional Figure 2A). In case of the Δlon and the $\Delta lon \Delta clpP$ mutants, these protein

level reductions were reflected in a reduced biofilm formation. In order to rule out indirect effects of the proteases on PgaD levels (e.g. through transcription and/or translation), protease deletions were analyzed in a strain that expresses the *pga* operon from the L-arabinose-dependent P_{ara} promoter (including the 5' untranslated leader sequence from *araB*). While the deletion of *lon* gave similar results than before, the PgaD steady state level of a $\Delta clpP$ mutant was again strongly reduced, but did not seem to show strong *ydeH*-dependent fluctuations this time (Additional Figure 2B). Using a slightly different experimental setup (ectopic expression of *pgaD* from plasmid), a similar phenotype was observed for the $\Delta clpP$ mutant when comparing PgaD levels of a *csrA* and a *csrA* $\Delta 7$ (see chapter 3.2) strain (Additional Figures 2C and 2D). In contrast to the almost c-di-GMP-independent PgaD protein levels, biofilm formation still reacted to c-di-GMP. This can readily be explained by the fact that PgaD stabilization seems to be a secondary effect of c-di-GMP-dependent allosteric PgaCD GT activation (see chapter 3.2). However, it remains a mystery why biofilm formation of a *csrA* $\Delta clpP$ mutant is only reduced by a factor of two compared to the *clpP*⁺ strain, while its PgaD level is reduced much more (Additional Figures 2C and 2D). Thus, the correlation between biofilm formation and PgaD levels seems to be somehow altered in a $\Delta clpP$ mutant background. Interestingly, the $\Delta clpP$ deletion resulted in a very weak, but poly-GlcNAc-independent attachment GOF phenotype in a *csrA* $\Delta 7$ c-di-GMP^{low} strain (Additional Figure 2D).

Since some of the results described above may suggest an involvement of ClpP in the degradation of PgaD in response to low cellular c-di-GMP concentrations, it was tested whether a $\Delta clpP$ deletion would prolong the half life of PgaD-3xF in a strain with low levels of c-di-GMP (*csrA* $\Delta ydeH$) as determined when blocking translation of exponentially growing cells with translation inhibitors (see chapter 3.2). As shown in Additional Figure 2E, the deletion of *clpP* did not rescue the instability of PgaD in cells with a low c-di-GMP concentration. This result thus strongly suggests that ClpP is not the sought-after protease.

The fact that the PgaD level even in a *csrA* $\Delta clpP$ mutant fully depended on the presence of *pgaC* (Additional Figure 2D), implies that uncomplexed PgaD is removed from the cell by another protease than ClpP. Therefore, PgaD accumulation upon the expression from plasmid was assayed in the absence of PgaC (*csrA*⁺ strain) in dependence of *lon*, *clpP* and *ftsH*. While no increase in the PgaD protein level was observed in the Δlon and $\Delta clpP$ mutants compared to the wildtype, PgaD slightly accumulated in a $\Delta ftsH$ deletion mutant (Additional Figure 2F). The difference between the wildtype and the $\Delta ftsH$ mutant may even be underestimated, since the control protein PgaC showed reduced levels in the $\Delta ftsH$ mutant compared to the wildtype. Next, it was tested whether FtsH may be the protease involved in PgaD degradation under low c-di-GMP conditions.

As shown in Additional Figure 2G, biofilm formation as well as PgaD steady state protein levels remained *ydeH*-dependent in a Δ *ftsH* mutant. It is worth mentioning however that the overall attachment and PgaD levels were found to be elevated in the Δ *ftsH* mutant compared to the *ftsH*⁺ strain (Additional Figure 2G), thus implying a potential role for FtsH in the removal of uncomplexed PgaD.

To make a long story short, none of the three main *E. coli* proteases seems to be the one that degrades PgaD under low c-di-GMP conditions. This could either be explained by a strong redundancy among the main proteases for PgaD degradation or by the involvement of another (maybe less well characterized) protease. If it is one specific protease, it may be found by performing a genetic screen (e.g. transposon mutagenesis) with the goal of isolating mutants that show an increased PgaD level in a *csrA* Δ 7 c-di-GMP^{low} strain. Theoretically, if a protein fusion between PgaD and the kanamycin resistance protein would promote c-di-GMP-dependent *E. coli* growth, the protease involved in PgaD degradation could be found by selecting for cell survival.

Towards understanding ppGpp-mediated control of PgaA levels

As we have previously reported (Boehm *et al*, 2009), PgaA steady state protein levels are negatively controlled by the bacterial signalling molecule ppGpp. In *E. coli*, the alarmone ppGpp is produced from ATP and GTP by RelA and SpoT. While RelA only harbors a ppGpp synthetase domain, SpoT is a bifunctional enzyme harboring a ppGpp synthetase and hydrolase domain (Potrykus & Cashel, 2008; Dalebroux & Swanson, 2012). A *csrA* Δ *relA* Δ *spoT* (ppGpp⁰) mutant formed very strong poly-GlcNAc-dependent biofilms and showed a strongly increased level of the outer membrane protein PgaA compared to the *csrA* mutant control. Since the PgaD levels were unaltered in a ppGpp⁰ strain, it was hypothesized that ppGpp influences the PgaA level post-transcriptionally (Boehm *et al*, 2009).

In order to substantiate a post-transcriptional control mechanism, the protein levels of all four components of the Pga machinery were individually analyzed using 3xFlag-tagged versions. The absence of ppGpp strongly affected the steady state level of PgaA, while the other three protein levels remained more or less constant (Additional Figure 3A). This suggests that the high PgaA level may be the reason for elevated biofilm formation in the absence of ppGpp. However, overexpression of PgaA in a *csrA* mutant background did not cause any biofilm induction (data not shown), indicating that the relatively low PgaA level in this strain is not the only limiting factor for strong biofilm formation.

In agreement with biofilm formation data (Boehm *et al*, 2009), the high PgaA protein level was found to be due to the total absence of ppGpp. A *csrA* Δ *relA* mutant did not show an increased

protein level (Additional Figure 3B). Since the strong biofilm formation of a ppGpp⁰ strain is fully dependent on the presence of the DGC-encoding gene *ydeH* (Boehm *et al*, 2009), it was tested whether the same is true for the PgaA protein level. As shown in Additional Figure 3C, PgaA levels stayed high upon deletion of *ydeH*, arguing that c-di-GMP is not involved in the control of PgaA protein levels.

The expression of outer membrane proteins is often regulated on a post-transcriptional level by bacterial small non-coding RNAs (sRNAs) (Vogel & Papenfort, 2006; Storz *et al*, 2011). In many cases, the RNA binding protein Hfq assists the sRNAs by facilitating their pairing with target mRNAs (Vogel & Luisi, 2011). The expression of *hfq* is known to be repressed by CsrA (Baker *et al*, 2007). Since PgaA is a porin-like outer membrane protein, the effect of a Δhfq deletion on the PgaA steady state protein level was tested. Interestingly, a Δhfq deletion caused a strong increase of the PgaA level in a *csrA* mutant, while the deletion did not lead to an increase of the protein level in a *csrA* ppGpp⁰ strain background (Additional Figure 3D). Thus, the negative impact of ppGpp on PgaA levels seems to be mediated through Hfq. However, it remains unclear whether the *hfq*-mediated effect is specific for PgaA, since it was previously found that a Δhfq mutant also showed increased PgaD protein levels (Master Thesis A. Casanova, 2009). To test whether the inhibitory effect of *hfq* on PgaA levels depends on the *pga* operon promoter and 5' untranslated leader sequence, the native chromosomal region was replaced with the corresponding region of the L-arabinose-dependent P_{ara} promoter. Even in this strain background, *hfq* negatively controlled PgaA protein levels (Additional Figure 3E). Although one cannot rule out indirect effects in general or negative effects of *hfq* on e.g. the 5' untranslated leader sequence of *araB*, the data described above suggest that Hfq does not target the 5' untranslated region of *pgaA*, but rather affects translation of *pgaA* by acting within the *pgaA* ORF. This is likely also true for the ppGpp-mediated control mechanism, since a translational *pgaA-lacZ* fusion did not respond to the deletions of *relA* and *spoT* (ppGpp⁰) (Master Thesis S. Steiner, 2007).

In summary, the findings discussed above suggest a highly speculative model in which a ppGpp-controlled sRNA represses the translation of PgaA in an Hfq-dependent manner. sRNAs (e.g. RybB and MicA) that are ppGpp-dependent due to being controlled by the membrane stress sigma factor σE have previously been described (Johansen *et al*, 2006; Costanzo & Ades, 2006; Udekwu & Wagner, 2007; Thompson *et al*, 2007). sRNA-mediated translational control within the coding region of target genes is rather uncommon, but has been reported in the past (Bouvier *et al*, 2008; Pfeiffer *et al*, 2009). Interestingly, the CRP-regulated sRNA McaS was recently shown to control *pgaA* expression in *E. coli* via a yet unknown, but *pga* operon promoter and/or 5' untranslated region-dependent mechanism (Thomason *et al*, 2012).

There are several open questions remaining: Is the elevated PgaA level in a ppGpp⁰ strain background physiologically relevant at all? If yes, what are the molecular mechanisms behind it? And finally, how are c-di-GMP- and ppGpp-mediated control mechanisms integrated on the functioning of the Pga machinery?

3.3.2 Additional figures, tables and figure legends

Additional Figure 1 Searching c-di-GMP-modified peptides following UV light-induced crosslinking with [³²P]c-di-GMP. (A) Membranes containing PgaC and PgaD were UV-crosslinked in the presence of [³²P]c-di-GMP. The concentrations of [³²P]c-di-GMP and competing unlabeled c-di-GMP are indicated. Following Flag IP, the samples were analyzed by autoradiography. SDS-resistant heterodimeric PgaCD complexes are indicated (PgaC + PgaD). (B) HPLC elution profile of the tryptic digest of Flag IP-enriched PgaC and PgaD eluted at 25 µl/min from an Agilent ZORBAX SB-C18 column. The effluent was recorded at 214 nm. Fractions of 15 µl were collected. (C) Localization of [³²P]c-di-GMP-modified peptides in the HPLC fractions. All 80 fractions collected during the HPLC run were individually spotted onto a silica gel plate and visualized by autoradiography. The order of the fractions is A1-H1, A2-H2, A3-H3 and so on. (D) Searching c-di-GMP-modified peptides with c-di-GMP-specific fragment ions (m/z 248.1 and m/z 540.0; right spectra) (Simm *et al*, 2004) liberated from the 2326 Da precursor ion (left spectrum).

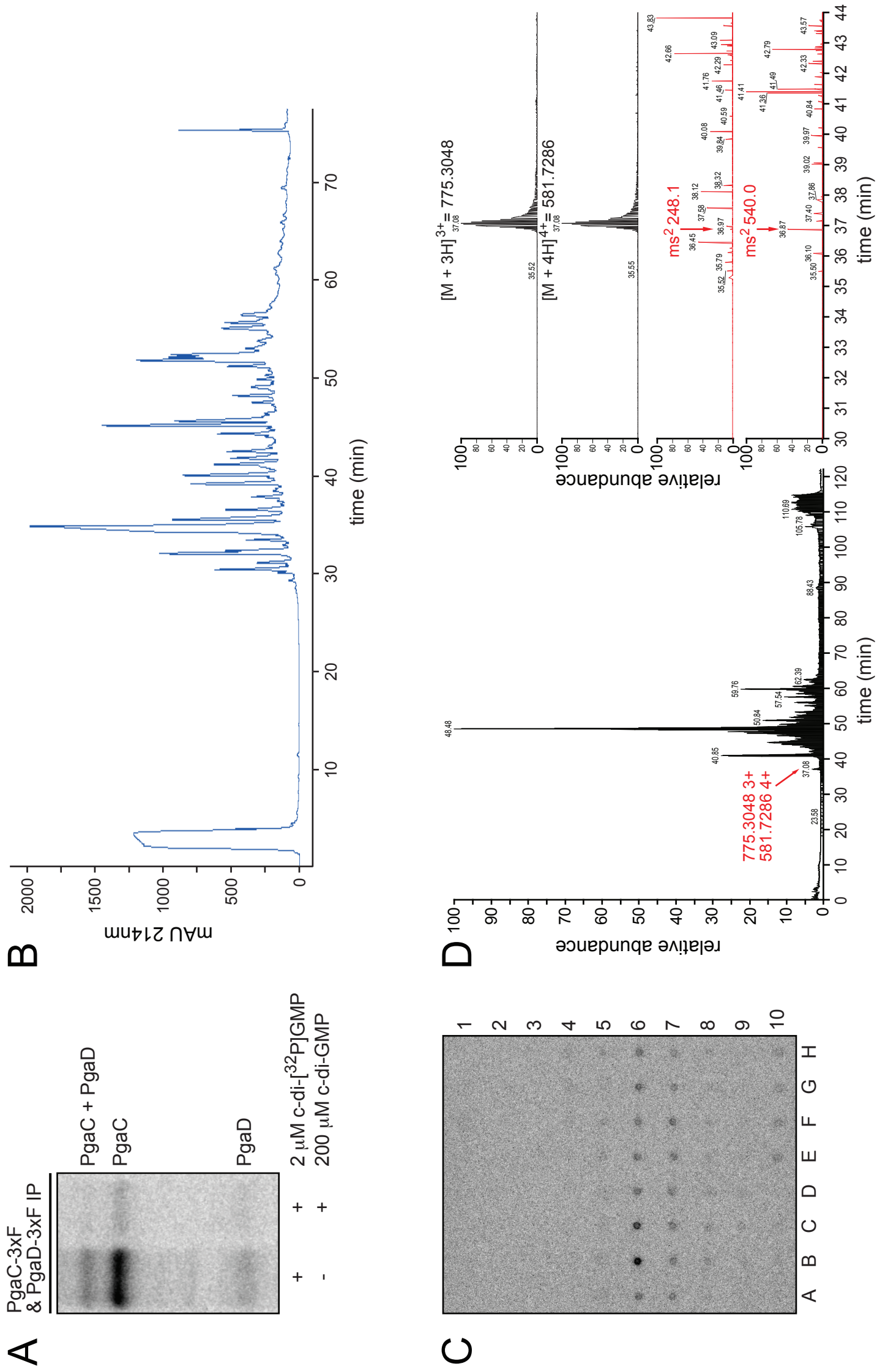
Additional Figure 2 ClpP, Lon and FtsH seem not to be involved in PgaD degradation in response to a low cellular c-di-GMP concentration. (A) Biofilm formation and immunoblot analysis of PgaD steady state protein levels in response to protease deletions and c-di-GMP (*ydeH*⁺/*ΔydeH*). Error bars are standard deviations. A C-terminally 3xFlag-tagged construct was used for PgaD detection. (B) Immunoblot analysis of PgaD steady state protein levels in response to protease deletions and c-di-GMP (*ydeH*⁺/*ΔydeH*). The native *pga* promoter has been replaced with the L-arabinose-dependent *P_{ara}* promoter. The resulting strains harbor an *araB-pgaA* translational fusion with the promoter and the 5' untranslated region of the *pga* operon being replaced with the corresponding regions of the *araBAD* operon. Expression was induced with 0.00002% arabinose. A C-terminally 3xFlag-tagged construct was used for PgaD detection. (C) Biofilm formation and immunoblot analysis of PgaD steady state protein levels in response to protease deletions and c-di-GMP (*csrA Δ7/csrA*). Error bars are standard deviations. A C-terminally 3xFlag-tagged construct was used for PgaD detection. Expression of *pgaD* was not induced (basal level). (D) A *ΔclpP* mutant shows a partially c-di-GMP-independent PgaD steady state level. Biofilm formation and immunoblot analysis of PgaD steady state protein levels in response to *ΔclpP* deletions and c-di-GMP (*csrA Δ7/csrA*). Error bars are standard deviations. A C-terminally 3xFlag-tagged construct was used for PgaD detection. Expression of *pgaD* was not induced (basal level). (E) c-di-GMP-dependent *in vivo* PgaD stability is not affected in a *ΔclpP* mutant as determined by a translation block experiment. Translation was inhibited in exponentially growing cells by the addition of 300 µg/ml erythromycin. Expression of *pgaD* was not induced (basal level). Left: Quantification of

relative PgaD protein levels over time following translation inhibition. Right: Immunoblot analysis of PgaD protein levels over time following translation inhibition. A C-terminally 3xFlag-tagged construct was used for PgaD detection. Time after translation inhibition (min) is indicated. (F) A *ΔftsH* mutant shows a higher PgaD steady state protein level than the wildtype. Immunoblot analysis of PgaC and PgaD steady state protein levels in response to protease deletions. C-terminally 3xFlag-tagged constructs were used for PgaC and PgaD detection. Expression of plasmid constructs was induced as indicated. All strains harbor chromosomal *pgaC* and *pgaD* in addition. *sfhC21* is a suppressor mutation that allows the deletion of *ftsH* (Ogura *et al*, 1999). (G) FtsH seems not to be involved in c-di-GMP-dependent PgaD level fluctuations. Left: Biofilm formation shows a response to c-di-GMP (*ydeH*⁺/*ΔydeH*) in a *ΔftsH* deletion mutant background. Error bars are standard deviations. Right: Biofilm formation and immunoblot analysis of PgaD steady state protein levels in response to *ΔftsH* deletions and c-di-GMP (*ydeH*⁺/*ΔydeH*). Error bars are standard deviations. A C-terminally 3xFlag-tagged construct was used for PgaD detection. Left and right graphs show experiments performed with isogenic strains that have been constructed using a different approach.

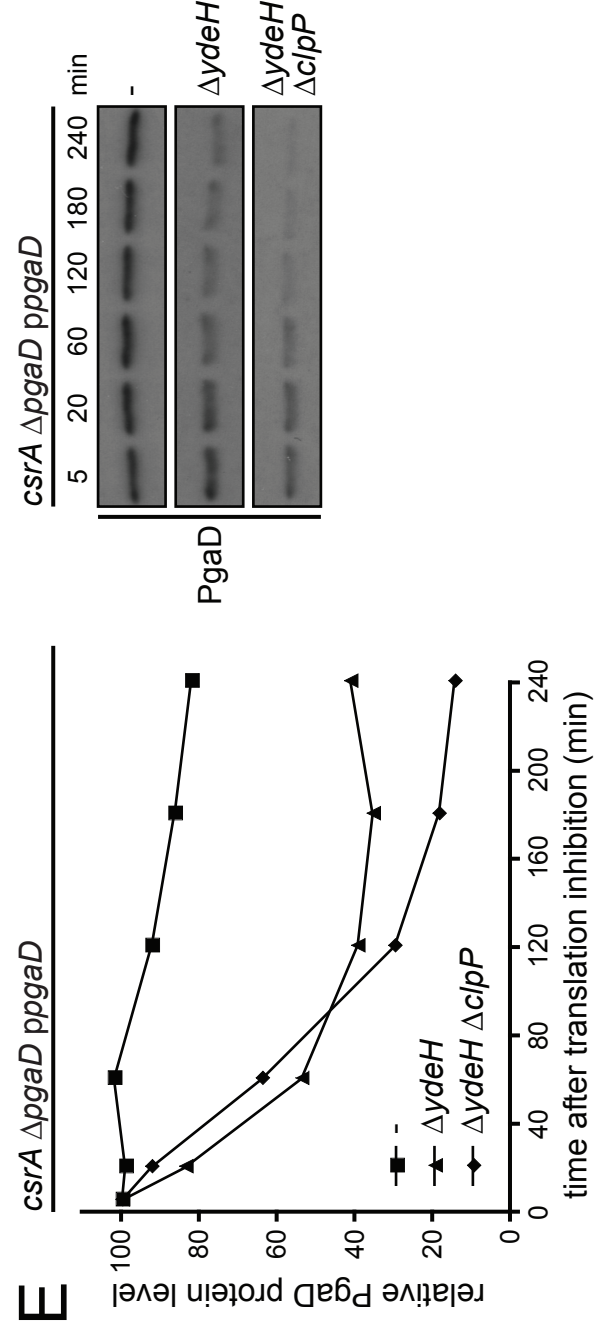
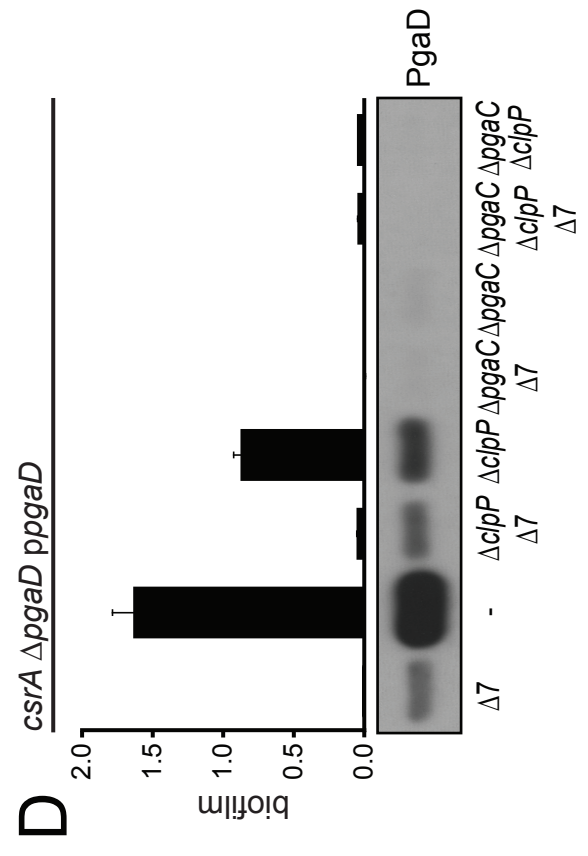
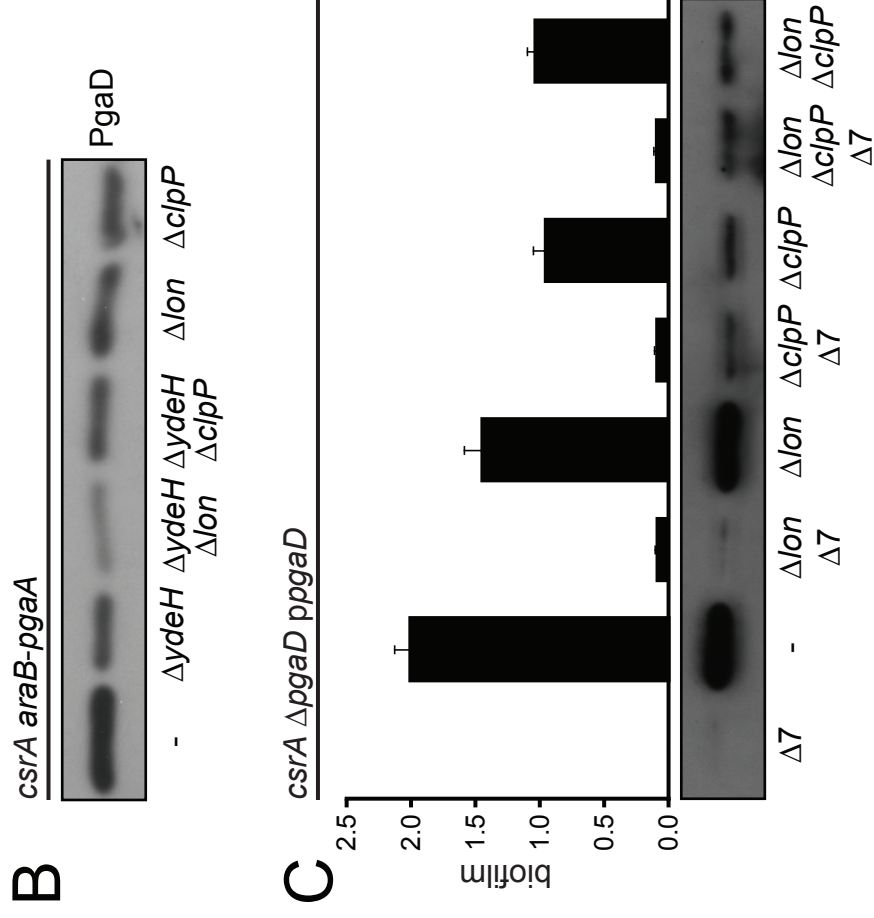
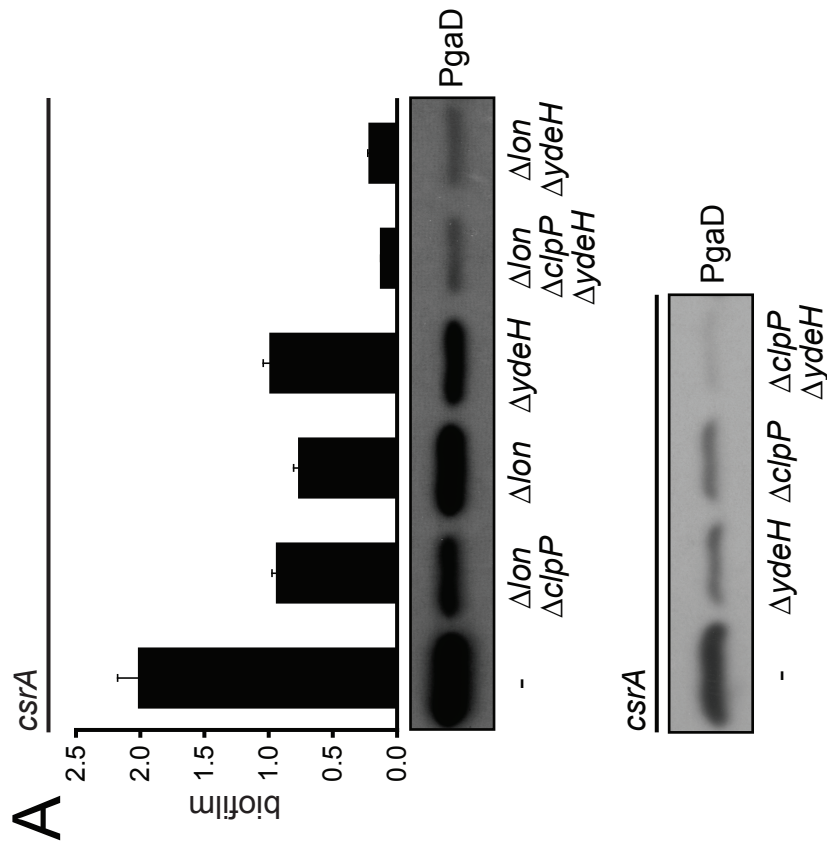
Additional Figure 3 The upregulation of PgaA levels in the absence of ppGpp seems to depend on *hfq*. (A) Immunoblot analysis of Pga steady state protein levels in response to ppGpp (ppGpp⁺/ppGpp⁰ (*ΔrelA ΔspoT*)). C-terminally 3xFlag-tagged constructs were used for protein detection. Strains for PgaA analysis carried a *ΔpgaBCD* deletion, strains for PgaB analysis a *ΔpgaCD* deletion and strains for PgaC analysis a *ΔpgaD* deletion. (B) Immunoblot analysis of PgaA steady state protein levels in different mutant backgrounds. A C-terminally 3xFlag-tagged construct was used for PgaA detection. Strains for PgaA analysis carried a *ΔpgaBCD* deletion. (C) A *csrA* ppGpp⁰ *ΔydeH* mutant does not show a reduced PgaA level. Immunoblot analysis of PgaA steady state protein levels in different mutant backgrounds. A C-terminally 3xFlag-tagged construct was used for PgaA detection. Strains for PgaA analysis carried a *ΔpgaBCD* deletion. (D) PgaA accumulates in a *Δhfq* mutant. Immunoblot analysis of PgaA steady state protein levels in different mutant backgrounds. A C-terminally 3xFlag-tagged construct was used for PgaA detection. Strains for PgaA analysis carried a *ΔpgaBCD* deletion. (E) Immunoblot analysis of PgaA steady state protein levels in response to a *Δhfq* deletion. The native *pga* promoter has been replaced with the L-arabinose-dependent P_{ara} promoter. The resulting strains harbor an *araB-pgaA* translational fusion with the promoter and the 5' untranslated region of the *pga* operon being replaced with the corresponding regions of the *araBAD* operon. Expression was induced as

indicated. A C-terminally 3xFlag-tagged construct was used for PgaA detection. Strains for PgaA analysis carried a $\Delta pgaBCD$ deletion.

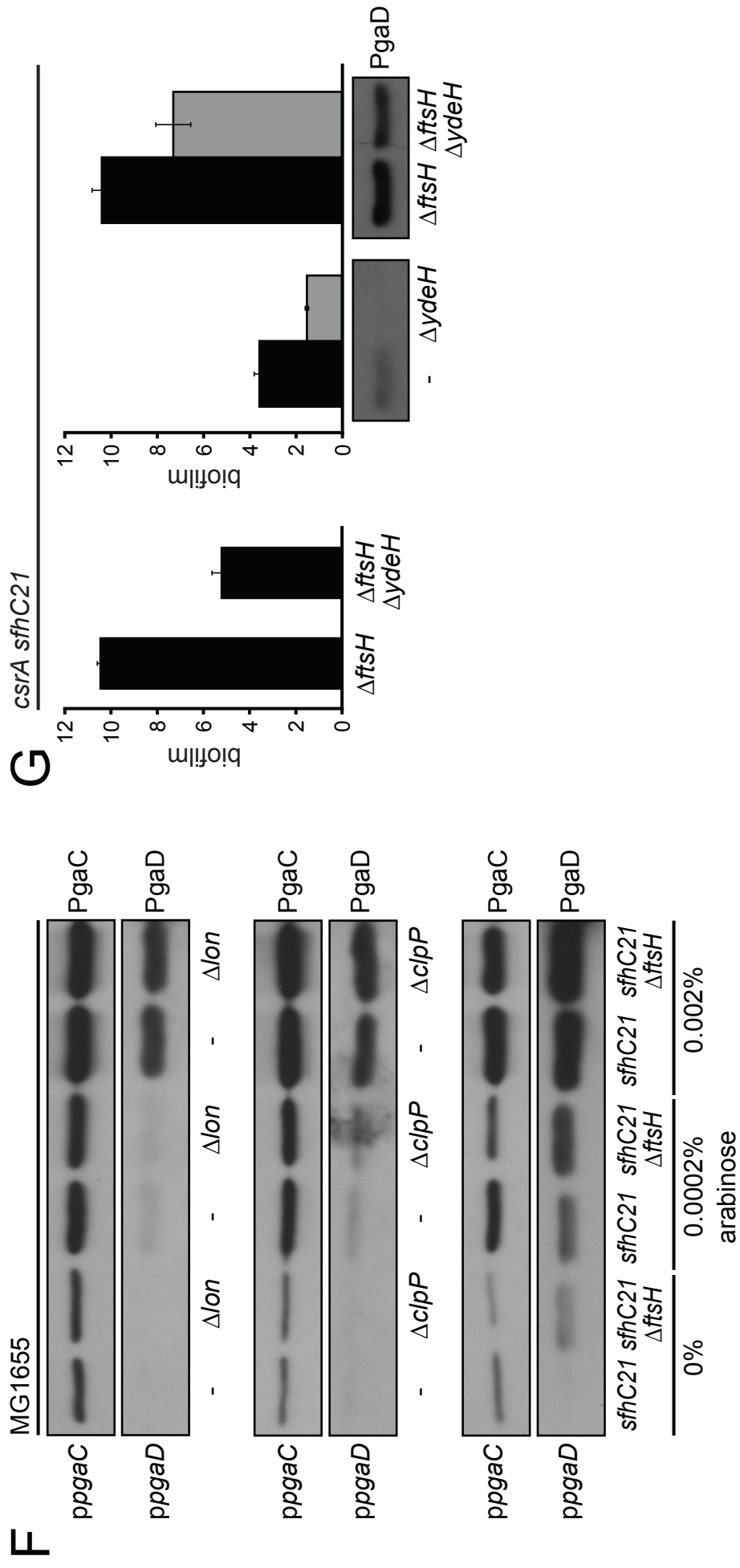
Additional Figure 1



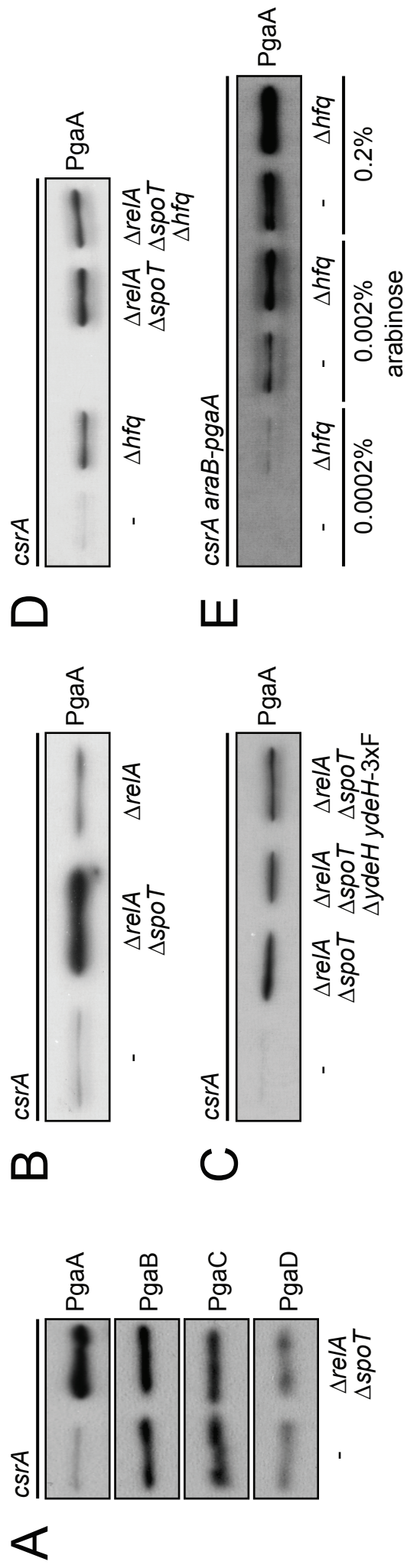
Additional Figure 2



Additional Figure 2



Additional Figure 3



Additional Table 1

Additional Table 1 Strains and plasmids used for Additional results.

E. coli strains

Name	Relevant genotype	Description/comments	Source/reference
MG1655	wildtype	<i>E. coli</i> K-12 wildtype	(Blattner <i>et al</i> , 1997)
AB330	DY330 λ cI ⁸⁵⁷ Δ (<i>cro-bioA</i>)	temperature sensitive, λ RED system	(Yu <i>et al</i> , 2000)
AB958	<i>csrA::Tn5</i> Δ (<i>kan</i>):: <i>Frt</i>	ancestor of most strains used in this study	(Boehm <i>et al</i> , 2009)
AB959	<i>csrA::Tn5</i> Δ (<i>kan</i>):: <i>Frt</i> Δ <i>ydeH</i> :: <i>Frt</i>		(Boehm <i>et al</i> , 2009)
AB1062	<i>csrA::Tn5</i> Δ (<i>kan</i>):: <i>Frt</i> <i>pgaD</i> -3xFlag- <i>kan</i>		(Boehm <i>et al</i> , 2009)
AB1063	<i>csrA::Tn5</i> Δ (<i>kan</i>):: <i>Frt</i> Δ <i>ydeH</i> :: <i>Frt</i> <i>pgaD</i> -3xFlag- <i>kan</i>		(Boehm <i>et al</i> , 2009)
AB1091	<i>csrA::Tn5</i> Δ (<i>kan</i>):: <i>Frt</i> Δ <i>relA</i> :: <i>Frt</i> Δ <i>spoT</i> :: <i>Frt</i> <i>pgaD</i> -3xFlag- <i>kan</i>		(Boehm <i>et al</i> , 2009)
AB1094	<i>csrA::Tn5</i> Δ (<i>kan</i>):: <i>Frt</i> <i>Frt-araC-araB</i> <i>pgaA</i> (tl.) <i>pgaD</i> -3xFlag- <i>Frt</i> Δ <i>araBC</i> :: <i>Frt</i>	translational <i>araB-pgaA</i> fusion, <i>kan-araC-P_{ara}</i> amplified from TB55	(Steiner <i>et al</i> , in prep)
AB1138	<i>csrA::Tn5</i> Δ (<i>kan</i>):: <i>Frt</i> <i>pgaC</i> -3xFlag Δ <i>pgaD</i> :: <i>kan</i>		This work
AB1416	<i>csrA::Tn5</i> Δ (<i>kan</i>):: <i>Frt</i> <i>Frt-araC-araB</i> <i>pgaA</i> (tl.) <i>pgaD</i> -3xFlag- <i>Frt</i> Δ <i>araBC</i> :: <i>Frt</i> Δ <i>ydeH</i> :: <i>Frt</i>	translational <i>araB-pgaA</i> fusion, <i>kan-araC-P_{ara}</i> amplified from TB55	(Steiner <i>et al</i> , in prep)
AB1417	<i>csrA::Tn5</i> Δ (<i>kan</i>):: <i>Frt</i> <i>pgaA</i> -3xFlag Δ <i>pgaBCD</i> :: <i>kan</i>		(Boehm <i>et al</i> , 2009)
AB1418	<i>csrA::Tn5</i> Δ (<i>kan</i>):: <i>Frt</i> <i>pgaB</i> -3xFlag Δ <i>pgaCD</i> :: <i>kan</i>		(Steiner <i>et al</i> , in prep)
AB1433	<i>csrA::Tn5</i> Δ (<i>kan</i>):: <i>Frt</i> Δ <i>araBC</i> :: <i>Frt</i> <i>Frt-kan-Frt-araC-araB</i> <i>pgaA</i> -3xFlag (tl.) Δ <i>pgaBCD</i> :: <i>cat</i>	translational <i>araB-pgaA</i> fusion, <i>kan-araC-P_{ara}</i> amplified from TB55	(Steiner <i>et al</i> , in prep)
AB1470	<i>csrA::Tn5</i> Δ (<i>kan</i>):: <i>Frt</i> Δ <i>relA</i> :: <i>Frt</i> Δ <i>spoT</i> :: <i>Frt</i> <i>pgaA</i> -3xFlag Δ <i>pgaBCD</i> :: <i>kan</i>		(Boehm <i>et al</i> , 2009)
AB1471	<i>csrA::Tn5</i> Δ (<i>kan</i>):: <i>Frt</i> Δ <i>relA</i> :: <i>Frt</i> Δ <i>spoT</i> :: <i>Frt</i> <i>pgaB</i> -3xFlag Δ <i>pgaCD</i> :: <i>kan</i>		This work
AB1472	<i>csrA::Tn5</i> Δ (<i>kan</i>):: <i>Frt</i> Δ <i>relA</i> :: <i>Frt</i> Δ <i>spoT</i> :: <i>Frt</i> <i>pgaC</i> -3xFlag Δ <i>pgaD</i> :: <i>kan</i>		This work
AB1569	<i>csrA::Tn5</i> Δ (<i>kan</i>):: <i>Frt</i> Δ <i>pgaD</i> :: <i>Frt</i>		(Steiner <i>et al</i> , in prep)
AB1570	<i>csrA::Tn5</i> Δ (<i>kan</i>):: <i>Frt</i> Δ <i>ydeH</i> :: <i>Frt</i> Δ <i>pgaD</i> :: <i>Frt</i>		(Steiner <i>et al</i> , in prep)
AB1638	<i>csrA::Tn5</i> Δ (<i>kan</i>):: <i>Frt</i> Δ <i>araBC</i> :: <i>Frt</i> Δ <i>pgaABCD</i> :: <i>Frt</i>	strain used for overexpressions (c-di-GMP binding assays)	(Steiner <i>et al</i> , in prep)
AB1668	<i>csrA::Tn5</i> Δ (<i>kan</i>):: <i>Frt</i> Δ <i>relA</i> :: <i>Frt</i> Δ <i>spoT</i> :: <i>Frt</i> <i>pgaA</i> -3xFlag Δ <i>pgaBCD</i> :: <i>kan</i> <i>ydeH</i> -Flag- <i>cat</i>		This work
AB1673	<i>csrA::Tn5</i> Δ (<i>kan</i>):: <i>Frt</i> Δ <i>relA</i> :: <i>Frt</i> Δ <i>spoT</i> :: <i>Frt</i> Δ <i>ydeH</i> :: <i>Frt</i> <i>pgaA</i> -3xFlag Δ <i>pgaBCD</i> :: <i>kan</i>		This work
AB1685	<i>csrA::Tn5</i> Δ (<i>kan</i>):: <i>Frt</i> Δ <i>relA</i> :: <i>Frt</i> <i>pgaA</i> -3xFlag Δ <i>pgaBCD</i> :: <i>kan</i>		This work
AB1699	<i>csrA::Tn5</i> Δ (<i>kan</i>):: <i>Frt</i> Δ <i>hfq</i> :: <i>Frt</i> <i>pgaA</i> -3xFlag Δ <i>pgaBCD</i> :: <i>kan</i>		This work
AB1700	<i>csrA::Tn5</i> Δ (<i>kan</i>):: <i>Frt</i> Δ <i>relA</i> :: <i>Frt</i> Δ <i>spoT</i> :: <i>Frt</i> Δ <i>hfq</i> :: <i>Frt</i> <i>pgaA</i> -3xFlag Δ <i>pgaBCD</i> :: <i>kan</i>		This work
AB1764	<i>csrA::Tn5</i> Δ (<i>kan</i>):: <i>Frt</i> <i>pgaD</i> -3xFlag- <i>kan</i> Δ <i>lon</i> Δ <i>clpP</i> :: <i>cat</i>	Δ <i>lon</i> Δ <i>clpP</i> :: <i>cat</i> construct from ' Δ <i>lon</i> <i>clpP</i> :: <i>cat</i> ' (Hallez <i>et al</i> , 2010)	This work
AB1765	<i>csrA::Tn5</i> Δ (<i>kan</i>):: <i>Frt</i> Δ <i>ydeH</i> :: <i>Frt</i> <i>pgaD</i> -3xFlag- <i>kan</i> Δ <i>lon</i> Δ <i>clpP</i> :: <i>cat</i>	Δ <i>lon</i> Δ <i>clpP</i> :: <i>cat</i> construct from ' Δ <i>lon</i> <i>clpP</i> :: <i>cat</i> ' (Hallez <i>et al</i> , 2010)	This work
AB1766	<i>csrA::Tn5</i> Δ (<i>kan</i>):: <i>Frt</i> <i>pgaD</i> -3xFlag- <i>kan</i> Δ <i>lon</i> :: <i>tet</i>	Δ <i>lon</i> :: <i>tet</i> construct from ' <i>lon</i> :: <i>tet</i> ' (Hallez <i>et al</i> , 2010)	This work
AB1767	<i>csrA::Tn5</i> Δ (<i>kan</i>):: <i>Frt</i> Δ <i>ydeH</i> :: <i>Frt</i> <i>pgaD</i> -3xFlag- <i>kan</i> Δ <i>lon</i> :: <i>tet</i>	Δ <i>lon</i> :: <i>tet</i> construct from ' <i>lon</i> :: <i>tet</i> ' (Hallez <i>et al</i> , 2010)	This work
AB1780	<i>csrA::Tn5</i> Δ (<i>kan</i>):: <i>Frt</i> Δ <i>araBC</i> :: <i>Frt</i> Δ <i>hfq</i> :: <i>Frt</i> <i>Frt-kan-Frt-araC-araB</i> <i>pgaA</i> -3xFlag (tl.) Δ <i>pgaBCD</i> :: <i>cat</i>	translational <i>araB-pgaA</i> fusion, <i>kan-araC-P_{ara}</i> amplified from TB55	This work

Additional Table 1

Name	Relevant genotype	Description/comments	Source/reference
AB1782	<i>csrA::Tn5Δ(kan)::Frt pgaD-3xFlag-kan ΔclpP::cat</i>	$\Delta clpP::cat$ construct from ' <i>clpP::cat</i> ' (Hallez <i>et al</i> , 2010)	This work
AB1783	<i>csrA::Tn5Δ(kan)::Frt ΔydeH::Frt pgaD-3xFlag-kan ΔclpP::cat</i>	$\Delta clpP::cat$ construct from ' <i>clpP::cat</i> ' (Hallez <i>et al</i> , 2010)	This work
AB1787	<i>sfhC zad220::Tn10</i>	construct from UJ646	This work
AB1799	<i>csrA::Tn5Δ(kan)::Frt Frt-araC-araBfgaA</i> (tl.) <i>pgaD-3xFlag-Frt ΔaraBC::Frt ΔclpP::cat</i>	translational <i>araB-pgaA</i> fusion, <i>kan-araC-P_{ara}</i> amplified from TB55, $\Delta clpP::cat$ construct from ' <i>clpP::cat</i> ' (Hallez <i>et al</i> , 2010)	This work
AB1800	<i>csrA::Tn5Δ(kan)::Frt Frt-araC-araBfgaA</i> (tl.) <i>pgaD-3xFlag-Frt ΔaraBC::Frt ΔydeH::Frt ΔclpP::cat</i>	translational <i>araB-pgaA</i> fusion, <i>kan-araC-P_{ara}</i> amplified from TB55, $\Delta clpP::cat$ construct from ' <i>clpP::cat</i> ' (Hallez <i>et al</i> , 2010)	This work
AB1801	<i>csrA::Tn5Δ(kan)::Frt Frt-araC-araBfgaA</i> (tl.) <i>pgaD-3xFlag-Frt ΔaraBC::Frt Δlon::tet</i>	translational <i>araB-pgaA</i> fusion, <i>kan-araC-P_{ara}</i> amplified from TB55, $\Delta lon::tet$ construct from ' <i>lon::tet</i> ' (Hallez <i>et al</i> , 2010)	This work
AB1802	<i>csrA::Tn5Δ(kan)::Frt Frt-araC-araBfgaA</i> (tl.) <i>pgaD-3xFlag-Frt ΔaraBC::Frt ΔydeH::Frt Δlon::tet</i>	translational <i>araB-pgaA</i> fusion, <i>kan-araC-P_{ara}</i> amplified from TB55, $\Delta lon::tet$ construct from ' <i>lon::tet</i> ' (Hallez <i>et al</i> , 2010)	This work
AB1813	<i>sfhC zad220::Tn10 ΔftsH3::kan</i>	constructs from UJ646	This work
AB1815	$\Delta clpP::cat$	$\Delta clpP::cat$ construct from ' <i>clpP::cat</i> ' (Hallez <i>et al</i> , 2010)	This work
AB1816	$\Delta lon::tet$	$\Delta lon::tet$ construct from ' <i>lon::tet</i> ' (Hallez <i>et al</i> , 2010)	This work
AB1879	<i>sfhC zad220::Tn10 ΔftsH3::kan csrA::Tn5Δ(kan)::Frt</i>	<i>sfhC zad220::Tn10</i> and $\Delta ftsH3::kan$ constructs from UJ646	This work
AB1887	<i>sfhC zad220::Tn10 ΔftsH3::kan csrA::Tn5Δ(kan)::Frt ΔydeH::Frt</i>	<i>sfhC zad220::Tn10</i> and $\Delta ftsH3::kan$ constructs from UJ646	This work
AB1888	<i>sfhC zad220::Tn10 pgaD-3xFlag-Frt ΔydeH::Frt csrA::Tn5Δ(kan)::Frt</i>	<i>sfhC zad220::Tn10</i> construct from UJ646	This work
AB1889	<i>sfhC zad220::Tn10 pgaD-3xFlag-Frt ΔydeH::Frt ΔftsH3::kan csrA::Tn5Δ(kan)::Frt</i>	<i>sfhC zad220::Tn10</i> and $\Delta ftsH3::kan$ constructs from UJ646	This work
AB1896	<i>sfhC zad220::Tn10 pgaD-3xFlag-Frt csrA::Tn5Δ(kan)::Frt ydeH-Flag-cat</i>	<i>sfhC zad220::Tn10</i> construct from UJ646	This work
AB1897	<i>sfhC zad220::Tn10 pgaD-3xFlag-Frt ΔftsH3::kan csrA::Tn5Δ(kan)::Frt ydeH-Flag-cat</i>	<i>sfhC zad220::Tn10</i> and $\Delta ftsH3::kan$ constructs from UJ646	This work
AB2022	<i>csrA::Tn5Δ(kan)::Frt ΔydeH::Frt ΔyegE::Frt ΔycdT::Frt ΔyfiN::Frt ΔyhjK::Frt ΔydaM::Frt ΔyneF::Frt pgaB-3xFlag ΔpgaCD::kan</i>	c-di-GMP ^{low} $\Delta 7$ mutant	(Steiner <i>et al</i> , in prep)
AB2043	<i>csrA::Tn5Δ(kan)::Frt ΔydeH::Frt ΔyegE::Frt ΔycdT::Frt ΔyfiN::Frt ΔyhjK::Frt ΔydaM::Frt ΔyneF::Frt ΔpgaABCD::Frt ΔaraBC::Frt</i>	strain used for overexpressions (c-di-GMP binding assays), c-di-GMP ^{low} $\Delta 7$ mutant	(Steiner <i>et al</i> , in prep)
AB2134	<i>csrA::Tn5Δ(kan)::Frt ΔydeH::Frt ΔyegE::Frt ΔycdT::Frt ΔyfiN::Frt ΔyhjK::Frt ΔydaM::Frt ΔyneF::Frt ΔpgaD::kan</i>	c-di-GMP ^{low} $\Delta 7$ mutant	(Steiner <i>et al</i> , in prep)
AB2135	<i>csrA::Tn5Δ(kan)::Frt ΔpgaD::kan</i>		(Steiner <i>et al</i> , in prep)
AB2151	<i>csrA::Tn5Δ(kan)::Frt ΔydeH::Frt ΔyegE::Frt ΔycdT::Frt ΔyfiN::Frt ΔyhjK::Frt ΔydaM::Frt ΔyneF::Frt ΔpgaD::kan Δlon::tet</i>	$\Delta lon::tet$ construct from ' <i>lon::tet</i> ' (Hallez <i>et al</i> , 2010), c-di-GMP ^{low} $\Delta 7$ mutant	This work
AB2152	<i>csrA::Tn5Δ(kan)::Frt ΔydeH::Frt ΔyegE::Frt ΔycdT::Frt ΔyfiN::Frt ΔyhjK::Frt ΔydaM::Frt ΔyneF::Frt ΔpgaD::kan Δlon ΔclpP::cat</i>	$\Delta lon \Delta clpP::cat$ construct from ' <i>lon clpP::cat</i> ' (Hallez <i>et al</i> , 2010), c-di-GMP ^{low} $\Delta 7$ mutant	This work
AB2153	<i>csrA::Tn5Δ(kan)::Frt ΔpgaD::kan Δlon::tet</i>	$\Delta lon::tet$ construct from ' <i>lon::tet</i> ' (Hallez <i>et al</i> , 2010)	This work

Additional Table 1

Name	Relevant genotype	Description/comments	Source/reference
AB2154	<i>csrA::Tn5Δ(kan)::Frt ΔpgaD::kan Δlon ΔclpP::cat</i>	<i>Δlon ΔclpP::cat</i> construct from ' <i>Δlon clpP::cat</i> ' (Hallez <i>et al</i> , 2010)	This work
AB2155	<i>csrA::Tn5Δ(kan)::Frt ΔydeH::Frt ΔyegE::Frt ΔycdT::Frt ΔyfiN::Frt ΔyhjK::Frt ΔydaM::Frt ΔyneF::Frt ΔpgaD::kan ΔclpP::cat</i>	<i>ΔclpP::cat</i> construct from ' <i>clpP::cat</i> ' (Hallez <i>et al</i> , 2010), c-di-GMP ^{low} $\Delta 7$ mutant	This work
AB2156	<i>csrA::Tn5Δ(kan)::Frt ΔpgaD::kan ΔclpP::cat</i>	<i>ΔclpP::cat</i> construct from ' <i>clpP::cat</i> ' (Hallez <i>et al</i> , 2010)	This work
AB2187	<i>csrA::Tn5Δ(kan)::Frt ΔydeH::Frt ΔpgaD::Frt ΔclpP::cat</i>	<i>ΔclpP::cat</i> construct from ' <i>clpP::cat</i> ' (Hallez <i>et al</i> , 2010)	This work
AB2188	<i>csrA::Tn5Δ(kan)::Frt pgaB-3xFlag ΔpgaCD::kan ΔclpP::cat</i>	<i>ΔclpP::cat</i> construct from ' <i>clpP::cat</i> ' (Hallez <i>et al</i> , 2010)	This work
AB2189	<i>csrA::Tn5Δ(kan)::Frt ΔydeH::Frt ΔyegE::Frt ΔycdT::Frt ΔyfiN::Frt ΔyhjK::Frt ΔydaM::Frt ΔyneF::Frt pgaB-3xFlag ΔpgaCD::kan ΔclpP::cat</i>	<i>ΔclpP::cat</i> construct from ' <i>clpP::cat</i> ' (Hallez <i>et al</i> , 2010), c-di-GMP ^{low} $\Delta 7$ mutant	This work
TB55	DY329 P _{minC} <>(kan-araC-P _{ara})	used for amplification of <i>kan-araC-P_{ara}</i> to construct translational <i>araB</i> fusions	(Bernhardt & de Boer, 2004)
UJ646	W3110 <i>sfhC zad220::Tn10 ΔftsH3::kan</i>		(Tatsuta <i>et al</i> , 1998)
DH5 α	(F-) F' <i>endA1 hsdR17</i> (rK-mK plus) <i>glnV44 thi1 recA1 gyr Δ(Nal^R) relA1 Δ(lacZYA-argF)U169 deoR</i> ($\Phi 80d/lac \Delta(lacZ)$ M15)	used for general cloning purposes	(Woodcock <i>et al</i> , 1989)

Plasmids

Name	Relevant genotype	Description/comments	Source/reference
pKD3	Amp ^R Cm ^R	Frt-flanked Cm ^R gene, for chromosomal gene disruptions	(Datsenko & Wanner, 2000)
pKD4	Amp ^R Km ^R	Frt-flanked Km ^R gene, for chromosomal gene disruptions	(Datsenko & Wanner, 2000)
pKD46	λ RED ⁺ Amp ^R	arabinose-inducible expression of λ RED system	(Datsenko & Wanner, 2000)
pCP20	FLP ⁺ Amp ^R Cm ^R	temperature-sensitive replication and thermal induction of FLP synthesis	(Cherepanov & Wackernagel, 1995)
pSUB11	3xFlag Km ^R	3xFlag-tagging of chromosomal genes	(Uzzau <i>et al</i> , 2001)
pSU313	Flag Cm ^R	Flag-tagging of chromosomal genes	(Uzzau <i>et al</i> , 2001)
pBAD18	<i>araC⁺ bla⁺ ParaBAD</i> (Amp ^R)	arabinose-inducible expression vector	(Guzman <i>et al</i> , 1995)
p1a	pBAD18:: <i>pgaA</i>	insert not fully sequenced, complements Δ <i>pgaA</i>	This work
p2a	pBAD18:: <i>pgaA-3xF</i>	<i>pgaA-3xF</i> amplified from AB1417, insert not fully sequenced, complements Δ <i>pgaA</i>	This work
p6a	pBAD18:: <i>pgaC-3xF</i>		(Steiner <i>et al</i> , in prep)
pins1	pBAD18:: <i>pgaD-3xF</i>		(Steiner <i>et al</i> , in prep)
p2-3xF	pBAD18:: <i>pgaC-3xF pgaD-3xF</i>		(Steiner <i>et al</i> , in prep)

3.3.3 Materials and methods

Only additional Materials and methods are described in detail here. See chapters 3.1 and 3.2 for more information.

Strains, plasmids, growth conditions and genetic constructions

Strains and plasmids used for Additional results are listed in Additional Table 1. Chromosomal *ydeH*-Flag construct was generated with the help of pSU313 (Uzzau *et al*, 2001). All Δ *ftsH* mutants were constructed by the successive P1 transduction (Miller, 1972) of the Tn10-linked *sfhC21* suppressor allele and the Δ *ftsH* deletion from UJ646 (Tatsuta *et al*, 1998). Hypersensitivity to rifampicin (inability to form colonies in the presence of 1 μ g/ml rifampicin at 30°C) was used to screen for the successful co-transduction of the Tn10 marker and the *sfhC21* allele (Ogura *et al*, 1999). pBAD18 derivatives were generated by ligation of PCR products between the *NheI* and *KpnI* sites.

c-di-GMP binding site probed by mass spectrometry

UV light-induced crosslinking was performed with crude membranes from strain AB1638 harboring p2-3xF as described in chapter 3.2. For tracing c-di-GMP-modified peptides, the crosslinking approach was scaled up to 30 25 μ l samples (plus experiment and competition control in triplicates as a control). 1 μ M radiolabeled [³²P]c-di-GMP was used for crosslinking. After the anti-Flag M2 magnetic beads (Sigma) were washed several times with IP Wash Buffer B (50 mM Tris HCl pH 7.5, 1 M NaCl, 5% glycerol, 0.1% DDM), the beads were pooled, split in 5 equal aliquots and all supernatants were completely aspirated with a Hamilton syringe. Immunoprecipitated proteins were eluted with 150 μ l Elution Buffer (0.1 M glycine HCl pH 3.5, 0.1% DDM) for 7 min at 25°C with gentle shaking. Beads were pelleted and supernatants were added to 15 μ l Take Up Buffer (1 M Tris HCl pH 8, 1.5 M NaCl, 10 mM CaCl₂, 1% DDM). The combined eluates were digested with 0.5 μ g endoproteinase Lys-C (Wako Chemicals, Germany) for 2 h at 37°C, then with 0.5 μ g trypsin (Modified, Sequencing Grade, Promega, USA) for 2 h at 37°C and finally with another 0.5 μ g trypsin overnight at 37°C with gentle shaking. Digestion was stopped by the addition of 1% TFA. The digest was injected onto a C18 ZORBAX SB-C18 column (0.5 x 150 mm) and bound peptides were eluted at 25 μ l/min with a gradient of 0.1% TFA (solvent A) and 80% acetonitrile/0.09% TFA (solvent B). The gradient was as follows: 0 min 2% B, 10 min 2% B, 70 min 75% B, 80 min 75% B. Eluting peptides were recorded at 214 nm and 15 μ l fractions were collected. To locate [³²P]c-di-GMP-labeled peptides, 5 μ l per fraction were spotted onto a

silica gel plate (Merck, Germany) and analyzed by autoradiography. The fraction with the highest radioactivity was dried in a speed vac, dissolved in 50 μ l 0.1% TFA and analyzed by capillary liquid chromatography tandem MS (LC/MS/MS) using a setup of a ProteoCol trap C-18 column (0.15 x 10 mm, 3 μ m particle size, 300 \AA) (SGE Analytical Science, Australia) and a separating column (0.1 mm x 10 cm) that had been packed with Magic 300 \AA C18 reverse phase material (5 μ m particle size, Swiss Bioanalytics, Switzerland). The columns were connected on line to an Orbitrap FT hybrid instrument (Thermo Finnigan, USA). The solvents used for peptide separation were 0.1% acetic acid in water (solvent A) and 0.1% acetic acid and 80% acetonitrile in water (solvent B). Peptides were injected via a 2 μ l loop onto the trap column with the capillary pump of an Agilent 1200 system set to 4 μ l/min. After 15 min, the trap column was switched into the flow path of the separating column. A linear gradient from 2 to 35% solvent B in solvent A in 60 min was delivered with an Agilent 1200 nano pump at a flow rate of 300 nl/min. After 60 min the percentage of solvent B was increased to 60% in ten minutes and further increased to 80% within 2 min. The eluting peptides were ionized at 1.7 kV. The mass spectrometer was operated in a data-dependent fashion. The precursor scan was done in the Orbitrap set to 60'000 resolution, while the fragment ions were mass analyzed in the LTQ instrument. A top five method was run so that the five most intense precursors were selected for fragmentation. The MS/MS spectra were then searched against an *E. coli* database using Mascot software (Perkins *et al*, 1999). The results were filtered with Proteome Discoverer version 1.2.0.208 by setting the precursor ion tolerance to 10 ppm, while the fragment ion tolerance was set to 0.8 Da. The false-discovery-rate was set to 0.01. Spectra were manually screened for precursor ions that liberated c-di-GMP-specific fragment ions (Simm *et al*, 2004).

C O N C L U S I O N S &
P E R S P E C T I V E S

4 Conclusions & perspectives

The first part of this work investigated the signalling events that trigger poly-GlcNAc-dependent biofilm formation in response to impaired ribosomal function that is e.g. caused by the action of subinhibitory concentrations of translation inhibitors. The presented data support a model in which in response to the partial inhibition of ribosome functioning, a SpoT-mediated reduction of ppGpp levels leads to the upregulation of Pga machinery components and increased poly-GlcNAc production. In addition, the second messenger c-di-GMP was identified as a post-transcriptional modulator of poly-GlcNAc-dependent biofilm formation. It appeared that a maximal poly-GlcNAc expression depends on the exact ratio between ppGpp and c-di-GMP. For the future, it would be of interest to investigate by which mechanisms impaired ribosome performance is signaled to SpoT. Does SpoT associate with the ribosome? Which parameters of ribosome function are measured? Additionally, the physiological role and the molecular details underlying the negative regulation of PgaA protein levels by ppGpp remain to be elucidated. Is the effect mediated by a sRNA as suggested in chapter 3.3? How does an enhanced PgaA level influence poly-GlcNAc secretion? Are there other reasons besides the elevated PgaA level for the high biofilm formed by a ppGpp⁰ mutant? And finally, how is the effect of ppGpp integrated with the c-di-GMP-mediated allosteric activation of the PgaCD complex to produce a secretion-compatible Pga machinery?

In the second and main part of this thesis, the PgaCD complex was identified as a novel type c-di-GMP receptor, in which two proteins have to tightly interact for specific ligand binding. As discussed in chapter 3.2, c-di-GMP-mediated allosteric activation of GT complexes involved in EPS biogenesis seems to be a general phenomenon. In this case however, none of the previously described and characterized c-di-GMP binding domains and/or motifs are associated with the Pga machinery. Gain-of-function, loss-of-function and truncated alleles that were analyzed in this study proposed that c-di-GMP interacts with the PgaCD complex in the vicinity of the cytoplasmic membrane. Arginine 222 of PgaC was suggested to be involved in the coordination of c-di-GMP. Clearly, the localization and characterization of the ligand binding site within the PgaCD complex, which is presumably formed by amino acid residues of both complex subunits, remains an important issue to be addressed in the future. So far, attempts to probe the c-di-GMP binding site by mass spectrometry were very promising, but yet unsuccessful. The approach that was performed to find the [³²P]c-di-GMP-modified peptide following UV light-induced crosslinking and some ideas on how to improve these experiments were shortly discussed in chapter 3.3. It is however questionable if such data would be very conclusive in the absence of any structural information about the PgaCD complex. Therefore, a crystal structure of the complex with c-di-

GMP bound seems to be inevitable for a better understanding of the nature of the ligand binding pocket.

Besides the characterization of the c-di-GMP binding site, further biochemical and structural analysis is also needed to unravel the exact structural and functional role of PgaD. The model that was proposed in chapter 3.2, in which the integration of the two transmembrane helices of PgaD into the core of transmembrane helices formed by PgaC triggers the opening of a poly-GlcNAc translocation pore upon c-di-GMP binding, may be further substantiated by e.g. performing chemical cysteine crosslinking experiments to map specific interactions between transmembrane helices (Chen *et al*, 2006; Moore & Fillingame, 2008). In addition, the postulated c-di-GMP-mediated pore formation may be directly monitored by studying the release of a dye from PgaCD-containing liposomes (Medina *et al*, 2012).

Based on the observations that PgaD is essential for poly-GlcNAc production both *in vivo* and *in vitro* and that the instability of PgaD under low cellular c-di-GMP conditions seems not to be the cause of Pga machinery control, but rather a consequence thereof, a role for PgaD in shutting-off the Pga machinery in response to a sudden drop in c-di-GMP levels and in temporarily uncoupling the Pga machinery from c-di-GMP signalling was suggested in chapter 3.2. Together with the fact that the expression of the *pga* operon and *ydeH*, which encodes the major DGC that stimulates poly-GlcNAc production, is coupled via CsrA, the instability of PgaD may represent a novel model for the molecular basis of specificity of c-di-GMP signalling systems. Once a cell is devoid of PgaD in the absence of a Csr cascade input signal, c-di-GMP produced by other unrelated DGCs cannot affect poly-GlcNAc production. Whether this scenario indeed holds true or can at least be simulated *in vivo* has to be carefully addressed in the future.

B I B L I O G R A P H Y

5 Bibliography

- Abu Khweek A, Fetherston JD & Perry RD (2010) Analysis of HmsH and its role in plague biofilm formation. *Microbiology* **156**: 1424-1438
- Akiyama Y (2009) Quality control of cytoplasmic membrane proteins in Escherichia coli. *J Biochem* **146**: 449-454
- Amikam D & Galperin MY (2006) PilZ domain is part of the bacterial c-di-GMP binding protein. *Bioinformatics* **22**: 3-6
- Babitzke P & Romeo T (2007) CsrB sRNA family: sequestration of RNA-binding regulatory proteins. *Curr Opin Microbiol* **10**: 156-163
- Baker CS, Eöry LA, Yakhnin H, Mercante J, Romeo T & Babitzke P (2007) CsrA inhibits translation initiation of Escherichia coli hfq by binding to a single site overlapping the Shine-Dalgarno sequence. *J Bacteriol* **189**: 5472-5481
- Becker S, Soares C & Porto LM (2009) Computational analysis suggests that virulence of Chromobacterium violaceum might be linked to biofilm formation and poly-NAG biosynthesis. *Genet Mol Biol* **32**: 640-644
- Beloin C, Roux A & Ghigo J-M (2008) Escherichia coli biofilms. *Curr Top Microbiol Immunol* **322**: 249-289
- Benach J, Swaminathan SS, Tamayo R, Handelman SK, Folta-Stogniew E, Ramos JE, Forouhar F, Neely H, Seetharaman J, Camilli A & Hunt JF (2007) The structural basis of cyclic diguanylate signal transduction by PilZ domains. *EMBO J* **26**: 5153-5166
- Bentancor LV, O'Malley JM, Bozkurt-Guzel C, Pier GB & Maira-Litrán T (2012) Poly-N-acetyl-beta-(1-6)-glucosamine is a target for protective immunity against Acinetobacter baumannii infections. *Infect Immun* **80**: 651-656
- Bernhardt TG & de Boer PAJ (2004) Screening for synthetic lethal mutants in Escherichia coli and identification of EnvC (YibP) as a periplasmic septal ring factor with murein hydrolase activity. *Mol Microbiol* **52**: 1255-1269
- Beyhan S, Bilecen K, Salama SR, Casper-Lindley C & Yildiz FH (2007) Regulation of rugosity and biofilm formation in Vibrio cholerae: comparison of VpsT and VpsR regulons and epistasis analysis of vpsT, vpsR, and hapR. *J Bacteriol* **189**: 388-402
- Blattner FR, Plunkett IG, Bloch CA, Perna NT, Burland V, Riley M, Collado-Vides J, Glasner JD, Rode CK, Mayhew GF, Gregor J, Davis NW, Kirkpatrick HA, Goeden MA, Rose DJ, Mau B & Shao Y (1997) The complete genome sequence of Escherichia coli K-12. *Science* **277**: 1453-1462
- Bobrov AG, Kirillina O & Perry RD (2005) The phosphodiesterase activity of the HmsP EAL domain is required for negative regulation of biofilm formation in Yersinia pestis. *FEMS Microbiol Lett* **247**: 123-130
- Bobrov AG, Kirillina O, Forman S, Mack D & Perry RD (2008) Insights into Yersinia pestis biofilm development: topology and co-interaction of Hms inner membrane proteins involved in exopolysaccharide production. *Environ Microbiol* **10**: 1419-1432
- Bobrov AG, Kirillina O, Ryjenkov DA, Waters CM, Price PA, Fetherston JD, Mack D, Goldman WE, Gomelsky M & Perry RD (2011) Systematic analysis of cyclic di-GMP signalling enzymes and their role in biofilm formation and virulence in Yersinia pestis. *Mol Microbiol* **79**: 533-551
- Boehm A, Kaiser M, Li H, Spangler C, Kasper CA, Ackermann M, Kaefer V, Sourjik V, Roth V & Jenal U (2010) Second messenger-mediated adjustment of bacterial swimming velocity. *Cell* **141**: 107-116
- Boehm A, Steiner S, Zaehring F, Casanova A, Hamburger F, Ritz D, Keck W, Ackermann M, Schirmer T & Jenal U (2009) Second messenger signalling governs Escherichia coli biofilm induction upon ribosomal stress. *Mol Microbiol* **72**: 1500-1516
- Bouvier M, Sharma CM, Mika F, Nierhaus KH & Vogel J (2008) Small RNA binding to 5' mRNA coding region inhibits translational initiation. *Mol Cell* **32**: 827-837

- Branda SS, Vik A, Friedman L & Kolter R (2005) Biofilms: the matrix revisited. *Trends Microbiol* **13**: 20-26
- Burdette DL, Monroe KM, Sotelo-Troha K, Iwig JS, Eckert B, Hyodo M, Hayakawa Y & Vance RE (2011) STING is a direct innate immune sensor of cyclic di-GMP. *Nature* **478**: 515-519
- Cerca N, Maira-Litrán T, Jefferson KK, Grout M, Goldmann DA & Pier GB (2007) Protection against *Escherichia coli* infection by antibody to the *Staphylococcus aureus* poly-N-acetylglucosamine surface polysaccharide. *Proc Natl Acad Sci USA* **104**: 7528-7533
- Chan C, Paul R, Samoray D, Amiot NC, Giese B, Jenal U & Schirmer T (2004) Structural basis of activity and allosteric control of diguanylate cyclase. *Proc Natl Acad Sci USA* **101**: 17084-17089
- Chatterji D, Fujita N & Ishihama A (1998) The mediator for stringent control, ppGpp, binds to the beta-subunit of *Escherichia coli* RNA polymerase. *Genes Cells* **3**: 279-287
- Chavez RG, Alvarez AF, Romeo T & Georgellis D (2010) The physiological stimulus for the BarA sensor kinase. *J Bacteriol* **192**: 2009-2012
- Chen Z, Akin BL, Stokes DL & Jones LR (2006) Cross-linking of C-terminal residues of phospholamban to the Ca²⁺ pump of cardiac sarcoplasmic reticulum to probe spatial and functional interactions within the transmembrane domain. *J Biol Chem* **281**: 14163-14172
- Cheng N, Merrill JBM, Painter GR, Frick LW & Furman PA (1993) Identification of the nucleotide binding site of HIV-1 reverse transcriptase using dTTP as a photoaffinity label. *Biochemistry* **32**: 7630-7634
- Cherepanov PP & Wackernagel W (1995) Gene disruption in *Escherichia coli*: TcR and KmR cassettes with the option of Flp-catalyzed excision of the antibiotic-resistance determinant. *Gene* **158**: 9-14
- Chin K-H, Lee Y-C, Tu Z-L, Chen C-H, Tseng Y-H, Yang J-M, Ryan RP, McCarthy Y, Dow JM, Wang AH-J & Chou S-H (2010) The cAMP receptor-like protein CLP is a novel c-di-GMP receptor linking cell-cell signaling to virulence gene expression in *Xanthomonas campestris*. *J Mol Biol* **396**: 646-662
- Choi AHK, Slamti L, Avci FY, Pier GB & Maira-Litrán T (2009) The pgaABCD locus of *Acinetobacter baumannii* encodes the production of poly-beta-1-6-N-acetylglucosamine, which is critical for biofilm formation. *J Bacteriol* **191**: 5953-5963
- Christen B, Christen M, Paul R, Schmid F, Folcher M, Jenoe P, Meuwly M & Jenal U (2006) Allosteric control of cyclic di-GMP signaling. *J Biol Chem* **281**: 32015-32024
- Christen M, Christen B, Allan MG, Folcher M, Jenö P, Grzesiek S & Jenal U (2007) DgrA is a member of a new family of cyclic diguanosine monophosphate receptors and controls flagellar motor function in *Caulobacter crescentus*. *Proc Natl Acad Sci USA* **104**: 4112-4117
- Christen M, Christen B, Folcher M, Schauerte A & Jenal U (2005) Identification and characterization of a cyclic di-GMP-specific phosphodiesterase and its allosteric control by GTP. *J Biol Chem* **280**: 30829-30837
- Ciocchini AE, Roset MS, Briones G, Iñón de Iannino N & Ugalde RA (2006) Identification of active site residues of the inverting glycosyltransferase Cgs required for the synthesis of cyclic beta-1,2-glucan, a *Brucella abortus* virulence factor. *Glycobiology* **16**: 679-691
- Conover MS, Sloan GP, Love CF, Sukumar N & Deora R (2010) The Bps polysaccharide of *Bordetella pertussis* promotes colonization and biofilm formation in the nose by functioning as an adhesin. *Mol Microbiol* **77**: 1439-1455
- Costanzo A & Ades SE (2006) Growth phase-dependent regulation of the extracytoplasmic stress factor, sigmaE, by guanosine 3',5'-bispyrophosphate (ppGpp). *J Bacteriol* **188**: 4627-4634
- Dalebroux ZD & Swanson MS (2012) ppGpp: magic beyond RNA polymerase. *Nat Rev Microbiol* **10**: 203-212
- Datsenko KA & Wanner BL (2000) One-step inactivation of chromosomal genes in *Escherichia coli* K-12 using PCR products. *Proc Natl Acad Sci USA* **97**: 6640-6645

- Duerig A, Abel S, Folcher M, Nicollier M, Schwede T, Amiot N, Giese B & Jenal U (2009) Second messenger-mediated spatiotemporal control of protein degradation regulates bacterial cell cycle progression. *Genes Dev* **23**: 93-104
- Fang X & Gomelsky M (2010) A post-translational, c-di-GMP-dependent mechanism regulating flagellar motility. *Mol Microbiol* **76**: 1295-1305
- Fazli M, O'Connell A, Nilsson M, Niehaus K, Dow JM, Givskov M, Ryan RP & Tolker-Nielsen T (2011) The CRP/FNR family protein Bcam1349 is a c-di-GMP effector that regulates biofilm formation in the respiratory pathogen *Burkholderia cenocepacia*. *Mol Microbiol* **82**: 327-341
- Ferreira RBR, Chodur DM, Antunes LCM, Trimble MJ & McCarter LL (2012) Output targets and transcriptional regulation by a cyclic dimeric GMP-responsive circuit in the *Vibrio parahaemolyticus* Scr network. *J Bacteriol* **194**: 914-924
- Forman S, Bobrov AG, Kirillina O, Craig SK, Abney J, Fetherston JD & Perry RD (2006) Identification of critical amino acid residues in the plague biofilm Hms proteins. *Microbiology* **152**: 3399-3410
- Gerke C, Kraft A, Süßmuth R, Schweitzer O & Götz F (1998) Characterization of the N-acetylglucosaminyltransferase activity involved in the biosynthesis of the *Staphylococcus epidermidis* polysaccharide intercellular adhesin. *J Biol Chem* **273**: 18586-18593
- Goller C, Wang X, Itoh Y & Romeo T (2006) The cation-responsive protein NhaR of *Escherichia coli* activates *pgaABCD* transcription, required for production of the biofilm adhesin poly-beta-1,6-N-acetyl-D-glucosamine. *J Bacteriol* **188**: 8022-8032
- Gottesman S (1996) Proteases and their targets in *Escherichia coli*. *Annu Rev Genet* **30**: 465-506
- Gudapaty S, Suzuki K, Wang X, Babitzke P & Romeo T (2001) Regulatory interactions of Csr components: the RNA binding protein CsrA activates *csrB* transcription in *Escherichia coli*. *J Bacteriol* **183**: 6017-6027
- Guzman L-M, Belin D, Carson MJ & Beckwith J (1995) Tight regulation, modulation, and high-level expression by vectors containing the arabinose PBAD promoter. *J Bacteriol* **177**: 4121-4130
- Habazettl J, Allan MG, Jenal U & Grzesiek S (2011) Solution structure of the PilZ domain protein PA4608 complex with cyclic di-GMP identifies charge clustering as molecular readout. *J Biol Chem* **286**: 14304-14314
- Hallez R, Geeraerts D, Sterckx Y, Mine N, Loris R & Van Melderen L (2010) New toxins homologous to ParE belonging to three-component toxin-antitoxin systems in *Escherichia coli* O157:H7. *Mol Microbiol* **76**: 719-732
- He Y-W & Zhang L-H (2008) Quorum sensing and virulence regulation in *Xanthomonas campestris*. *FEMS Microbiol Rev* **32**: 842-857
- Heldermon C, DeAngelis PL & Weigel PH (2001) Topological organization of the hyaluronan synthase from *Streptococcus pyogenes*. *J Biol Chem* **276**: 2037-2046
- Hengge R (2009) Principles of c-di-GMP signalling in bacteria. *Nat Rev Microbiol* **7**: 263-273
- Hickman JW & Harwood CS (2008) Identification of FleQ from *Pseudomonas aeruginosa* as a c-di-GMP-responsive transcription factor. *Mol Microbiol* **69**: 376-389
- Hinnebusch BJ & Erickson DL (2008) *Yersinia pestis* biofilm in the flea vector and its role in the transmission of plague. *Curr Top Microbiol* **322**: 229-248
- Hinnebusch BJ, Perry RD & Schwan TG (1996) Role of the *Yersinia pestis* hemin storage (*hms*) locus in the transmission of plague by fleas. *Science* **273**: 367-370
- Hong SH, Hegde M, Kim J, Wang X, Jayaraman A & Wood TK (2012) Synthetic quorum-sensing circuit to control consortial biofilm formation and dispersal in a microfluidic device. *Nat Commun* **3**: 613-623
- Huang B, Whitchurch CB & Mattick JS (2003) FimX, a multidomain protein connecting environmental signals to twitching motility in *Pseudomonas aeruginosa*. *J Bacteriol* **185**: 7068-7076
- Ito K & Akiyama Y (2005) Cellular functions, mechanism of action, and regulation of FtsH protease. *Annu Rev Microbiol* **59**: 211-231

- Itoh Y, Rice JD, Goller C, Pannuri A, Taylor J, Meisner J, Beveridge TJ, Preston JF & Romeo T (2008) Roles of pgaABCD genes in synthesis, modification, and export of the Escherichia coli biofilm adhesin poly-beta-1,6-N-acetyl-D-glucosamine. *J Bacteriol* **190**: 3670-3680
- Izano E a, Sadovskaya I, Vinogradov E, Mulks MH, Velliyagounder K, Ragunath C, Kher WB, Ramasubbu N, Jabbouri S, Perry MB & Kaplan JB (2007) Poly-N-acetylglucosamine mediates biofilm formation and antibiotic resistance in Actinobacillus pleuropneumoniae. *Microb Pathog* **43**: 1-9
- Izano EA, Sadovskaya I, Wang H, Vinogradov E, Ragunath C, Ramasubbu N, Jabbouri S, Perry MB & Kaplan JB (2008) Poly-N-acetylglucosamine mediates biofilm formation and detergent resistance in Aggregatibacter actinomycetemcomitans. *Microb Pathog* **44**: 52-60
- Johansen J, Rasmussen AA, Overgaard M & Valentin-Hansen P (2006) Conserved small non-coding RNAs that belong to the sigmaE regulon: role in down-regulation of outer membrane proteins. *J Mol Biol* **364**: 1-8
- Jonas K, Edwards AN, Ahmad I, Romeo T, Römling U & Melefors O (2010) Complex regulatory network encompassing the Csr, c-di-GMP and motility systems of Salmonella Typhimurium. *Environ Microbiol* **12**: 524-540
- Jonas K, Edwards AN, Simm R, Romeo T, Römling U & Melefors O (2008) The RNA binding protein CsrA controls cyclic di-GMP metabolism by directly regulating the expression of GGDEF proteins. *Mol Microbiol* **70**: 236-257
- Kazmierczak BI, Lebron MB & Murray TS (2006) Analysis of FimX, a phosphodiesterase that governs twitching motility in Pseudomonas aeruginosa. *Mol Microbiol* **60**: 1026-1043
- Kirillina O, Fetherston JD, Bobrov AG, Abney J & Perry RD (2004) HmsP, a putative phosphodiesterase, and HmsT, a putative diguanylate cyclase, control Hms-dependent biofilm formation in Yersinia pestis. *Mol Microbiol* **54**: 75-88
- Kirstein J, Molière N, Dougan DA & Turgay K (2009) Adapting the machine: adaptor proteins for Hsp100/Clp and AAA+ proteases. *Nat Rev Microbiol* **7**: 589-599
- Ko J, Ryu K-S, Kim H, Shin J-S, Lee J-O, Cheong C & Choi B-S (2010) Structure of PP4397 reveals the molecular basis for different c-di-GMP binding modes by PilZ domain proteins. *J Mol Biol* **398**: 97-110
- Kotzyba-Hibert F, Kapfer I & Goeldner M (1995) Recent trends in photoaffinity labeling. *Angew Chem Int Edit* **34**: 1296-1312
- Krasteva PV, Fong JCN, Shikuma NJ, Beyhan S, Navarro MVAS, Yildiz FH & Sondermann H (2010) Vibrio cholerae VpsT regulates matrix production and motility by directly sensing cyclic di-GMP. *Science* **327**: 866-868
- Kulshina N, Baird NJ & Ferré-D'Amaré AR (2009) Recognition of the bacterial second messenger cyclic diguanylate by its cognate riboswitch. *Nat Struct Mol Biol* **16**: 1212-1217
- Lapouge K, Schubert M, Allain FH-T & Haas D (2008) Gac/Rsm signal transduction pathway of gamma-proteobacteria: from RNA recognition to regulation of social behaviour. *Mol Microbiol* **67**: 241-253
- Leduc JL & Roberts GP (2009) Cyclic di-GMP allosterically inhibits the CRP-like protein (Clp) of Xanthomonas axonopodis pv. citri. *J Bacteriol* **191**: 7121-7122
- Lee ER, Baker JL, Weinberg Z, Sudarsan N & Breaker RR (2010) An allosteric self-splicing ribozyme triggered by a bacterial second messenger. *Science* **329**: 845-848
- Lee VT, Matewish JM, Kessler JL, Hyodo M, Hayakawa Y & Lory S (2007) A cyclic-di-GMP receptor required for bacterial exopolysaccharide production. *Mol Microbiol* **65**: 1474-1484
- Leitner A, Sturm M & Lindner W (2011) Tools for analyzing the phosphoproteome and other phosphorylated biomolecules: a review. *Anal Chim Acta* **703**: 19-30
- Lewis CT, Seyer JM & Carlson GM (1992) Photochemical cross-linking of guanosine 5'-triphosphate to phosphoenolpyruvate carboxykinase (GTP). *Bioconjugate Chem* **3**: 160-166
- Li T-N, Chin K-H, Fung K-M, Yang M-T, Wang AH-J & Chou S-H (2011) A novel tetrameric PilZ domain structure from xanthomonads. *PLoS ONE* **6**: e22036

- Lim B, Beyhan S, Meir J & Yildiz FH (2006) Cyclic-diGMP signal transduction systems in *Vibrio cholerae*: modulation of rugosity and biofilm formation. *Mol Microbiol* **60**: 331-348
- Ma Q, Yang Z, Pu M, Peti W & Wood TK (2011) Engineering a novel c-di-GMP-binding protein for biofilm dispersal. *Environ Microbiol* **13**: 631-642
- Mack D, Fischer W, Krokotsch A, Leopold K, Hartmann R, Egge H & Laufs R (1996) The intercellular adhesin involved in biofilm accumulation of *Staphylococcus epidermidis* is a linear beta-1,6-linked glucosaminoglycan: purification and structural analysis. *J Bacteriol* **178**: 175-183
- Maira-Litrán T, Kropec A, Goldmann DA & Pier GB (2005) Comparative opsonic and protective activities of *Staphylococcus aureus* conjugate vaccines containing native or deacetylated *Staphylococcal* poly-N-acetyl-beta-(1-6)-glucosamine. *Infect Immun* **73**: 6752-6762
- Mattick JS (2002) Type IV pili and twitching motility. *Annu Rev Microbiol* **56**: 289-314
- Medina AP, Lin J & Weigel PH (2012) Hyaluronan synthase mediates dye translocation across liposomal membranes. *BMC Biochem* **13**:
- Meisenheimer KM & Koch TH (1997) Photocross-linking of nucleic acids to associated proteins. *Crit Rev Biochem Mol* **32**: 101-140
- Merighi M, Lee VT, Hyodo M, Hayakawa Y & Lory S (2007) The second messenger bis-(3'-5')-cyclic-GMP and its PilZ domain-containing receptor Alg44 are required for alginate biosynthesis in *Pseudomonas aeruginosa*. *Mol Microbiol* **65**: 876-895
- Miller JH (1972) Experiments in molecular genetics. Cold Spring Harbor Laboratory (Cold Spring Harbor, N.Y)
- Moore KJ & Fillingame RH (2008) Structural interactions between transmembrane helices 4 and 5 of subunit a and the subunit c ring of *Escherichia coli* ATP synthase. *J Biol Chem* **283**: 31726-31735
- Navarro MVAS, De N, Bae N, Wang Q & Sondermann H (2009) Structural analysis of the GGDEF-EAL domain-containing c-di-GMP receptor FimX. *Structure* **17**: 1104-1116
- Navarro MVAS, Newell PD, Krasteva PV, Chatterjee D, Madden DR, O'Toole GA & Sondermann H (2011) Structural basis for c-di-GMP-mediated inside-out signaling controlling periplasmic proteolysis. *PLoS Biol* **9**: e1000588
- Newell PD, Boyd CD, Sondermann H & O'Toole GA (2011) A c-di-GMP effector system controls cell adhesion by inside-out signaling and surface protein cleavage. *PLoS Biol* **9**: e1000587
- Newell PD, Monds RD & O'Toole GA (2009) LapD is a bis-(3',5')-cyclic dimeric GMP-binding protein that regulates surface attachment by *Pseudomonas fluorescens* Pf0 – 1. *Proc Natl Acad Sci USA* **106**: 3461-3466
- Oglesby LL, Jain S & Ohman DE (2008) Membrane topology and roles of *Pseudomonas aeruginosa* Alg8 and Alg44 in alginate polymerization. *Microbiology* **154**: 1605-1615
- Ogura T, Inoue K, Tatsuta T, Suzaki T, Karata K, Young K, Su LH, Fierke CA, Jackman JE, Raetz CR, Coleman J, Tomoyasu T & Matsuzawa H (1999) Balanced biosynthesis of major membrane components through regulated degradation of the committed enzyme of lipid A biosynthesis by the AAA protease FtsH (HflB) in *Escherichia coli*. *Mol Microbiol* **31**: 833-844
- O'Gara JP (2007) ica and beyond: biofilm mechanisms and regulation in *Staphylococcus epidermidis* and *Staphylococcus aureus*. *FEMS Microbiol Lett* **270**: 179-188
- Pannuri A, Yakhnin H, Vakulskas CA, Edwards AN, Babitzke P & Romeo T (2012) Translational repression of NhaR, a novel pathway for multi-tier regulation of biofilm circuitry by CsrA. *J Bacteriol* **194**: 79-89
- Parise G, Mishra M, Itoh Y, Romeo T & Deora R (2007) Role of a putative polysaccharide locus in *Bordetella* biofilm development. *J Bacteriol* **189**: 750-760
- Paul K, Nieto V, Carlquist WC, Blair DF & Harshey RM (2010) The c-di-GMP binding protein YcgR controls flagellar motor direction and speed to affect chemotaxis by a "backstop brake" mechanism. *Mol Cell* **38**: 128-139

- Paul R, Weiser S, Amiot NC, Chan C, Schirmer T, Giese B & Jenal U (2004) Cell cycle-dependent dynamic localization of a bacterial response regulator with a novel di-guanylate cyclase output domain. *Genes Dev* **18**: 715-727
- Perkins DN, Pappin DJC, Creasy DM & Cottrell JS (1999) Probability-based protein identification by searching sequence databases using mass spectrometry data. *Electrophoresis* **20**: 3551-3567
- Perry RD, Bobrov AG, Kirillina O, Jones HA, Pedersen L, Abney J & Fetherston JD (2004) Temperature regulation of the hemin storage (Hms+) phenotype of *Yersinia pestis* is posttranscriptional. *J Bacteriol* **186**: 1638-1647
- Petters T, Zhang X, Nesper J, Treuner-Lange A, Gomez-Santos N, Hoppert M, Jenal U & Søgaard-Andersen L (2012) The orphan histidine protein kinase SgmT is a c-di-GMP receptor and regulates composition of the extracellular matrix together with the orphan DNA binding response regulator DigR in *Myxococcus xanthus*. *Mol Microbiol* **84**: 147-165
- Pfeiffer V, Papenfort K, Lucchini S, Hinton JCD & Vogel J (2009) Coding sequence targeting by MicC RNA reveals bacterial mRNA silencing downstream of translational initiation. *Nat Struct Mol Biol* **16**: 840-846
- Potrykus K & Cashel M (2008) (p)ppGpp: still magical? *Annu Rev Microbiol* **62**: 35-51
- Pratt JT, Tamayo R, Tischler AD & Camilli A (2007) PilZ domain proteins bind cyclic diguanylate and regulate diverse processes in *Vibrio cholerae*. *J Biol Chem* **282**: 12860-12870
- Pérez-Mendoza D, Coulthurst SJ, Sanjuán J & Salmond GPC (2011) N-acetyl-glucosamine-dependent biofilm formation in *Pectobacterium atrosepticum* is cryptic and activated by elevated c-di-GMP levels. *Microbiology* **157**: 3340-3348
- Qi Y, Chuah MLC, Dong X, Xie K, Luo Z, Tang K & Liang Z-X (2011) Binding of cyclic diguanylate in the non-catalytic EAL domain of FimX induces a long-range conformational change. *J Biol Chem* **286**: 2910-2917
- Rahav-Manor O, Carmel O, Karpel R, Taglicht D, Glaser G, Schuldiner S & Padan E (1992) NhaR, a protein homologous to a family of bacterial regulatory proteins (LysR), regulates nhaA, the sodium proton antiporter gene in *Escherichia coli*. *J Biol Chem* **267**: 10433-10438
- Ramelot TA, Yee A, Cort JR, Semesi A, Arrowsmith CH & Kennedy MA (2007) NMR structure and binding studies confirm that PA4608 from *Pseudomonas aeruginosa* is a PilZ domain and a c-di-GMP binding protein. *Proteins* **66**: 266-271
- Richter FM, Hsiao H-H, Plessmann U & Urlaub H (2009) Enrichment of protein-RNA crosslinks from crude UV-irradiated mixtures for MS analysis by on-line chromatography using titanium dioxide columns. *Biopolymers* **91**: 297-309
- Robinette D, Neamati N, Tomer KB & Borchers CH (2006) Photoaffinity labeling combined with mass spectrometric approaches as a tool for structural proteomics. *Expert Rev Proteomic* **3**: 399-408
- Romeo T, Gong M, Liu MY & Brun-Zinkernagel A (1993) Identification and molecular characterization of *csrA*, a pleiotropic gene from *Escherichia coli* that affects glycogen biosynthesis, gluconeogenesis, cell size, and surface properties. *J Bacteriol* **175**: 4744-4755
- Ross P, Mayer R, Weinhouse H, Amikam D, Huggirat Y & Benziman M (1990) The cyclic diguanylic acid regulatory system of cellulose synthesis in *Acetobacter xylinum*. *J Biol Chem* **265**: 18933-18943
- Ross P, Weinhouse H, Aloni Y, Michaeli D, Weinberger-Ohana P, Mayer R, Braun S, Vroom E de, Van der Marel GA, Van Broom JH & Benziman M (1987) Regulation of cellulose synthesis in *Acetobacter xylinum* by cyclic diguanylic acid. *Nature* **325**: 279-281
- Ryan RP, Fouhy Y, Lucey JF, Crossman LC, Spiro S, He Y-W, Zhang L-H, Heeb S, Cámara M, Williams P & Dow JM (2006) Cell-cell signaling in *Xanthomonas campestris* involves an HD-GYP domain protein that functions in cyclic di-GMP turnover. *Proc Natl Acad Sci USA* **103**: 6712-6717
- Ryjenkov DA, Simm R, Römling U & Gomelsky M (2006) The PilZ domain is a receptor for the second messenger c-di-GMP: the PilZ domain protein YcgR controls motility in enterobacteria. *J Biol Chem* **281**: 30310-30314

- Saxena IM & Brown RM (1997) Identification of cellulose synthase(s) in higher plants: sequence analysis of processive beta-glycosyltransferases with the common motif "D, D, D35Q(R,Q)XRW". *Cellulose* **4**: 33-49
- Schirmer T & Jenal U (2009) Structural and mechanistic determinants of c-di-GMP signalling. *Nat Rev Microbiol* **7**: 724-735
- Shin J-S, Ryu K-S, Ko J, Lee A & Choi B-S (2011) Structural characterization reveals that a PilZ domain protein undergoes substantial conformational change upon binding to cyclic dimeric guanosine monophosphate. *Protein Sci* **20**: 270-277
- Shivanna BD, Mejillano MR, Williams TD & Himes RH (1993) Exchangeable GTP binding site of beta-tubulin. *J Biol Chem* **268**: 127-132
- Simm R, Morr M, Kader A, Nimtz M & Römling U (2004) GGDEF and EAL domains inversely regulate cyclic di-GMP levels and transition from sessility to motility. *Mol Microbiol* **53**: 1123-1134
- Skurnik D, Davis MRJ, Benedetti D, Moravec KL, Cywes-Bentley C, Roux D, Traficante DC, Walsh RL, Maria-Litràn T, Cassidy SK, Hermos CR, Martin TR, Thakkappalli EL, Vargas SO, McAdam AJ, Lieberman TD, Kishony R, LiPuma JJ, Pier GB, Goldberg JB, *et al* (2012) Targeting pan-resistant bacteria with antibodies to a broadly conserved surface polysaccharide expressed during infection. *J Infect Dis*
- Smith KD & Strobel SA (2011) Interactions of the c-di-GMP riboswitch with its second messenger ligand. *Biochem Soc Trans* **39**: 647-651
- Smith KD, Lipchock SV, Ames TD, Wang J, Breaker RR & Strobel SA (2009) Structural basis of ligand binding by a c-di-GMP riboswitch. *Nat Struct Mol Biol* **16**: 1218-1223
- Smith KD, Shanahan CA, Moore EL, Simon AC & Strobel SA (2011) Structural basis of differential ligand recognition by two classes of bis-(3'-5')-cyclic dimeric guanosine monophosphate-binding riboswitches. *Proc Natl Acad Sci USA* **108**: 7757-7762
- Srivastava D, Harris RC & Waters CM (2011) Integration of cyclic di-GMP and quorum sensing in the control of vpsT and aphA in *Vibrio cholerae*. *J Bacteriol* **193**: 6331-6341
- Steen H & Jensen ON (2002) Analysis of protein-nucleic acid interactions by photochemical cross-linking and mass spectrometry. *Mass Spectrom Rev* **21**: 163-182
- Storz G, Vogel J & Wassarman KM (2011) Regulation by small RNAs in bacteria: expanding frontiers. *Mol Cell* **43**: 880-891
- Sudarsan N, Lee ER, Weinberg Z, Moy RH, Kim JN, Link KH & Breaker RR (2008) Riboswitches in eubacteria sense the second messenger cyclic di-GMP. *Science* **321**: 411-413
- Sun Y-C, Koumoutsi A, Jarrett C, Lawrence K, Gherardini FC, Darby C & Hinnebusch BJ (2011) Differential control of *Yersinia pestis* biofilm formation in vitro and in the flea vector by two c-di-GMP diguanylate cyclases. *PLoS ONE* **6**: e19267
- Suzuki K, Babitzke P, Kushner SR & Romeo T (2006) Identification of a novel regulatory protein (CsrD) that targets the global regulatory RNAs CsrB and CsrC for degradation by RNase E. *Genes Dev* **20**: 2605-2617
- Suzuki K, Wang X, Weilbacher T, Pernestig A-K, Melefors Ö, Georgellis D, Babitzke P & Romeo T (2002) Regulatory circuitry of the CsrA/CsrB and BarA/UvrY systems of *Escherichia coli*. *J Bacteriol* **184**: 5130-5140
- Tagliabue L, Antoniani D, Maciag A, Bocci P, Raffaelli N & Landini P (2010) The diguanylate cyclase YddV controls production of the exopolysaccharide poly-N-acetylglucosamine (PNAG) through regulation of the PNAG biosynthetic pgaABCD operon. *Microbiology* **156**: 2901-2911
- Takeuchi K, Kiefer P, Reimann C, Keel C, Dubuis C, Rolli J, Vorholt JA & Haas D (2009) Small RNA-dependent expression of secondary metabolism is controlled by Krebs cycle function in *Pseudomonas fluorescens*. *J Biol Chem* **284**: 34976-34985
- Tao F, He Y-W, Wu D-H, Swarup S & Zhang L-H (2010) The cyclic nucleotide monophosphate domain of *Xanthomonas campestris* global regulator Clp defines a new class of cyclic di-GMP effectors. *J Bacteriol* **192**: 1020-1029

- Tatsuta T, Tomoyasu T, Bukau B, Kitagawa M, Mori H, Karata K & Ogura T (1998) Heat shock regulation in the ftsH null mutant of Escherichia coli: dissection of stability and activity control mechanisms of sigma32 in vivo. *Mol Microbiol* **30**: 583-593
- Thomason MK, Fontaine F, De Lay N & Storz G (2012) A small RNA that regulates motility and biofilm formation in response to changes in nutrient availability in Escherichia coli. *Mol Microbiol* **84**: 17-35
- Thompson KM, Rhodius VA & Gottesman S (2007) SigmaE regulates and is regulated by a small RNA in Escherichia coli. *J Bacteriol* **189**: 4243-4256
- Timmermans J & Van Melderen L (2010) Post-transcriptional global regulation by CsrA in bacteria. *Cell Mol Life Sci* **67**: 2897-2908
- Tuckerman JR, Gonzalez G & Gilles-Gonzalez M-A (2011) Cyclic di-GMP activation of polynucleotide phosphorylase signal-dependent RNA processing. *J Mol Biol* **407**: 633-639
- Tuckerman JR, Gonzalez G, Sousa EHS, Wan X, Saito JA, Alam M & Gilles-Gonzalez M-A (2009) An oxygen-sensing diguanylate cyclase and phosphodiesterase couple for c-di-GMP control. *Biochemistry* **48**: 9764-9774
- Udekwu KI & Wagner EGH (2007) Sigma E controls biogenesis of the antisense RNA MicA. *Nucleic Acids Res* **35**: 1279-1288
- Uzzau S, Figueroa-Bossi N, Rubino S & Bossi L (2001) Epitope tagging of chromosomal genes in Salmonella. *Proc Natl Acad Sci USA* **98**: 15264-15269
- Vogel J & Luisi BF (2011) Hfq and its constellation of RNA. *Nat Rev Microbiol* **9**: 578-589
- Vogel J & Papenfort K (2006) Small non-coding RNAs and the bacterial outer membrane. *Curr Opin Microbiol* **9**: 605-611
- Wang X, Dubey AK, Suzuki K, Baker CS, Babitzke P & Romeo T (2005) CsrA post-transcriptionally represses pgaABCD, responsible for synthesis of a biofilm polysaccharide adhesin of Escherichia coli. *Mol Microbiol* **56**: 1648-1663
- Wang X, Preston JF & Romeo T (2004) The pgaABCD locus of Escherichia coli promotes the synthesis of a polysaccharide adhesin required for biofilm formation. *J Bacteriol* **186**: 2724-2734
- Wassmann P, Chan C, Paul R, Beck A, Heerklotz H, Jenal U & Schirmer T (2007) Structure of BeF3--modified response regulator PleD: implications for diguanylate cyclase activation, catalysis, and feedback inhibition. *Structure* **15**: 915-927
- Weilbacher T, Suzuki K, Dubey AK, Wang X, Gudapaty S, Morozov I, Baker CS, Georgellis D, Babitzke P & Romeo T (2003) A novel sRNA component of the carbon storage regulatory system of Escherichia coli. *Mol Microbiol* **48**: 657-670
- Wilksch JJ, Yang J, Clements A, Gabbe JL, Short KR, Cao H, Cavaliere R, James CE, Whitchurch CB, Schembri MA, Chuah MLC, Liang Z-X, Wijburg OL, Jenney AW, Lithgow T & Strugnell RA (2011) MrkH, a novel c-di-GMP-dependent transcriptional activator, controls Klebsiella pneumoniae biofilm formation by regulating type 3 fimbriae expression. *PLoS Pathog* **7**: e1002204
- Woodcock DM, Crowther PJ, Doherty J, Jefferson S, DeCruz E, Noyer-Weidner N, Smith SS, Michael MZ & Graham MW (1989) Quantitative evaluation of Escherichia coli host strains for tolerance to cytosine methylation in plasmid and phage recombinants. *Nucleic Acids Res* **17**: 3469-3478
- Yakandawala N, Gawande PV, LoVetri K, Cardona ST, Romeo T, Nitz M & Madhyastha S (2011) Characterization of the poly-beta-1,6-N-acetylglucosamine polysaccharide component of Burkholderia biofilms. *Appl Environ Microbiol* **77**: 8303-8309
- Yu D, Ellis HM, Lee EC, Jenkins NA, Copeland NG & Court DL (2000) An efficient recombination system for chromosome engineering in Escherichia coli. *Proc Natl Acad Sci USA* **97**: 5978-5983
- Zhou G, Charbonneau H, Colman RF & Zalkin H (1993) Identification of sites for feedback regulation of glutamine 5-phosphoribosylpyrophosphate amidotransferase by nucleotides and relationship to residues important for catalysis. *J Biol Chem* **268**: 10471-10481

A P P E N D I X

6 Appendix

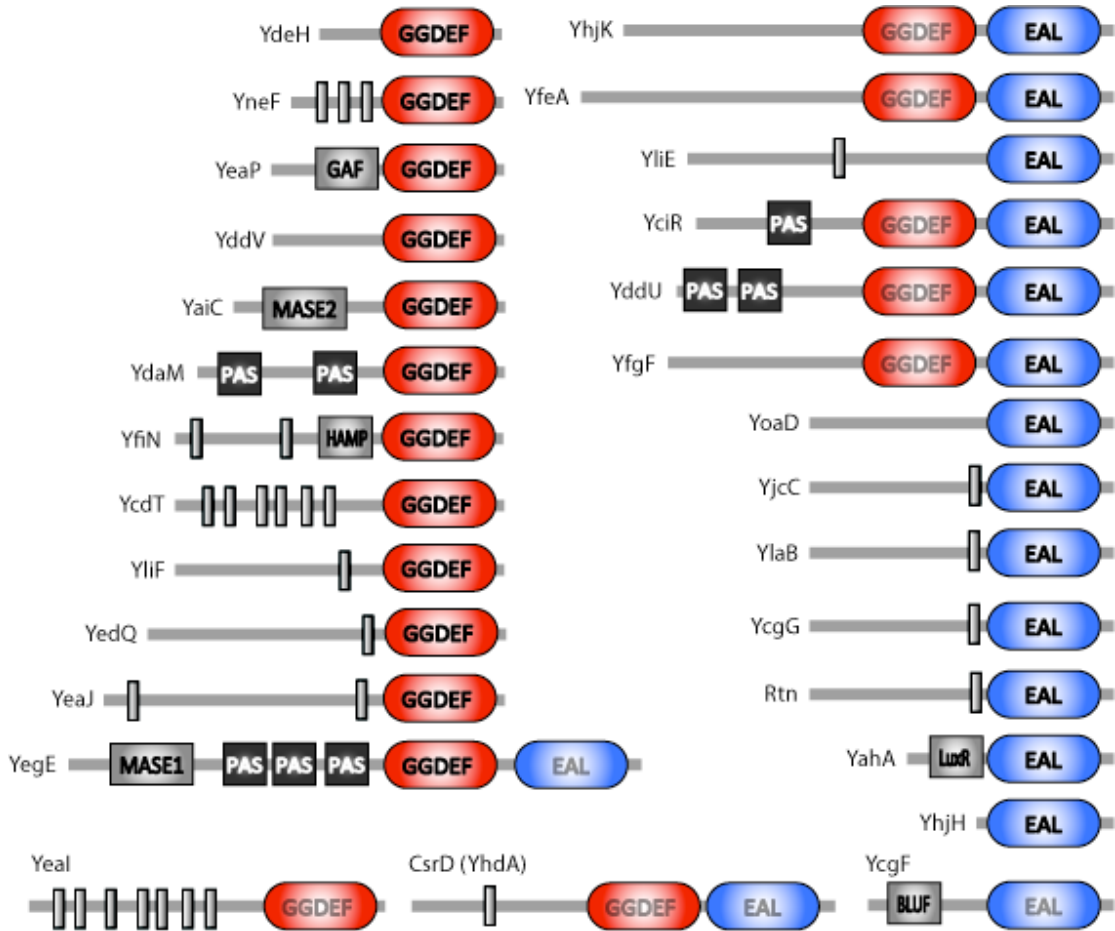


Figure 4: Schematic overview of the *E. coli* K-12 c-di-GMP signalling proteins. GGDEF and EAL written in grey letters indicates degenerate domains that presumably show no catalytic activity. Predicted transmembrane helices are shown as grey vertical bars. Figure by courtesy of A. Boehm.

A C K N O W L E D G E M E N T S

7 Acknowledgements

This work was carried out in the research group of Prof. Dr. Urs Jenal at the Biozentrum of the University of Basel, Switzerland.

I am grateful to my supervisor Prof. Dr. Urs Jenal for the opportunity to perform my PhD thesis in his lab on this very interesting, exciting and challenging topic, for the continuous support and for many fruitful scientific discussions.

I would also like to thank the members of my PhD committee, Prof. Dr. Dirk Bumann and Prof. Dr. Michael Hall for their scientific advice and constructive criticism at the yearly committee meetings.

I am especially thankful to Alex Boehm for supervising me during my Master thesis, for the continuous great support during the four years of my PhD (when he was still in Basel, but also afterwards) and for many inspiring scientific and non-scientific discussions.

Special thanks also go to Christian Lori for the excellent teamwork, for stimulating discussions and the fun we had during his time as a Master student under my supervision.

I am very grateful to Paul Jenö and Suzette Moes for their great help and contribution in the tricky MS project.

I furthermore thank Régis Hallez and Alain Casanova for their helpful and ingenious input and many science- and non-science-related discussions.

I would also like to thank all other former and current members of the Jenal group for the very nice and pleasant atmosphere in as well as outside the lab: Alberto, Anna, Annina, Benoît, Elli, Fabs, Imke, Isabelle, Jake, Jenny, Jutta, Kathrin, Lucie, Marc, Marco, Matthias, Micael, Raphy, Shogo, Sören, Svetlana, Tabitha, Tina, Ursula and Yaniv.

Thanks to all the people from the 4th floor for making it such a great place to work!

Last but not least, I would like to sincerely thank my family and friends for the continuous support and encouragement during the last years.

C U R R I C U L U M V I T A E

8 Curriculum vitae

Curriculum vitae

Personal Details

Name	Samuel Steiner
Address	Theodorsgraben 10 CH-4058 Basel Switzerland
Phone	+ 41 61 681 24 68
Mobile	+ 41 79 286 35 49
E-Mail	samuel.steiner@stud.unibas.ch
Date of birth	April 19 th , 1983
Hometown	Walterswil (BE), Switzerland
Nationality	Swiss

Education

Mar. 2008 - present	PhD thesis with Prof. Dr. Urs Jenal “Cyclic di-GMP-mediated regulation of the Pga exopolysaccharide secretion machinery in <i>Escherichia coli</i> ” Biozentrum, University of Basel, Switzerland
Sept. 2006 - Dec. 2007	Master of Science in Molecular Biology with Prof. Dr. Urs Jenal “Molecular mechanisms of <i>Escherichia coli</i> biofilm induction by translation inhibitors” Biozentrum, University of Basel, Switzerland
2003 - 2006	Bachelor of Science in Molecular Biology University of Basel, Switzerland
1999 - 2002	Matura Typ C Gymnasium Oberwil (BL), Switzerland

Working experience

Mar. 2008 - present	PhD thesis with Prof. Dr. Urs Jenal Biozentrum, University of Basel, Switzerland
---------------------	---

Teaching experience

2008 - 2011	Assistant in annual student course (Blockcourse Microbiology) 1 week/year; Biozentrum, University of Basel, Switzerland
-------------	--

Aug. 2010 - Jan. 2012 Supervision of Master student Christian Lori
Biozentrum, University of Basel, Switzerland

Presentations & Posters

- 2007 Annual Assembly of the SSM, Interlaken, Switzerland
Poster: "Role of c-di-GMP Signaling for *Escherichia coli* Biofilm Induction by Subinhibitory Concentrations of Translation Inhibitors"
- 2007 SWIMM, Villars-sur-Ollon, Switzerland
Poster: "Role of c-di-GMP Signaling for *Escherichia coli* Biofilm Induction by Subinhibitory Concentrations of Translation Inhibitors"
- 2008 Biozentrum Symposium, Basel, Switzerland
Poster: "Pas de deux: Two bacterial second messengers induce biofilm formation through antagonistic control of a surface adhesin"
- 2009 Annual Assembly of the SSM, Lausanne, Switzerland
Poster: "Two bacterial second messengers antagonistically control an *Escherichia coli* surface adhesin" (1st posterprize)
- 2009 Biozentrum PhD Retreat, Engelberg, Switzerland
Poster: "Two bacterial second messengers antagonistically control an *Escherichia coli* surface adhesin"
- 2010 Monod Minisymposium, Paris, France
Poster: "Two bacterial second messengers antagonistically control an *Escherichia coli* surface adhesin"
- 2010 Biozentrum PhD Retreat, Interlaken, Switzerland
Poster: "Second messenger-mediated control of an exopolysaccharide-secreting machinery in *Escherichia coli*"
- 2010 BacNet Conference, Sant Feliu de Guixols, Spain
Poster: "c-di-GMP-mediated control of an exopolysaccharide secretion machinery in *Escherichia coli*"
- 2011 Biozentrum Symposium, Basel, Switzerland
Poster: "c-di-GMP-mediated control of an exopolysaccharide secretion machinery in *Escherichia coli*"
- 2011 Mol Micro Meeting, Würzburg, Germany
Poster: "c-di-GMP-mediated control of an exopolysaccharide secretion machinery in *Escherichia coli*"

2011 Biozentrum PhD Retreat, Fribourg, Switzerland
Poster: "c-di-GMP-mediated control of an exopolysaccharide secretion machinery in *Escherichia coli*"

2011 FEMS Congress, Geneva, Switzerland
Poster: "c-di-GMP-mediated control of an exopolysaccharide secretion machinery in *Escherichia coli*"

2011 10 Years Infection Biology Symposium, Basel, Switzerland
Poster: "c-di-GMP-mediated control of an exopolysaccharide secretion machinery in *Escherichia coli*"

2012 Biozentrum Symposium, Bettingen, Switzerland
Poster: "Allosteric activation of exopolysaccharide synthesis through cyclic di-GMP-mediated protein-protein interplay in *Escherichia coli*" (1st posterprize)

Publications

2009 Boehm A *, **Steiner S** *, Zaehring F, Casanova A, Hamburger F, Ritz D, Keck W, Ackermann M, Schirmer T, Jenal U (2009) Second messenger signalling governs *Escherichia coli* biofilm induction upon ribosomal stress. *Mol Microbiol* **72**: 1500–1516
(* Both authors contributed equally to this work)

Fellowships

2008 - 2011 Werner Siemens Foundation (WSF) Fellowship, International PhD Program; Biozentrum, University of Basel, Switzerland

Language skills

German	Mother tongue
English	Fluent
French	Good knowledge
Japanese	Basic knowledge